AD-A084 924   NAVAL POSTGRADUATE SCHOOL MONTEREY CA   F/G 17/2
                A FLUIDIC VOICE COMMUNICATION SYSTEM AND DATA LINK.(U)
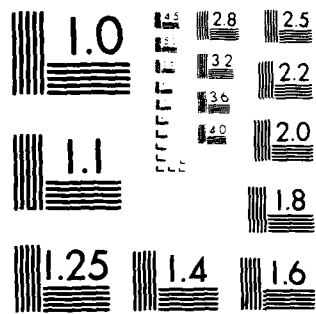   MAR 80   T M DRZEWIECKI

UNCLASSIFIED   NL

1 OF 3

AD
A084 924

	1.0			2.8		2.5
	1.1			3.2		2.2
				3.6		
				4.0		2.0
						1.8
	1.25		1.4			1.6

MICROCOPY RESOLUTION TEST CHART

NATIONAL BUREAU OF STANDARDS-1963-A

NAVAL POSTGRADUATE SCHOOL
Monterey, California

DTIC
ELECTE
JUN 3 1980

C

THESIS

A FLUIDIC VOICE COMMUNICATION SYSTEM
AND DATA LINK

by

Tadeusz M. Drzewiecki

March 1980

Thesis Advisor: R. H. Nunn

Approved for public release; distribution unlimited.

80 5 30 064

DISCLAIMER NOTICE

THIS DOCUMENT IS BEST QUALITY PRACTICABLE. THE COPY FURNISHED TO DTIC CONTAINED A SIGNIFICANT NUMBER OF PAGES WHICH DO NOT REPRODUCE LEGIBLY.

REPORT DOCUMENTATION PAGE		READ INSTRUCTIONS BEFORE COMPLETING FORM
1. REPORT NUMBER	2. GOVT ACCESSION NO. AD-A084 924	3. RECIPIENT'S CATALOG NUMBER
4. TITLE (and Subtitle) A FLUIDIC VOICE COMMUNICATION SYSTEM AND DATA LINK.		5. TYPE OF REPORT & PERIOD COVERED Doctor's Dissertation March, 1980
		6. PERFORMING ORG. REPORT NUMBER
7. AUTHOR(s) Tadeusz M. Drzewiecki Harry Diamond Laboratories Adelphi, MD 20783		8. CONTRACT OR GRANT NUMBER(s)
9. PERFORMING ORGANIZATION NAME AND ADDRESS Naval Postgraduate School Monterey, CA 93940		10. PROGRAM ELEMENT, PROJECT, TASK AREA & WORK UNIT NUMBERS
11. CONTROLLING OFFICE NAME AND ADDRESS Naval Postgraduate School Mechanical Engineering Department		12. REPORT DATE March 1980
		13. NUMBER OF PAGES 262
14. MONITORING AGENCY NAME & ADDRESS(If different from Controlling Office)		15. SECURITY CLASS. (of this report) Unclassified
		15a. DECLASSIFICATION/DOWNGRADING SCHEDULE

16. DISTRIBUTION STATEMENT (of this Report)

Approved for public release; distribution unlimited.

17. DISTRIBUTION STATEMENT (of the abstract entered in Block 20, if different from Report)

18. SUPPLEMENTARY NOTES

19. KEY WORDS (Continue on reverse side if necessary and identify by block number)

Fluidics
Laminar Proportional Amplifier
Communications

20. ABSTRACT (Continue on reverse side if necessary and identify by block number)

This thesis presents a comprehensive dynamic analysis of fluidic laminar proportional amplifiers (LPA) and a subsequent design of a broad-band voice communication system and narrow-band data link that demonstrates the utility of the analysis.

Starting from first principles, the governing equations for the lumped parameter representation of the various flow regimes found in an LPA are derived. From these governing equations, in the Laplace domain, equivalent

DD FORM 1473 EDITION OF 1 NOV 68 IS OBSOLETE
(Page 1) S/N 0102-014-6601

#20. ABSTRACT (continued)

electrical circuits are derived. The input of the LPA is determined to have a fifth order impedance. The transmission of the signal from input ot output is delayed by a transport time, determined both phenomenologically and experimentally, to be twice the average particle transit time. A pressure is developed at the output that is dependent on the loading and the vent conditions. This pressure is acoustically fed gack to the control fregion of the jet, augmenting jet deflection when in phase. The vent inductance has the effect of producing a low frequency himp on the Bode plot. The regions of enhanced gain correspond almost exactly to the edge-tone eigenfrequencies reported in the literature and as such the theory developed herein may be used to predict not only the ratios of eigen frequencies, but also their actual values. Experiments have shown good agreement between theory and data for the amplitude frequency response of LPAs and excellent agreement for their phase shift.

Using the analysis as a tool, an engineering guide was developed for the dynamic characteristics of LPAs especially the HDL STD MOD 3.1.1.8. Operating bandwidths of greater than 14 kHz can be expected for amplifiers with a nozzle width of 0.25 mm. Ultrasonic operation is feasible with smaller devices.

Using the engineering guide, an intercom and an FM data transmission system were designed, built and experimentally evaluated. Performance parameters include a bandwidth of 1-4 kHz for the voice system and a narrow band of 6-6.7 kHz for the FM carrier. FM demodulation results in a dynamic range of 400 at 3 Hz with a frequency discrimination of 0.5 - 40 Hz depending on input amplitude. Transmission distances of 5-10 m have been demonstrated.

Accession For

NTIS GRA&I
DDC TAB
Unannounced
Justification

By
Distribution/

Availability Codes

Avail and/or
Dist   special

A

A FLUIDIC VOICE COMMUNICATION SYSTEM AND DATA LINK

by

Tadeusz M. Drzewiecki

B.E. (Mechanical), City College of the City University of New York, 1966

M.E. (Mechanical), City College of the City University of New York, 1968

Submitted in partial fulfillment of the requirements
for the degree of

DOCTOR OF ENGINEERING
from the

NAVAL POSTGRADUATE SCHOOL

March 1980

Author _____

Approved by _____   _____
D. J. Collins, Professor   T. M. Houlihan, Assoc. Prof.
Aeronautics   Mechanical Engineering

_____   _____
D. E. Kirk, Professor   J. M. Kirshner
Electrical Engineering   Harry Diamond Laboratories

_____   _____
P. J. Marto, Professor   R. H. Nunn, Assoc. Professor
Mechanical Engineering   Mechanical Engineering

_____
R. D. Strum, Assoc. Professor
Electrical Engineerirg

Approved by _____
Chairman, Department of Mechanical Engineering

Approved by _____
Academic Dean

ABSTRACT

This thesis presents a comprehensive dynamic analysis of fluidic laminar proportional amplifiers (LPA) and a subsequent design of a broad-band voice communication system and narrow-band data link that demonstrates the utility of the analysis.

Starting from first principles, the governing equations for the lumped parameter representation of the various flow regimes found in an LPA are derived. From these governing equations, in the Laplace domain, equivalent electrical circuits are derived. The input of the LPA is determined to have a fifth order impedance. The transmission of the signal from input to output is delayed by a transport time, determined both phenomenologically and experimentally, to be twice the average particle transit time. A pressure is developed at the output that is dependent on the loading and the vent conditions. This pressure is acoustically fed back to the control region of the jet, augmenting jet deflection when in phase. The vent inductance has the effect of producing a low frequency hump on the Bode plot. The regions of enhanced gain correspond almost exactly to the edge-tone eigenfrequencies reported in the literature and as such the theory developed herein may be used to predict not only the ratios of eigen frequencies, but also their actual values. Experiments have shown good agreement between theory and data for the amplitude frequency response of LPA's and excellent agreement for their phase shift.

Using the analysis as a tool, an engineering guide was developed for the dynamic characteristics of LPA's especially the HDL STD MOD 3.1.1.8. Operating bandwidths of greater than 14 kHz can be expected for amplifiers with a nozzle width of 0.25 mm. Ultrasonic operation is feasible with smaller devices.

i

Using the engineering guide, an intercom and an FM data transmission system were designed, built and experimentally evaluated. Performance parameters include a bandwidth of 1-4 kHz for the voice system and a narrow band of 6-6.7 kHz for the FM carrier. FM demodulation results in a dynamic range of 400 at 3 Hz with a frequency discrimination of 0.5 - 40 Hz depending on input amplitude. Transmission distances of 5-10 m have been demonstrated.

ACKNOWLEDGEMENT

FOREWORD

The analysis of fluidic amplifiers has been considered by many authors, but I would like to think that the present effort culminates the pioneering work started by Frank Manion of the Harry Diamond Laboratories. It was his experience and insight that led to the successful development of laminar jet devices as we know them today. It was his dynamism and keen engineering acumen that resulted eventually in the successes of laminar systems such as the tank turret stabilization system. I hope that this thesis will be accepted as a contribution to the technology, but it should be remembered that the original concepts of laminar systems are attributable to Frank Manion.

TABLE OF CONTENTS

Table of Contents (continued)

LIST OF FIGURES

List of Figures (con't)

List of Figures (con't)

xi

List of Figures (con't)

xiii

List of Figures (con't)

NOMENCLATURE

a_1 - spillback coefficient

A   - cross-section area, m^2

b   - channel width, m

B   - dimensionless channel width, b/b_s

c   - speed of sound, m/s

c_d - LPA supply nozzle discharge coefficient

c_θ - LPA supply nozzle momentum flux discharge coefficient

C   - capacitance, m^3/Pa

d   - internal tube diameter, m

db   - decibel

E   - electric potential, volts

f   - frequency, Hz

F   - dimensionless frequency, $f\, b_s/(c_d(\ 2P_s/\rho)^{1/2})$

F_y - force in y-direction, N

G_p - pressure gain, dp_o/dp_c

h   - height, m

Hz   - hertz

I   - electric current, amperes

j   - $(-1)^{1/2}$,

k   - empirical constant in duct resistance equation

$K_{1,2}$ - constants in transfer function consolidation

ℓ - length, m

L   - inductance, kg/m^4

LPM   - litres per minute

m   - mass, kg

mmHg   - millimeters of mercury of pressure

Nomenclature (con't)

n	-	integer number
N_R	-	Reynolds number, $(b_s/\nu)(2 P_s/\rho)^{1/2}$
N'_R	-	modified Reynolds number $N_R/((x_{th}/b_s+1)(1+1/\sigma)^2)$
p	-	pressure, Pa
P	-	dimensionless pressure, p/P_s
Q	-	volumetric flow, m^3/s
r	-	radius, m
R	-	resistance, $kg/(m^4 s)$
R_g	-	gas constant, $m^2/(s^2 \, °K)$
s	-	Laplace operator
t	-	time,s
T	-	temperature, °K
u	-	x direction velocity, m/s
U_s	-	x-direction supply nozzle velocity, m/s
v	-	y-, or lateral direction, velocity, m/s
V_s	-	Bernoulli velocity, $(2p_s/\rho)^{1/2}$, m/s
V	-	general velocity, m/s
x	-	length dimension, m, or coordinate axis
X	-	dimensionless length, x/b_s
Y	-	complex admittance, 1/Z, $m^4 s/kg$
z	-	coordinate axis, m
Z	-	complex impedance, $kg/(m^4 s)$

Nomenclature (con't)

Greek Symbols

β	-	bulk modulus, Pa
δ	-	deflected jet space, m
Δ	-	change
ζ	-	attenuation factor
λ	-	wavelength, m
μ	-	absolute viscosity, kg/(m s)
ν	-	kinematic viscosity, μ/ρ , m^2/s
π	-	3.14159
ρ	-	density, kg/m^3
σ	-	aspect ratio, h/b_s
τ	-	transport time, s
τ	-	RC time constant, s
τ_w	-	wall shear stress, Pa
ω	-	circular frequency, rad/s
Ω	-	dimensionless circular frequency, $b_s/c_d V_s$

Nomenclature (con't)

Subscripts

B	-	blocked
bw	-	bandwidth
c	-	control
d	-	spill back resistance
e	-	entrained
f	-	fitting
fb	-	feedback
g	-	gas
h	-	hydraulic
i	-	input or integer
in	-	in
j	-	jet
k	-	pseudo-impedance
L	-	load
LPA	-	laminar proportional amplifier
LJARS	-	laminar jet angular rate sensor
m	-	modulus
min	-	minimum
n	-	integer
N	-	noise
o	-	output
out	-	out
r	-	returned
RC	-	resistive capacitive
RL	-	resistive inductive
s	-	supply
sp	-	splitter
t	-	distance between downstream control edges

Nomenclature (con't)

Subscripts (con't)

th	-	supply nozzle straight section
v	-	vent
w	-	wall
x	-	x-direction
XSP	-	distance to splitter
XVI	-	distance to vent vane
y	-	y-direction
1	-	side 1
2	-	side 2
∞	-	ambient or atmospheric
δ	-	deflection of jet

Superscripts

$^{-}$	-	"bar," average value
$^{\prime}$	-	"prime"
$^{\cdot\cdot}$	-	"double dot," second derivative with time

1. INTRODUCTION

1.1 A Historical Perspective

Communication of data, speech and other information in the military and civilian sphere probably goes back as far as the time when the first cave man grunted once for danger and twice for all clear to his compatriots during a hunt. Oral and acoustic communication has persisted through the ages until the dawn of the electronic age with the invention of the telegraph which permitted the virtually instantaneous transfer of electrical pulses along a conductor that were later converted into sounds. With growing sophistication telegraphic information could be imposed directly into markings on paper thus providing a permanent record of the data transmitted. The telephone and finally the radio permitted the transfer of much more data content and of actual speech. These inventions revolutionized the economic, social and military environments. They enabled the military to broaden their scope of operations with information regarding the enemy and deployment of friendly forces. The modern age of electronics ushered in during World War II dramatically increased the rate and quantity of data being transmitted. In addition, with the invention of the radar, electronic air waves were being used for detection as well as transmission. During all this technological expansion, simultaneous efforts were being made to provide for secure transmission as well as the overt and covert interruption and interception of transmissions. Jamming signals were added to the ever increasing spectrum of electromagnetic (EM) signals propagating through space. With the advent of the electronic computer the data rates and handling capabilities took a quantum jump. The number of channels in the radio frequency (RF) spectrum has become fantastic. Sophisticated techniques to increase the capacity of a single channel have allowed the RF spectrum to keep up with demand. With the EM spectrum already

crowded, the nuclear age has provided yet another source of radiated energy, and the recent development of EMP (electromagnetic pulse) devices and particle beam weapons provides more. The overt disruptive transmission of energy such as jamming, EMP and particle beam weapons is aimed at destroying the transmissive medium or the actual transmitting or receiving devices. In a recent article in SIGNAL magazine[1*], the authors describe the modern battlefield and its requirements for reliable communication. This battlefield is a blaze of light and noise in addition to a mass of radio transmissions. Hearing, sight and speech are impaired as well as are electromagnetic transmissions.

Let us regress in time for a moment and paint a different scenario. The preceeding perspective has primarily relied on a land based view. Consider, however, the problems of communication within a rigidly bounded structure as in a naval vessel, an aircraft, or for that matter, a large residential dwelling. Ever since the days of the Roman warships directional acoustic transmission of voice has been used. The Romans used crude megaphones to channel human voice energy into a small section of space, while on steamships, passive speaking tubes were effective in providing a communications link between the bridge and various deck levels such as the boiler room. These same tubes were commonly in use at the turn of the century in large residences and hotels as means of summoning servants and relaying household requirements. The electronic age had its effect on this mode of communication wherein the telephone or intercom has replaced these old standby's. The development of the aircraft occurred totally within the electronic age time frame and as such was not touched by such quaint antiques as the speaking tubes.

---

*Numerical superscripts refer to bibliographical references.

The development of the battleship and aircraft carrier as
a wholly self contained entity or community has posed an interesting
dilemma regarding the safety aspects as of high intensity of electro-
magnetic radiation. Fuel and munitions are stored in this hazardous
EM environment. Fumes are ever-present below decks even in well ven-
tilated places, hence, there is an ever-present danger of conflagration
or explosion due to electrical sparks, heating or radiation. An inter-
esting example of the latter is the propensity of small bridge wires,
used to detonate munitions, to act as antennae for RF signals thus
inducing a current and hence producing sufficient heat for initiation
of a charge. The safety aspect is the reason why the Navy has been
most interested in nonelectrical schemes for doing things, to include
communications.

The historical perspective on interpersonal communication systems
is one of rapid development following the invention of the tele-
graph with an ever increasing traffic load and mutual and active
interference. As an exalmple of this interference, even hard wire
intercoms in an armored vehicle suffer tremendously during the heat
of battle with intelligibility deteriorating to the point that com-
munications are often lost between a commander and driver over a
space as short as two meters. It is this problem, the loss of com-
munications at relatively close quarters, that this work attempts
to solve by applying the non-electrical technology of fluidics.

1.2 The Role of Fluidics in Communication

In 1959, Horton, Bowles and Warren coined the term "fluid
amplification" for the process of controlling relatively high energy
streams or jets of fluid by low energy ones. Kirshner[2] relates that
the principles of this new technology were disclosed in a press release
in March 1960. The basis of operation of a fluidic amplifier is shown
in figure 1.

LAMINAR ANALOG FLUIDIC AMPLIFIER
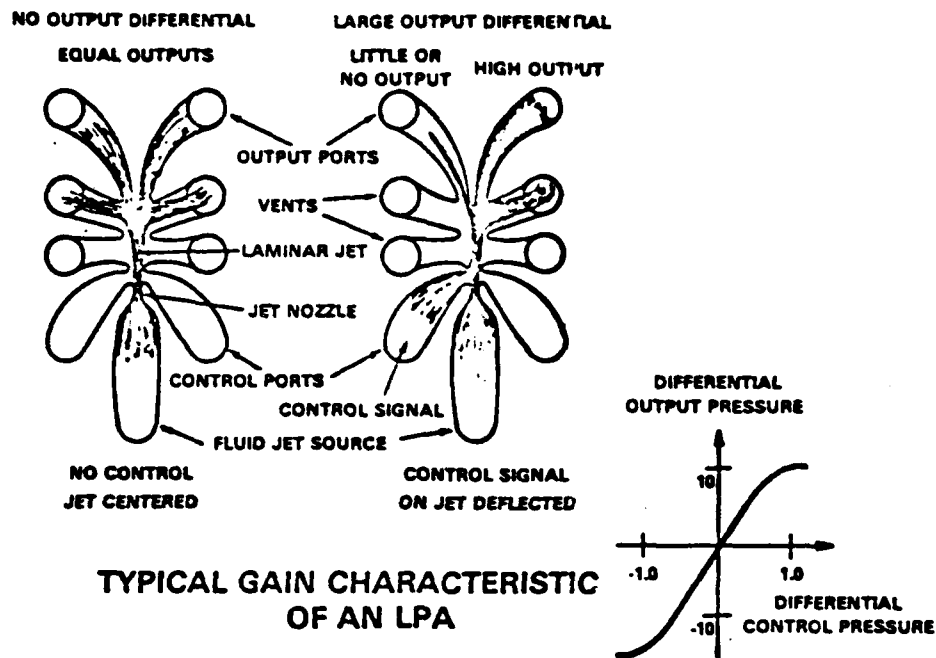
Figure 1. Operation of a fluidic amplifier

In the neutral, undeflected or centered position, a jet of fluid
emanates from a nozzle, traverses a given distance, and impinges on a
dividing wedge commonly called a splitter, whereupon the flow divides
equally. If there is no restriction in the channels on either side
of the splitter, then equal amounts of flow will exit through the output
ports. If the output ports are restricted, then the flow will turn
approximately 90° and exit through the vents to ambient. While the
flow undergoes the 90° change in direction, it develops equal static
pressures at the output ports. When a low energy stream of fluid (or
a small pressure difference) is applied to the jet in the vicinity
of the nozzle exit, the effect is to deflect it slightly. This small
deflection becomes considerable, by geometry, at some distance downstream,
hence the amount of fluid impinging on one output is increased and

4

simultaneously reduced on the other. This, then, produces a differential
pressure at the outputs that is considerably greater than the dif-
ferential pressure that produced the deflection. The ratio of the
output pressure differential to the input or control differential
describes the function of signal or input amplification, and is called,
therefore, "gain." Although this principle has been known and used
since 1959, it was not until the early part of the 1970's that low
noise, high input impedance, laminar proportional amplifiers (LPA)
became available for convenient systems utilization[3,4,5,6]. The
laminar nature of the flow accounts for the low noise, and since the
narrow disturbance-free jet may be caused to flow in such a way as to
almost block off the control channels, the input impedance is made
quite high.

Despite the lack of availability of such critical components as
the LPA, the basic concept of a fluidic amplifier as a pressure amplifier
coupled with the fact that sound is a pressure wave phenomenon led
Horton in 1960 to propose the fluidic speech amplifier shown in figure 2.[7]
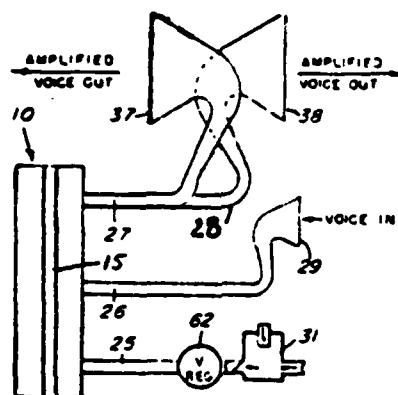
Figure 2. Horton's speech amplifier concept.

He described the function in the following manner:

"In this figure exponentially curved horn 29 is attached
to tube 26. Source 31 provides a constant, continuous
source of air to nozzle 15. Anyone speaking into the

5

enlarged end of this horn will cause pressure pulsation to
occur in tube 26. These pulsations will be amplified by
system 10. The amplified pulsations pass through tubes 27
and 28 and into horns 37 and 38 respectively. Amplified
voice issues from horns 37 and 38."

This simple idea lay fallow for many years for the already cited
lack of proper components of sufficient bandwidth and dynamic range.
In 1969 HDL working under a Navy contract studied a public address
system for use on flight decks[8,9,10], resulting in a public demon-
stration of the system at the 10th Anniversery of Fluidics ASME
sponsored meeting at Georgia Tech In 1970. Although this system did
not meet the Navy requirements at that time, it did demonstrate that
the bandwidth of fluidic amplifiers was adequate to pass speech. Sub-
sequently, in 1976, a laminar fluidic public address system was built
and demonstrated again at the Harry Diamond Laboratories (HDL). The
most objectionable drawback, that of background hiss or noise was
eliminated. In addition, the task was performed with LPA's that were
twice the size of those used previously and since there was considerably
more gain and bandwidth, fewer stages of amplification were required.
Also due to the laminar nature of the flow, the operating power pressure
was considerably lower, 3 kPa as opposed to 45 kPa.

Another fluidic technique for speech amplification and trans-
mission originated a few years after Horton's disclosure of his
beam deflection amplifier (figure 1 shows the jet being deflected
much as a rigid beam, hence the term beam deflection amplifier)
that utilized the inherent amplification of disturbances of a parti-
cular frequency in a free shear layer. Unfried[12] discusses such a
system and uses the inherent non-linearities to provide modulation
and demodulation of a basic carrier frequency at bandwidths to 8 kHz
on carriers of up to 17.5 kHz. Figure 3 shows schematically Unfried's

Acoustic Amplitude Modulated Wave
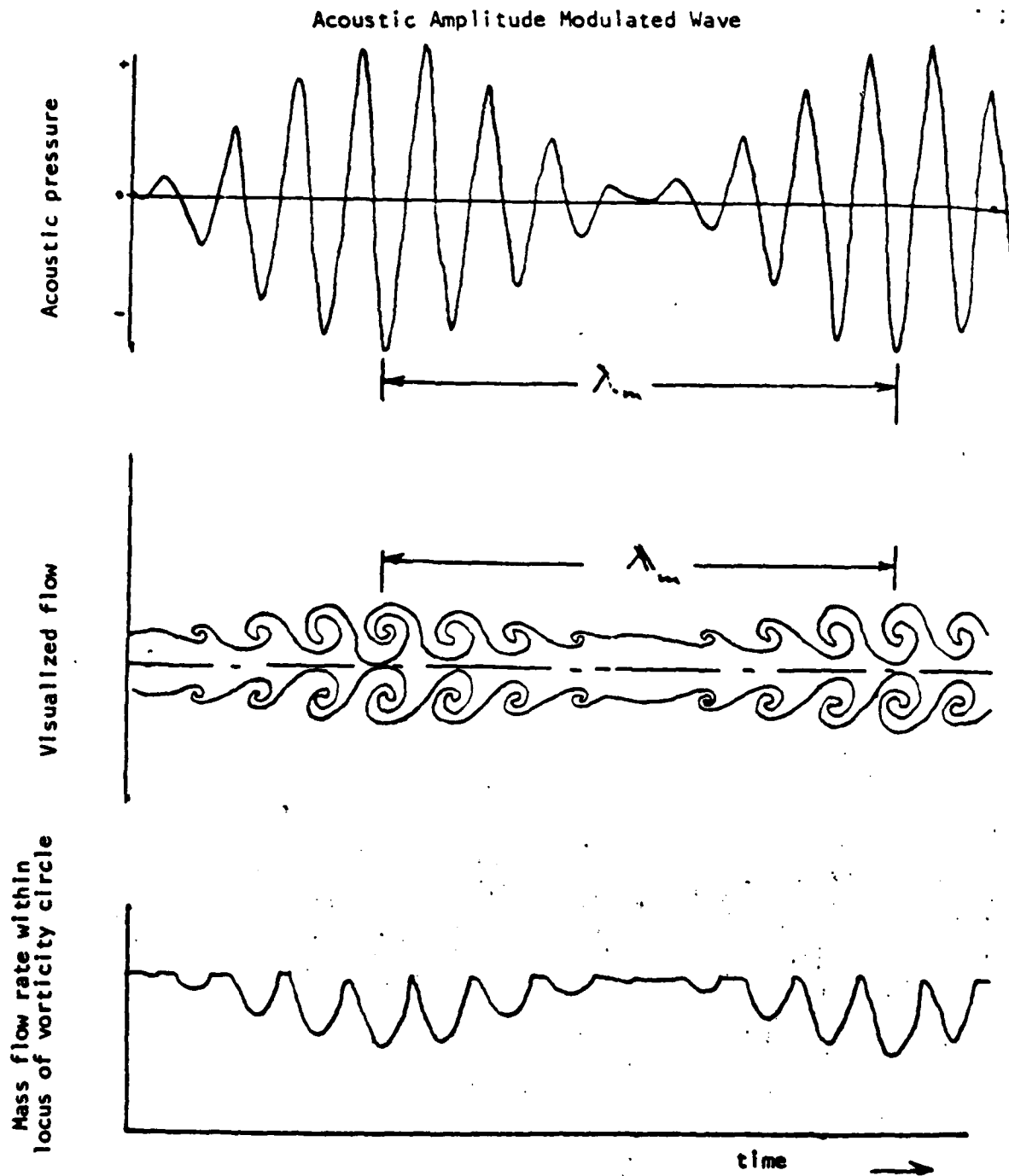
Figure 3.   Unfried's[12] free shear layer acoustic amplifier concept.

concept. The chief drawback of this system was the requirement
of a transitional free jet where the breakdown eddies would be
modulated. This type of jet is very susceptible to being tripped
into turbulence[13,14] and requires quite precise flow regulation to
maintain the appropriate Strouhal and Reynolds numbers.

The transmission of data insofar as communications is concerned
can occur at any frequency as is obvious from a comparison of the low
bit-rate of the original hand coded Morse messages to the super sophis-
ticated computer-controlled systems used to transmit data from satellites
at huge baud rates. All fluidic systems, in fact all communication
systems, involve the transmission of data over some distance at some
bandwidth. Maximum distance for transmission of fluidic signals with
closed loop control is about 10 meters in order to keep the acoustic
delay low enough so that the overall bandwidth is over 40 Hz in air. Trans-
mission of data up to 100 meters is discussed by Kirszenblat.[15] The
theory of acoustic transmission lines is well developed. Almost any
text on acoustics deals with the subject. For example, Rschevkin[16]
has an excellent treatment. Indeed, his treatment of the fundamental
lumped parameter approach to acoustics is excellent and forms the
basis for much analysis in the literature. With regard to fluidic
transmission lines, Kirshner and Katz[17] present an excellent treatise
thereof. They consider both the lumped and distributed parameters
approach and present a quasi-method of characteristics for the
solution of the signal propagation problem in long ducts. Roffman and
Deadwyler[8] consider signal transmission through circular cross-section
lines for their public address system and conclude that   audio band
pass is possible.

Finally, the concept of an intravehicular fluidic communication
system was published by Alexander and Drzewiecki[1] and is shown in
figure 4.

FLUID TRANSMISSION LINES

AMPLIFIED SOUND
PRESSURE WAVE

NORMAL VOICE
LEVEL SOUND

OUTPUTS

RECEIVER

NORMAL SPEECH
SOUND WAVES

FLUID JET MOVES BACK
AND FORTH WITH INPUT
PRESSURE WAVE

INPUT TUBE

INPUT

SOUND PRESSURE
WAVE

SPEAKER

FLUID JET SOURCE

FLUIDIC AMPLIFIER

←———COMMUNICATION DISTANCE———→
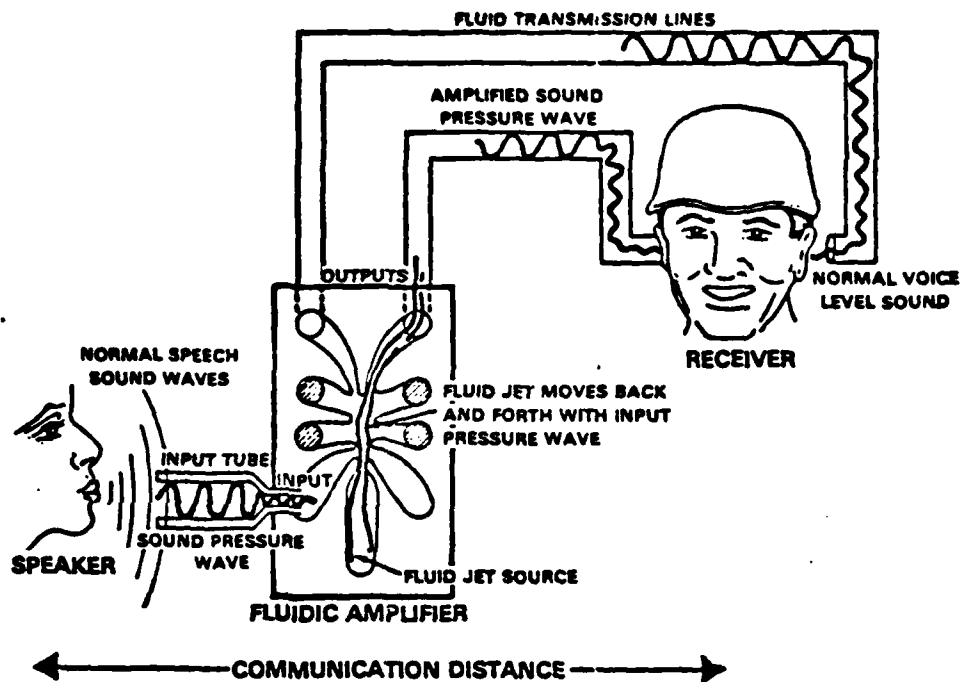
Figure 4. A fluidic voice communication system schematic.

At this point excerpts from the introduction to the proposal for this thesis cover some of the remaining points.

"The ability to communicate in the military environment constitutes perhaps the one most important factor that determines the outcome of armed combat. Whether it is the tank commander talking with his gunner, the pilot talking with his bombardier or the ship's captain talking with his missile officer, if there is any loss of information content then there exists an excellent chance that either the target will be lost or that the tables will be turned. With the expansion of modern day technology to include computers, microprocessors and other sophisticated electronics in most major weapons systems, the area of communications has expanded to include man-

9

machine interaction in addition to the already mentioned man-to-
man interaction. Ship control may be communicated to the steering
mechanism by electronic means, from a potentiometer to a servo
mechanism. The fly-by-wire concept introduced in both the Navy
and Air Force and currently used on the F-16 aircraft is an excel-
lent example of man-machine interaction in that it requires that
human command information be transmitted to the actuators and con-
trollers by wire. Introduce now the electronic warfare environment-
-jamming, broad-band electromagnetic (EM) signal traffic, and spurious
EM effects from motors, engines and electronic devices. It has
been estimated that hard-wire radio communications within an M60
tank in a typical combat EM environment can be reduced to as little
as 30-35% information content. There are no comparable figures
available on the failure rate of electronic control systems in EM
environments; however, current design practice for military avionics
requires six-times redundant control paths and control systems.
The use of Kalman filters has become increasingly popular in radar
and fire-control systems but has not as yet made an impact in other
areas, perhaps due to the added complexity."

1.3 Statement of the Problem

While there is some repetition from the earlier two sections,
this helps focus the problem. It is clear that two main areas of
work are identified--research and development.

The research must necessarily involve the mathematical analysis
from first principles of the frequency response of fluidic amplifiers
so that rational design may proceed. As early as 1965[18] researcher's
have remarked on the high order frequency response of fluidic pro-
portional amplifiers. They noted the appearance of high gain, high
frequency regions that they tacitly assumed could not be explained
by lumped parameter equivalent circuit techniques. Figure 5 is
typical of the observed frequency response at relatively high aspect
ratios (nozzle height-to-width ratio, $h/b_s = \sigma$) $\sigma = 2.5$, for a turbu-
lent jet device. The solid line has been faired in to point out the
multiply resonant character of the amplitude response. In 1967, Moore
et al[19] attempted to capitalize on the resonant regions by enhancing
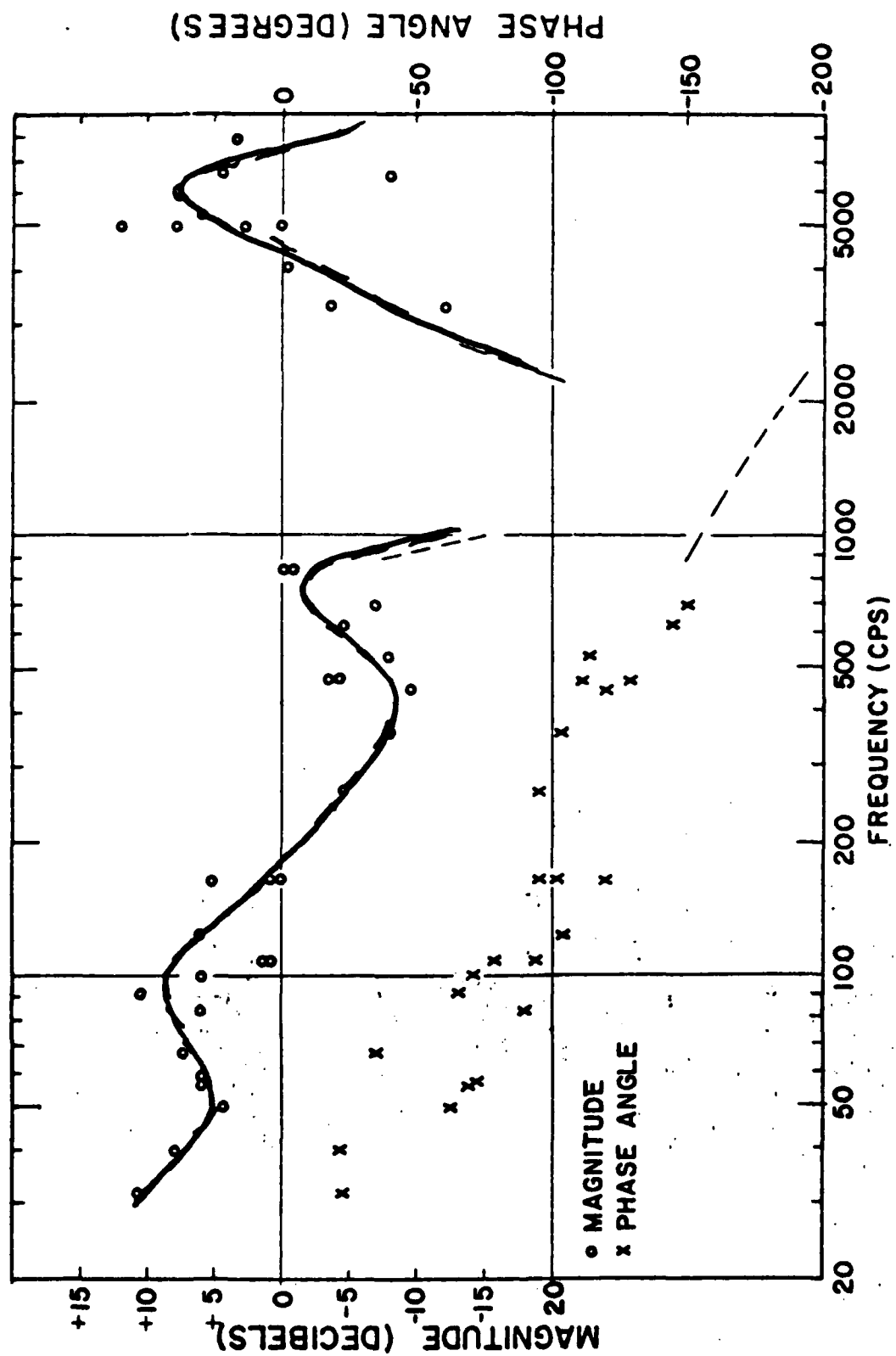
Figure 5. Frequency response of a turbulent fluidic amplifier due to Roffman[18].

11

them and thus getting high frequency and high Q, hence good noise rejection in otherwise very low signal-to-noise turbulent devices. They met with limited success in that they were only able to achieve about 1.5 kHz operation. They did, however, provide experimental evidence of the high order modes of operation as shown in figure 6. The solid line represents their attempt to represent the observed data trends
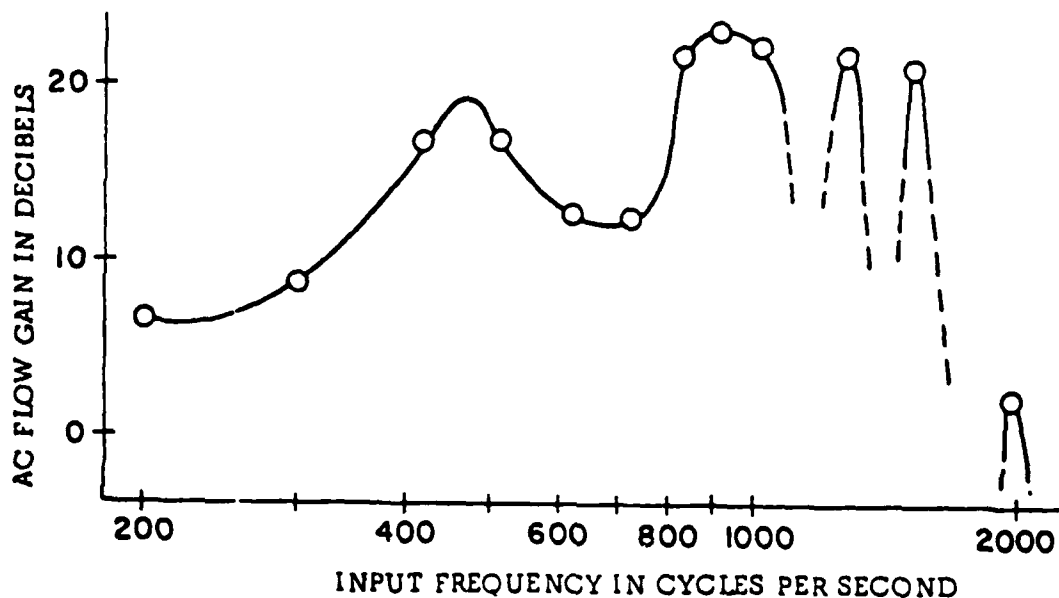
Figure 6. Typical response data from Moore et al[19].

between actual data points depicted by circles. The fluidic amplifier used in obtaining these data is shown in figure 7 to distinguish it from the laminar devices shown in figure 1.

SPLITTER   OUTPUT LINE

RECEIVER WIDTH

VENT

CONTROL EDGE

UPPER CONTROL PORTS INPUT

VENT   SUPPLY NOZZLE
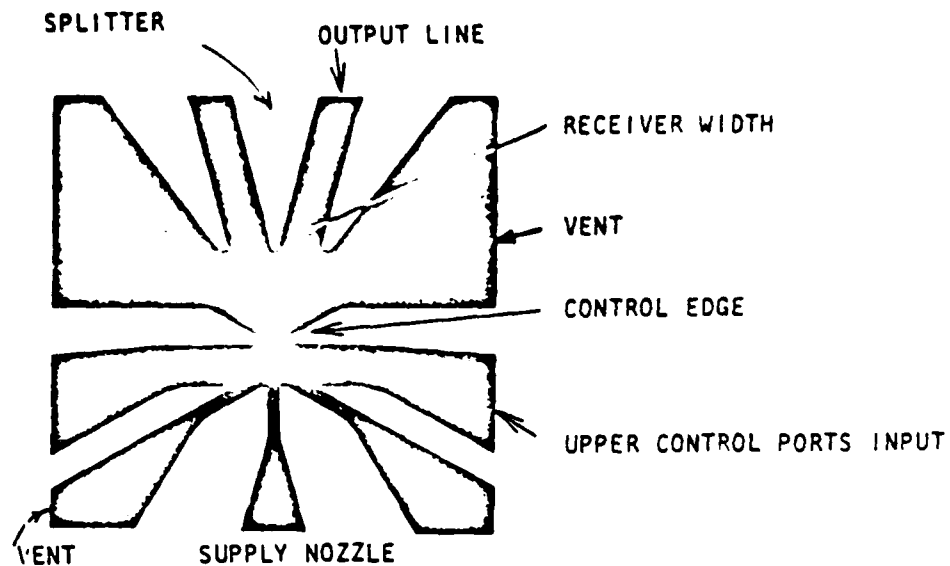
Figure 7.   Typical geometry of fluidic amplifier used
by Moore et al.[19]

The devices all are turbulent and would involve considerably more
empiricism to analyse than would a laminar device.   In 1973 Healey
and Shipp[20] summarized the available work on proportional amplifiers
and presented data of their own.   Typical of the results for amplifiers
with adjustable vents are those shown in figure 8 where the three in-
dividual curves correspond to three operating supply pressures.   Healey[21]
comments on this behaviour to the effect that the high frequency behaviour
is a jet dynamic effect and he limits his discussion of amplifier op-
eration to frequencies well below this point.   He also states that no
satisfactory theory exists to quantitatively predict the high frequency
gain although a qualitative jet bending argument can be made for their
general existence.   Up to this point all amplifiers examined were tur-
bulent.   However, in 1972, Manion and Mon[13] published their results
on laminar proportional amplifiers (LPA's).   These were inherently low
frequency devices because of the predominant wide control ports that
are of a low pass nature.   Kirshner and Katz[17] describe the jet dynamics

13
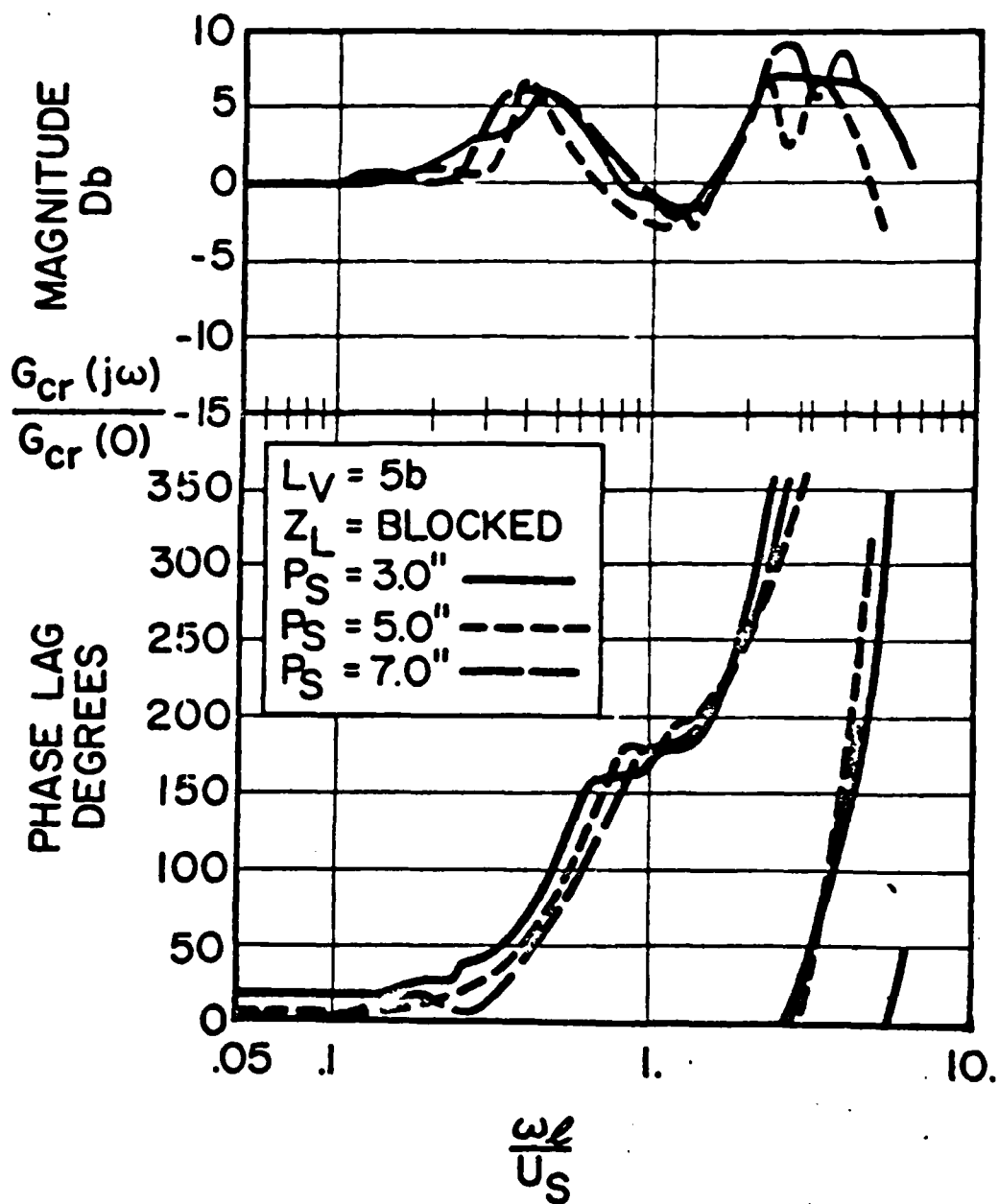
Figure 8. Turbulent amplifier frequency response from Healey et al.[20],[21]

as a pressure feedback phenomenon; however, they also do not show any numerical examples related specifically to fluidic amplifiers.

It follows, therefore, that consideration must be given to the behavior of an LPA at high frequencies. As such, this effort will consider the fluid dynamics of the flows through the LPA passages and will consider the overall jet coupling with the structure.

Insofar as the development of a communication system is concerned, it is an objective of this thesis to present feasibility arguments for a design and a working demonstration of fluidic communication. To this end, broad band voice transmission and amplification will be considered and, to demonstrate overall utility (although probably not practicality), a duplex system for the simultaneous transmission of frequency modulated data will be built. It is intended that this overall system will demonstrate all the capabilities of LPA's in the high frequency modes.

In keeping with the engineering design/analysis tenor of this work, the analysis will be approached from a control volume, block diagram aspect.

The thesis is divided into 12 sections as follows:

1. INTRODUCTION - An outline of the problem, a literature survey, plan of analytical attack and design methodology.

2. ANALYSIS - The governing equations for an LPA will be developed, tying together past analyses and introducing the additional dynamics. Control volume methods will be stressed. Flow visualization data will be used to demonstrate step response and signal eddy convection. A block diagram approach will then be used to develop the overall transfer function and an equivalent lumped parameter circuit approach will be used to develop the input and loading dynamic response. Comparison will be presented between theory and data.

3. <u>VOICE SYSTEM DESIGN</u> - This section will be broken down into the sub-systems outlined in a matrix. Each part will have its own analysis, computation, and hardware section. In addition, there will be a section dealing with human engineering as well as system engineering.

4. <u>DATA LINK SYSTEM DESIGN</u> - This section also will be broken down into sub-systems outlined in a matrix as in part 3. Performance data and characteristics will be presented.

5. <u>SYSTEM IMPLEMENTATION</u> - This section will deal with the installation of FVCDL systems in military vehicles to include M60 and XM-1 class tanks, F-14, 15, 16 type fighter aircraft and LVTP-type assault craft.

6. <u>ENVIRONMENTAL SENSITIVITY</u> - This section will be divided in two major subsections: gaseous property changes due to temperature and altitude and basic environment such as contamination, vibration and EMI/EMP/nuclear effects.

7. <u>COST AND RELIABILITY</u> - This section will consider the production costs, producibility, life-cycle costs, maintainability and overall system life. Based on studies conducted on typical fluidic systems, all this information can be extracted.

8. <u>SUMMARY</u>

9. <u>CONCLUSIONS</u>

10. <u>RECOMMENDATIONS</u>

11. <u>BIBLIOGRAPHY</u>

12. <u>APPENDICES</u> - This will be the repository for the various computer programs used.

2. ANALYSIS

This section will deal with the theoretical considerations involved with the problem. The first section shall deal with the dynamic modeling of the laminar proportional amplifier (LPA). The next two sections will deal with transmission lines and passive components, respectively.

2.1 The Laminar Proportional Amplifier (LPA)

Considerable mention has been made of the LPA in the text so far. Historically, this device has evolved for three distinct reasons. The first is the dynamic range. In the early portion of the seventies the problem of fluidically stabilizing a gun turret in two axes was posed. It was established that in order to meet the specifications of a maximum rate of 100°/s and a threshold of 0.1°/s an overall dynamic range of 1000:1 was required. Since no turbulent device has a signal-to-noise ratio of any better than 500:1[3], it was clear that the specification could not be met by any combination of turbulent devices. Griffin and Gebben[22] disclosed an amplifier that was subsequently used in the laminar regime[3] and was the basis for the evolution of the HDL LPA. Significantly, at about the same time G.E. showed operation of their commercially available amplifier in the laminar regime; however, with significant loss in gain.[23] The ultimate LPA dynamic range is essentially unmeasurable since in the limit only thermal noise due to random molecular motion exists; however, practically flow-borne noise and common-mode ambient disturbances in conjunction with a finite common-mode rejection ratio normally limit the dynamic range of multiple LPA systems to the order of 100,000:1[24]. For most practical applications this is quite sufficient.
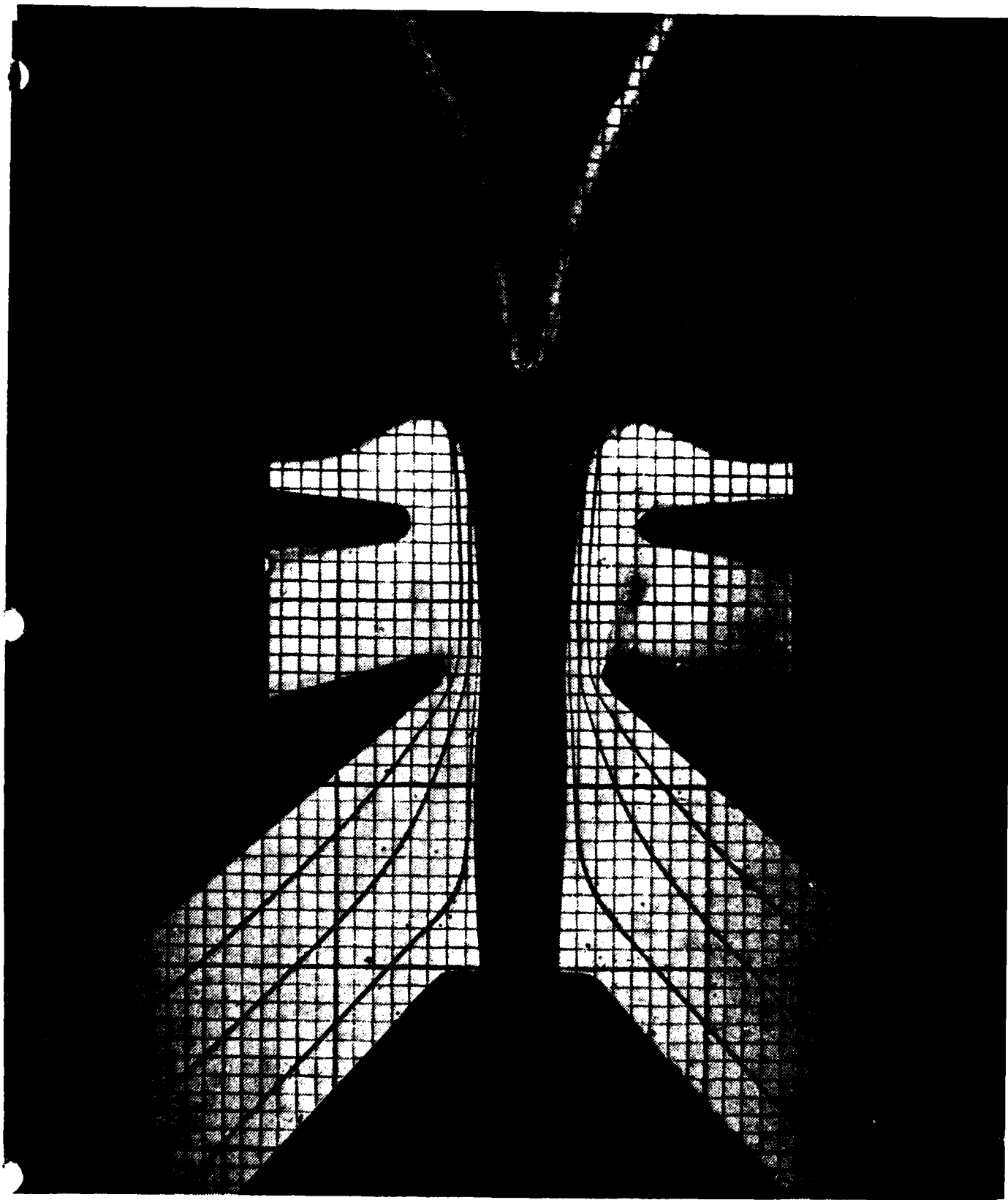
Figure 9. Flow visualization photograph of an LPA interaction region. Dark flow is the power jet.

The second reason for laminar flow devices was that the reduction in entrained flow allowed the placement of the laminar jet in such a way as to effectively block off the control channel as shown in figure 9, thus giving rise to a high input impedance.

The third reason for the use of laminar devices is their inherent low power consumption. Normally operating in air only several millimeters of mercury pressure, only a few milliwatts of power are required as opposed to a typical value of almost one watt for turbulent devices operating at 10 kPa.

It is of interest, therefore, to examine the LPA to see what its bandwidth is and to see if the design can be improved.

2.1.1 Flow Through Ducts and Channels

Consider therefore the LPA geometry shown in figure 10.
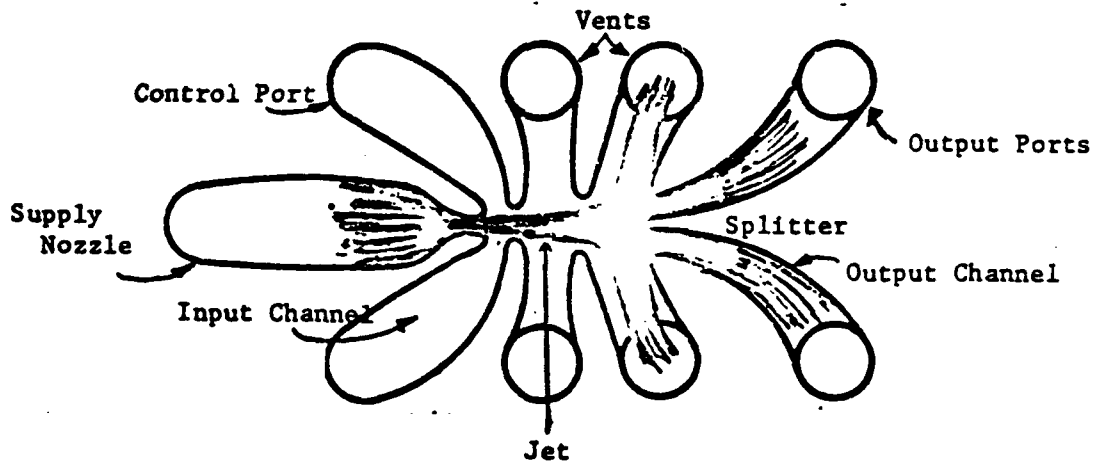
Figure 10. Schematic of a laminar proportional amplifier.

With the exception of the vent vanes and the close proximity of the control edges, this is the same as the beam deflection amplifier described in the literature.[25,26,27,17] It is composed of inflow,

outflow, and through flow passages. Thus, the behavior of flow through
rectangular cross-section channels forms the basis of this analysis.
The steady flow character of these channels is well understood and
documented in the literature.[6] The frequency response is also known
under certain circumstances.[17] With the requirement of small ampli-
tude deviations around steady flow, it has been found that the
pressure drop is made up of steady and reactive components. Iseman[28]
goes to particular pains to describe the equivalent circuit topology
(network arrangement) of capillaries as various combinations of single
resistances, inductances and capacitances, and Kirshner and Katz[17]
go into some considerable discussions of rectangular passages. Un-
fortunately, there has not been any real effort to describe the
equivalent circuit of an LPA device other than in the simplest terms.
Following the example of Kirshner and Katz[17] where they describe the
differential ecuivalent circuit of a transmission line as an "ell"
circuit shown in figure 11 this author will attempt to describe a
useful equivalent lumped circuit for a short channel such as the input
or output of an LPA.
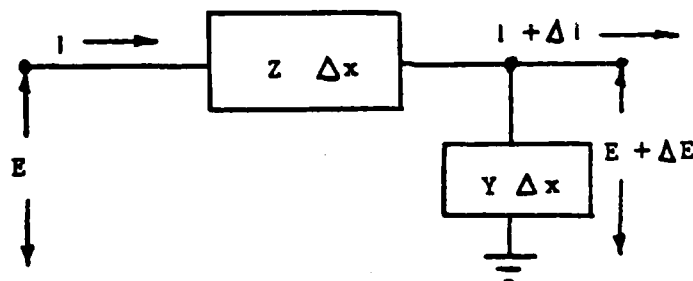
Figure 11.   Infinitesimal transmission line element after
             Kirshner and Katz[17].

The equivalent circuit of figure 11 is only valid in the infini-
tesimal size when one may make the assumption that the voltage across
the admittance Y is approximately E. Consider how this analogy was

developed. Zalmanzon[29] derives the momentum and continuity equations for a control volume in a duct. This derivation is presented here in a slightly altered fashion. Consider a duct and a control volume within that duct as shown in figure 12.
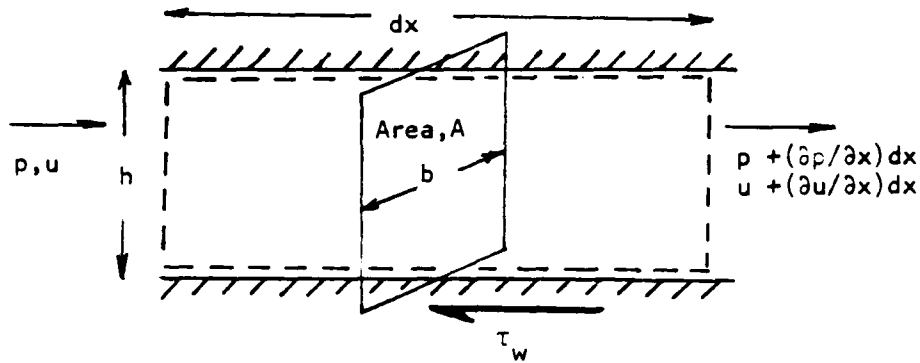
Figure 12. Control volume in a duct.

The forces acting on this differential element must equal the mass times the acceleration of the fluid according to Newton's Second Law. Hence

$$p A - A(p + \frac{\partial p}{\partial x} dx) - 2\tau_w dx(b + h) = \rho A dx \frac{\partial u}{\partial t} \tag{1}$$

or

$$- \frac{\partial p}{\partial x} - 2\tau_w \frac{(b + h)}{A} = \rho \frac{\partial u}{\partial t} \tag{2}$$

Defining the flow Q = Au then

$$- \frac{\partial p}{\partial x} = 2 \frac{\tau_w (b + h)}{A} + \frac{\rho}{A} \frac{\partial Q}{\partial t} \tag{3}$$

The continuity equation states that mass is conserved hence

$$\rho uA - A\rho (u + \frac{\partial u}{\partial x} dx) = \frac{dm}{dt} = \frac{d}{dt} \rho A dx \tag{4}$$

21

or
$$-\rho \, \frac{\partial Q}{\partial x} = A \, \frac{\partial \rho}{\partial t}$$

$$(5)$$

For a gas, the equation of state will be

$$p = \rho R_g T \tag{6}$$

For a liquid $\quad dp = \beta_m d\rho/\rho \tag{7}$

so that the derivative of density in (5) can be replaced. Consider the gaseous, isothermal case

$$\frac{\partial \rho}{\partial t} = \frac{1}{R_g T} \, \frac{\partial p}{\partial t} \tag{8}$$

hence equation (5) becomes

$$- \rho \frac{\partial Q}{\partial x} = \frac{A}{R_g T} \frac{\partial p}{\partial t} = - \frac{p}{R_g T} \, \frac{\partial Q}{\partial x}$$

where the ambient density,ρ, is related to the absolute ambient pressure,$\bar{p}$, and the absolute temperature, T.

or
$$- \frac{\partial Q}{\partial x} = \frac{A}{\bar{p}} \, \frac{\partial p}{\partial t}$$

$$(9)$$

Equations (3) and (9) form a set of differential equations that when $\tau_w = 0$ are identical to the wave equation. Taking now the Laplace transform of both equations result in

$$- \frac{\partial P}{\partial x} = \frac{2\tau_w (h + b)}{A} + \frac{\rho}{A} s \quad Q \tag{10}$$

$$- \frac{\partial Q}{\partial x} = \frac{As}{\bar{p}} \quad P \tag{11}$$

Now the term with the friction forces is represented by the pressure
drop due to friction per unit length of a given duct. The resistance of
a duct is defined as

$$R \equiv \frac{\Delta P}{Q} \tag{12}$$

analogous to the electrical voltage drop divided by current where
pressure is analogous to voltage and volume flow to current. The
pressure drop per unit length is then

$$\frac{RQ}{\ell}$$

where R has been computed for various geometries by various authors.
For circular ducts it is determined by the Hagen-Poiseuielle equation

$$R = 8 \ \mu\ell/\pi r^4 \tag{13}$$

For rectangular ducts the Cornish[30] solution may be used, but an
approximate solution by Kirshner and Katz[17] has been improved with
an empirical constant by Manion and Drzeweicki[4] and Drzewiecki[6]
so that

$$R = \frac{12 \ \mu\ell}{(hb)^2} \ [b/h + h/b + k] + \frac{0.475 \ \rho Q}{(bh)^2} \tag{14}$$

where $0.35 \leq k \leq 0.5$, $1 \leq b/h \leq 2$
and $\quad k = 0.5$ for $b/h \geq 2$

Notice here that entrance effects have been considered giving an
accurate representation for all laminar flows for ducts of length ℓ .
The pressure per unit length is substituted into equation (10) yielding

$$-\partial P/\partial x = RQ/\ell + (\rho \ s/A) \ Q = (R/\ell + \rho s/A) \ Q \tag{15}$$

along with equation (11)

$$-\partial Q/\partial x = (A/\bar{\rho}) \ s \ P \tag{16}$$

23

Equations (15) and (16) form the governing equations for an infinitesimal
section of flow through a duct. Now recall the equivalent circuit of
a transmission line segment of figure 11. The governing equations
are obtained from the input impedance and shunt admittance. The
voltage drop ΔE is

$$\Delta E = -(Z \, \Delta x) \, I \tag{17}$$

and the current drop is

$$\Delta I = - (Y \, \Delta x) \, (E + \Delta E) \tag{18}$$

where Z and Y are the impedance and admittance per unit length.
Neglecting second order terms and taking the limit as $\Delta x \to 0$, these
two equations become

$$\frac{\partial E}{\partial x} = -ZI \tag{19}$$

$$\frac{\partial I}{\partial x} = -YE \tag{20}$$

Differentiating equation (19), with respect to x and substituting
in equation (20) yields the wave equation

$$\frac{\partial^2 E}{\partial x^2} = ZYE \tag{21}$$

However, note the form of equations (19) and (20) and notice that
they are identical to (15) and (16) when P is analogous to E, I to Q,
and

$$Z = (\frac{R}{\ell} + \frac{\rho}{A} s) \tag{22}$$

and

$$Y = \frac{A}{\overline{\rho}} s \tag{23}$$

This then means that an infinitestimal section of a duct may be
represented by a resistive, inductive (inertive) and capacitive
circuit in an "ell" as in figure 13.
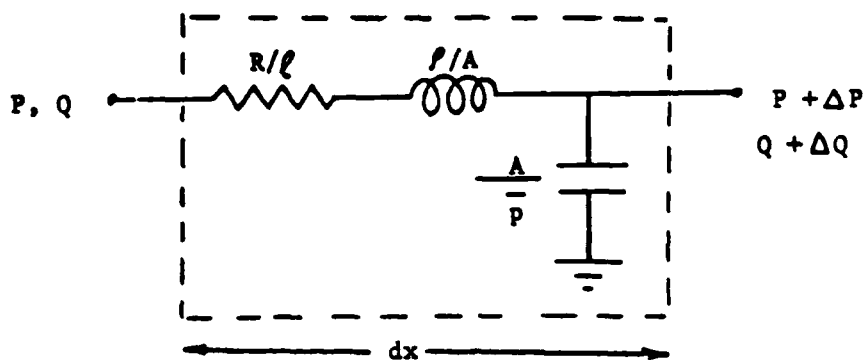
Figure 13.   Equivalent circuit for an infinitesimal section
of a duct.

The question now arises, "What equivalent circuit does one use
for a single-lump model of a duct?" Most workers in fluidics have
opted for the "ell" RLC of figure 13.   Iseman[28], Beisterling[27],
Kirshner[17], Foster et al[26] all tacitly assume this form.   Blackburn
et al[31], however, assume a different form for hydraulic lines.   They
arbitrarily chose a "tee" as in figure 14 and do not offer any reasons.
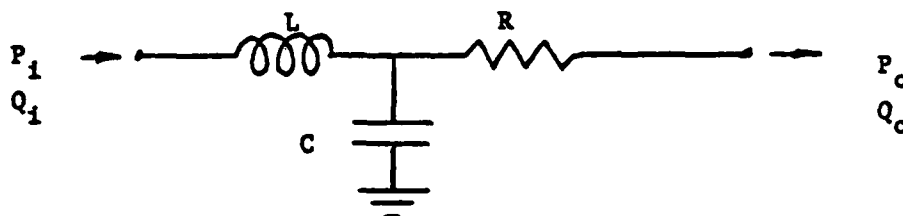
Figure 14.   Lumped parameter representation of a hydraulic
transmission line after Blackburn et al.[31]

Drzewiecki[32] found that lines used as loads on fluidic elements
were best modeled by a "tee" also but with the resistance first
as in figure 15.
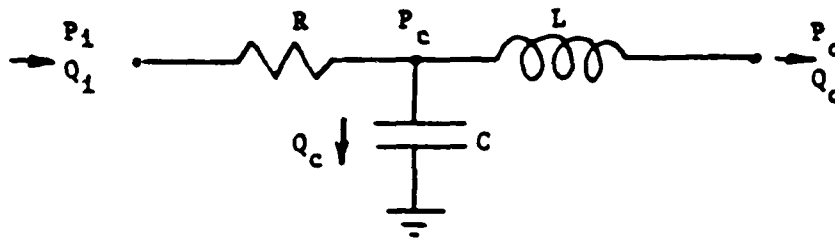
Figure 15.   Lumped parameter representation of a fluidic line
after Drzewiecki.[32]

The basic argument for placing the capacitance (due to fluid
compressibility) in the middle was that the average amount of com-
pression is due to an average pressure which is better represented
by the node pressure in the middle rather than at either end.   Ac-
tually, a more satisfying model would be one that is symmetric about
the capacitance as in figure 16.
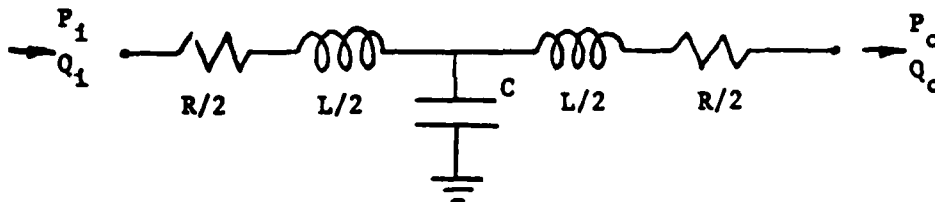
Figure 16.   Symmetric equivalent circuit model of a duct.

The disadvantage is, of course, the increased complexity.   Con-
sider now the governing equations for the duct as a whole single
lump.   Equations (15) and (16) become

$$P_1 - P_2 = (R + \frac{\rho \ell}{A} \ s) \ Q \qquad\qquad (24)$$

26

and

$$Q_1 - Q_2 = \frac{A\ell}{\rho} s\, P \tag{25}$$

Now the equivalent circuit of figure 11 no longer holds for the second order. Terms cannot be neglected in writing the flow through the shunt. Consider, however, the "tee" circuit of figure 15 as a single normal circuit. The pressure drop is

$$\Delta P = P_o - P_1 = -RQ_1 - LsQ_o$$

$$Q_o = Q_1 - Q_c = Q_1 - \frac{P_c}{Z_c}$$

where $Z_c = \frac{1}{Cs}$

so that

$$\Delta P = -R\, Q_1 - Ls\left(Q_1 - P_c/Z_c \right)$$

$$\Delta P = -(R + Ls)\, Q_1 - \omega^2 LCP_c$$

where $j\omega = s$, ω is the circular frequency and $j = \sqrt{-1}$. When

$$\frac{P_c \omega^2 LC}{(R + Ls)Q_1} \ll 1,$$ then the pressure drop is

$$-\Delta P = (R + Ls)\, Q_1 \tag{26}$$

Similarly the flow drop ΔQ is

$$\Delta Q = Q_o - Q_1 = -Q_c = -CsP_c$$

so that

$$\Delta Q = \frac{P_c - P_o}{Ls} - \frac{P_1 - P_c}{R} \text{ and eliminating } P_c,$$

$$\Delta Q = -(Z_c \Delta Q + P_o)/Ls - (P_1 + Z_c \Delta Q)/R$$

or

$$-\Delta Q = P_o/(Ls + 1/Cs + L/CR) + P_1/(R + R/(LCs^2) + 1/Cs)$$

27

when R is sufficiently small this reduces to

$$Q_i - Q_o = C \, s P_i \tag{27}$$

Now we compare equations (26) and (27) to (24) and (25) and find that they are identical when the inductance (called by Blackburn et al[31] and others in fluidics inertance, due to inertia forces),

$$L \equiv \rho \ell / A \tag{28}$$

and the capacitance is

$$C \equiv \frac{A\ell}{\bar{P}} \tag{29}$$

The resistance R is already understood.

The restrictions on frequency and resistance are that they be small. The frequency limitations can be estimated by requiring that

$$\omega^2 LC = 0.1$$

The following typical values

$L = \rho \ell / A$ and $C = \ell \, A / \bar{P}$

$\rho = 1.2059 \ kg/m^3$ (density of air at STP)

$\ell = 0.005 \ m$

$\bar{P} = 1.01 \times 10^5 \ Pa$ (atmospheric pressure)

yield $\quad \omega = \dfrac{0.1}{\sqrt{LC}} = \dfrac{0.1}{\sqrt{\rho \ell^2}/\rho} = 5800 \ rad/s$

or $\quad f = 924 \ Hz$

Therefore, the equivalent circuit of figure 15 will be valid for frequencies roughly below 1 kHz for the dimensions given as typical of moderate size LPA. This is not to say that the LPA will not

28

operate at higher frequencies, but that accurate modelling beyond 1 kHz may require a more complex equivalent circuit.

The equivalent circuit of figure 15 is therefore chosen to describe the input and output channels of the LPA shown in figure 10.

The supply nozzle is described merely as a nozzle since no dynamics are associated with it. It merely supplies a constant flow of fluid. This is true as long as the dc level at the nozzle exit is constant in time. This requires the assumption of push-pull signals at either side of the jet or essentially infinite common mode rejection. The nozzle is treated as an ideal orifice with a discharge coefficient. Drzewiecki[33,34] has solved the general problem of flow through a planar nozzle by solution of the modified Karman-Pohlhausen integral equation that describes the displacement thickness boundary layer growth. He has found that for most smoothly converging nozzles there exists a single function that describes the discharge coefficient c_d. This implicit function is given in equation (30). Figure 17 is a plot of this equation taken from reference (33) showing numerous experimental data verifying its universatility.

$$c_d \, N_R{}' = 2.667 \, (e^{6.6c_d{}^2} - 1) \tag{30}$$

The flow through a space defined by an edge and a jet barrier as is seen in figure 9 and through which the streamlines in that photograph pass, is described as that through an ideal orifice of unity discharge coefficient if the flow is in the direction of the jet stream. If, on the other hand, the flow is from the vents to the controls, the discharge coefficient is chosen to be, quite arbitrarily, one half. The present analysis does not consider the latter case but to justify the choice of unity c_d one can look at figure 18 where an artist's rendition of the velocity profile demonstrates the argument that reduction in flow due to wall shear

29
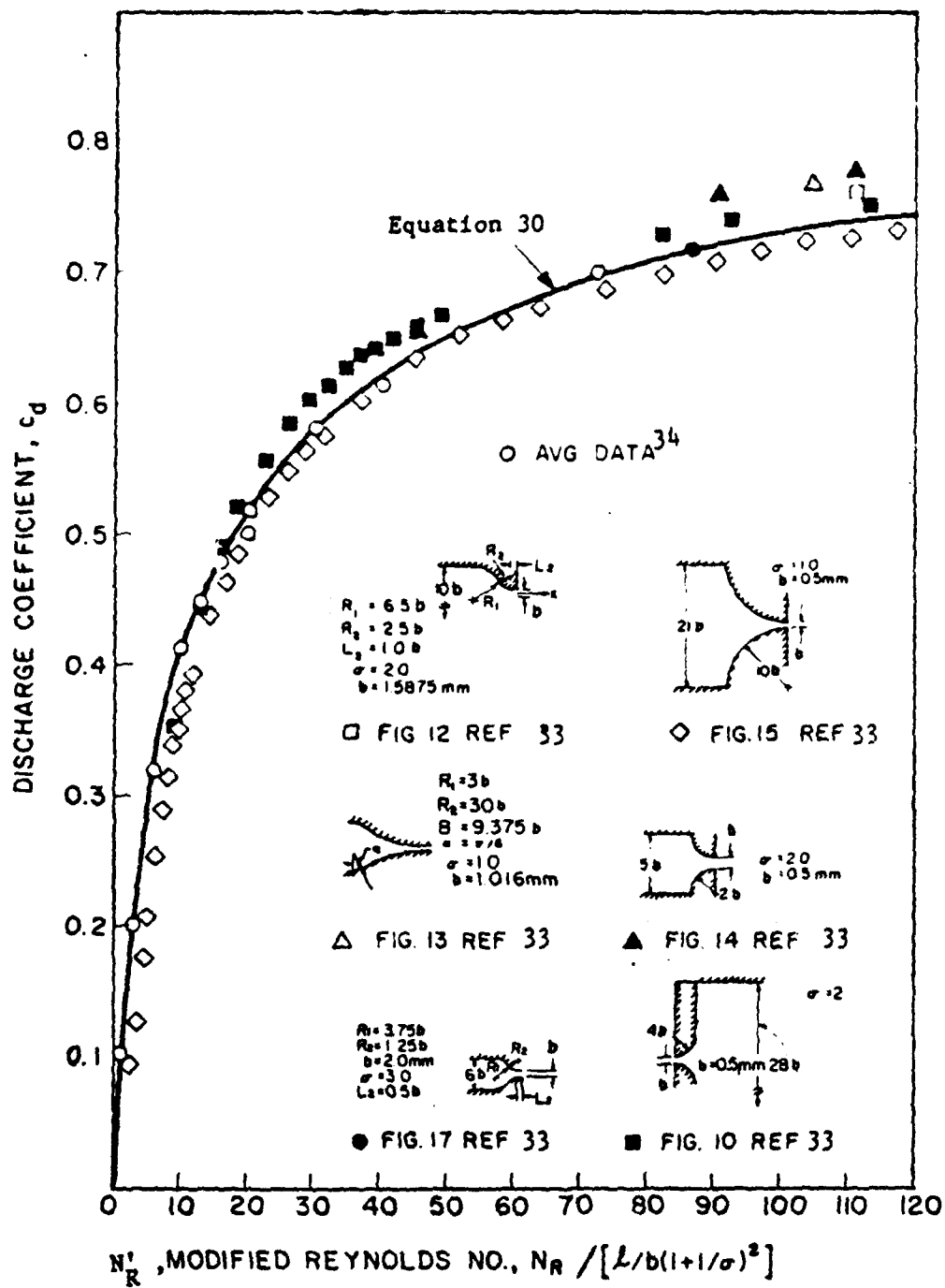
Figure 17. Comparison of theory and data for discharge coefficient
for nozzles of widely varying planview and low
Reynolds number.

Is offset by flow Increase by viscous drag In the vicinity of the
jet.
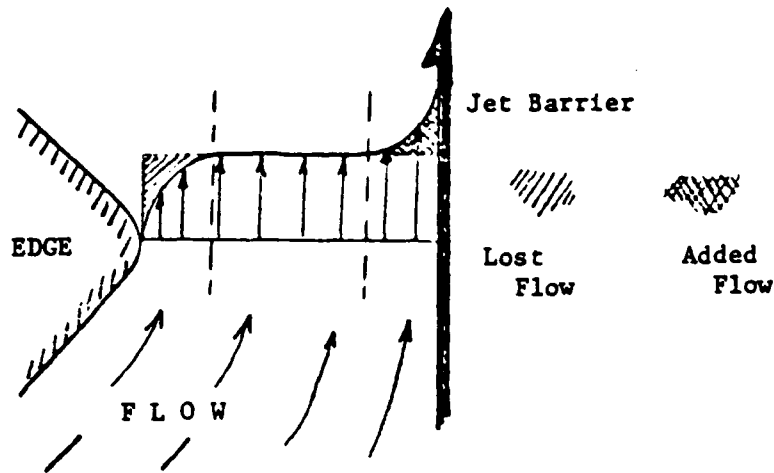
Figure 18. Flow past an edge by a jet barrier.

While no actual solution of the flow field or comparison with
velocity data has been made, this assumption appears to be valid
In that It gives good agreement with actually measured LPA input
resistances[6]. The volume of the orifice Is exceedingly small, hence,
there Is no capacitance but there are Inertia effects requiring an
Inertance (Inductance) term as previously derived. Rschevkin[16]
describes In detail the Inductive properties of orifices and In
table 6 pp 238-244 lists the common equivalent circuits for acoustic
components. The Inertance, however, Is defined In equation 28.

One comment has to be made. The channels of an LPA are hardly
ever of constant cross-section viz. figure 10. However, typically
the flow rate Is very small, hence, the Reynolds numbers are small
especially In the Inputs. Here the flows are of the order of 5% of
the jet flow through areas 3-5 times the nozzle area. For typical
nozzle Reynolds numbers of 1000 this means the channel Reynolds
numbers are about 10. Viscous effects predominate over the accelera-
tion terms and the width averaged over the length may be used with
no ill effects.[6]

Lastly, the flow of the jet from the nozzle between parallel plates to the splitter is observed to be a steady dc axial flow since there is no axial forcing. There are viscous losses as described by Manion and Drzewiecki[4] and by Drzewiecki[35]. There is a lateral time dependent motion but for the time being, this is assumed, as others have done, not to be impeded by either inertial or viscous forces. The major frequency dependent contribution of the jet stream is the time delay which occurs at one half the jet average velocity. A signal at the nozzle exit forms a signal eddy that has a centroid that travels like a wheel at about one-half the outer velocity which is typically the average jet velocity. This is depicted pictorially in figure 19.
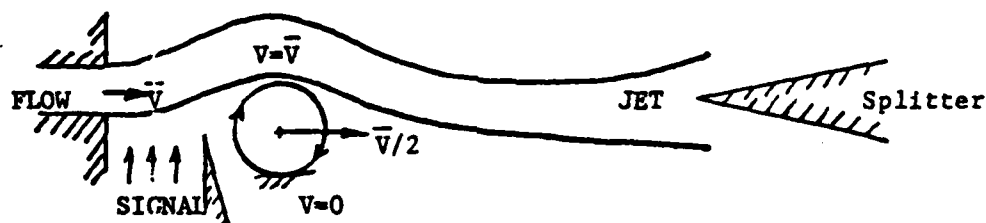
Figure 19. Signal convection along a jet.

This then completes the review and analysis of the through flows to be encountered in analysing an LPA.

2.1.2. Amplifier Input Analysis

Now that the basic flow parameters have been identified, consider the control-volume modeling for the input impedance dynamics of an LPA. A pressure is imposed on an input causing flow to enter the LPA and deflect the jet. A control volume is drawn in the vicinity of the jet edge in order to determine the pressure therein and, hence, the amount of jet deflection. Figure 20 shows such a control volume.
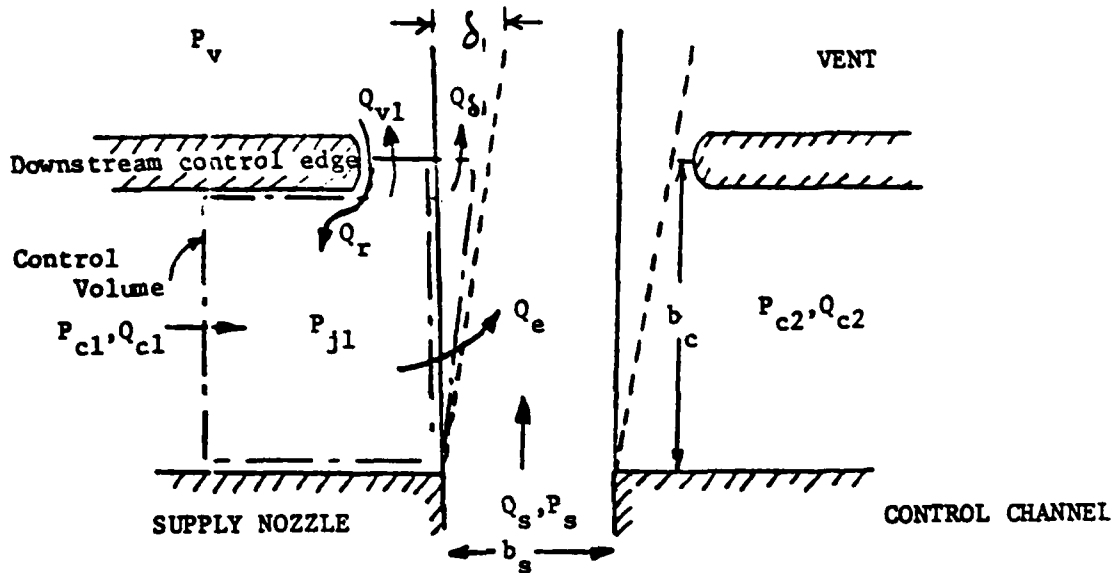
Figure 20. Control volume for jet edge pressure.

The terms in the figure are defined below.

Q_c - control flow

Q_v - flow to vent

Q_r - flow returned to control volume due to spillage

Q_e - entrained flow

Q_δ - flow through deflected space

Q_s - supply jet flow

b_d - control width

b_s - supply width

33

δ -   deflected space width at downstream control edge

P_c -   input or control pressure

P_s -   supply pressure

P_j -   jet edge pressure

P_v -   pressure in vent downstream of control

1,2   -   side 1 or side 2, respectively

Following the established procedure for determining the input impedance (see for example Manion and Drzewiecki[4]) one now writes the continuity equation for the control volume.

$$Q_{c1} - Q_e - Q_{v1} - Q_{\delta 1} + Q_{r1} = \frac{d \ (\text{Volume})}{dt} \qquad (31)$$

Now using the chain rule

$$\frac{d \ (\text{Volume})}{dt} = \frac{d \ (\text{Volume})}{dp} \frac{dP}{dt} \qquad (32)$$

The change in volume with pressure is called the compliance and is a capacitive term. This term has been modelled in several ways. Kirshner and Katz examine it from both a jet barrier approach and a jet dynamic approach, the latter reducing to the jet barrier solution at frequencies encountered in fluidics. The jet barrier capacitance is the change of volume due to jet deflection relative to the change in pressure required to cause the deflection. Consider a fluid slug issuing from a nozzle as in figure 21 at the average jet exit velocity $\bar{u}$.

Depth is h
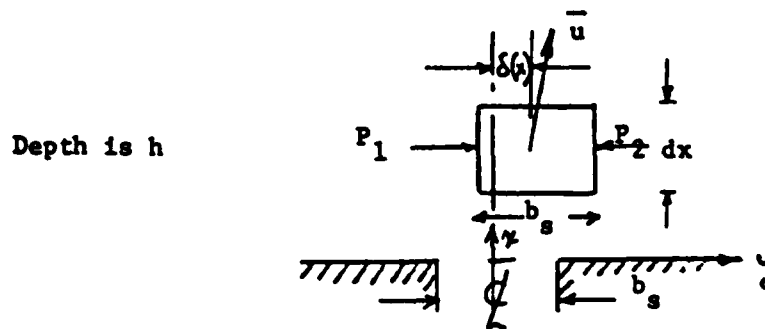
Figure 21. Slug of fluid under the action of a uniform pressure difference.

Newton's Second Law requires that the lateral displacement of this slug
be such that the sum of the lateral forces equal that mass times the
acceleration

$$\Sigma F_y = m\ddot{y} = P_1 \, dx \, h - P_2 \, dx \, h$$

or

$$\ddot{y} = (P_1 - P_2) \, dx \, h \, / \, (\rho dx \, h \, b_s)$$

so that

$$\ddot{y} = (P_1 - P_2)/ \rho b_s$$

$$(33)$$

with zero initial conditions. Under a constant pressure difference
the displacement as a function of time is then

$$y(t) = (P_1 - P_2) \, t^2 \, / \, (2b_s \rho)$$

The displacement as a function of downstream distance is determined
by the time it takes to travel the distance x, t_x,

$$t_x = x/ \, \bar{u}$$

where $\bar{u}$ is the x-velocity at which the particle is traveling assuming
small deflections. Hence

$$y(x) = (P_1 - P_2) \, x^2/(2 \, b_s \, \rho \bar{u}^2)$$

$$(34)$$

Now notice that this is in effect an interaction of the pressure with
the jet momentum flux $\rho \, A\bar{u}^2.$ This may be written in terms of the jet
supply pressure in that

$$\rho \bar{u}^2 = 2c_\theta P_s$$ $$(35)$$

where c_θ is the momentum flux discharge coefficient or the ratio of actual flux to ideal flux. This term has been developed for nozzles by Manion and Drzewiecki[4] and related to the discharge coefficient c_d where

$$c_\theta = 1.32 \, c_d^2$$

When equation (35) is substituted into (34), one gets

$$y(x) = \frac{P_1 - P_2}{4 b_s c_\theta P_s} x^2 \tag{36}$$

The volume per unit depth swept out by this deflection over the control width can be calculated from the integral of equation (36):

$$\Delta(\text{VoL}) = h \int_0^{b_c} y(x) \, dx = \frac{b_c^3 \, h \, (p_1 - p_2)}{12 \, c_\theta P_s} \tag{37}$$

One may therefore define the jet capacitance as

$$\frac{\Delta(\text{VoL})}{\Delta P} \equiv C_j = \frac{b_c^3 \, h}{12 c_\theta P_s} \tag{38}$$

Now if one considers only push-pull signals so that the increase in pressure on one side is equal to the decrease on the other, then $\Delta P_{j1} = 0.5 \, \Delta P$ and equation (38) for the capacitance may be written for the change in pressure on one side as

$$C_{j1} \equiv \Delta(\text{Vol})/\Delta P_{j1} = b_c^3 \, h/6 \, c_\theta P_s \tag{39}$$

This forms the basis for a complex impedance $Z_j = 1/C_{j1}s$ of the jet. In a more detailed jet impedance analysis, Kirshner and Katz[17] have found that this impedance has a dissipative component due to particles being swept out of the control volume. This term is $R_j/R_s = 6 c_d^2/B_c^2$, so that $Z_j = R_j + 1/C_{j1}s$. Now take the Laplace transform of the continuity equation (31)

$$Q_{c1}(s) - Q_e(s) - Q_v(s) - Q_{\delta 1}(s) + Q_{r1}(s) = \frac{P_{j1}(s)}{Z_j} \tag{40}$$

and

$$Q_{c1} = (P_{c1} - P_{j1})/Z_{c1} \tag{41a}$$

$$Q_{v1} = (P_{j1} - P_v)/Z_v \tag{41b}$$

$$Q_{\delta 1} = (P_{j1} - P_v)/Z_{\delta 1} \tag{41c}$$

so that

$$\frac{P_{c1} - P_{j1}}{Z_{c1}} - \frac{(P_{j1} - P_v)}{Z_v} - \frac{(P_{j1} - P_v)}{Z_{\delta 1}} - (Q_e - Q_{r1}) = P_{j1}/Z_j \tag{42}$$

where the channel impedance is characterized by the equivalent circuits as before in 2.1.1. The resistive part of the impedance to vent Z_v has been shown[4] to be a constant. The inductance is due to the slug inertia. The impedance $Z_{\delta 1}$, is merely the resistance of an orifice of width δ and an inertia of a slug of the same width, hence, the d.c. flow is defined by

$$Q_{\delta 1} = \delta_1 h \sqrt{2(P_{j1} - P_v)/\rho} \tag{43}$$

so that the resistance is

$$R_{\delta 1} = \frac{P_{j1} - P_v}{Q_{\delta 1}} = \frac{\sqrt{\rho(P_{j1} - P_v)/2}}{\delta_1 h} \tag{44}$$

and the complex impedance is

$$Z_{\delta 1} = R_{\delta 1} + \frac{x_{\delta 1}}{\delta_1 h} \rho s \qquad (45)$$

where from equation (28) the inductance in its general form $\rho L/A$ is here $\rho x_{\delta 1}/\delta_1 h$. The length is $x_{\delta 1}$. It is somewhat difficult to assign a value to this dimension since the gap, δ_1, is bounded on one side by a curved wall of small radius. I have chosen twice this radius as $x_{\delta 1}$. Now let the jet impedance be as before

$$Z_j = \frac{1}{C_{j1} s} + R_j \qquad (46)$$

so that equation (42) becomes

$$\frac{P_{c1} - P_{j1}}{Z_c} - P_{j1} \left(\frac{1}{Z_v} + \frac{1}{Z_{\delta 1}} + \frac{1}{Z_j}\right) = Q_e - Q_{r1} \qquad (47)$$

Now one notes that we are looking for an expression for the small signal input impedance while the jet is deflected through an additional deflection, δ,

$$Z_1 = \frac{dP_c}{dQ_c}$$

which by the chain rule is

$$Z_1 = \frac{dP_c}{d\delta} \frac{d\delta}{dQ_c}$$

Therefore, differentiate equation (47) with respect to δ, a small deflection of the jet relative to the deflected position δ_1. Equation (47) thus becomes, when P_v is assumed to be zero,

38

$$(\partial P_{c1}/\partial\delta \; - \; \partial P_{j1}/\partial\delta)/Z_c \; - \; (1/Z_v + 1/Z_{\delta 1} + 1/Z_j) \; \partial P_{j1}/\partial\delta$$

$$- \; P_{j1} \; [h(1/(\rho P_{j1}/2)^{1/2} + \rho x_\delta s)] \; - \; \delta_1 h \; \{[0.5(\rho P_{j1}/2)^{1/2} + x_{\delta 1}\rho s]/$$

$$[(\rho P_{j1}/2)^{1/2} + x_{\delta 1}\rho s]^2\} \; (\partial P_{j1}/\partial\delta) = \partial(Q_e - Q_{r1})/\partial\delta \qquad (48)$$

Now recall the jet deflection from equation (36) and note the assumption of push-pull pressure where $P_{j1} = 0.5 \; P_j$ then with $x = b_c$ and $y(x) = \delta$

$$\frac{\partial P_{j1}}{\partial\delta} = 2 \; c_\theta b_s P_s/b_c^{\;2} \qquad (49)$$

Substituting equation (49) into (48) and solving for $\frac{\partial P_{c1}}{\partial\delta}$ for the symmetrical case, $\delta_1 = 0$, yields.

$$\partial P_{c1}/\partial\delta = (2c_\theta b_s P_s/b_c^2)(1 + \; Z_c(1/Z_v + 1/Z_j)) +$$
$$Z_c P_{j1} h/((\rho P_{j1}/2)^{1/2} + \rho x_{\delta 1} s) +$$
$$Z_c \; \partial(Q_e - Q_{r1})/ \; \partial\delta \qquad (50)$$

Drzewiecki[6] has determined the term

$$(2 \; b_s/Q_s) \; \; \partial(Q_e - Q_{r1})/\partial\delta$$

as the net entrainment coefficient a_1, which is a constant for a given geometry and flow condition. This term is computed by the program given in Appendix 1. No reactive component is ascribed to this term. Experimental evidence of this is shown later. If now equation (50) is normalized by P_s and b_s and $R_s = P_s/Q_s$, so that capitalized dimensions are normalized, e.g. $B_c = b_c/b_s$, $X = x /b_s$ etc., then

$$\partial(P_{c1}/P_s)/\partial(\delta/b_s) = (2c_\theta \; B_c^2)(\; 1 + Z_c(1/Z_v + 1/Z_j)) +$$
$$(Z_c Q_s/P_s)(hb_s P_{j1}/((\rho P_{j1}/2)^{1/2} + \rho x_\delta s)Q_s + a_1/2)$$

39

and

$$\partial\,(P_{c1}/P_s)/\partial(\delta/b_s) = (2c_\theta/B_c^2)(\ 1 + (Z_c/R_s)(R_s/Z_v + R_s/Z_j)) +$$

$$(Z_c/R_s)(\ (P_{j1}/P_s)/(2c_d((P_{j1}/P_s)^{1/2}/2 + j\Omega X_\delta c_d) + a_1/2))$$

(51)

where Ω – normalized radian frequency $= \omega b_s/c_d\ (\dfrac{2P_s}{\rho})^{1/2}$ and c_d is defined by equation (30). Now define a normalized pseudo-impedance

$$Z_k = (c_d\ \sqrt{(P_{j1} - P_v)/P_s}\ + 2\ c_d^{\,2}\ X_\delta \Omega j)/(P_{j1}/P_s) \qquad (52)$$

and note that it is of the form

$$Z_k = R_k + j\,L_k\,\Omega \qquad (53)$$

where R_k and L_k are the resistance and inertance, respectively. Simillarly define a pseudo-resistance

$$R_d/R_s = 2/a_1 \qquad (54)$$

Equation (51) becomes

$$\frac{\partial(P_{c1}/P_s)}{\partial(\delta/b_s)} = \frac{2c_\theta}{B_c^{\,2}}\ [1 + \frac{Z_c}{R_s}\ (\frac{R_s}{Z_v} + \frac{R_s}{Z_j})] + \frac{Z_c}{R_s}\ [\ \frac{R_s}{Z_k} + \frac{R_s}{R_d}] \qquad (55)$$

Notice that normalization of any impedance by $R_s = P_s/Q_s$ results in a normalized time or frequency term as shown below.

$$Z/R_s = R/R_s + j\omega\ L/R_s = R/R_s + j\omega\rho x\ /(bhR_s)$$

where x and b are the length and breadth of some channel.

Now

$$R_s = P_s/Q_s = P_s/(c_d b_s h \ \sqrt{2P_s/\rho}) = \sqrt{\rho P_s/2}/(c_d b_s h)$$

Therefore

$$Z/R_s = R/R_s + J\omega\rho x c_d b_s h/(bh \ \sqrt{\rho P_s/2})$$

The reactive term alone is

$$J\omega\rho x c_d b_s/(b \ \sqrt{\rho P_s/2}) = J\omega \ \sqrt{\rho} x c_d/B \ \sqrt{P_s/2}$$

where $\qquad B = b/b_s$

but $\tau = b_s/(c_d(2P_s/\rho)^{1/2})$ is the transport time for one nozzle width

so that $\omega\tau$ is the radian frequency per transport time, or Ω. The reactive term thus becomes

$$\frac{J\omega \ \sqrt{\rho} x c_d}{B \ \sqrt{P_s/2}} \quad \frac{b_s c_d \ \sqrt{2P_s/\rho}}{b_s c_d \ \sqrt{2P_s/\rho}} = J\Omega 2 X c_d^2/B \qquad (56)$$

so that inertance is $2 \ X \ c_d^2/B$ in the normalized frequency domain.

Now recall that one must obtain $\partial Q_c/\partial\delta$ to complete the derivation of the input impedance. Consider, therefore, again equation (40) in its Laplace transformed state and differentiate it with respect to the deflection.

$$Q_{c1} - Q_v - Q_\delta + Q_{r1} - Q_e = P_{j1}/Z_j$$

$$\frac{\partial Q_{c1}}{\partial\delta} - \frac{\partial Q_v}{\partial\delta} - \frac{\partial Q_\delta}{\partial\delta} - \frac{\partial}{\partial\delta}(Q_e - Q_{r1}) = \frac{1}{Z_j} \ \frac{\partial P_{j1}}{\partial\delta} \qquad (57)$$

and solving for $\partial Q_{cl}/\partial\delta$ and substituting for Q_v and Q_δ yields

$$\frac{\partial Q_{cl}}{\partial\delta} = \frac{1}{Z_v}\frac{\partial P_{j1}}{\partial\delta} + \frac{\partial}{\partial\delta}\left(\frac{P_{j1}-P_v}{Z_\delta}\right) + \frac{1}{Z_j}\frac{\partial P_{j1}}{\partial\delta} + \frac{\partial(Q_e - Q_{rl})}{\partial\delta}$$

and remembering that $\partial P_{j1}/\partial\delta$ is defined by the jet deflection equation (49), performing the differentiation on the deflected impedance of equation (45) as before and normalizing results in

$$\frac{\partial(Q_{cl}/Q_s)}{\partial(\delta/b_s)} = \frac{2c_\theta}{B_c^2}\left(\frac{R_s}{Z_v} + \frac{R_s}{Z_j}\right) + \left(\frac{R_s}{R_d} + \frac{R_s}{Z_k}\right) \tag{58}$$

When this result is divided into equation (55), the complex input deflection impedance is obtained

$$\frac{\partial(P_{cl}/P_s)}{\partial(Q_{cl}/Q_s)} = \frac{Z_c}{R_s} + \cfrac{1}{\frac{R_s}{Z_v} + \frac{R_s}{Z_j} + \frac{B_c^2}{2c_\theta}\left(\frac{R_s}{Z_k} + \frac{R_s}{R_d}\right)} \tag{59}$$

Now let all normalized terms appear without their normalizing parameter. In other words, all quantities of pressure, flow, impedance and dimensions appear now as normalized quantities (e.g. $b/b_s \to B$, $P/P_s \to P$, $Q/Q_s \to Q$, $Z/R_s \to Z$, etc.). In addition, define two new pseudo-impedances

$$R_D = \frac{2c_\theta}{B_c^2} R_d \text{ and } Z_K = \frac{2c_\theta}{B_c^2} Z_k \tag{60}$$

and remember that symmetry has been assumed where $P_{cl} = \Delta P_c/2$, etc., then equation (59) becomes

$$Z_I = \partial(\Delta P_c)/\partial(\Delta Q_c) = Z_c + 1/(1/Z_v + 1/Z_j + 1/Z_K + 1/R_D) \qquad (61)$$

When the control channel is assumed to have a capacitance due to compressibility in a shunt to ground as previously discussed, equation (61) becomes

$$Z_I = R_c + 1/(\frac{1}{Z_A + Z_L} + \frac{1}{Z_P}) \qquad (61a)$$

where $1/Z_A = 1/Z_v + 1/Z_j + 1/Z_K + 1/R_D$, $Z_L = L_c s$ and $Z_P = 1/C_c s$

Equation (61a) is the input impedance of an LPA or that impedance seen by a differential input signal. Consider now the equivalent circuit between the input, the jet edge and ground (the vent pressure) that this circuit describes. It is a series combination of a channel impedance with a lumped parallel combination of the vent, deflection, bias effect $(\alpha \bar{P}_j)$ and jet compliance impedances. This is shown in figure 22. Note that the node pressure is the jet edge pressure since the pressure drop across the channel is defined as the drop from the input to the jet edge pressure.
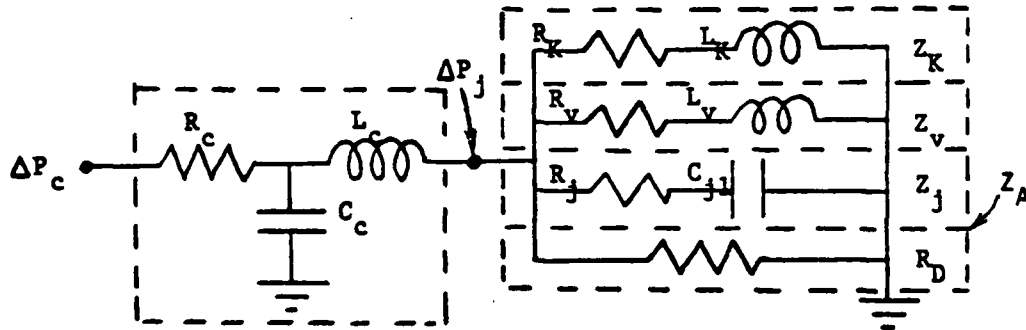
Figure 22. Equivalent circuit of LPA input impedance.

The normalized quantities are defined by the following equations:

$$R_c = 24 X_c c_d (\sigma/\bar{B}_c + \bar{B}_c/\sigma + K)/(\bar{B}_c^2 \, \mathsf{J} N_R) + 0.95 \, c_d^2 \, Q_c/B_{cmin}^2 \tag{62a}$$

$$L_c = 2 \, c_d^2 \, X_c/\bar{B}_c \tag{62b}$$

$$C_c = \bar{a}_c X_c \, (P_s/P_\infty) \quad (P_\infty - \text{absolute ambient pressure}) \tag{62c}$$

where $P_s/P_\infty = (N_R'/120)^2 \, (1/\sigma^2) \, (1/b_s^2) \, 760$ with b_s in mm.

$$R_D = 4 \, c_\theta/(a_1 B_c^2) \tag{62d}$$

$$c_{j1} = B_c^3/6 \, c_\theta \tag{62e}$$

$$R_K = 2 \, c_\theta c_d/(B_c^2 \sqrt{(P_{j1} - P_v)}) \tag{62f}$$

$$L_K = 4 \, c_\theta c_d^2 \, X_\delta/(B_c^2 (P_{j1} - P_v)) \tag{62g}$$

$$L_V = 2 \, c_d^2 \, X_\delta/B_j \tag{62h}$$

$$R_j = 6 \, c_d^2/B_c^2 \tag{62i}$$

where
$\bar{B}_c$ - average channel width
σ - aspect ratio
K - empirical constant $0.35 \leq K \leq 0.5$
B_{cmin} - minimum channel width
X_c - channel length
X_δ - length of jet-edge space
B_j - width of jet-edge space $= (B_t - 1)/2$
B_t - distance between downstream control edges.

B_c - control width

N_R - Reynolds number - $(b_s/\nu) \sqrt{2 P_s/\rho}$

are all constant for a given LPA and operating point.

The vent resistance, R_V, has been determined as a function of average bias pressure by Manion and Drzewiecki[4]. The value must be calculated for each geometry and is in general proportional to the jet edge gap size but depends also on how far downstream from the nozzle it is because it depends on the jet spreading. Hence, it is also dependent on control width. A typical value for $R_V = 3.0$ when $B_c = 1$, $B_t = 1.25$.

It is interesting to compare this model, that has been essentially derived from first principles, to those used by others for the inputs of fluidic amplifiers. Figure 23 shows three such circuits.
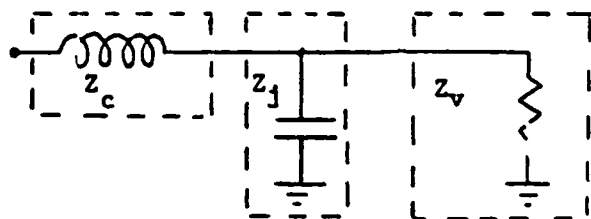
(a) Amplifier input due to Beisterling[27]
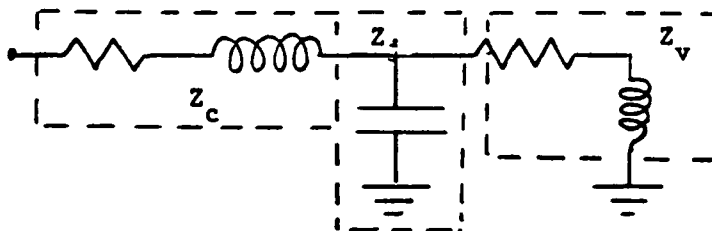
(b) LPA input due to Manion and Mon[3]
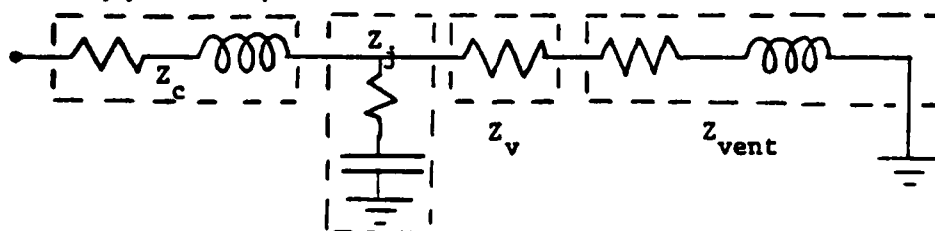
(c) LPA input due to Kirshner and Katz[17]

Figure 23. Various equivalent circuits used for amplifier inputs.

Beisterling[27] considers the input as a simple second-order R-L-C as in 23a. Manion and Mon[3] are much closer, as in figure 23b, to the complete equations in that they consider a second inertive term. It is not clear, however, how they derived their added inductance. In Kirshner's[17] work, see figure 23(c), the jet edge inductance is neglected; however, a vent impedance is assumed which gives rise to additional terms. Kirshner also derives an energy loss term in the form of a resistance in series with the jet compliance and explains its function as representing the energy lost from the control volume due to particles being swept out by the jet. In each case the capacitance of the control channel is neglected. This is not always a valid assumption. Equations (62c) and (62e) define the two capacitances in the model. Consider an LPA of $\sigma = 0.25$, $X_c = 10$, $B_c = 2.75$, $B_c = 1.50$, $P_s = 64$ mmHg, $P_\infty = 760$ mmHg and $b_s = 0.5$ mm. This yields capacitances of

$$C_c = 2.3 \quad C_j = 0.879$$

which indicates that for low aspect ratio, fairly high pressure, LPA operation, the channel capacitance is predominant and may not be neglected.

The assumptions used in the foregoing analysis should be recapitulated and the inferred ones stated for clarity.

1. Laminar flow, $(c_d N_R/(1 + 1/\sigma)^2 \leq 180)$
2. Small amplitude signals (so that derivatives are good approximations).
3. Small compressibility effects - fluid is essentially incompressible thus reducing the problem to one of acoustics.
4. Dimensions small compared to wavelengths--implies constant pressures in control volumes and low frequencies.
5. Two-dimensional laminar jet net entrainment characteristics but not necessarily velocity distributions.
6. The pressure downstream of the control jet edge region is constant and ambient.
7. The mean pressure level at the jet edge $(P_{j1} + P_{j2})/2 =$ constant-push-pull signals.
8. Geometrical symmetry about the LPA centerline.

The last assumption allows the solution of the governing equations around the the point of zero jet deflection. For static cases, the problem of non-symmetry is examined by Drzewiecki and Manion,[35]. In general, it was found that offsets produce deterioration of gain.

Low frequency increases in gain could possibly be due to a frequency dependence of the mean pressure level. Perhaps if $\bar{P}_j$ were a function of frequency, it would explain the low frequency "hump" in the frequency response as shown for example by Healey[21] in figure 8. The mean value of the jet edge pressure is predominantly a function of the jet entrainment characteristics, hence, if entrainment were to dramatically increase with frequency, then the input impedance could resonate as can be seen from the R_k term which, in itself, depends on $\bar{P}_j$. Experiments by Roffman and Toda[14] and Hoglund and Simcox[36], the results of which are shown in figures 24 and 25, indicate that spreading significantly affects entrainment. Sato[13] indicates also that sound may affect laminar jet spreading. Shields and Karamcheti[37] present instantaneous

Pressure profiles measured with various frequency sound signals

MEASURED AT 18 w
DOWNSTREAM
$P_j = 1$ KN/m^2 = 0.145 psi

- NO SIGNAL
- 1.5 KHz
- 4.81 KHz

LATERAL POSITION OF JET NORMALIZED BY NOZZLE WIDTH

PRESSURE NORMALIZED BY MAXIMUM PRESSURE WITH NO SIGNAL
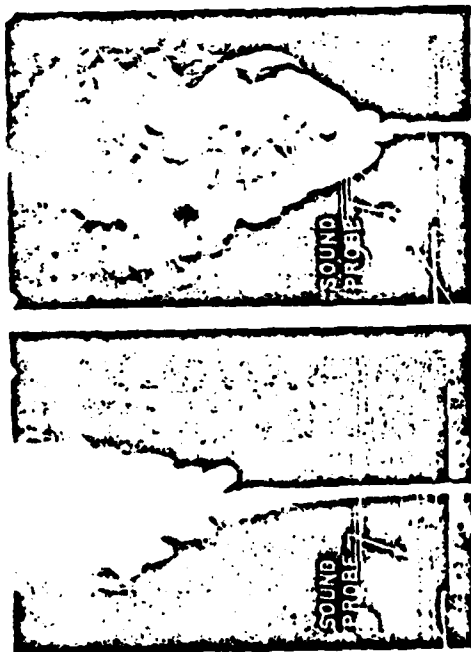
(a) Without sound
(b) With sound

Powerjet pressure is 0.051 cm H_2O, Reynolds number is 307, and excitation frequency applied through polyflow tube is 180 Hz
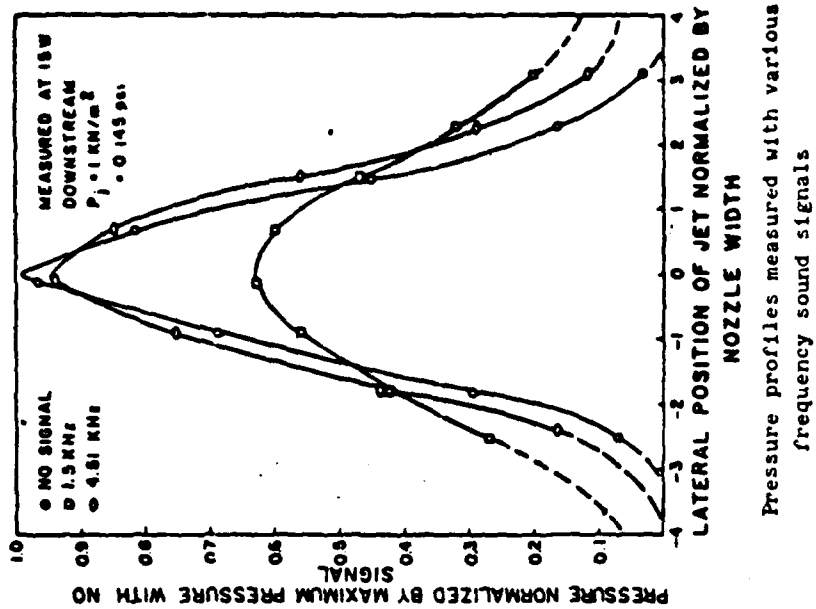
Figure 24. Jet spreading data due to Roffman and Toda[14].
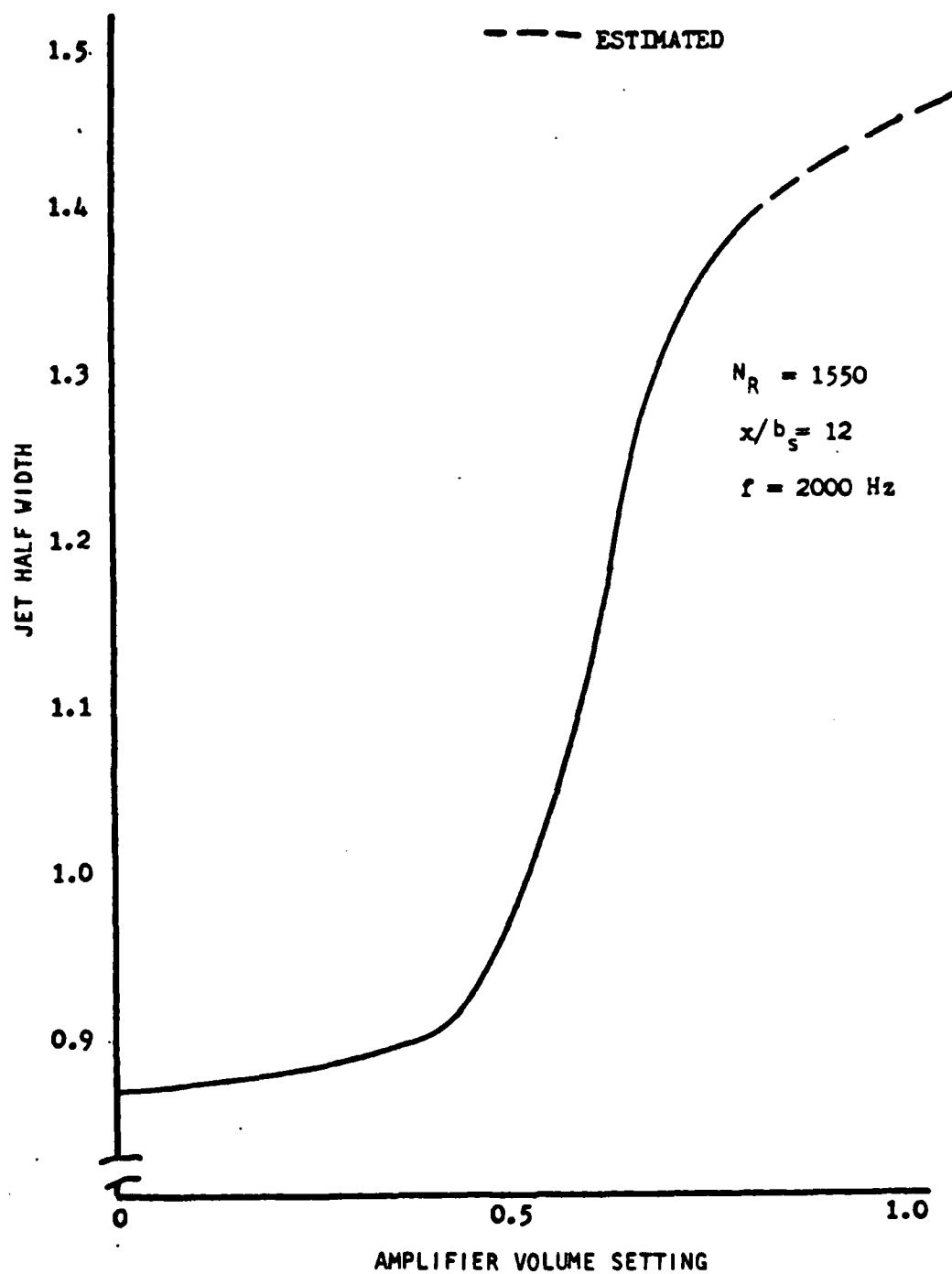
Figure 25. Change in turbulent jet spreading with sound amplitude after Hoglund and Simcox [36].

velocity profile data on a laminar jet in an edgetone oscillation as
shown in figure 26. There is considerable skewing and distortion of the
profiles. Kirshner[17] speculates on this and offers the explanation that
the slower velocity particles at the jet edges are in the force field
longer than the peak velocity particles, hence, they get out of phase.
While this probably leads to phase distortion, it does not appear to
affect the overall entrainment of the jet although there may be some
apparent periodicity of entrainment. This appears as a broadening of
the jet on one side and a narrowing on the other. There is also some
periodic increase in the velocity gradients so that mixing, if it were
a factor could increase. Since the flow is laminar, this does not
seem to be the case. The jet, however, except for some skewing due to
the phase difference of various slower travelling particles, merely
deflects as is assumed in the quasi-steady assumption. For frequencies
below a value determined Stiffler and Shearer,[38] turbulent jets show
no added spreading at all when under the influence of sinusoidal pres-
sures, thus verifying the quasi-steady assumption.[38] The fact that
laminar entrainment is not affected is dramatically proven by experi-
ments that were carried out under the aegis of this program. If the
entrainment changes, then the mean pressure will change. This mean
pressure was measured in three different aspect ratio LPA's as a
function of frequency by a static tap mounted just at the end of the
control passage as shown in figure 27. The frequency was varied to
3 kHz (essentially the whole bandpass of an LPA of nozzle width
b_s = 0.5 mm). The results are shown in figure 28. As can be seen, there
is no deviation from constancy (except for some experimental noise).
This is an important verification of one of the simplifying assump-
tions in the model. From this assumption one also can make the state-
ment that the change of entrainment with deflection is negligible,
hence, the only parameter that may be frequency dependent is the returned
flow. The assumption here, however, is that there is no significant
dynamic contribution of this term.
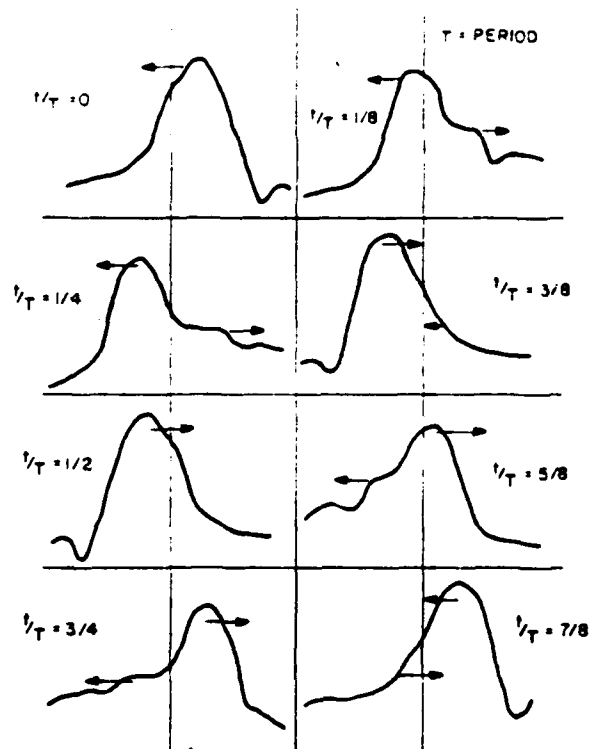
Figure 26. Instantaneous mean jet profiles due to Shields and Karamcheti[37].
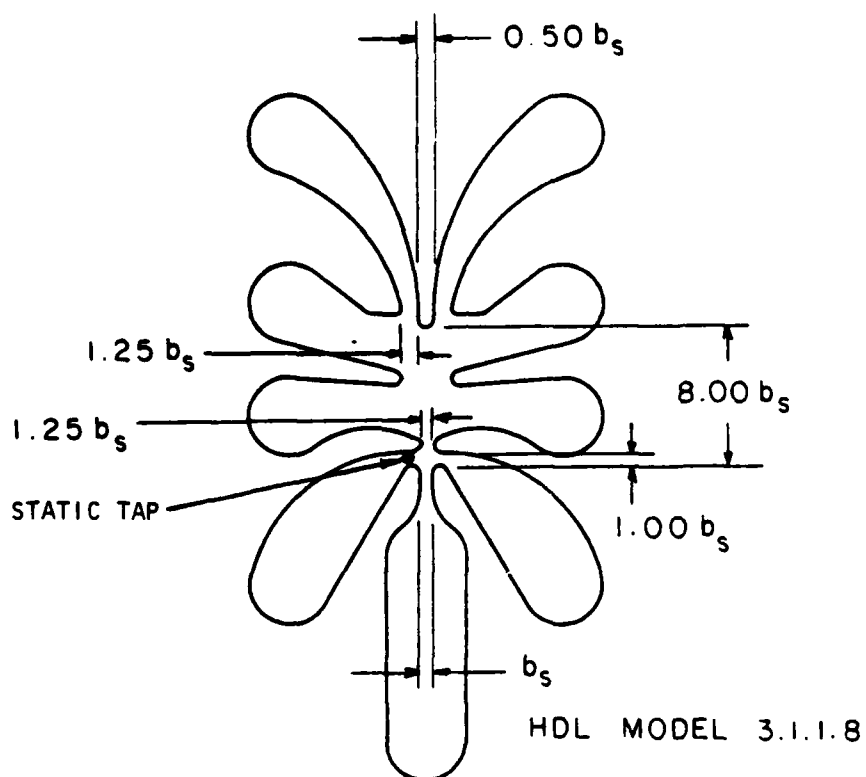
Figure 27. Line drawing of the standard HDL LPA 3.1.1.8 showing the location of a static tap used to measure the mean jet edge pressure.

MEAN JET EDGE PRESSURE, mmHg

σ = 0.5
P$_s$ = 16 mmHg

MEAN DATA AS OBSERVED AT STATIC TAP
WITH BAROCEL WITH 3Hz LOW PASS FILTER

b$_s$ = 0.5 mm
INPUT AMPLITUDE = 80 db

σ = 1.0
P$_s$ = 4 mmHg

σ = 2.0
P$_s$ = 1 mmHg

5

4

3

2

1

0

500   1000   2000   4000

FREQUENCY, hertz
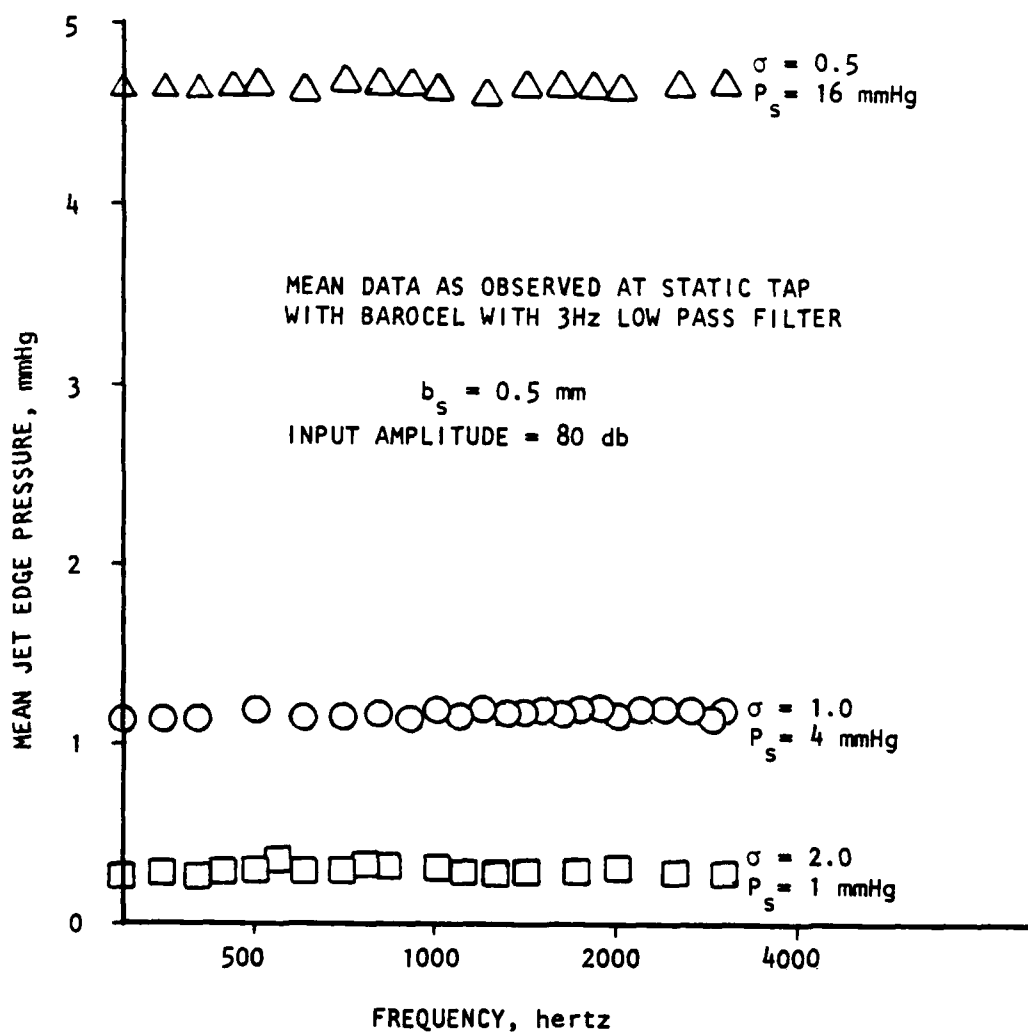
Figure 28. Experimental data for the mean jet edge pressure, $\bar{P}_j$, of an LPA.

This then concludes the analysis of the input of an LPA. What
now remains is to tie this to the complete device.

2.1.3 Modeling of the Complete LPA

Early dynamic tests on high aspect ratio LPA's indicated a region
of multiple resonances. In fact, as the Reynolds number was increased
to just below transition, sustained oscillations would occur attribu-
table only to some form of internal feedback. This coupled with the
insight gained from discussions with J. M. Kirshner, formerly of HDL,
and physical observations on a large scale water tunnel model of an LPA
led to the conclusion that jet dynamic effects and internal acoustic
feedback caused the resonances. In fact, if one considers an oscillating
jet in an LPA geometry, it seems clear that the spillage of flow to one
side or the other must cause a pressure to develop at the sides of the
jet. If this pressure feeds back to the sensitive area of the jet (the
controls) and it arrives in phase or 360° out of phase with the input,
it will augment deflection and give rise to a substantially greater
output due to positive feedback. Figure 29 is a series of photographs
taken during a single cycle of an LPA in oscillation. Figure 29(a)
shows the jet swinging to the left. Figure 29(b) shows the same jet
starting to swing to the right at the control region but still travel-
ling right near the outputs. In figure 29(c), the jet is swinging to
the right over its entire length. What should be observed is the modu-
lation of the flow through the upper vents. Consider, therefore, the
verbal description of the phenomenon. A signal is put in the control,
is attenuated and then deflects the jet. The jet deflection is delayed
by the jet transport time. The deflection reaches the outputs where
some jet flow is spilled to the vents and some is delivered to the out-
puts and hence the load. The flow into the vents causes a pressure to

54

Figure 29 a. Flow visualization photograph of an oscillating jet in an LPA.

(Jet is swinging from right to left.)

55

Figure 29 b. Flow visualization photograph of an oscillating jet in an LPA.

(Jet is swinging from left to right at the nozzle exit but
just at the end of right to left travel by the splitter.)

Figure 29 c. Flow visualization photograph of an oscillating jet in an LPA.

(Jet is swinging from left to right.)

57

develop that is radiated out acoustically. This signal reaches the control region and acts to help or hinder jet deflection. A block diagram of this is shown in figure 30.
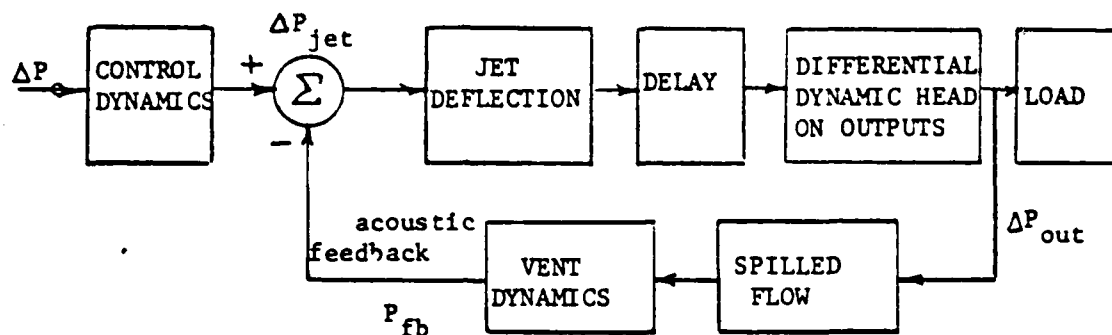
Figure 30. Conceptual block diagram for LPA dynamic response.

It is apparent that there may be multiple feedback paths if flow is spilled at more than one location. In the typical LPA, there are vent vanes (see for example in figure 29) where flow interaction may take place as, perhaps in figure 29b. Figure 31 illustrates this possibility.

Additional dynamic effects have been observed when a laminar jet is subjected to a step input. Rather than having a single sided pulse travel downstream, a whiplash effect is seen such as that shown in the photograph of figure 32. The physical explanation of this apparently anomolous behaviour is that the step control signal causes a pulse of high velocity flow (due to the tiny orifice between the jet and control edge) to form along side of the jet as shown in figure 33. This causes an initial or leading eddy to form and preceed the eddy that is

Figure 31. Oscillating Jet showing edge feedback interactions.
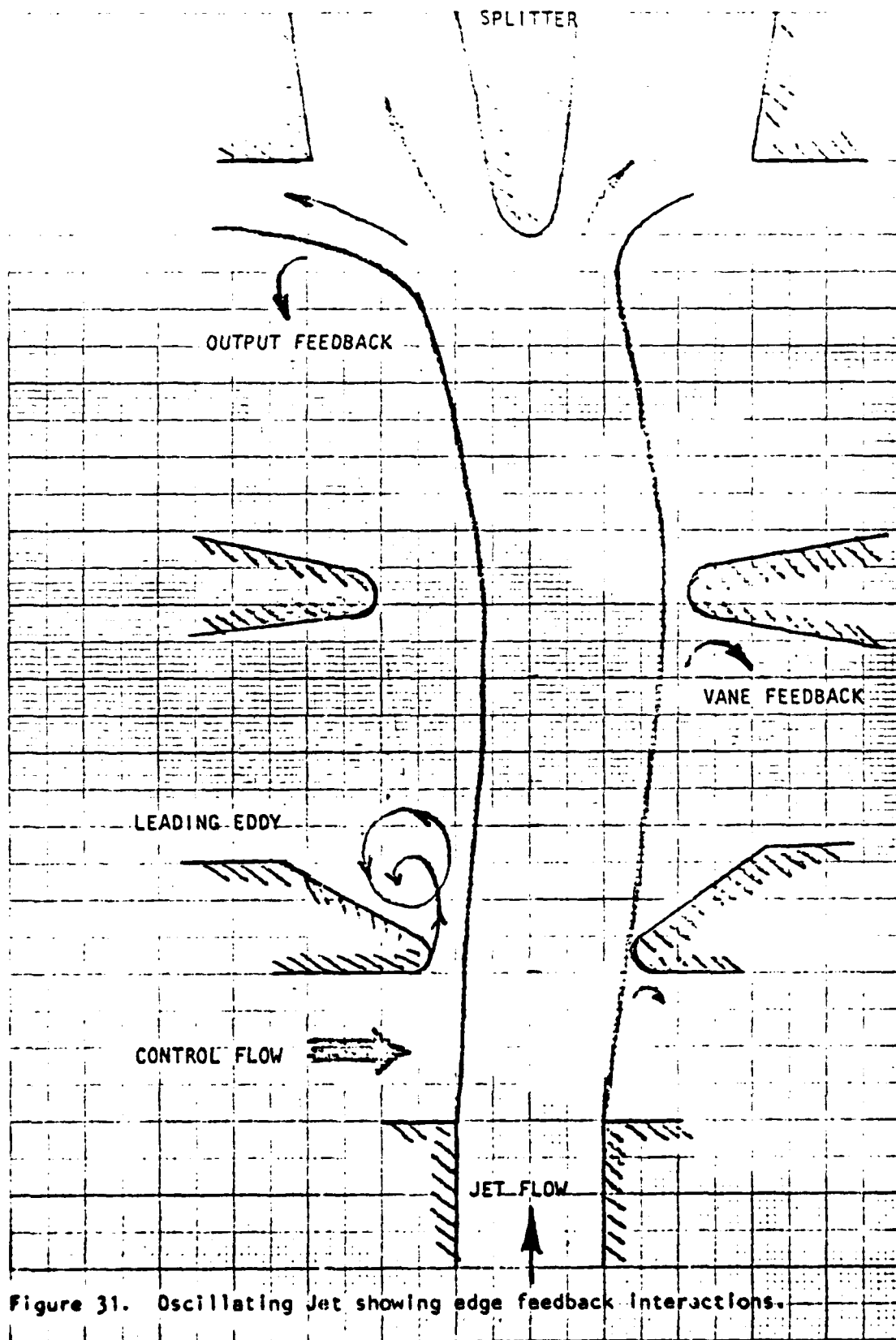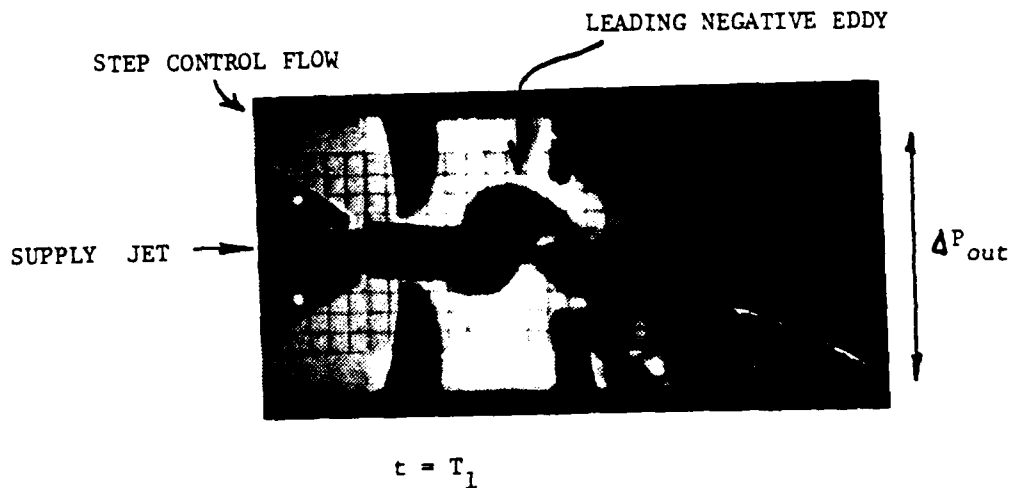
(a)   Jet deflection just after application of step in control flow.
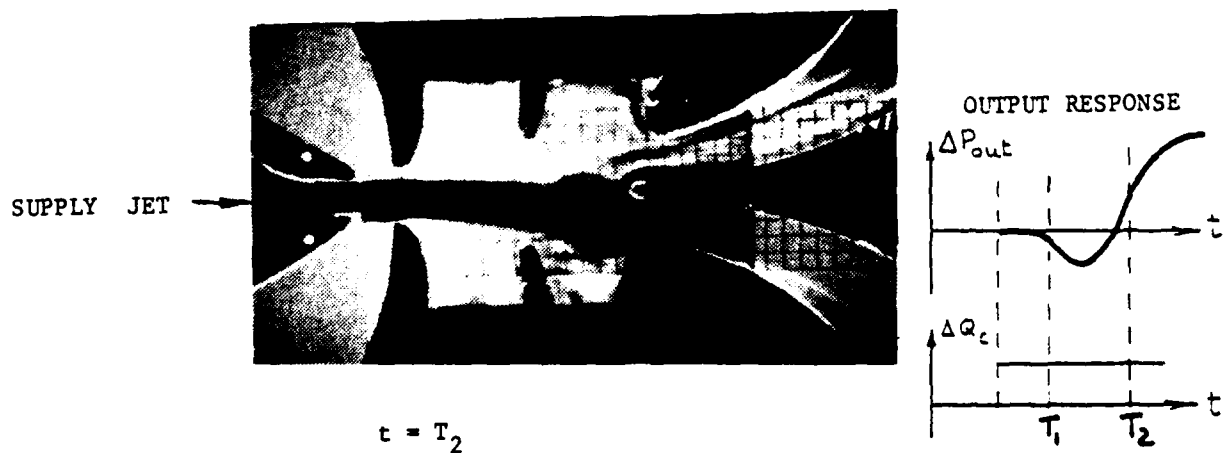
(b)   Jet deflection almost at steady state

Figure 32.   Flow visualization photographs of the step response of an HDL
standard LPA, illustrating a twin eddy, whiplash, effect.

60
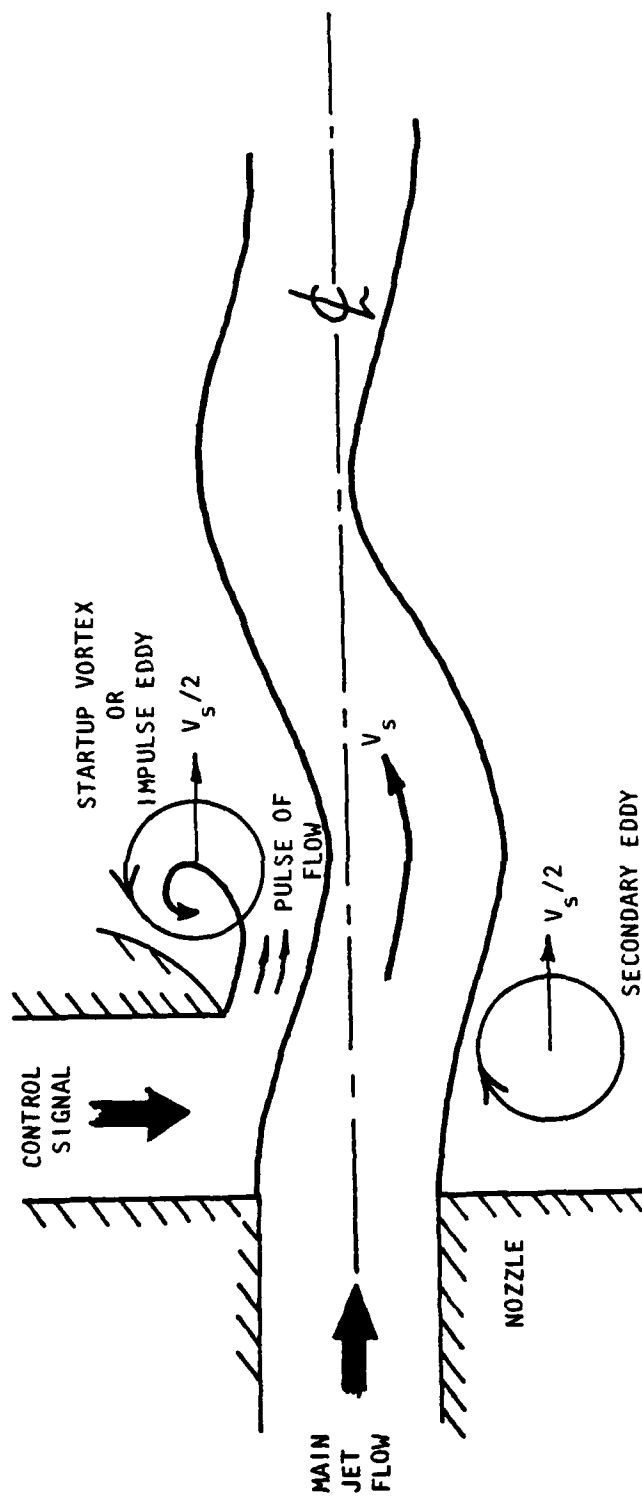
Figure 33. Sketch of the formation of the two eddies in the whiplash step response.

formed by the sudden acceleration of stagnant flow on the opposite side of the jet. Two eddies now must be convected to the outputs. The time required for this is longer than it would be if only   one eddy were being convected. The leading eddy also causes the jet to cross over the centerline and as a result, causes a negative differential pressure to occur prior to the establishment of the positive final steady state output pressure. This can be reasonably explained by the fact that the leading eddy grows in size as it is convected downstream. The velocity component of the leading edge of that eddy is in the negative lateral direction. This also can be seen in the sketch of figure 33. Clearly then, the step response is nonlinear and does not fall into the category of small signals as assumed in the analysis section.

It should be mentioned here that the presence of these two signal eddies is a strong argument for more time delay and hence added phase shift over that expected from assuming two transport times for a single eddy. Conceivably, four transport times could be argued as the time for signal propagation. Certainly this would hold true for large signals as observed in the present experiment and in experiments reported by Drzewiecki and Manion[35] when step changes in angular rates were applied to laminar jet angular rate sensors. Initial attempts at placing LPA resonances at low frequency involved using four transport time delay. Subsequent identification of the internal processes (feedback, etc.) allow the use of two transport times when considering small signals.

The acoustic feedback signal is attenuated by the viscous impedance of the bounding planes of the amplifier. Beranek[39] gives a relationship for the attenuation of nearly square passages that is proportional to the square root of the frequency and inversely proportional to a characteristic dimension, hence

$$20 \ \log \ (\frac{P(x)}{P_o}) = \frac{0.00664 \ \sqrt{f}}{h} \ x \, (db) \tag{63}$$

or

$$\frac{P_c}{P_{xsp}} = 10 \; (-2.767 \times 10^{-5} \; [c_d{}^\nu(\sigma N_R)/b_s{}^2]^{1/2} \; \sqrt{F} \; X_{sp}/\sigma^{3/2}) \qquad (63a)$$

Is assumed to be the attenuation of a square cross-section distance of length X_{sp} alongside the jet from the splitter back to the control. This agrees with experimental evidence that shows that as the aspect ratio or depth diminishes, the resonances disappear. Resonances also vanish, however, as the Reynolds number decreases.

As Reynolds number decreases the jet spreads out and reduces the space between itself and the vent vanes as shown in the following figure, figure 34. The fed back signal is thus further attenuated. Experimental evidence in the form of the frequency response of amplifiers with and without vent vanes illustrates this point quite dramatically as shown in figure 35. The response without the vanes is considerably more peaked indicating that feedback is enhancing gain at resonant points.

The model of an LPA thus is taken to follow the block diagram of figure 30. In figure 36 the complete model is shown in block diagram form. This feedback network may be reduced to the more compact form illustrated in figure 37. This transfer function and the expression for the impedances have been programmed in FORTRAN IV for an IBM 370/168 computer. The listing is given in Appendix I. A typical computer plot for a self-staged case (LPA driven by and loaded into an identical LPA) is shown in figure 38. Compare this typical plot to a typically obtained experiment plot of the frequency response of a high aspect ratio LPA as isshown in figure 39 (see also figure 35). Typical of the response is a very broad band hump centered at a normalized frequency of 0.01 that is predicted by the current model. This location and amplitude is found to be a function of the inductance of the
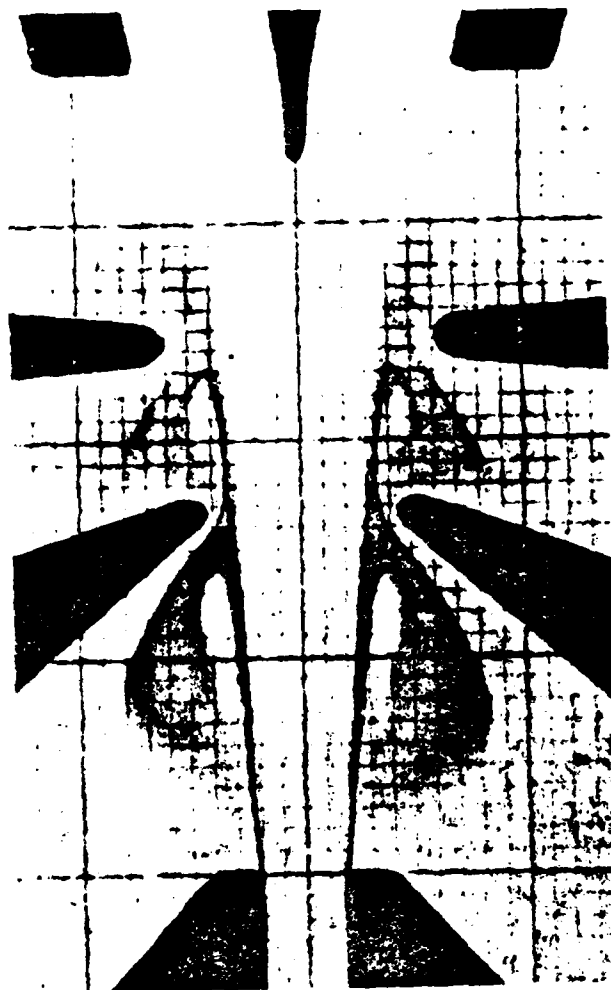
Figure 34. Jet spreading at low Reynolds number showing
interaction with vent vanes.
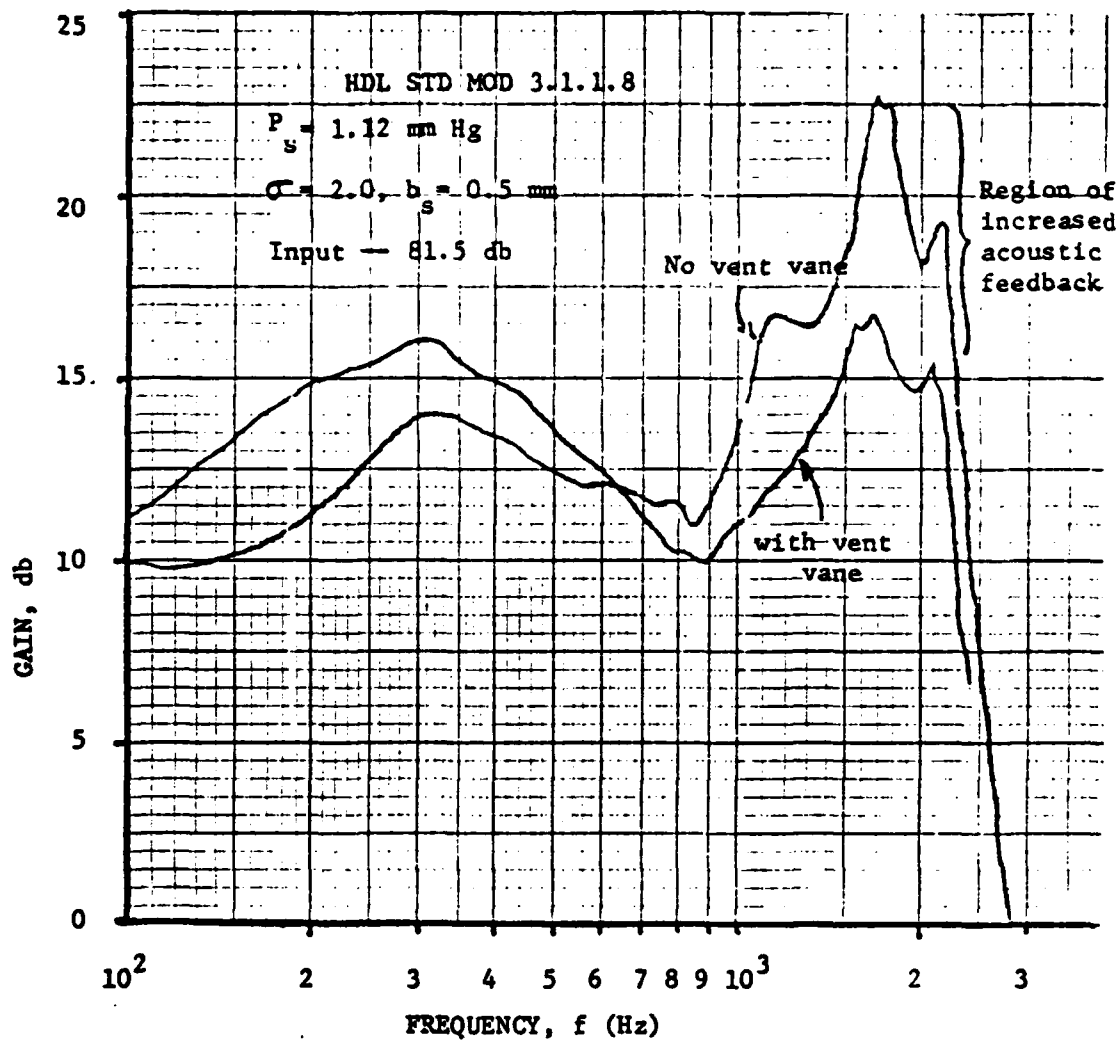
Figure 35. Experimental comparison of the effects of vent vanes on the acoustic feedback characteristics of LPA's.
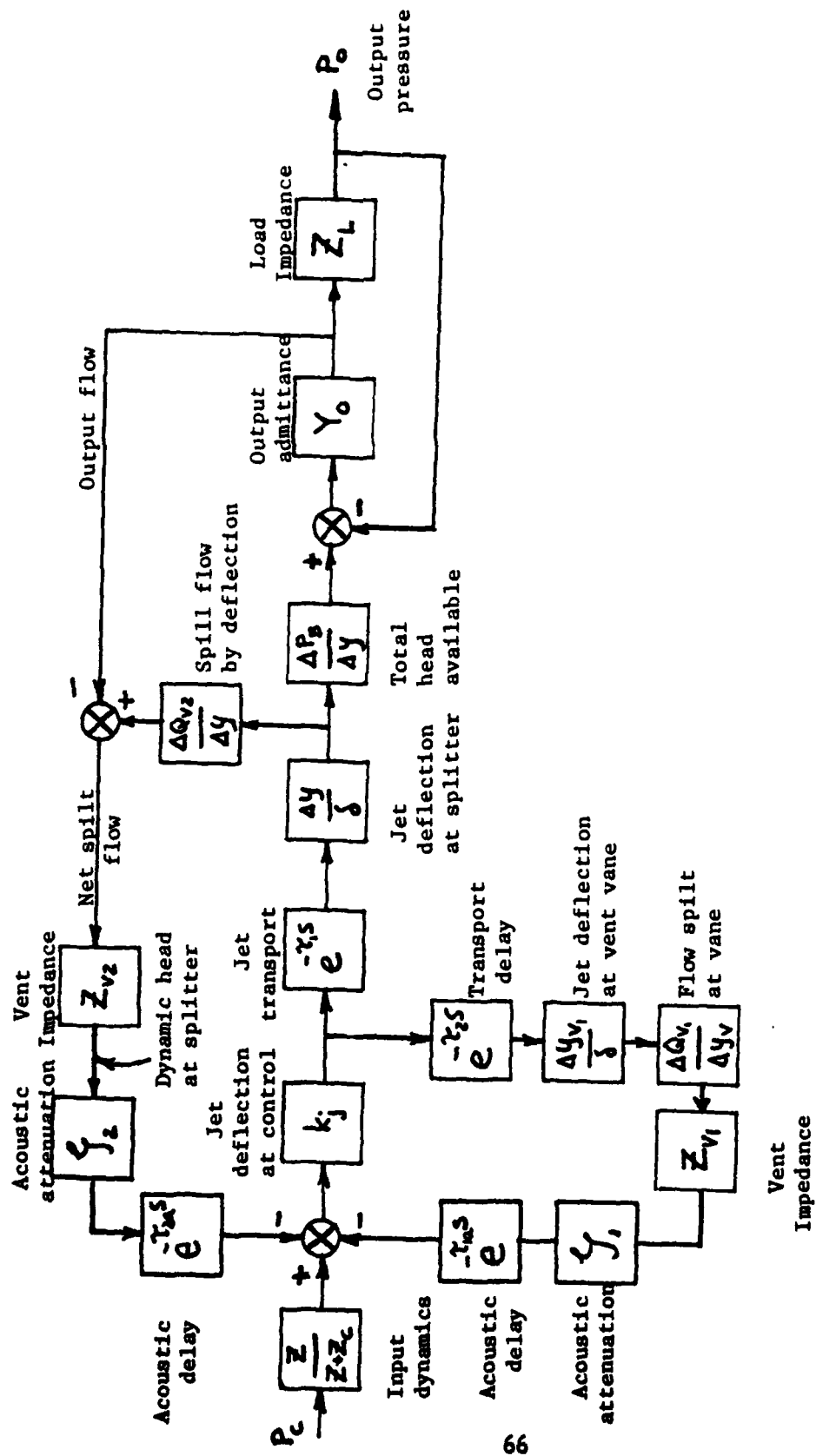
Figure 36. Full block diagram model of an LPA, including acoustic feedback.

66
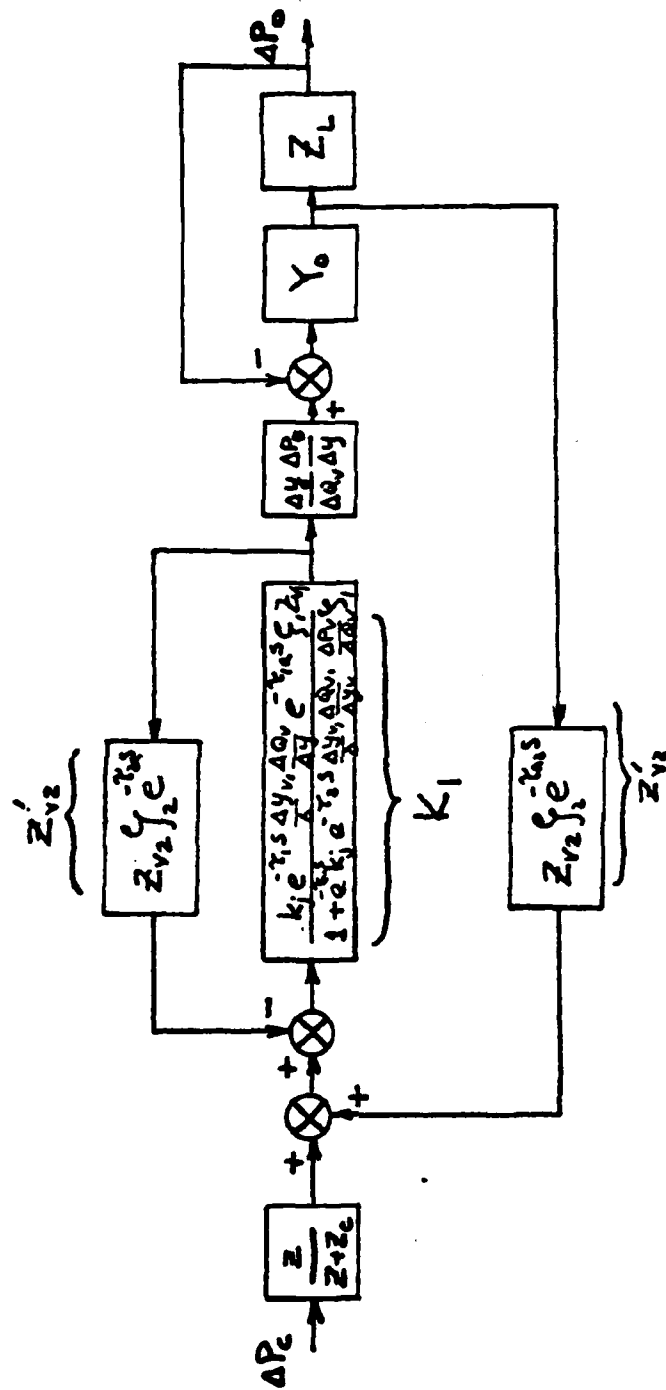
Figure 37. The LPA transfer function.

FREQUENCY RESPONSE OF AN LPA
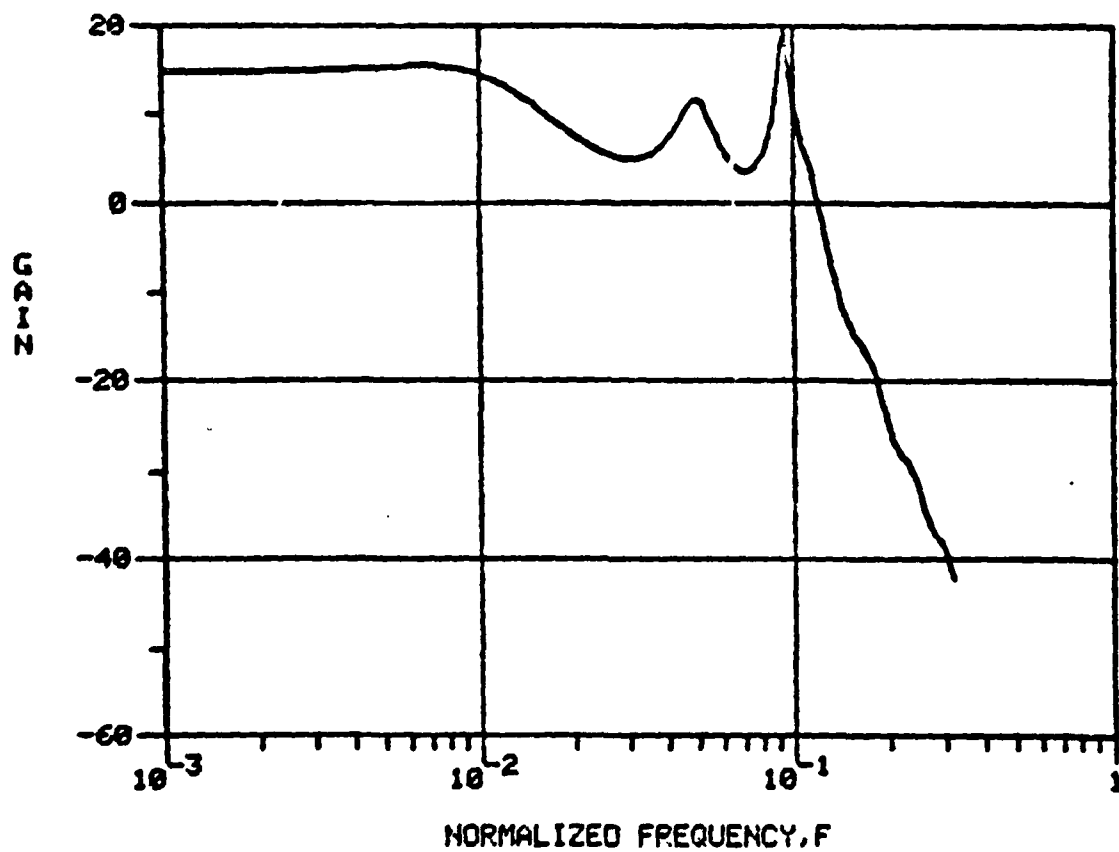
Figure 38. Computer plot of the frequency response of an LPA -- analytical.
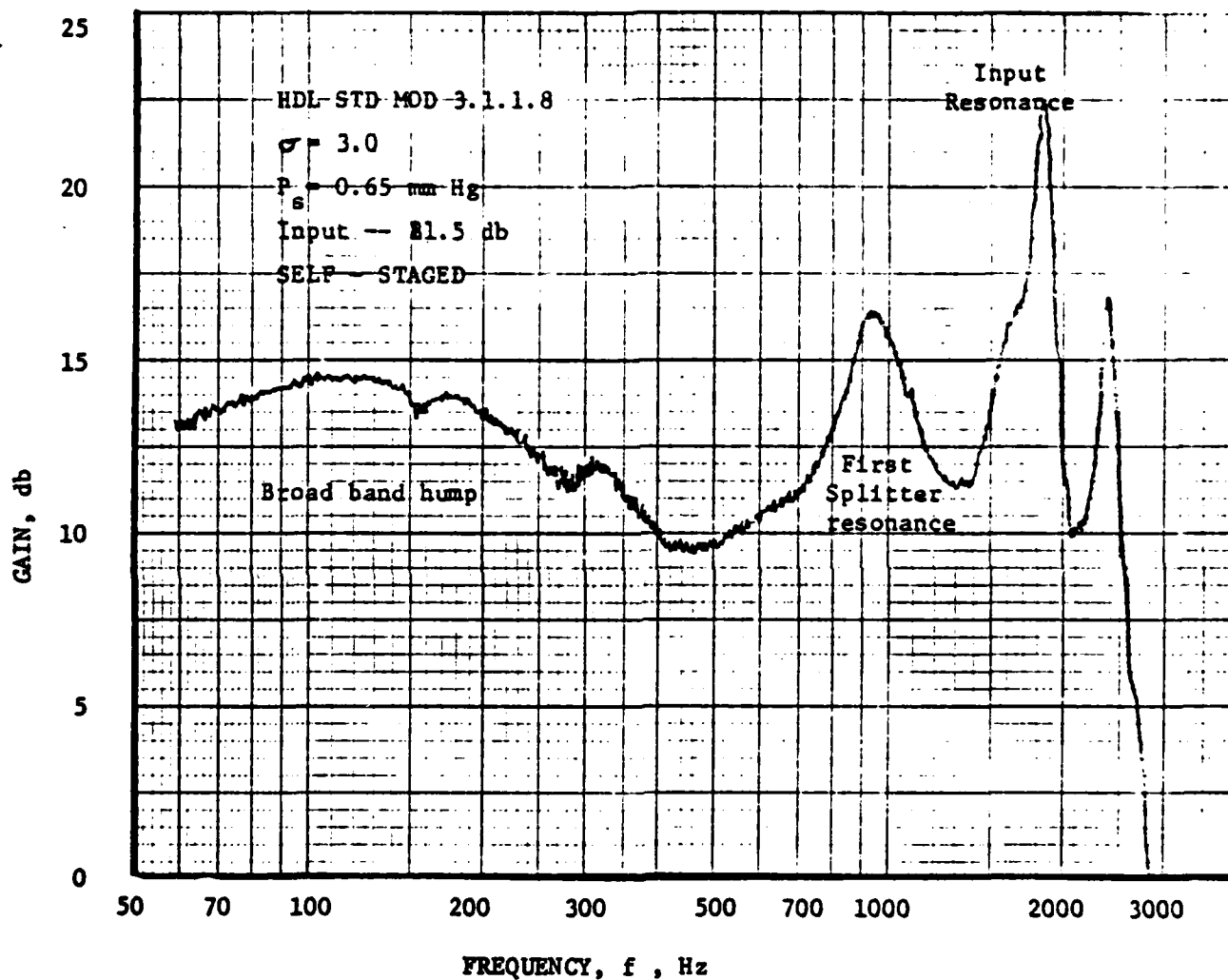
Figure 39. Experimental BAFCO gain plot of frequency response of the standard HDL LPA. High aspect ratio case.

69

downstream vents. When inductance is low, the response is flat as shown in figures 40 and 41. Figure 40 shows the self-staged response, and figure 41 shows the blocked ($Z_L = \infty$) response when the inductance is that for a channel one nozzle width long and four nozzle widths wide as opposed to the figure 38 response where the length was four nozzle widths. Notice that the locations of the second peak in figures 38 and 40, due to feedback from the splitter, are unaffected by the vent inductance. It is difficult to judge the values of inductance for all possible cases and configurations of manifolds and cover plates. For example, if the device is not cross-coupled and an apparently wide opening is provided for side venting, the vent may still have a considerable inductance if the length to width ratio is large. When the vents are collected through manifolds, as is often the case, the length and breadth of the channels prior to the common volume must be considered. In addition, if volumes are large, it is conceivable that capacitive effects may have to be considered. The low frequency gain increase is generally only 3-4 db and does not affect the bandwidth. It is of interest to note that this peak does not appear in the low aspect ratio cases where the velocities are much higher and the Reynolds number based on jet width is very high. In those cases, the feedback appears to be insignificant. The main resonances seem to line up fairly well as can be observed in figure 42 for the case when the load is an identical LPA. The phase shift is remarkably well predicted as shown in figure 43. Although of considerable importance, the experimental methods are not especially germaine to the topic at hand, so the details of the experiments and the gathering of data are relegated to Appendix II.

In order to see that the feedback terms in the model are having a significant effect, runs were made with the feedback terms zero. One such resulting Bode plot is shown in figure 44. As is observed, a single peak occurs that is due to a resonance of the inductive and

70
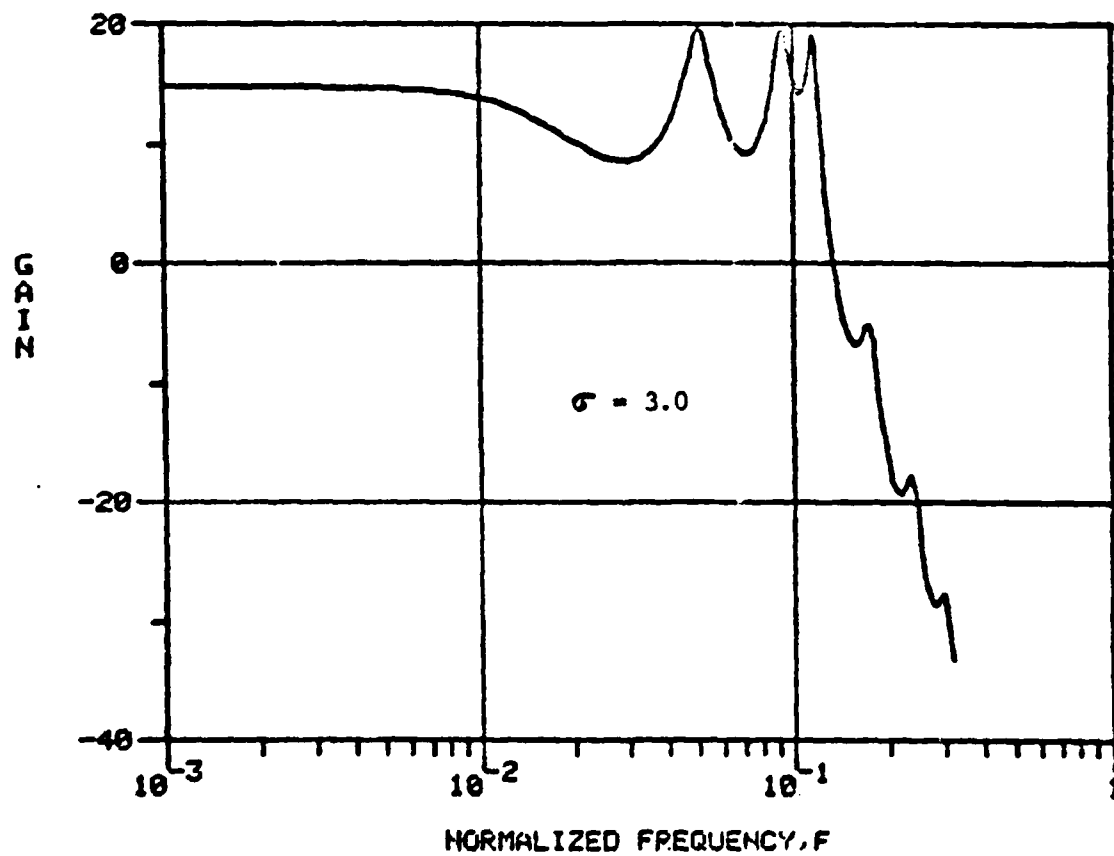
Figure 40. Theoretical frequency response of the standard HDL LPA with low vent inertance. Self-staged case.

71

FREQUENCY RESPONSE OF AN LPA

$\sigma = 3.0$
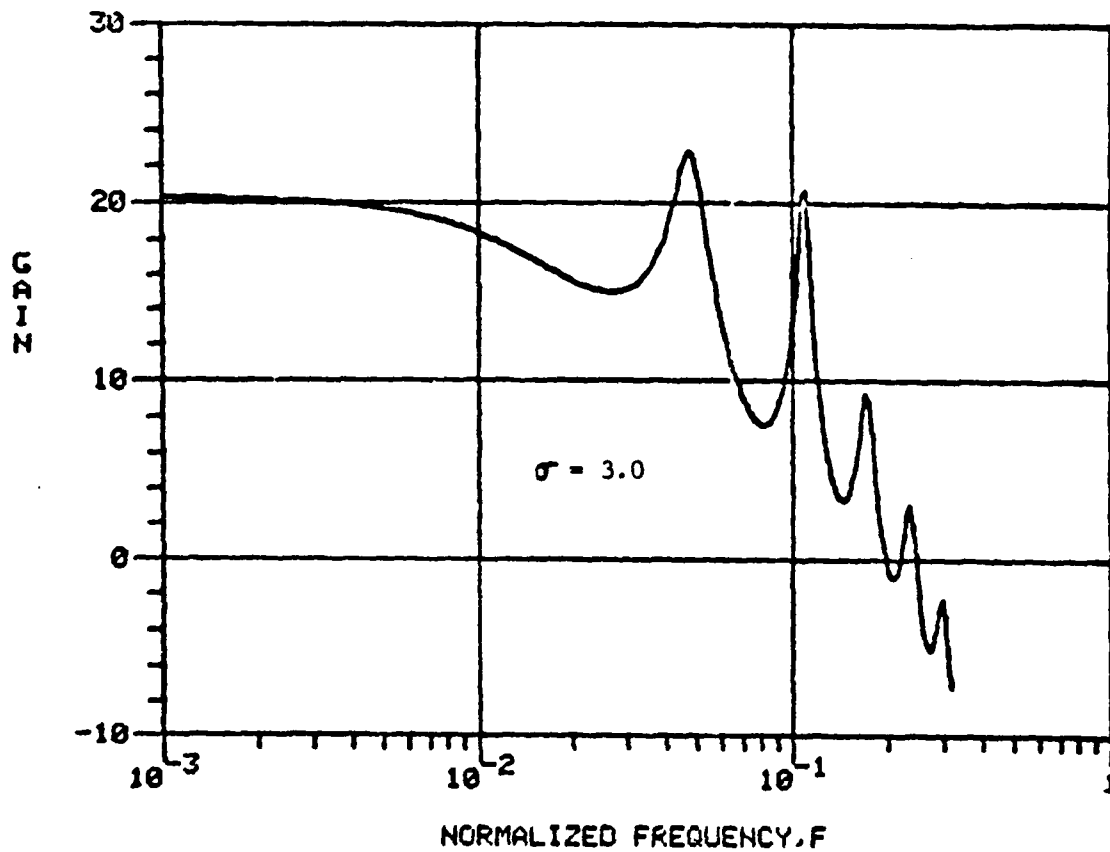
Figure 41. Theoretical frequency response of the standard HDL LPA with low vent inertance. Blocked output case.

AD-A084 924   NAVAL POSTGRADUATE SCHOOL MONTEREY CA   F/G 17/2
              A FLUIDIC VOICE COMMUNICATION SYSTEM AND DATA LINK.(U)
              MAR 80   T M DRZEWIECKI

UNCLASSIFIED   NL

1.0

1.1

1.25   1.4   1.6

2.8   2.5

3.2   2.2

3.6

4.0   2.0

1.8
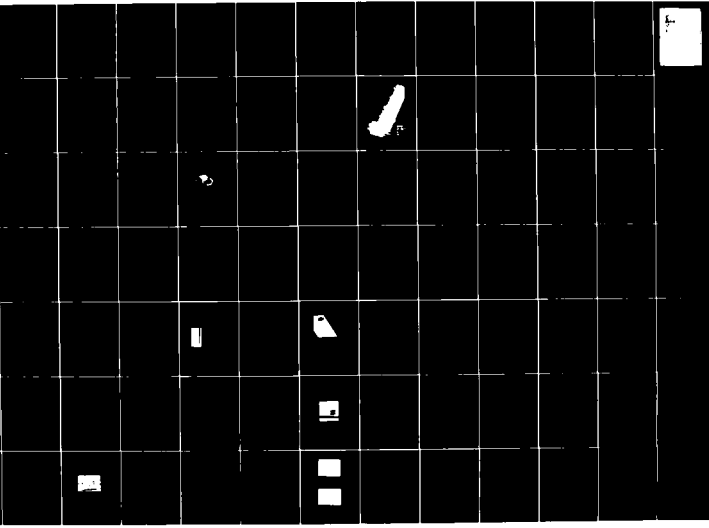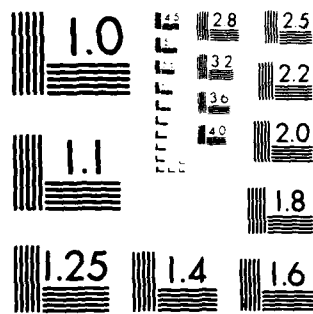
MICROCOPY RESOLUTION TEST CHART
NATIONAL BUREAU OF STANDARDS 1963 A
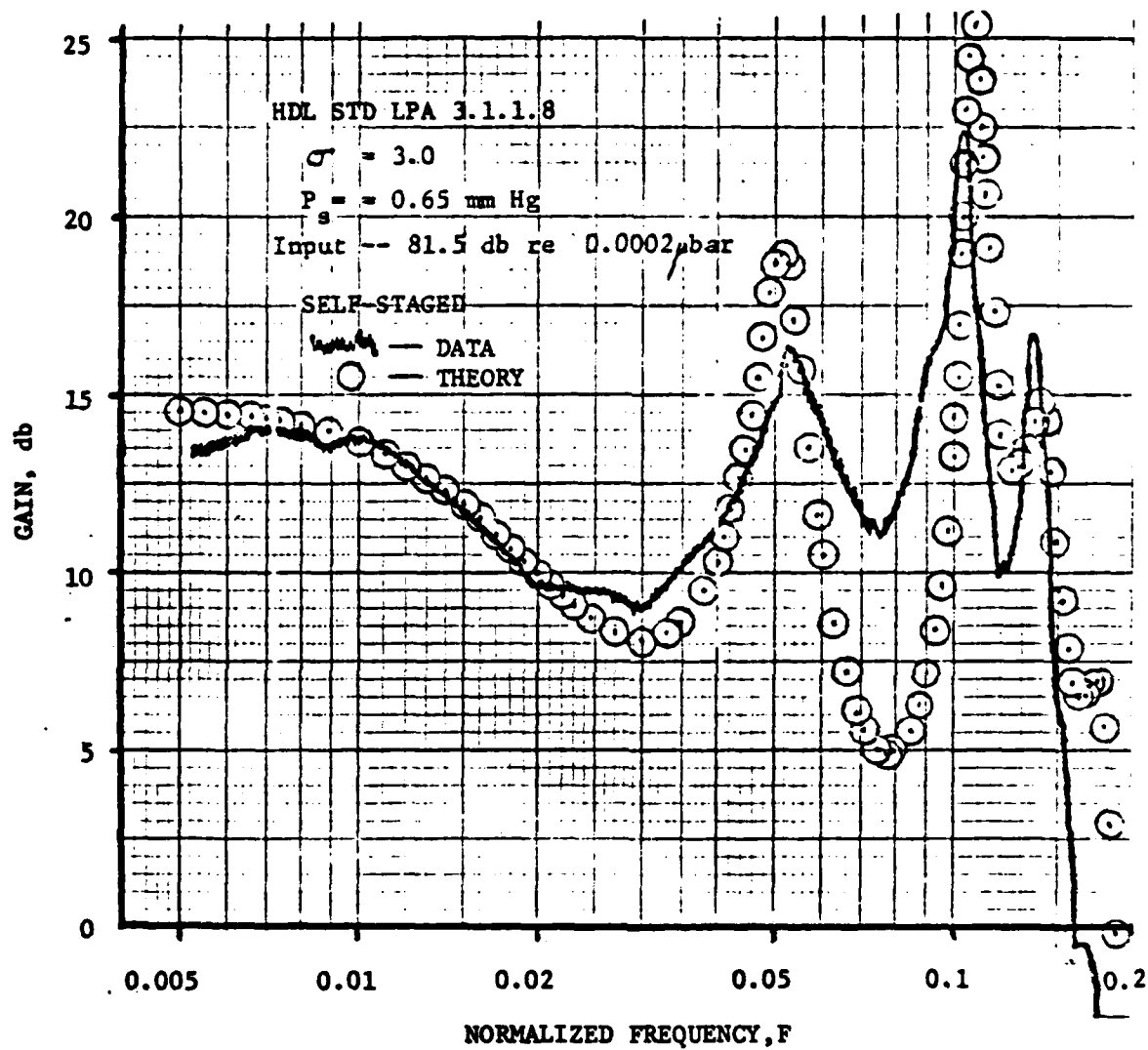
Figure 42. Comparison of theory and experiment for the frequency response of an HDL standard LPA at high aspect ratio.

73
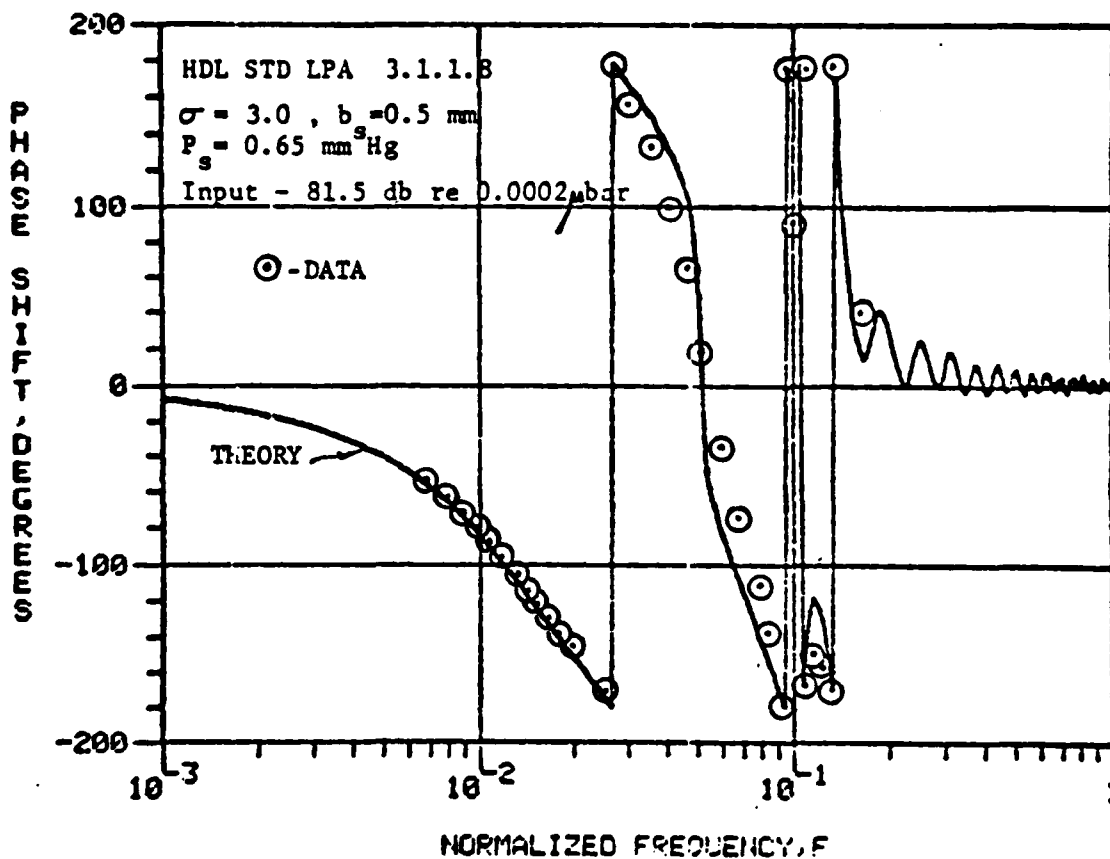
Figure 43. Comparison of theory and experiment for the phase
shift as a function of frequency in a high aspect
ratio HDL standard LPA. Self-staged case.
(Note: In order to display the phase angle within
the bounds of the figure, $\pm 360°$ has been added to
the results, where necessary.)

74

FREQUENCY RESPONSE OF AN LPA
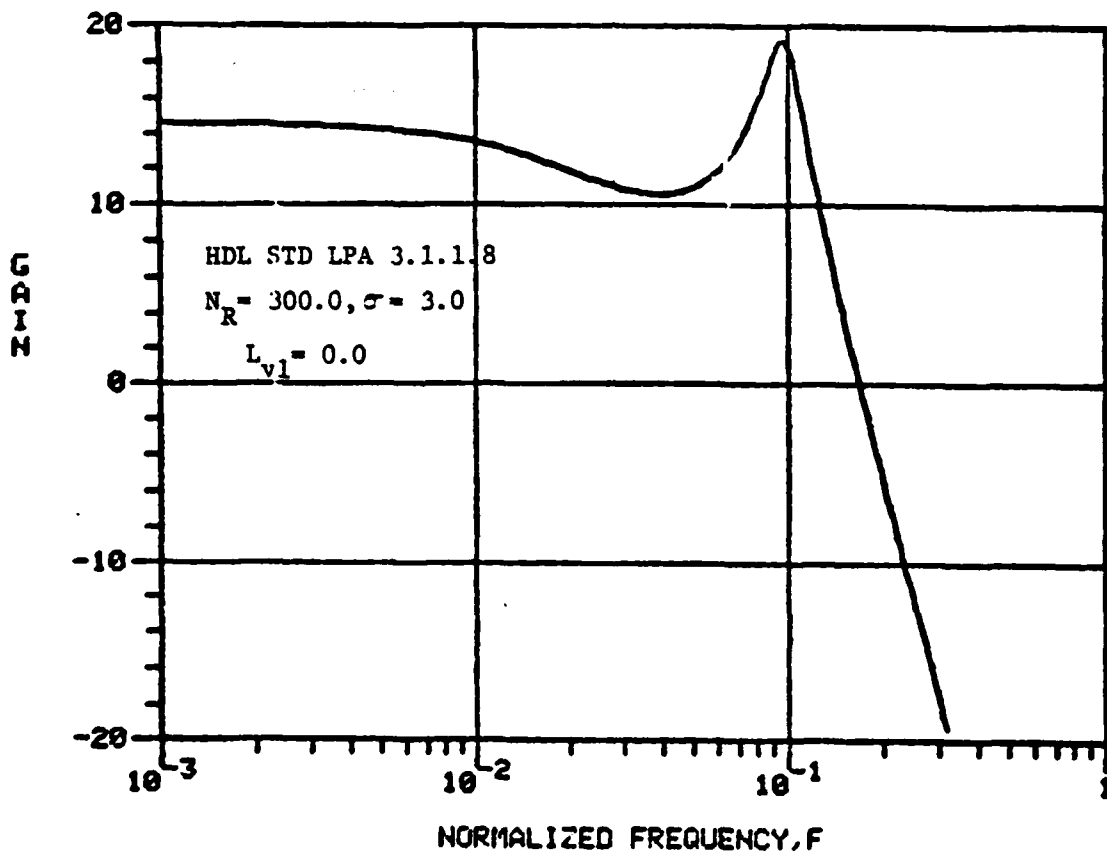
Figure 44. LPA frequency response when acoustic feedback is zero. (vents act as perfect ground of zero resistance)

compliant terms. Under the same conditions with non-zero feedback
terms but low values of inductance, the plot is as shown in figure 45.
The second peak is at the same frequency as the resonance of figure 44,
hence, it is not due to feedback; whereas, the first and all others are
due to feedback. For the case when the outputs are blocked ($Z_L = \infty$)
the resonances are more pronounced as shown in figure 46. When the
feedback terms are again neglected, no resonances occur as is seen in
figure 47. This then explains the origin of the second resonance in
the self-staged case and the increase in overall gain as being due to
the lead function of the load (the LPA input).

Coming back for a moment to the feedback mechanism of the reso-
nances, it is essentially the same as postulated for edgetones by
Kirshner[17]. It is therefore of interest to see if the regions of high
gain correspond to the edgetone eigenfrequencies. In figure 46 the
resonances are due only to acoustic feedback hence let us examine them.
The theoretically observed resonant normalized frequencies are:

$$F_i = 0.05, \; 0.113, \; 0.175, \; 0.27$$

and the ratios relative to the first are

$$F/F_i = 1.0, \; 2.26, \; 3.5, \; 5.4$$

These values are not harmonics and are very close to the edgetone
eigenfrequency ratios reported by Brown[40].

$$f/f_i = 1.0, \; 2.3, \; 3.8, \; 5.4 = j_i$$

If now the frequency is put into Brown's form

$$f = 0.466(u_o/\ell)j_i \tag{64}$$

FREQUENCY RESPONSE OF AN LPA

HDL STD LPA 3.1.1.8
N_R=300.0 , σ = 3.0
L_{v1}=0.25
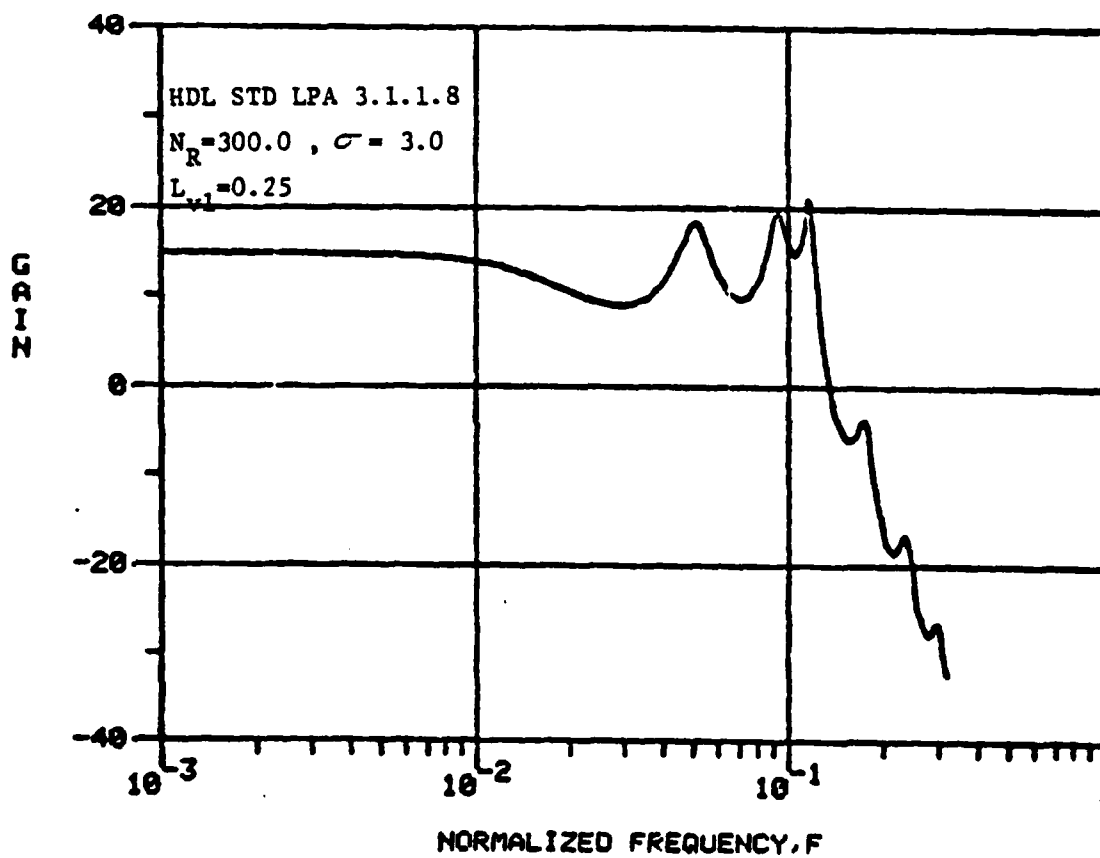
Figure 45.   Theoretical LPA frequency response for small values of vent inertance.
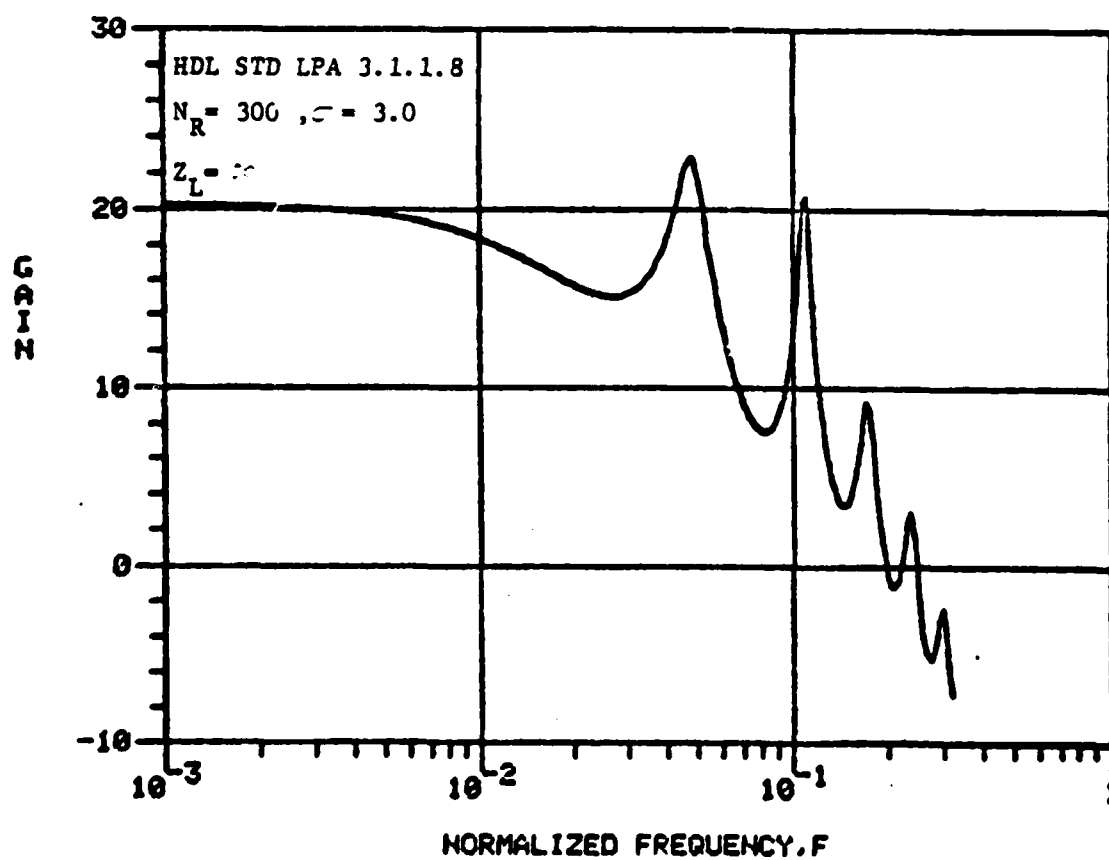
Figure 46. Theoretical blocked output LPA frequency response for the same conditions as in figure 45.

FREQUENCY RESPONSE OF AN LPA
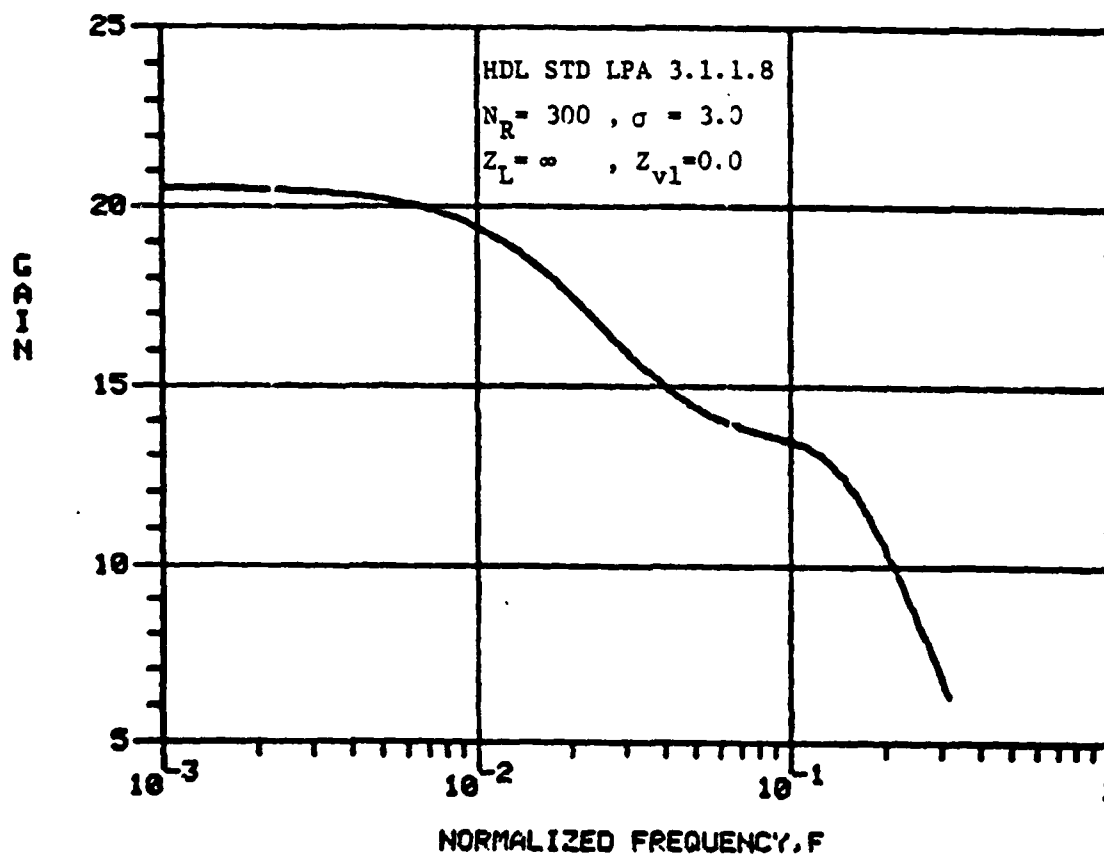
Figure 47. Theoretical LPA frequency response for a blocked output case
with no acoustic feedback.

where $u_o = c_d V_s$ the average jet exit velocity, then

$$f = 0.466 \, (c_d V_B / x_{sp})(X_{sp} F_i / 0.466) \tag{65}$$

where by inspection

$$j_i = X_{sp} F_i / 0.466 = 17.167 \, F_i \tag{66}$$

where $X_{sp} = 8.00$. In such a case then the matched eigenfrequencies are

$$j_i = 0.858, \ 1.94, \ 3.0, \ 4.635$$

These represent the absolute values of frequency at which oscillations would occur given sufficient gain. They are close to those values observed by Brown. It is of interest to note that this result was obtained by a lumped parameter approach as opposed to a particle mechanics or other more detailed approach. This independently supports the theoretical analysis and indicates perhaps some generality.

Following this edgetone problem a little further, one may observe that when the Reynolds number is decreased, the predominance of the second resonance is reduced in favor of the first as can be seen in figure 48 where the Reynolds number is one-half of that previously shown ($N_R = 150$ as opposed to 300 for the previous cases). The reason for this is seen in the values of the parameters as a function of Reynolds number. The vent impedances are predominantly inductive as can be seen in comparing terms for a typical geometry, hence

$$Z_v = R_v + j\omega L_v \tag{67}$$

For a short channel $X_v = 1$, $B_v = 4$, $N_R = 400$, $\sigma = 2$, $c_d = .7$ the equation for duct resistance gives

$$R_v = 0.003$$

FREQUENCY RESPONSE OF AN LPA
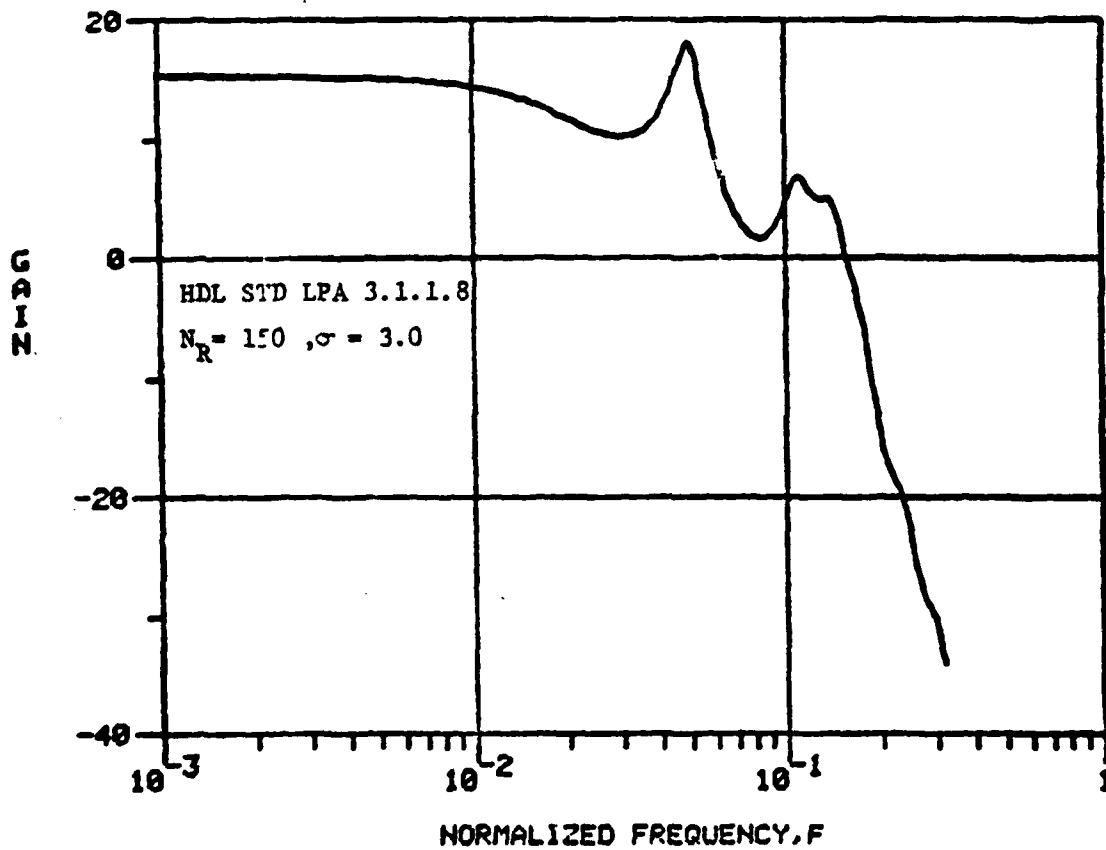
Figure 48. Theoretical LPA frequency resonse at reduced Reynolds number.

and the inertance

$$L_v = 2 c_d^2 X_v/B_v = 0.25$$

so that at high frequency, e.g. $F = 0.05$ or $\Omega = 2\pi F = 0.3$, the inductive reactance exceeds the resistive by a factor of almost 30. Now observe that as Reynolds number decreases, so does inertance since discharge coefficient decreases. This means that less pressure is developed to be fed back and as a consequence the resonances are smaller. At the same time the jet compliance is dramatically increasing since it depends on the inverse square of discharge coefficient. This means that the frequency response is rolling off sooner and the second resonance is down further while the first resonance is still near the flat response. This kind of superposition argument seems to be appropriate in light of observations.

That, indeed, a sustained oscillation like an edgetone is feasible is demonstrated by increasing the vent impedance to a large value about 20 times that found in a well vented LPA. Figure 49 shows the Bode plot for this case where the extremely dominant resonance indicates the point at which the device would oscillate. That this is qualitatively true has been observed time and again when inadequate venting is provided for LPA's. Experience has shown that jet devices must be well vented and cross-coupled to prevent oscillation.[35] Figures 50 and 51 are photographs of an LPA laminate with coverplates that allow venting directly at the edge of the jet. In effect, the jet is bounded by planes only over the lateral distance of full jet deflection, plus a bit. When such venting is not observed, the LPA will oscillate at high Reynolds numbers prior to transition-to-turbulence. As a matter of fact, the point of transition-to-turbulence is moved to a lower Reynolds number if laminar oscillations are allowed to occur due to poor venting. Figure 52 shows photographs of spectrum analyser traces of a poorly

FREQUENCY RESPONSE OF AN LPA
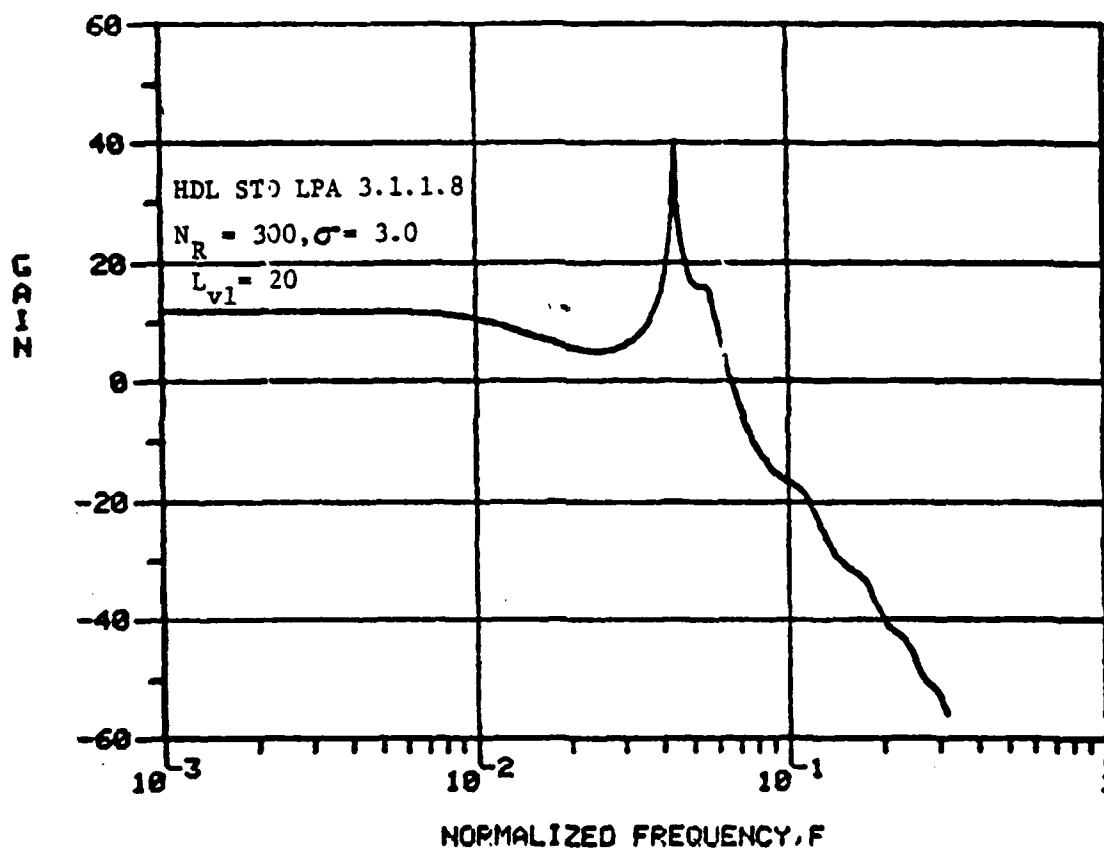
Figure 49. Theoretical LPA frequency response when a long vent with
high inertance (e.g. long manifold) occurs, showing high
resonant peak conducive to oscillation.

83

Figure 50. Photograph of an LPA lamination and its associated venting plate.
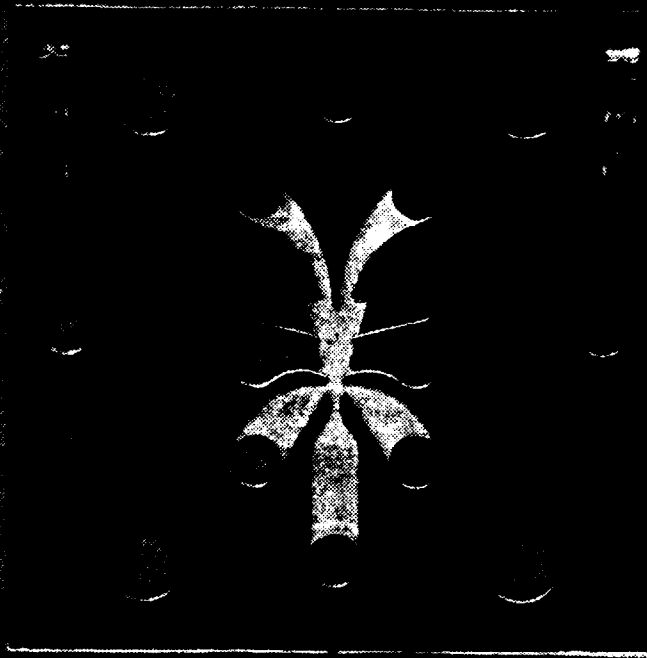
Figure 51. Photograph of an LPA lamination and its associated venting plate as found in normal stacking.
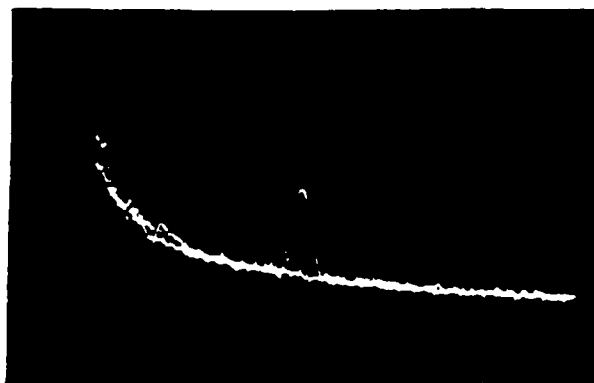
(a) $P_s = 17.4$ mm Hg
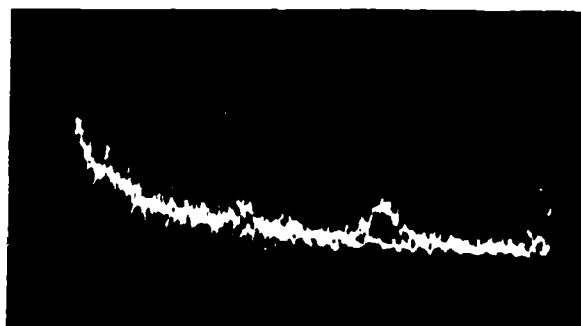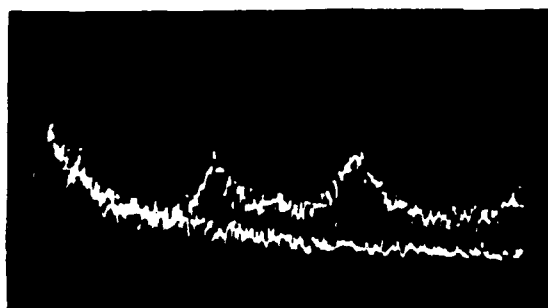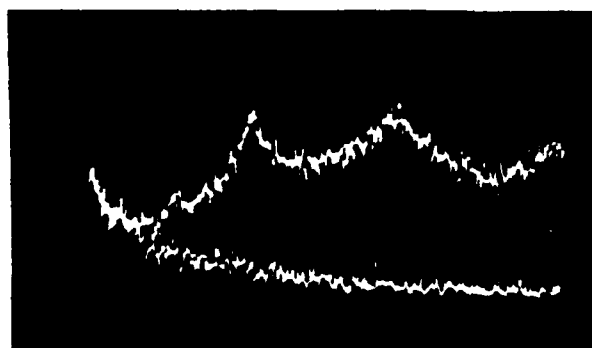
(b) $P_s = 25$ mmHg

                                                 GE built long
                                                 nozzle HDL LPA

(c) $P_s = 26.8$ mmHg

(d) $P_s = 36.8$ mm Hg

Figure 52. Spectrum analyser traces of transition to turbulence in an LPA,
            showing edgetone oscillation just prior to transition.

vented amplifier of a long nozzle LPA silhouette as shown. Figure 52(a) shows a clean, sharp resonance at 2500 Hz which is the first edgetone eigenfrequency (f = 2500 Hz corresponds to F = 0.05). Each photograph shows two traces; the lower one with no flow and the superimposed upper one with flow. When the two traces coincide as in 52(a) (except for the resonance), the flow is defined to be laminar. Figures 52(b), (c) and (d) show the progression of turbulence from high frequencies to low with 52 (b) showing that the oscillation vanishes just before transition. This seems to support the theoretical consideration since at transition the jet spreads and both gain and pressure recovery are lost so that oscillation ceases. If one were to attempt to tie the occurrence of edgetone oscillation to transition, it would require considerably more work and analysis into the hydrodynamic stability of the flow. It is not attempted here but note is made of it.

As the aspect ratio is decreased, one observes that to maintain the nominal operating modified Reynolds number, the supply pressure must be increased. This increases the parasitic or channel capacitance and also increases the feedback signal attenuation because the bounding walls are closer. These two effects both reduce the normalized bandwidth. The increased capacitance promotes faster rolloff by attenuating the input signal and the increased feedback attenuation reduces the acoustic feedback.

It should be remembered at this point, in defense of prior analyses, that the LPA has a geometry quite different from those in existence at the time of early work by those such as Brown[41], Belsterling[27], Healey[21] and Kirshner and Katz[17]. A particular difference lies in the high input impedance and close proximity of the jet to the control edges. Prior amplifiers always had large clearances so that the clearance reactance could be neglected.

This analysis is in relatively acceptable agreement both quali- tatively and quantitatively with experimental data as shown in figures

42 and 43 and in more detail in the Appendix II where various aspect
ratios and Reynolds numbers are considered. Therefore, it can be used
to generate the engineering guidelines that follow.

2.1.4 Bandwidth Guidelines

For the cases of various loading on the high aspect ratio,
HDL standard LPA, model 3.1.1.005 shown in figure 27, the frequency
characteristics will lie generally between the blocked case and the
self- staged case. In each case the overall maximum bandwidth over
which useful gain occurs is $F \sim 0.1$ so that a map of bandwidth, size,
aspect ratio and supply pressure can be made for a nominal modified
Reynolds number of 120 ($c_d \sim .7$). When modified Reynolds number N_R' =
$N_R / ((1 + X_{th})(1 + 1/\sigma)^2)$ is substituted into the normalized frequency
the actual frequency (bandwidth in hertz) is

$$f_{bw} = 16.8 \, \nu \quad (1 + 1/\sigma)^2 / b_s^2 \tag{68}$$

Now noting that supply pressure at N_R' = 120 is defined by

$$P_s \big|_{N_R'} = 120 = 28,800 \rho \, \nu^2 (1 + 1/\sigma)^4 / b_s^2 \tag{69}$$

then the aforementioned map is generated for air at 20°C where ν =
1.4864×10^{-5} m^2/s and ρ = 1.2059 kg/m^3 as shown in figure 53.
The numerical coefficients in equations (68) and (69) were obtained
using a nominal value of X_{th} = 1.0.
Similarly one notes in the frequency response characteristic
that there exists a region of essentially uniform gain . For the
blocked case, the gain is down 3 db at a frequency an order of magni-
tude lower than that given above or $F \sim 0.01$. For the self-staged case,
the lead in the load increases this bandwidth to $F \sim 0.03$. From these

88
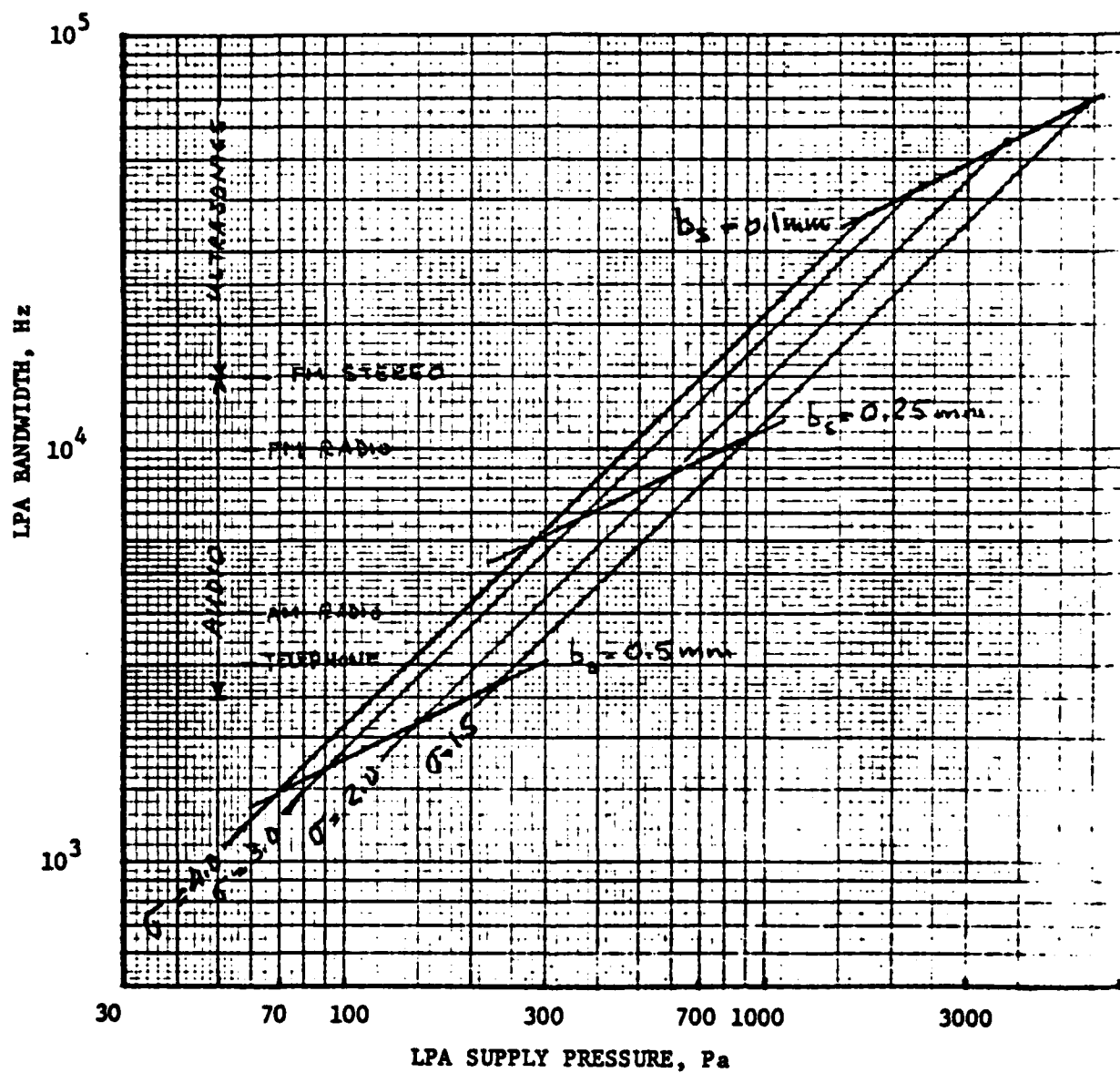
Figure 53. Engineering guide for the frequency response bandwidth of the HDL standard LPA, 3.1.1.8 for high aspect ratios.

observations one can stipulate a bandwidth for the worst case for a
single LPA as being $F \sim 0.01$. It should be noted, therefore, that if
many amplifiers are staged together in series and the last stage is
blocked, then care must be taken to describe the overall bandwidth with
the reduced frequency response of the last stage taken into account.
Looking ahead for a moment to the case where headsets are the load,
they are essentially an inductive load (e.g. a long, low-resistance
duct) and they may provide some gain compensation, (or "equalization"
as is the term used in acoustics).

Based on the premise that feedback from edges and protrusions
augments gain of an amplifier, a concept for a broadband amplifier aug-
mented by such feedback has been proposed and a patent disclosure made.
The patent disclosure is given in Appendix III. Basically, one may use
an extended distance to the splitter that gives increased gain and
several intermediate vent vanes to provide extra resonances. Several
such devices can be placed in parallel and operated at slightly
different supply pressures; thus, the peaks will be shifted from each
other. Addition of the output signals will be such that peaks of one
occur at anti-peaks of another so that a broad band, fairly uniform
gain may be achieved. A favorable internal review of this disclosure
has been made and a formal application has been made with in the U. S.
Patent Office.

This then completes the analysis of the LPA. As can be seen from
the various experimental and theoretical curves presented and especially
from the engineering guide in figure 53, the current HDL standard LPA
has sufficient bandwidth to be used in audio amplification and the
analytical means at hand are sufficient to understand why. Prognosis
for ultrasonic operation of these devices is excellent as long as the
small dimensions can be manufactured, see for example in figure 53
devices where $b_s = 0.25$ mm.

2.2 Transmission Lines

The communication system will necessarily require a means for transmission of speech and other data from one distant point to another. This will be accomplished by use of acoustic transmission lines. Acoustic transmission through ducts of constant area is treated in every elementary text on the subject, hence, no analysis will be presented here other than that already presented in the previous sections. The texts by Rshevkin[16], Zalmanzon[29] and Beranek[39] form the required background information. Beranek presents the most needed information in that the duct (transmission line) will attenuate the signal as a function of the square root of frequency and inversely as the radius. The pertinent loss coefficient is that the loss in db/meter is

$$0.278 \quad \sqrt{f(Hz)} \ /r(mm). \tag{70}$$

Kirszenblat[15] makes note that a transmission line will exhibit a resonant response if it is blocked, loaded with a termination other than the characteristic impedance ($Z = \rho c/A$, where c is the speed of sound, A is the cross-sectional area and ρ is the density), or has a sharp discontinuity or sudden change in areas such as an expansion or contraction. He points out that the use of matching exponential horns eases the problem of reflections and it is for that reason that all terminations in this project are matched through exponential horns.

2.3 Other Passive Components

Other components involved in the communication system are the exponential horns mentioned above, junctions and fittings.

The effects of fittings on the fluidic response are assumed to be negligible when the volumes are small and the changes in area smooth. Their effects in the acoustic region, however, are not small. When acoustic signals converge in a junction where the exit area equals the sum area of the input lines, acoustic summing occurs, wherein the amplitude of the fluctuations add. This is in contradistinction to the case of lumped parameter operation of the fluidics where flows add but not pressure. This brings up the very important distinction between what are called fluidic signals and acoustic signals. Fluidic signals require that the wavelength of a given frequency be large compared with the dimensions of the components under consideration. This is sometimes known as "slowly varying dc." It is intuitively obvious that pressure will distribute itself in such a manner as to accommodate a given flow-rate. However, when one operates acoustically, pressures can add as in the example of reverberant rooms with standing waves. This distinction has often been overlooked, especially when fluidics engineers--not acousticians--attempt to work with acoustics. A particular example is demonstrated in the work that was done on the public address system in 1976[11]. In order to get a high amplitude signal out of large exponential horns with a large column of air, 17 standard LPA's were paralleled to produce enough flow and provide dynamic matching. This is illustrated in figure 54 which shows the PA amplifier. Here five stages of amplifiers make up a three-stage pressure amplifier (pre-amplifier) and a two-stage flow (or power) amplifier that delivers the flow to move the large column of air in the horns. However, when preliminary audio amplifiers were made, the concept of power output was thought to be synonymous with loudness, and a two-parallel stage power amplifier was provided. Instead of an increase in loudness actually a slight decrease was observed. This was because the ear responds to pressure (see Randall[42]) and adding a parallel stage of amplification
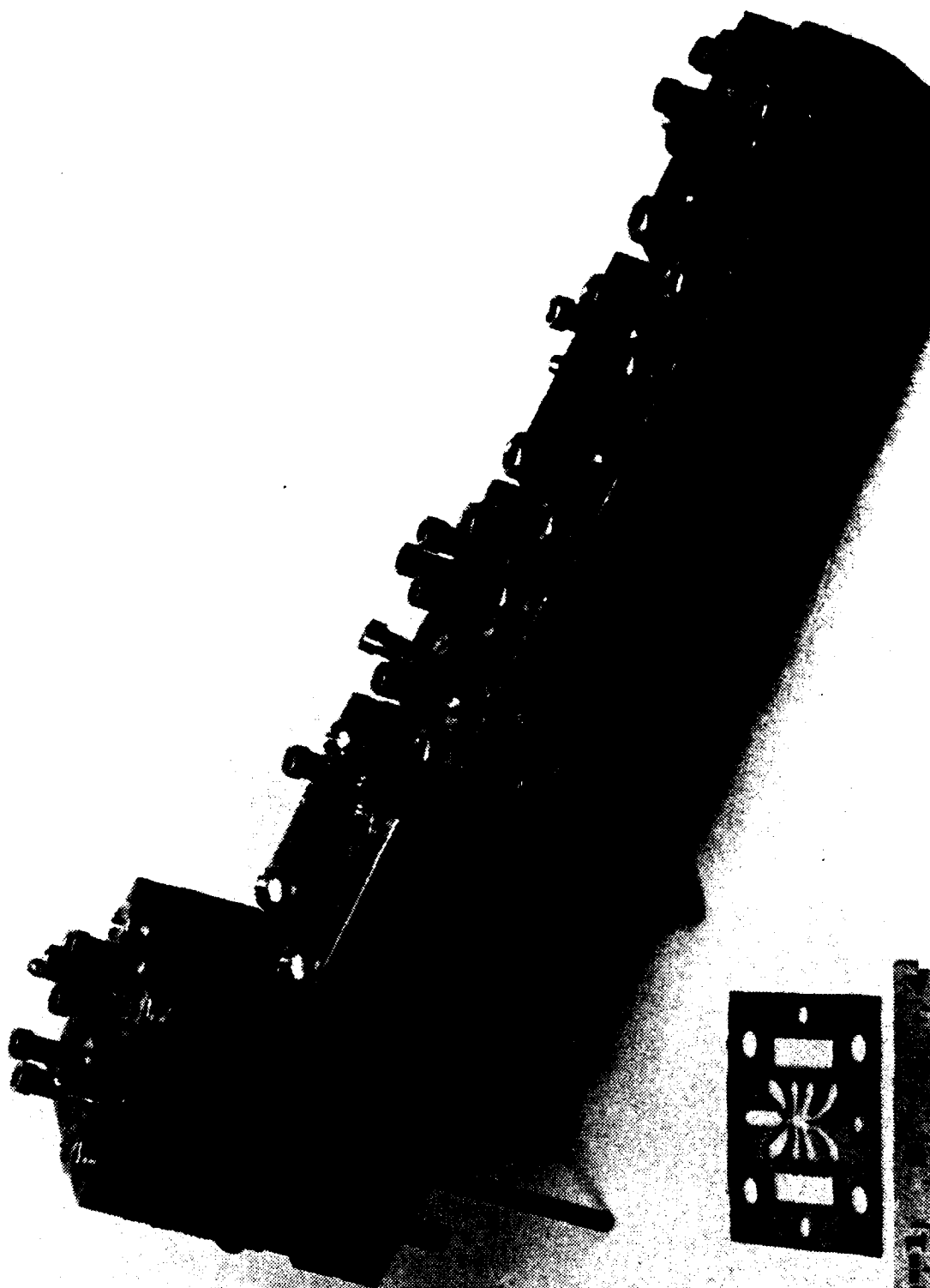
Figure 54. Photograph of a five stage LPA gain block used in a public address system

reduced the load impedance on the pre-amplifier and hence dropped the gain slightly. This occurred when the two amplifiers were stacked one on the other, and the pressure was drawn off a common port. When the parallel stages were separated and the signals drawn off separately and recombined in a constant cross- section junction, the loudness was considerably increased. Figure 55 shows schematically the physical arrangement.
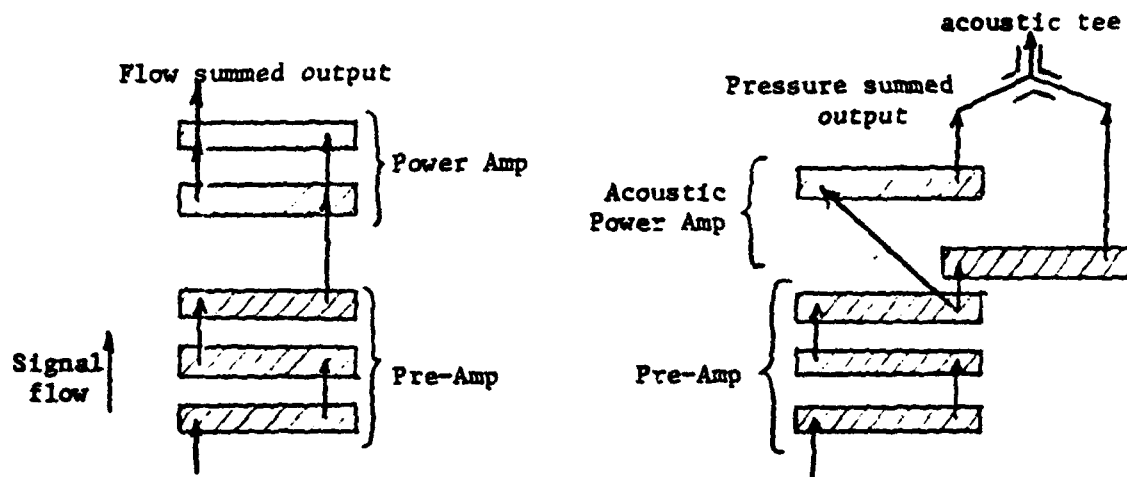
Figure 55. Schematic of flow and pressure summing schemes.

The signal transfer within the fluidics package itself is essentially identical; however, the resultant acoustic levels are considerably different. This type of "passive amplification" is very useful in personal-type communication systems and is quite often used by acousticians.

2.4 Concluding Remarks on the Analysis

This section has attempted to tie together many existing analyses, has expanded on them and has provided new insight into the lumped parameter approach for the analysis of the dynamics of fluidic components. As such, the significant results of the analytical and experimental effort are:

1. Entrainment effects such as bias pressures have been shown to be independent of frequency at least to frequencies in the bandwidth of LPA's.

2. The double eddy (whiplash) large signal transient or step response has been shown to be a nonlinear effect that does not materially affect the small signal frequency response; however, it does explain increases in phase shift observed when large signals are used.

3. The development of an improved high order equivalent circuit model for the input impedance of an LPA.

4. A combined acoustic feedback, lumped parameter model of an LPA has been developed that correctly predicts the performance and frequency character of LPA's from the initial broadband low frequency gain increase to the high frequency resonances which occur near the edgetone eigenfrequencies.

5. The prediction of the edgetone eigenfrequencies and their ratios. In addition, both the qualitative and quantitative description of their behavior, within an LPA, has developed as a function of Reynolds number. It is shown that for large Reynolds numbers, the higher edgetone frequencies give rise to resonant peaks in gain. An explanation for the propensity of edgetones to jump from one frequency to another is offered by noting that different peaks are higher (more energy) than others at different Reynolds numbers.

6. The development of engineering guidelines for the estimation of overall system bandwidth to include acoustic and fluidic considerations.

7. The identification of physical quantities such as geometry and fluid properties with equivalent circuit elements.

8. The development of an equivalent model for short fluidic channels as a "tee" network.

9. A broadband fluidic amplifier scheme has been proposed.

The above are highlights only. The insight and the intuition gained has been invaluable. Items of interest were noted in such a way that their relevance could be maintained intact when they were learned. What has really been learned is that there is a lot more that is unknown than is known. For example, the transition between fluidics and acoustics should be carefully examined. The role of edgetones or high frequency gain should be examined in terms of its effect on the transition-to-turbulence. Lumped parameter analysis approaches may be appropriate for a broader area of transition problems. The differences and similarities between a feedback system's stability and hydrodynamic stability of shear layers should be examined. The fluid mechanics of confined jet-like flows should be examined to tie in differences in phase. Integral and differential effects should be examined--for example, the effects of velocity profiles on transport delays.

These are only some of the fundamental single amplifier areas of interest that appear. Whole areas of multiple amplifier dynamic interactions appear as well as those fluidic/acoustic interactions between amplifier components and transmission components. The whole area of generation of interactive engineering models is opened up. Already this author is using the basic transfer function presented herein for multiple component analyses. This model is currently being examined by others as the basis for design of oscillators that will be used as pressure-to-frequency transducers. More will be said about this in a later section dealing with signal frequency generators.

96

3. FLUIDIC VOICE COMMUNICATION SUB-SYSTEM DESIGN

This section deals with the design and development of hardware
for the broad band audio transmission system and considers design
analysis and hardware development. The concluding parts of section 3
will be devoted to human and system engineering.

Consider, however, that both the voice and the data link systems
are composed of subsystems and components that can be tabulated into a
matrix. Both the voice and data subsystems have in common the following:
a signal generator, an input, a transmission section, an amplifier, a
signal processor, an output, and a power supply. These then form the
structure of the two systems.

3.1 The Voice System Feasibility

At the start of the experimental program, feasibility of speech
transmission was of paramount importance, so a rough cut
was made with an existing high gain amplifier that had dimensions and
an operating point that indicated probable voice bandwidth. This was
a three-stage, self-staged, ceramic amplifier manufactured to HDL speci-
fications (HDL-STD-MOD 3.1.1.8 amplifiers) by Corning of aspect ratio
$\sigma = 1.5$ and nozzle width, $b_s = 0.25$ mm. According to the engineering

map, see figure 53, and equations (68) and (69), this should require that the bandwidth f is in the range $(0.01 < F < 0.1)$ of:

$$100 \ \sqrt{P_s}/b_s < f < 1000 \ \sqrt{P_s \ (mmHg)} \ /b_s \ (mm) \tag{71}$$

so that at $P_s = 8$ mmHg (corresponding to $N_R = 120$, $\sigma = 1.5$) and $b_s = 0.25$ mm, the bandwidth should be between 1.1 and 11 kHz. This amplifier is shown in figure 56 and its single-sided frequency response (differential gain is 6 db higher) is shown in the Bode plot of figure 57. This frequency response very closely spans the human speech pressure spectrum given by Randall[42] in figure 58 and is no worse at frequencies below 2 kHz than a typical loudspeaker shown in figure 59 (also due to Randall[42]). This device was then tested as a speech processing unit by attaching airline-type headphones (merely a 1/8 in diameter plastic tube connected directly to the earhole) to the outputs. The signals in the two lines are 180° out of phase; however, the brain does not discriminate the phase relationship and allows the sound to appear twice as loud rather than cancelled. For the first tests an 1/8 in (3 mm) diameter input tube was connected to one control and a tank (low pass filter) to the other so that signals would enter only one control. Speech was not only passed but amplified as expected. The experiment was then broadened to make a full communication link by incorporating two amplifiers and two lines. This also was sucessful. Then, in an effort to cut down on the number of lines, and the dynamic absorption of the compliant plastic a single copper tube 12.5 mm ID and 10 meters long was used and the input teed in.

Several important design characteristics were discovered during this portion of the effort. The input could be achieved by a "throat microphone" consisting of a closely clamped "U" tube connected to the
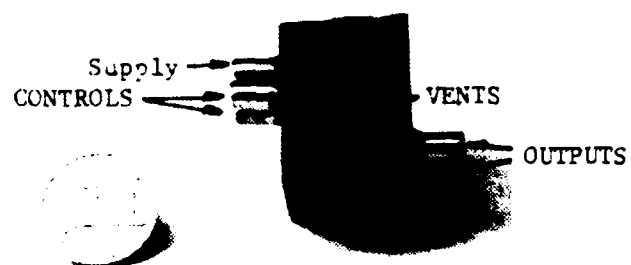
Figure 56. Photograph of a Corning-made three stage gain block
(HDL STD LPA 3.1.1.8[3])
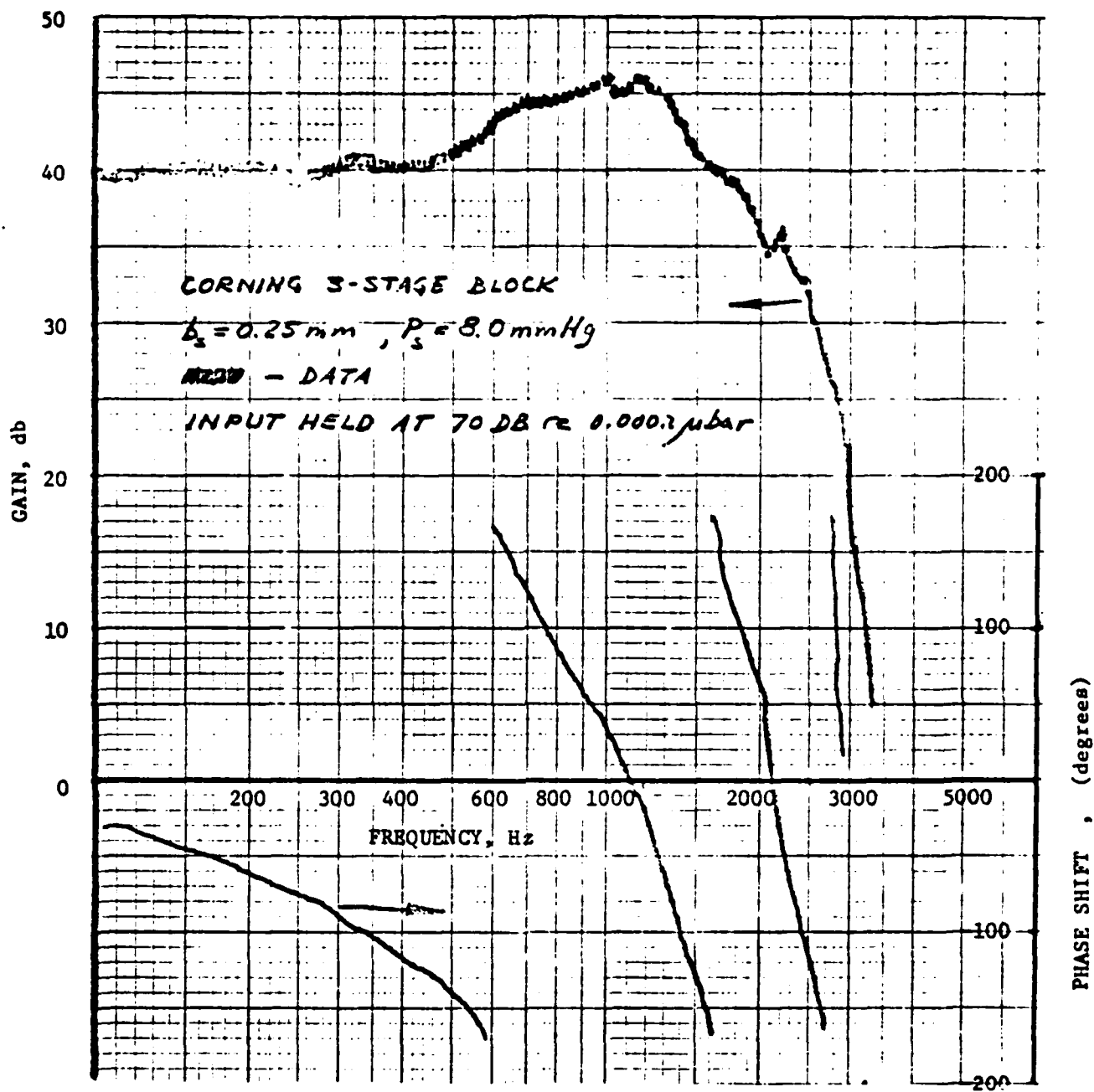
Figure 57. Frequency response Bode Plot of the ceramic Corning three stage audio amplifier (b_s = 0.25 mm).
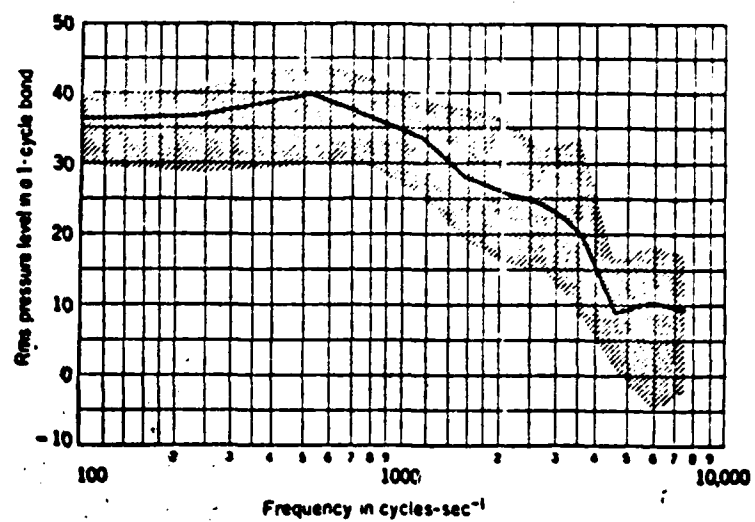
Figure 58. Pressure – frequency distribution in normal speech after Randall[42].
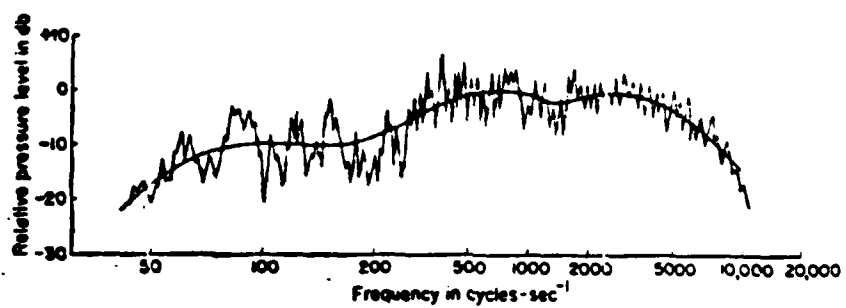
Figure 59. Typical measured response of a loudspeaker in a "live" room. Smooth line represents the effect to the average ear. (Randall [42]).

neck at or near the larynx. This was an extremely important finding
because of the superior background noise rejection afforded. Ambient
noise must pass through the tubing and through the skin/tube-end in-
terface. Ambient room noise suppression of as much as 40 db was found
compared with speaking into an open-ended tube. This type of speech
input was investigated because vehicular noise levels may approach 100
db and passing and amplifying this noise is one of the most severe draw-
backs of existing intercoms. Personal communication with individuals
with expertise in the tank intercom area has resulted in this author's
rejection of an open microphone concept. The Air Force routinely uses
throat microphones on aircraft for this very reason.

Another characteristic investigated empirically in the early
efforts was the output or the headphone arrangement. The best fidelity
and loudness could be achieved with the "airline-type" head sets where
the outputs of the amplifier were directly fitted into the ear. Expo-
nential horns that fit into ear protection devices as shown in figure
60 were examined. Under certain circumstances when the ear-headphone
cavity was large, it was found that loudness could be increased by
blocking the ends of the horns with a thin steel diaphragm. When the
horn was held directly against the ear, no appreciable difference was
noticed. The geometry of the horn was such that the neck diameter
was 3 mm flaring out exponentially to 37 mm over an 80 mm length.

The attenuation of the 10 m line is computed from equation (70)
based on the highest frequency to be passed, say 3 kHz. Then the
loss per meter is

$$\frac{0.278 \ \sqrt{3000}}{6.25} = 2.4 \text{ db/m}$$

or 24 db for a 10 m line. This implies that the gain of the system
must be greater than 24 db just to overcome line losses. From figure
57 it can be deduced that a gain of about 46 db is available from the
Corning units.

103

TUBE TO FLUIDIC OUTPUT

PADDING

METAL DIAPHRAGM

EAR PROTECTOR MUFF
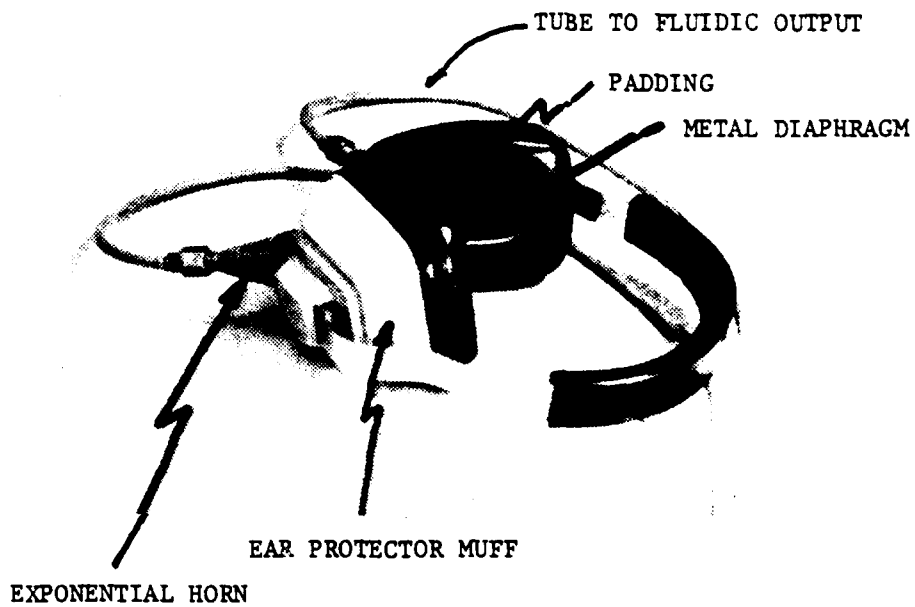
EXPONENTIAL HORN

Figure 60. Photograph of prototype fluidic headphone with exponential horns.

Commercial airline crew radios use headsets with metal tubes that
swivel and fit into the ear. These lightweight devices provide a
maximum of fidelity with a minimum of encumberance.

3.2 The Voice System Design

These preliminary tests proved feasibility of an intercom system
and validated the engineering guide to some extent. Consider therefore
the design of a workable system for inclusion in a combat vehicle such
as a tank or armored personnel carrier. The following matrix of compo-
nents in table 1 may now be used as a guide for the analysis and design
and appropriate choice for the final system.

Table 1. Voice Communication System Component Matrix

Parameter	Components	Comments
signal	human speech	external noise? engine
input	throat tube open tube diaphragm	external noise rejection vs. input loss
signal transmission	rigid tube compliant radiation tube	length and diameter to be determined
amplification	fluidic amplifier	size, gain
signal processing	output high pass passive input filter low pass filter	low frequency rumble
output	direct fitting exponential tubes horns	human engineering into helmets-comfort
power	self contained parasitic	reliability and redundancy
interconnections	acoustic flow	system integration penalties

3.2.1 The Signal

The signal to be transmitted is human voice. The signals available
are basically threefold: the voice; engine or operating noise; and
external random noise such as of the battlefield. Typically the ambient
sound level in a tank is of the order of 100 db re. 0.0002μbar, hence,
hearing protection is required. This is accomplished by ear muff type
headphones in the electronic system, which are mounted in a plastic
helmet as shown in figure 61. Notice also the boom type microphone that
is susceptible to all the sound airborne at the speaker's mouth. Normal
speech, 70 db at 1 meter, is a signal about 100 - 110 db at the larynx.

3.2.2 The Input

As previously noted, the feasibility studies were conducted using
a clamped tube at or near the larynx. This "throat mike" concept has
been chosen for this program primarily due to its superior noise re-
jection. This concept also removes an obstruction from the face;
however, the penalty is wearer discomfort. When the tube ends are
clamped very close to the larynx, unacceptable discomfort occurs,
but when the tube is placed too far away, the signal is lost. Based
on standard throat mike designs, a "U" tube spacing of 10 cm was settled
upon. This is consistent with the average neck dimensions of the
American male which is about 40 cm (16 inches) in circumference or
12.5 cm in diameter. The chosen microphone arrangement places two
open tubes flush against the neck at the one quarter point around the
neck centered on the larynx. The two tubes are joined together in an
equal area "tee" (the output area equals the input area) so that re-
flections and distortion are minimized.

Some consideration was given to the use of diaphragms or membranes
over the open tube ends to avoid system contamination by particles of
dust and moisture such as perspiration and to avoid dc flow saturation
of the LPA. Thin neoprene rubber about 0.05 mm (0.002 in) in thickness
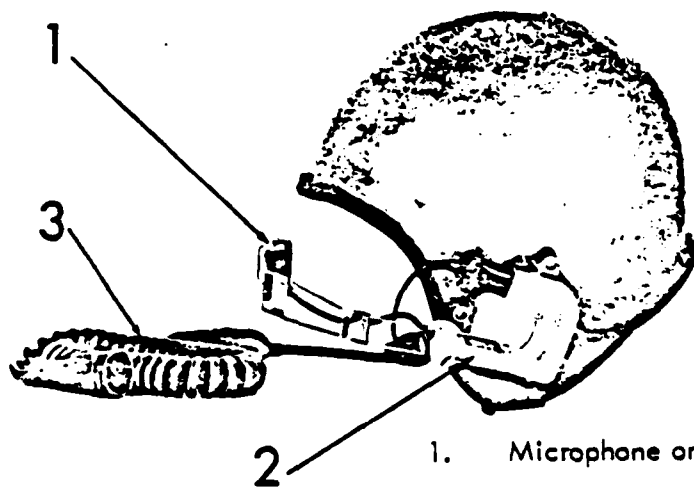
1. Microphone on adjustable boom.

2. Switch box with 3-position switch — forward (hold-on) to talk on radio; backward (lock-on) to talk on inter-com; center to listen only.

3. Cable with quick-disconnect plug, a clothes clip, and a coiled cord.
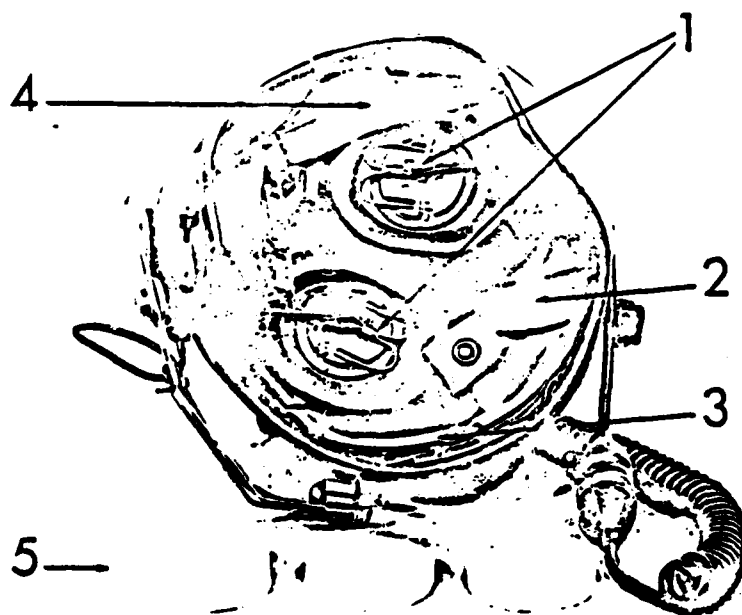
1. Earphones in earpads.

2. Three adjustable web straps.

3. Sweatband.

4. Neckband.

5. Sponge rubber spacers.

Figure 61. Standard issue US Army tankers helmet showing headphone installation

was found to have little or no attenuation since it lies flat on the skin and falls within the general dimensions of the epidermal layer of the human neck.

A disadvantage of the "throat mike" and blocking membrane concept is that it is a dc blockage that allows no entrained flow, hence, the controls of the amplifier would operate at a suction or negative head. This is undesirable from the standpoint of amplifier stability. LPA operation at negative bias is the basis for the digital operation of a laminar digital amplifier (LDA)[43,44]. Typically, the gain of an LPA increases with increasingly negative bias and becomes unstable. While the blocked control pressure is not very negative, only about -5% of supply pressure it still could be a problem. Provision of a bleed is one solution, but this provides for undesirable ingestion of ambient air. A slight pressurization of the common transmission line can however be achieved by providing a high resistance shunt from the main pressure supply.

The LPA is inherently a differential device where signals may enter either side. If a time varying signal is impressed on one side of the amplifier, the conditions of loading must be specified on the opposite side. If the condition is such that the opposite side is open to ambient (the opposite control pressure is zero gage) then the instantaneous differential pressure is merely the input signal ampli- tude since $\Delta P = P_1 - P_2$ and $P_2 = 0$ so that $\Delta P = P_1$. This, however, is not the case at hand. The opposite control must be shielded from all signals. Certainly the voice and noise will radiate towards that port. In addition, since the device is differential but operation is desired around jet centered conditions, the dc level on the opposite side must be adjusted for a dc null output condition. This is accom- plished by a variable resistor to ground. High frequency noise and

signals can be eliminated by placing a volume (tank) in series with the
resistor to provide a low pass filter. When one anticipates a high
pass output filter, as in the matrix of Table I, then the low frequencies
entering will wind up being filtered at the output. The variable re-
sistor (valve) will allow individual adjustment of null so that the
volume of the tank must be determined. The circuit, however, is com-
plicated by the fact that the amplifier input impedance is involved.
However, at low frequencies it is fortunately mostly resistive. The
equivalent circuit of the nulling low pass filter then is as shown
in figure 62.
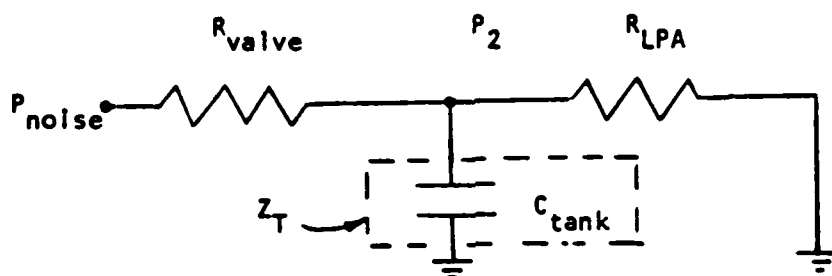
Figure 62. Equivalent circuit for nulling low pass circuit on
opposite control of an LPA.

This circuit has a transfer function

$$P_2/P_N = R_{LPA}Z_T/[R_{VALVE}\,(R_{LPA} + Z_T) + R_{LPA}Z_T]$$

which reduces to equation (72) when it is noted that $Z_T = 1/Cs$.

$$P_2/P_N = \cfrac{[R_{LPA}(R_{LPA} + R_{VALVE})]}{\left[\cfrac{R_{VALVE}\,R_{LPA}}{R_{VALVE} + R_{LPA}}\right]Cs + 1} \tag{72}$$

109

The break point frequency is $f(-3db) = 1/(2\pi \tau_{RC})$
where τ_{RC} is the RC time constant

$$\tau_{RC} = \frac{R_{VALVE}R_{LPA}}{R_{VALVE} + R_{LPA}} C \tag{73}$$

and where the volume capacitance is given as

$$C = V/P_\infty \tag{74}$$

With a breakpoint frequency of 100 Hz this results in a volume of

$$V = \frac{P_\infty}{200\pi} \left(\frac{1}{R_{VALVE}} + \frac{1}{R_{LPA}}\right) \tag{75}$$

For typical values of $R_{LPA} = 10^8$ Pa/(m^3/s), $R_{VALVE} = 10^9$ Pa/(m^3/s), and $P_\infty = 1.01 \times 10^5$ Pa, $V = 1.77 \times 10^{-6} m^3$ or a volume of 1.77 cm^3. This is fairly small, hence, any reasonable volume of several centimeters dimensions will provide more than adequate filtration.

With this nulling filter circuit as the load on the opposite control, the opposite side control pressure is a constant essentially equal to the blocked control bias pressure. This pressure is determined from the static characteristics of the LPA as determined by this author previously[6] and shown in figure 63. This program has been amended and rewritten in FORTRAN and the current dynamic analysis has been incorporated. The static analysis program is required to compute the various resistive parameters required herein. The complete listing is given in Appendix II. As can be observed from figure 63, the blocked control pressure is available from the centered jet input characteristic when FLOW = 0. This normalized pressure is -0.06 or -6% of supply pressure.
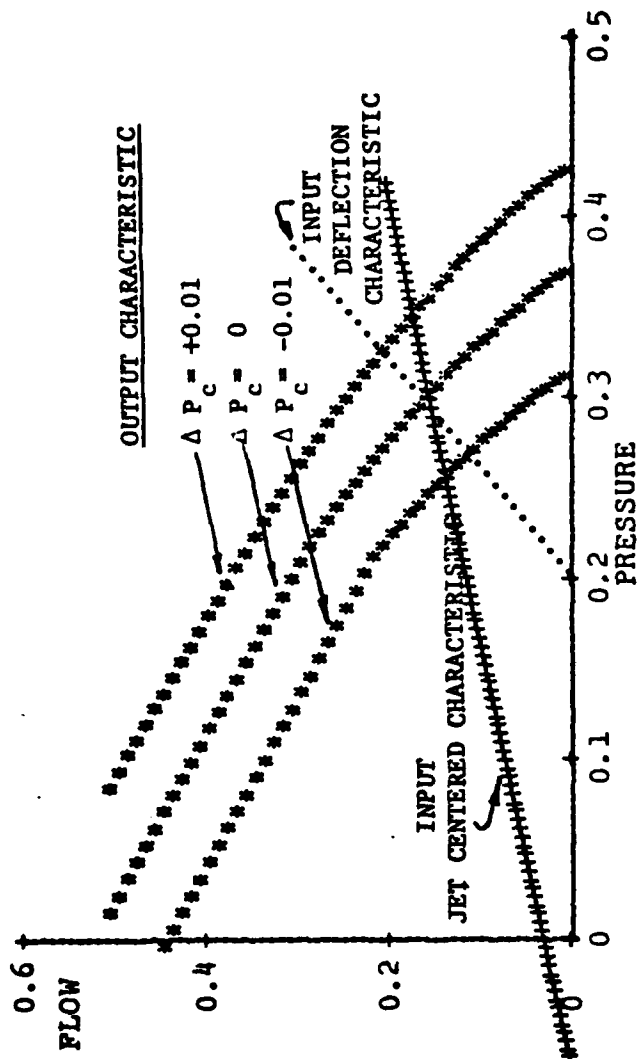
$RV = 2.283, NR = 355.5, NR' = 100.0, AR = 3.000, BC = 1.50, BT = 1.25, XSP = 8.00, CD = .708$

SELF-STAGED DEFL. RESIST. =   0.600
SELF-STAGED OUTPUT RESIST. =   -0.556
BLOCKED GAIN AT SELF-BIAS =   8.288
SELF-STAGED BIAS =   0.294
SELF-STAGED GAIN =   4.299

Figure 63.   Computer plots and printout for the static performance characteristics of a high aspect ratio
($\sigma = 3.0$) HDL standard LPA as computed by Drzewiecki's program.

3.2.3 Signal Transmission

It has already been demonstrated that audio signals can be transmitted over a distance of 10 m. It is now of concern to actually determine the distance required in a combat vehicle. The choice of vehicle is somewhat arbitrary, and since this author is involved and familiar with the M60 class of tanks, an M60 tank is chosen for this problem. Figure 64 shows the side and top views of an M60. The longest distance occurs between the driver in the front and the commander who sits up high in the turret. The straight line distance is 2 meters but allowing for bends and detours, 5 meters is the maximum distance encountered. It has been established that elastic tubes add considerable signal attenuation due to the added compliance, hence, they are ruled out. But even if not for that reason, elastic tubes act as antennas to motion since small geometric changes can induce pressure signals. Copper tubing was used in the feasibility demonstration; however, copper is expensive and relatively soft. For this reason rectangular cross-section wave guide was chosen. Studies on audio transmission through rectangular ducts indicate that circular duct analysis can be used if the hydraulic diameter is utilized. The hydraulic diameter is

$$d_h = 2\ bh/(b + h) \tag{76}$$

hence, in the present case $d_h = 1.667$ cm, and the attenuation from equation (70) is 1.8 db/m or 9.0 db for a 5 m length. It is desirable to keep the losses as small as possible since more losses are expected in connections and area mismatches.

3.2.4 Amplification

Randall[42] states that the ear is best attuned to understanding and intelligibility when the sound pressure level to the ear is about

6.93 m

STOWAGE BOXES

TURRET

DRIVER'S HATCH

GRILLE DOORS

US ARMY 983488

TRACKS

AIR CLEANER

SUSPENSION

USA REGISTRATION NUMBER

DRIVER'S CONTROLS AND INSTRUMENTS

PERSONNEL HEATER

FUEL TANKS

TRANSMISSION

FIXED FIRE EXTINGUISHER

AMMUNITION RACKS

ENGINE

FINAL DRIVES
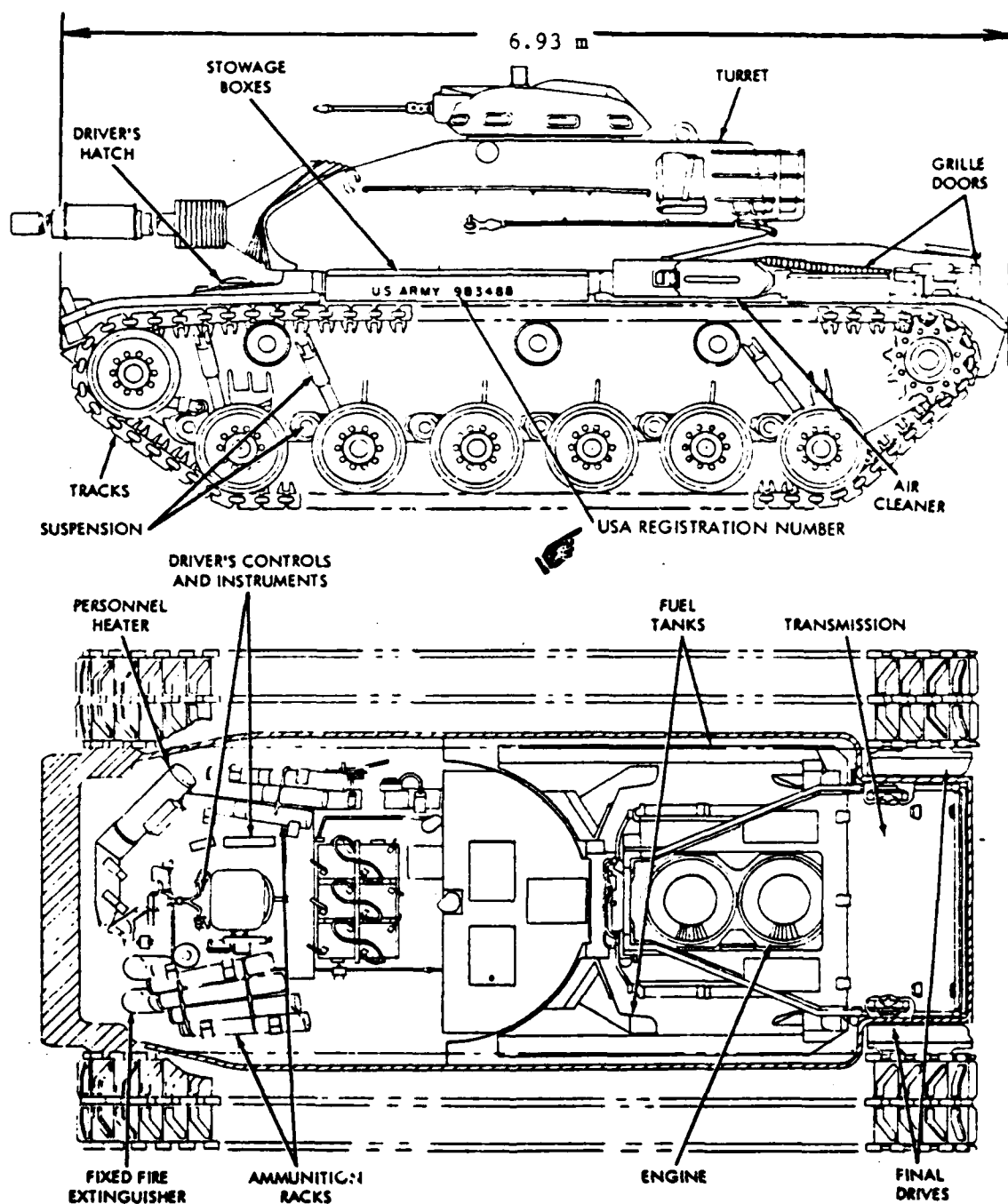
Figure 64. Side and top views of an M60 tank.

b ref. 0.0002 μ bar. The sound pressure level in a tank is about
db, but within the ear protection devices it is down 15-20 db at
ᴐ. Randall[42] further states that a certain background level must
ᴄceeded for intelligibility as shown in figure 65.
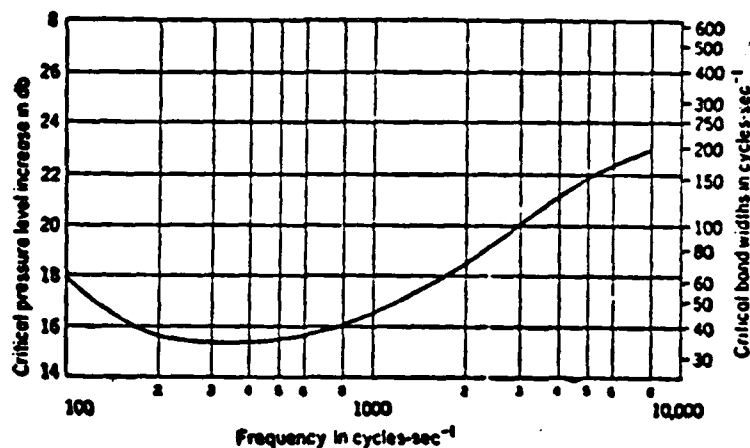
Figure 65. Increase of sound pressure level over a masking
background noise due to Randall[42].

the speech spectrum 100-3000 Hz the increase varies from a low
5 db to a maximum of 20 db. For engineering purpose then consider
signals must be a minimum of 20 db above the background noise to
nderstood and, say, 26 db (an extra factor of two) to include a
ᴄy factor and to prevent straining. Thus the signal to the ear
be at about 106 db. The input signal is at a similar level,
ᴄb, so that the amplification required must overcome only the losses.
Typically, losses are mainly due to area changes, and acoustic
ᴄs occur proportionately to the area change. Upon expansion, sound
ᴄre level is lost due to the Bernoulli effect--the velocity decreases.
ᴄhe area decreases, reflections are the main cause of signal
      Exponential horns reduce the losses considerably between tube

sections; however, the main losses due to area changes occur at the fitting as the circular cross-section changes to the planar cross-section. Assuming that the overall losses are minimized to the acoustic attenuation in lines, then the losses into an LPA can be characterized as ζ_{LPA}

$$\zeta_{LPA} = A_{FITTING}/A_{CONTROL} \tag{77}$$

where $A_{FITTING} = \pi d_f^2/4$, d_f is the internal diameter of the control port fitting which is usually made equal to the maximum width of the control. ζ_{LPA} is a measure of the energy allowed to pass into an LPA assuming that the incident energy is reflected back from the mismatched area. This can be seen on the drawing of the LPA in figure 77. The area of the control, $A_{CONTROL}$, is the maximum width, d_f, multiplied by the depth, $h = \sigma b_s$, hence the losses are

$$\zeta_{LPA} = \pi d_f/4b_s\sigma \tag{78}$$

For the standard LPA, however, $d_f/b_s = 4.65$ so that the input losses are

$$\zeta_{LPA} = 3.65/\sigma$$

where as expected the losses decrease with aspect ratio. This same ratio occurs on the outputs, hence, an engineering figure of merit can be obtained using $\zeta_{LPA} = 7.3/\sigma$ for the whole LPA.

The input tubing from the "throat mike" is 3.175 mm diameter so that equation (70) gives a loss of 9.6 db/meter. A 1.0 m section is used to connect to the transmission line to allow freedom of movement. Similarly, if a 1.0 m line of the same dimensions is used to transmit

115

the audio from the amplifier to the ear, then the total line losses
are 28.2 db. The loss in the LPA will depend on the aspect ratio of
the device. Taking a worst case of $\sigma = 0.6$ the loss will be 22 db. To
summarize then, if the output power is to equal the input power the
net amplifier gain must equal the sum of the losses, that is:

$$G_p = \zeta_{LPA} + \zeta_{transmission} + \zeta_{input} + \zeta_{output} + \zeta_{safety\ factor}$$
$$= 22.0 + 9.0 + 9.6 + 9.6 + 6.0 = 56.2$$

The gain of the LPA must therefore equal the predicted losses or
$G_p = 56.2$ db ($G_p = 630$) if a factor of 2 (6 db) is added to ensure
that there is sufficient bandwidth to pass audio. At very low fre-
quencies, of course, the losses are negligible so that not much dc
gain is needed.

The development of a gain block proceeds essentially from a static
analysis of single amplifiers. A three-stage self-staged gain block
will have a blocked gain of roughly 200, and a self-loaded gain of 125.
In any event an additional gain of less than 10 will put the device at
a gain greater than required here. The range of choices of staging
schemes is quite large. If one wishes to maximize dynamic range, then
each succeeding stage should be of a lower aspect ratio and operate at
a higher pressure as described by Manion et al[4] and Drzewiecki et al[5].
In such an arrangement a gain of 630 can easily be achieved in three
stages. Such a gain block can be constructed using the simple engineer-
ing guide lines given below for the HDL standard LPA:

1. The operating point is $\sigma N_R = 10^3$
2. At the operating point $c_d = 0.7$

3. The Reynolds number is $N_R = 1000\ b_s$ (mm) $\sqrt{P_s\ (mmHg)}$
4. The operating pressure is in mmHg

$$P_s = \left(\frac{N'_R}{120}\right)^2 \frac{1}{\sigma^2}\ \frac{1}{b_s^2} \ , \text{ where } b_s \text{ is in mm.}$$

5. The operating flow in LPM is

$$0.3 \ (N'_R/120)(b_s/0.5) = Q_s$$

6. The supply resistance is in mmHg/LPM

$$R_s = P_s/Q_s = 13.3 \ (N'_R/120)(1/\sigma)^2 \ (0.5/b_s)^3$$

7. The input resistance is

$$R_I = 0.75 \ R_s$$

8. The output resistance is

$$R_o = 0.5 \ R_s$$

9. The blocked gain is $G_{pB} = 10.0$

10. The loaded gain is

$$G_p = G_{pB} \ (1/(1 + R_o/R_L))$$

11. The saturation output signal is twice the pressure recovery where $P_R = 0.35 \ P_s$

The above are based on geometric similarity and Reynolds number scaling with a standard reference

$$b_s = 0.5 \ mm$$

$$\sigma = 1.0$$

$$N'_R = 120$$

$$P_s = 4 \ mmHg$$

$$Q_s = 0.3 \ LPM$$

and the results of the static computer program[6].

From this design guide it is apparent that staged gain is maximized when the load impedance is large compared with the output impedance. Dynamic range is the ratio of maximum input signal to minimum detectable input signal. This is similar to signal-to-noise ratio. If a staging arrangement is chosen so that the last stage saturates before first stage saturation occurs, then the first-stage dynamic range is reduced since the maximum output is limited to that which saturates the last stage. Dynamic range therefore is maximized when each succeeding stage saturates at the same time. This means that the saturation output of each preceeding stage should be sufficient to saturate its load stage so that with a gain of G_p, the output pressure of the $(n - 1)$ stage is related to the nth stage by:

$$P_{o(n-1)} = P_{on}/G_p$$

and since the supply pressure is related to the output saturation pressure, then

$$0.7\ P_{sn}/G_p = 0.7\ P_{s(n-1)}$$

so that $P_{s(n-1)} = P_{sn}/G_p$ or with $G_p = 10$ each succeeding stage must operate at a pressure equal to 10 times the latter stage. From guideline 4 the different aspect ratios can be determined

$$P_{s(n-1)} = (1/\sigma_{n-1})^2\ (1/b_{s(n-1)})^2 = (1/\sigma_n)^2\ (1/b_{sn})/G_p$$

so that for the same size $(b_{sn} = b_{s(n-1)})$

$$\sigma_n/\sigma_{n-1} = \sqrt{1/G_p} \simeq 0.3$$

Now the limit on aspect ratio is generally kept at $\sigma = 0.3$ for below this value gain and other characteristics are adversely affected due to viscous boundary layer losses. Hence, the last stage minimum is

$$\sigma_n = 0.3\ ,\ \text{then}\ \sigma_{n-1} = 1.0,\ \sigma_{n-2} = 3.3,\ \sigma_{n-3} = 11.0,\ \text{etc.}$$

It becomes clear very quickly that beyond three stages of the
same size the first stage aspect ratio is   large requiring a very low
pressure, perhaps beyond the realm of practicality. If the ratios of
aspect ratio are not optimum, then dynamic range is sacrificed and the
last stage will saturate before the first stage.

A three stage gain block of maximum dynamic range will have a
gain approaching 10^3 (60 db). Guideline 10 is used where

$$R_o/R_L = R_{o(n-1)}/R_{in} = 0.5 \, R_{s\,(n-1)}/0.75 \, R_{sn}$$

$$= 0.667 \, (\sigma_n/\sigma_{n-1})^2 = 0.0667$$

so that $G_{p\ total} = G_{p1} \, G_{p2} \, G_{p3B} = G_{pB}^3 \, (.9375)^2$

where the last stage is blocked so that a net gain of $G_p = 879$ is achiev-
able. Notice, however, that three separate pressures must be supplied.

If one pressure were supplied, thus eliminating manifolding and
reducing resistors to reduce line pressure, the load impedance ratio
would be self-staged $(R_{s1} = R_2 \ldots)$

$$R_o/R_L = 0.5 \, R_s/0.75 \, R_s = 0.667$$

so that a three-stage block would have a gain of 360 and a four stage
blocked gain of

$$G_{P_{total}} = G_{p1} G_{p2} G_{p3} G_{p4} = G_{pB}^4 \, (0.6)^3 = 2160$$

and self-loaded gain of 1296. This, then, allows a degree of flexibility
in the choice of circuit topology (choice of staging schemes) since either
3 or 4 stages can do the job.

Now the choice of size and aspect ratio must be involved with the
frequency response. Notice that a single stage response as shown in
figure 40 and 41 has useful gain out to a normalized frequency of
$F = 0.1$; however, there are regions of low gain which, when amplified
in multiple stages, cause considerable degradation. For example, the
low gain region between $F = 0.01$ and $F = 0.05$ is down only 5 db in a
single stage, but in a self-staged, four-stage block this will be down
20 db (a factor of 10). This is clearly undesirable. The gain should
be as uniform as possible over the desired bandwidth while non-uniform
high frequency gain beyond say 4 kHz may enhance, picking up and
transmitting some higher harmonics. The bandwidth chosen here is that
of a telephone, 3 - 4 kHz, since this is all that is required for in-
telligibility and individual recognition. The voice spectrum is down
14 db at 4 kHz so that if the amplifier is down, say 5 db at that point,
the signal should be still clear. The single amplifier transfer function
can be expanded to consider a multiple amplifier configuration by suc-
cessive multiplication of the transfer function for successive amplifiers.
In the self-staged case for moderate vent inductance (say due to extra
manifolding, $L_{V1} = 1.0$) a four stage frequency response is shown com-
puted in figures 66 and 67. The gain is down 6 db at a frequency of $F = 0.012$. However, in the maximum dynamic range case, each succeeding
stage has a higher actual frequency response so that when the first
stage is rolling off, no succeeding stage is yet doing so. In such a
case the -6 db point of a single amplifier can be used to determine the
bandwidth. From figure 42 the -6 db point occurs at about $F = 0.03$.
There can be considerable advantage to using the maximum dynamic range
scheme if the first-stage is the same as that in the self-staged com-
ponent. Not only is bandwidth increased, but also phase shift is re-
duced since most of the phase lag will occur in the slow first stage.
A three-stage gain block with a lower aspect ratio fourth stage can also

120

FREQUENCY RESPONSE OF AN LPA
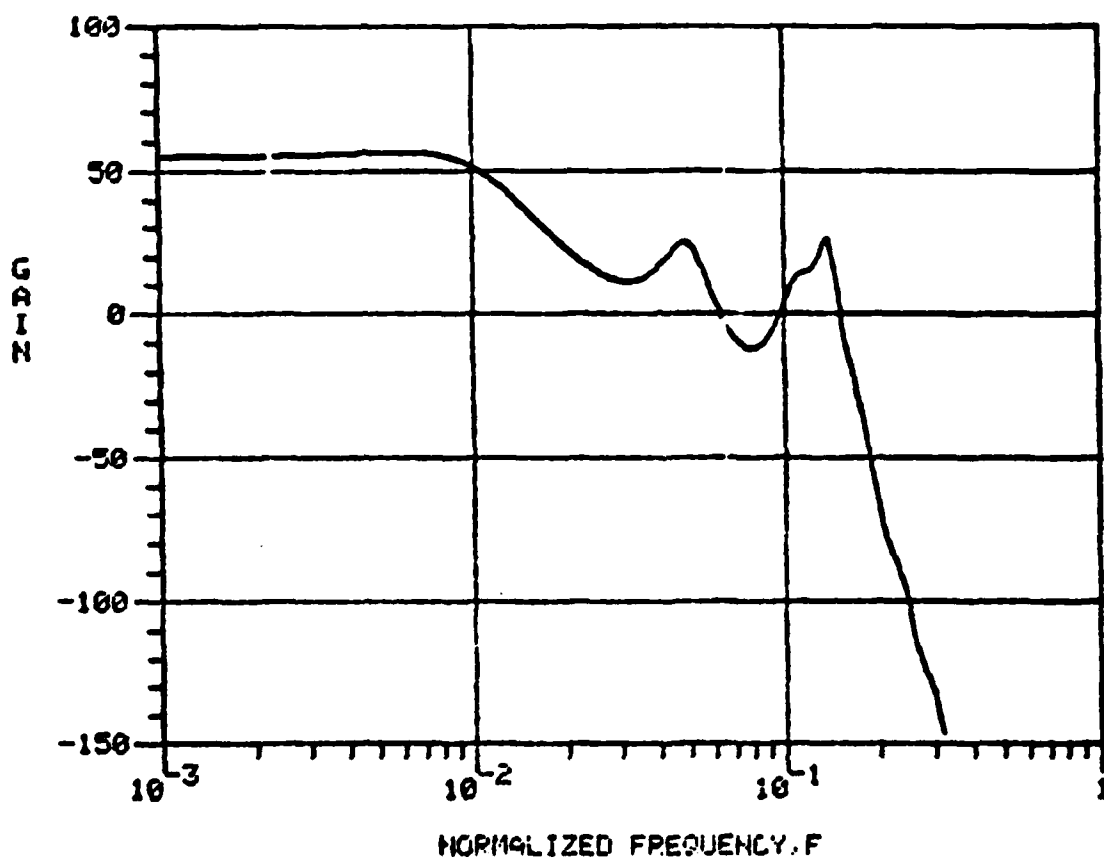
Figure 66.   Frequency response of a four stage, self staged LPA (gain only)
(theoretical).
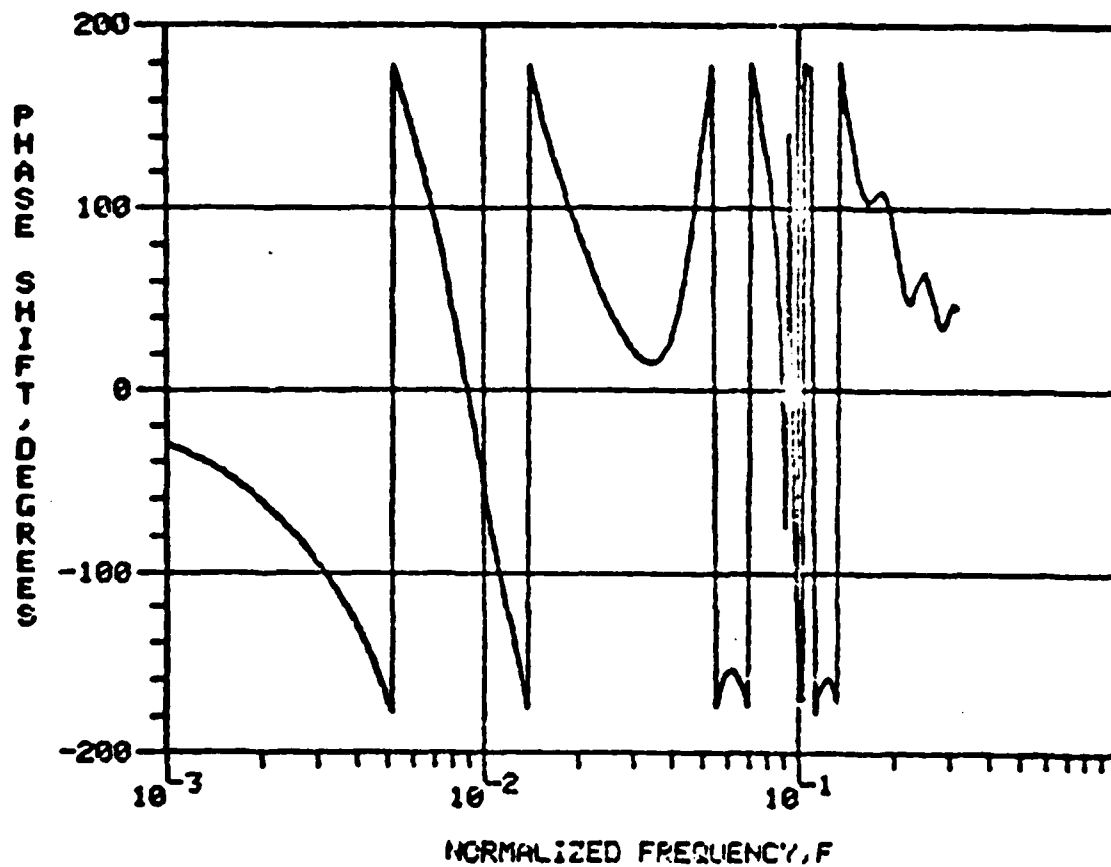
Figure 67. Frequency response phase shift of a four-stage,
self-staged LPA (theoretical).

(Note: In order to display the phase angle within
the bounds of the figure, ±360° has been added to
the results, where necessary.)

122

Increase the actual bandwidth in that the normalized frequency for three stages is F = 0.015 as can be deduced from the -6 db point from figure 68. With this one can deduce a function for the usable bandwidth of a gain block whose frequency response is limited by a different number of stages. This is shown in the log-log plot of figure 69.

The three stage gain block would require a first stage aspect ratio of σ = 3.3 if the normalized bandwidth is F = 0.03, or f_{bw} = 300 $\sqrt{P_s \text{ (mmHg)}}$ /b_s (mm). For σ = 3.3, P_s = 0.6 and 2.5 mmHg respectively for b_s = 0.5 mm and b_s = 0.25 mm. In the case of the smaller and higher frequency device, the bandwidth is only 1.9 kHz and, hence, not acceptable. For a four stage gain block whose first three stages are a selfstaged pre-amplifier, the limiting bandwidth would be

$$f = 150 \quad P_s \sqrt{\text{(mmHg)}} / b_s \text{ (mm)} \tag{82}$$

so that for f = 3000 Hz, P_s = 25 mmHg when b_s = 0.25 mm or σ = 0.8 and P_s = 100 mmHg when b_s = 0.5, or σ = 0.25. This latter case is beyond the limit for laminar operation and also an undesirably low aspect ratio. This analysis then shows that the size of the device should be smaller than b_s = 0.5 mm. The next size down that is readily available is b_s = 0.25 mm. The Corning 3-stage device of figure 57, σ = 1.5 and b_s = 0.25, is down 6 db at 2000 Hz at P_s = 8 mmHg. From the above theoretical equation we get 1700 Hz which is slightly low but still reasonably close. However, the theory is conservative and slightly underestimates bandwidth, so that higher aspect ratios can be used than predicted.

As a compromise therefore, let the preamplifier be of aspect ratio σ = 1.2 that operates at P_s = 10 mmHg. It is important to reduce the supply pressure on the initial stages so as to reduce power supply flow noise, which can be amplified by later stages when the common

FRECUENCY RESPONSE OF HI LPH
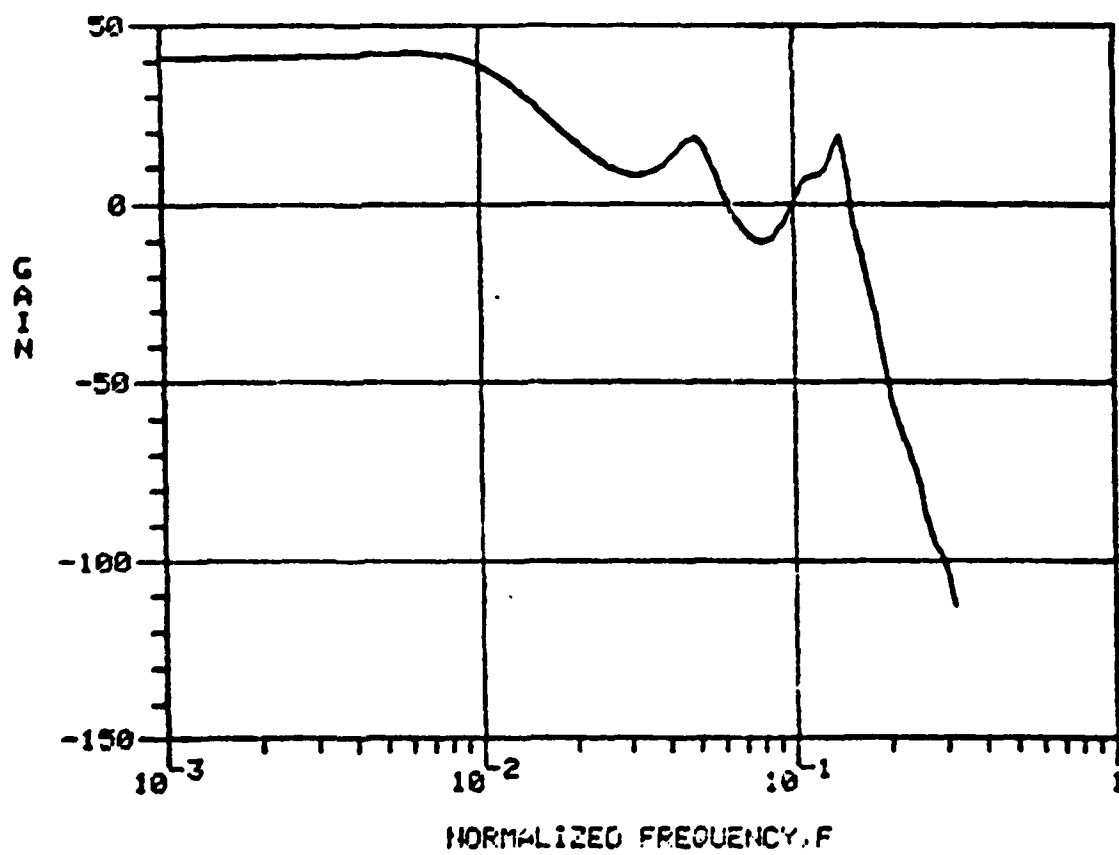
Figure 68. Gain frequency response of a three stage, self-staged LPA (theoretical).
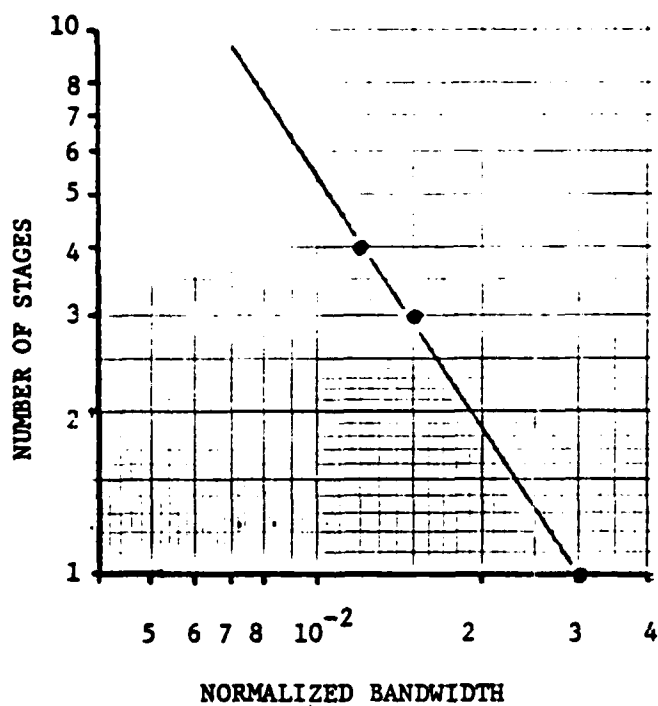
Figure 69.   Engineering guide for uniform bandwidth as a function of
number of stages that determine cutoff frequency.

mode rejection ratio is not infinite.[†] It is for this reason then
that it is desirable to operate at as high a first stage aspect ratio
as possible. The last stage is made to be aspect ratio $\sigma = 0.8$ since
its one-stage bandwidth is 6000 Hz and well above affecting the overall
bandwidth. Two such amplifiers in parallel will thus allow the ad-
dition of acoustic signals as described in section 2.3, figure 55
for some increased output. The two in parallel will load down the
pre-amplifier, but there still will be sufficient gain.

The gain of a four-stage amplifier comprising a three-stage pre-
amplifier of $\sigma = 1.2$ and an acoustic power amplifier of $\sigma = 0.8$ will
have a gain

$$G_p(4) = G_{pB}^{4} (0.6)^2 (1 + \frac{R_{o3}}{R_{14}})$$

but R_{14} will be one half of a single $\sigma = 0.8$ or

$$\frac{R_{o3}}{R_{14}} = \frac{2.2}{3} (\frac{\sigma_4}{\sigma_3})^2 = 0.593$$

and $\quad 1/(1 + R_{03}/R_{14}) = 0.63$
so that

$$G_p(4) = G_{pB}^{4} (.6)^2 (.63) = 2268$$

or a value just slightly greater than a four-stage self-staged device,
but with more dynamic range and bandwidth.

Just such an amplifier was constructed with photochemically metal
etched laminations that were over-etched slightly. The result was that
the blocked gain was 8.0 so that theoretically a four stage blocked gain
of 930 should have been recorded for the whole block and 110 for the
preamp. Figure 70 shows the pre-amplifier dc transfer characteristic as

---

[†] Common mode rejection ratio is a measure of the insensitivity of the
LPA to identical signals applied simultaneously to both controls.

126
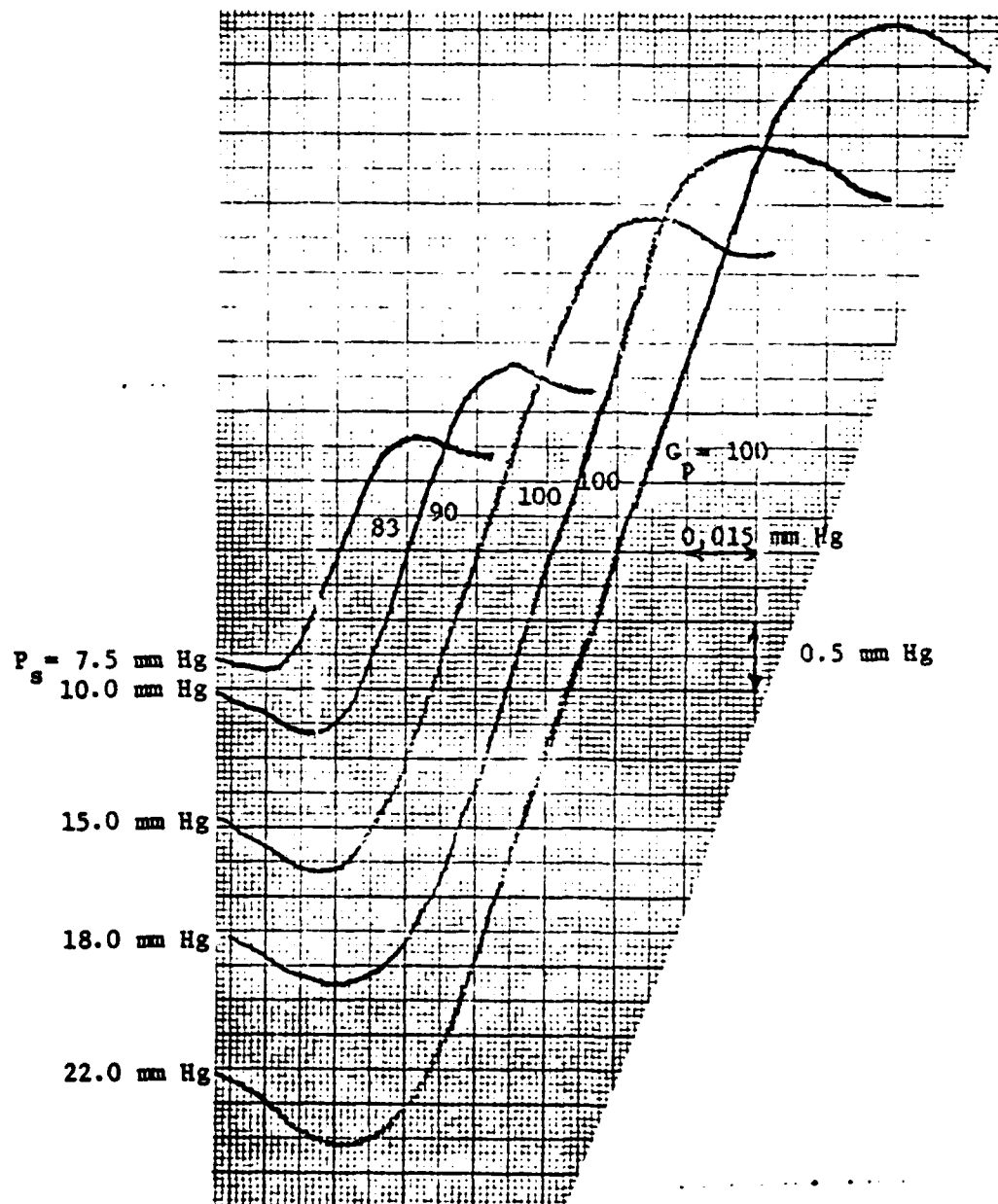
Figure 70. Experimental data for differential output pressure versus differential control pressure for the $\sigma = 1.2$ pre-amplifier. (Slope is the gain $G_p = dP_o/dP_c$)

taken on an x-y recorder with different supply pressures and G_p is seen
to be just over 100 so that with a last stage of gain of 8.0, 800 overall
gain can be achieved. (Note that the overall transfer function was not
measured at dc because a high pass filter is incorporated in the stack,
as will be discussed in the next section, which is an L-R shunt to
ground between the pre-amp and the last stage.) The Bode plot will be
shown later but the extrapolated dc gain is indeed about 58 db as de-
sired. A schematic of the gain block and manifolding is shown in figure
figure 71.

3.2.5 Signal Processing

It has already been mentioned that a high pass filter is to be
used. The purpose of this device is to remove unwanted low frequency
rumble and harmonics of 60 Hz found in machinery. Additional low
frequency (less than 800 Hz) noise comes from the engine and the
harmonics of the hull motion of the tank such as the suspension re-
sonances. A high pass filter in acoustics is merely an open ended
tube that is short compared with the wavelengths of the frequencies
to be considered. The tube segment can then be treated as a single
lumped inertance and parasitic resistance. When placed between two
stages of an LPA gain block, the output impedance of one stage and
the input of the next form the branches of a "tee" circuit. For low
frequencies, as before, treat these as resistances and the equivalent
circuit appears as in figure 72.

L-R SHUNT

$P_s = 24$ mm Hg

LAST
STAGE
SUPPLY

COVER PLATE

OUTPUTS

SEPARATOR TRANSFER PLATE

AMPLIFIER LAMINATIONS
AND VENTING MANIFOLDS

COVER PLATE

INPUT

SUPPLY DROPPING
RESISTOR

$P_s = 10$ mm HG

PREAMPLIFIER SUPPLY

— — — — SUPPLY PATH

———————— SIGNAL PATH
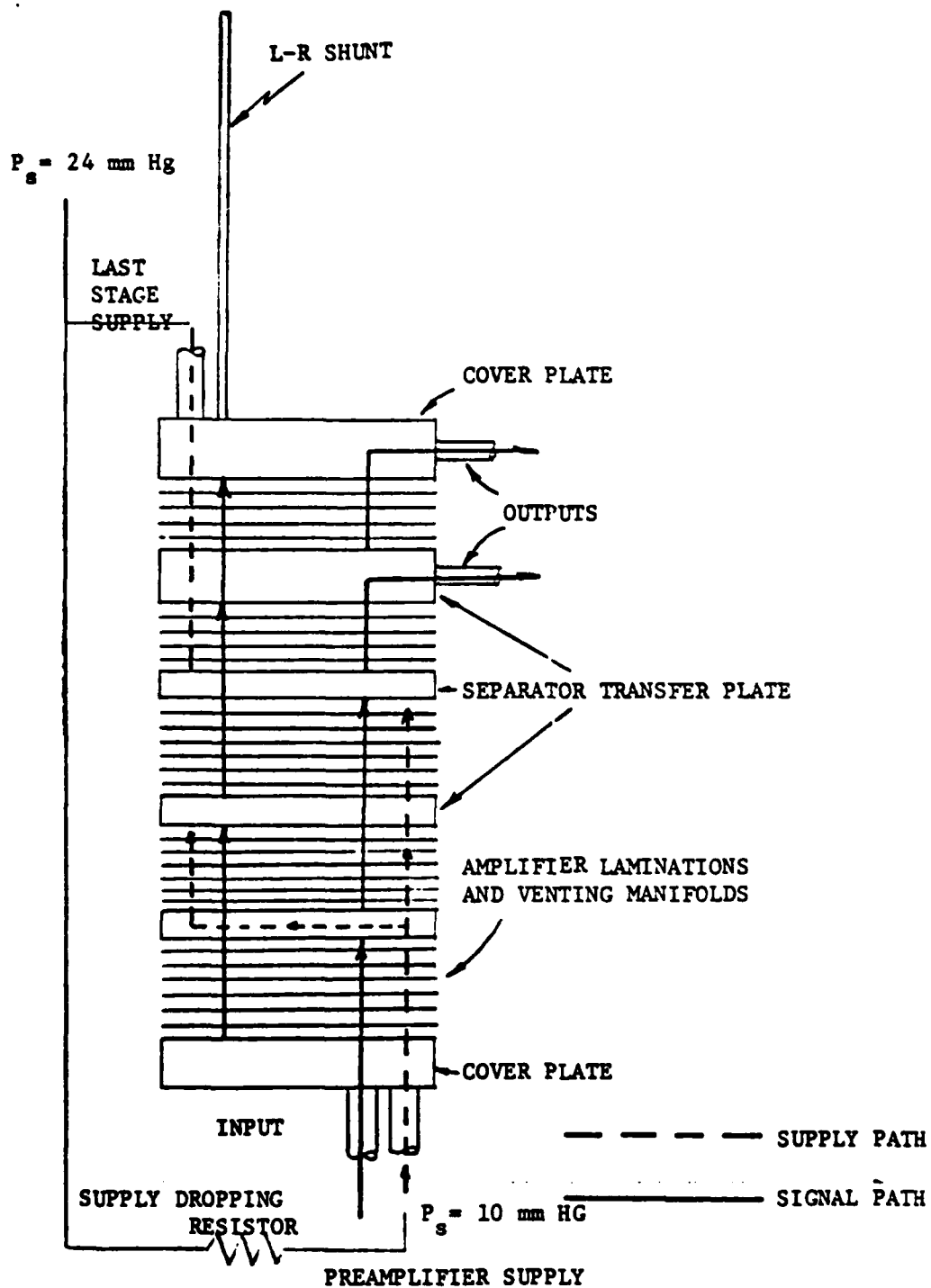
Figure 71. Schematic drawing of the four stage audio amplifier.
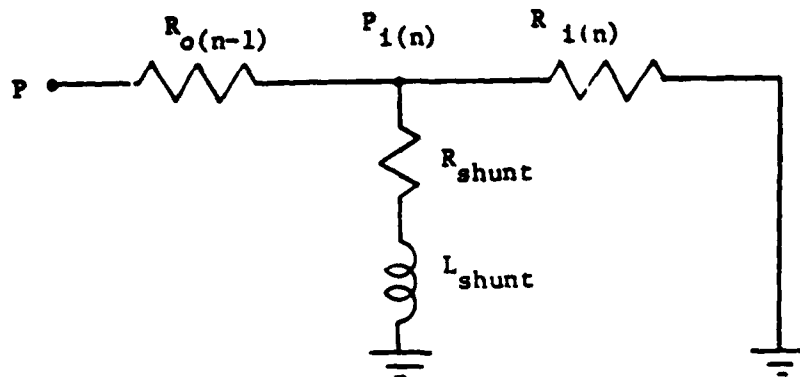
Figure 72. Equivalent circuit for an inductive shunt, high pass filter.

The input pressure to the last stage will be within 6 db of the pressure without a shunt when the magnitude of the shunt impedance equals the input resistance.

$$\sqrt{R_{SHUNT}^2 + L_{SHUNT}^2 \omega^2} = R_I$$

so that $\omega = \sqrt{R_I^2 - R_{SHUNT}^2}/L_{SHUNT}$ (83)

Since $L_{SHUNT} = \rho \ell / A_{SHUNT}$, the desired frequency $f = \omega/2\pi = 1000$ Hz and the area is the area of a control port fitting $A_{SHUNT} = d_f^2/4$ where $d_f = 1.2$ mm for a half-size device with $b_s = 0.25$ mm, then the length of tube required is 8.4 cm if the input resistance of two parallel amplifiers $\sigma = 0.8$ is $R_I = 5.6 \times 10^8$ Pa/m³/s. The shunt resistance $R_{SHUNT} = 8 \mu \ell / \pi r^4$ is very small compared with R_I. The frequency at which the length dimension is a half wavelength is about 2 kHz. At this frequency the acoustic signal leaving the shunt will

cause a rarefaction wave to be reflected back and will put a notch in the input signal.† The notch must be moved to a higher frequency to avoid interference with audio transmission. This can be done by halving the shunt length and area. The inductance remains the same, but the resonant frequency is doubled.

The final high pass filter then is a tube 4.0 cm long and 0.85 mm in diameter. With this filter installed between the pre-amplifier and the last stages, an additional benefit accrues--the d.c. signal is shorted to ground, hence, d.c. null offsets are eliminated preventing the saturation of the last stage due to asymmetries in the pre-amplifier. Figure 73 shows both a photograph of the final hardware of the gain block and its ultimate frequency response. Notice that the Bode plot is not very different from the Corning gain block except for the high pass characteristics at low frequencies and that the bandpass is greater. As pointed out in the previous section, the bandpass gain is about as expected and actually a bit higher due to the operation on the slight hump in the vicinity of $F = 0.01$.

Signal conditioning or processing also involves the conditioning of the power supply. As a general rule it is desirable to remove noise from the supply flow. This is normally done with a low-pass filter or a tank in-line with the supply flow. The dimensions are essentially the same as for the low-pass on the opposite control. Further conditioning is required if the power supply itself generates a particular frequency. In such a case a notch-filter using for example a blocked, resonant line tuned to the undesired frequency will additionally remove fluctuations of this particular frequency. Section 3.2.7 will discuss the power supply in detail.

---

† This is the basis of a notch filter temperature sensor described by Drzewiecki et al.[45]

131
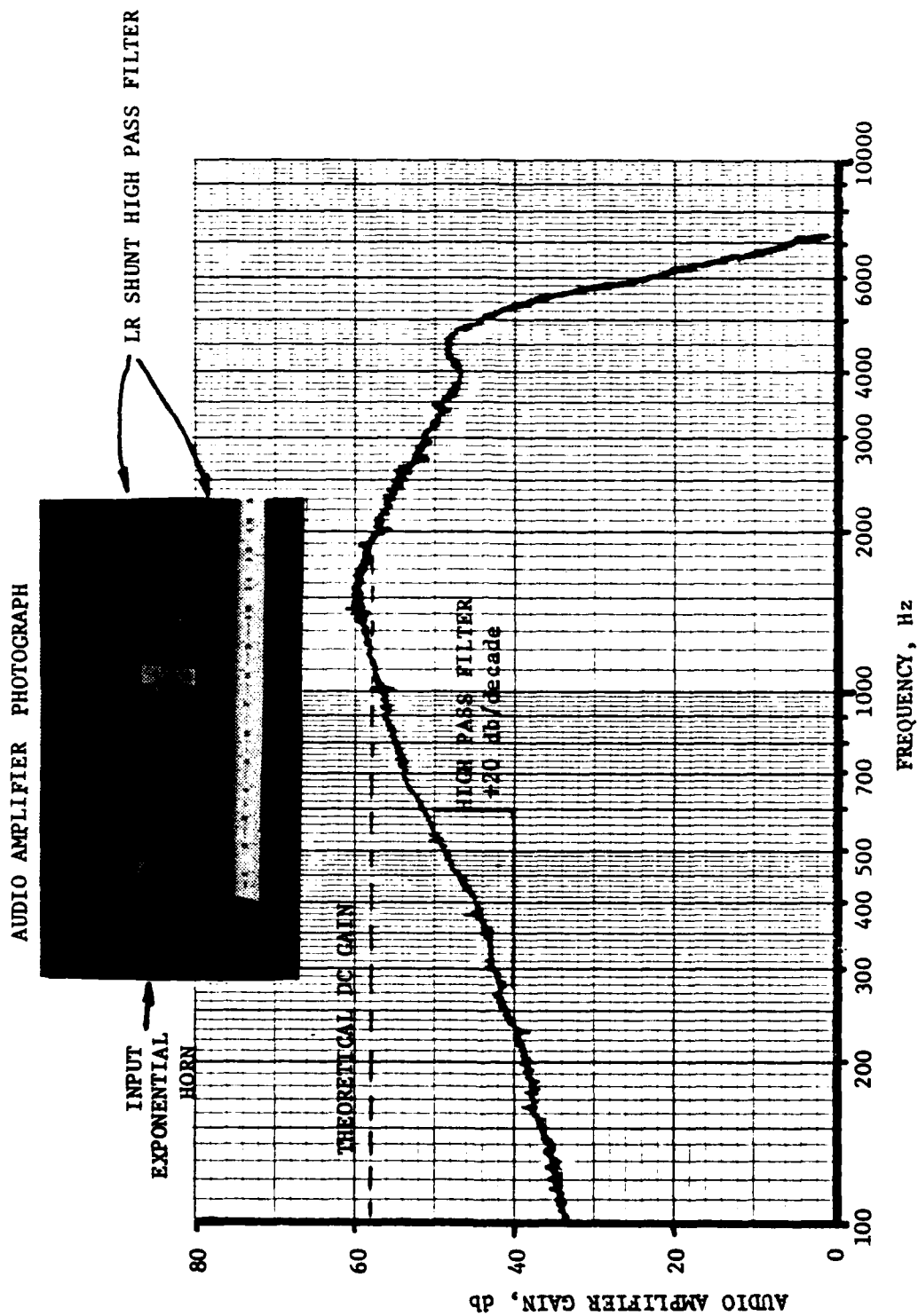
Figure 73. Experimental BAFCO Bode plot of the audio amplifier frequency response at $P_s = 22$ mm Hg.

3.2.6 The Output

The output is composed of the transmission lines from the audio
amplifier to the termination at the ear. The two types of terminations
considered have been discussed previously as direct termination in
the ear or termination in the volume of an ear protector through an
exponential horn. In either case the response is affected by the
resonances set up in the line. The effect is quite pronounced when
the terminations are direct; whereas, with the horns, reflections are
minimized. The low end cut off frequency of an exponential horn is
determined by its length. For a length less than a quarter wavelength,
low frequencies are reflected and a mismatch occurs.   The cutoff for
the 8 cm long horns described previously is 1 kHz. Since the band
pass is to be about 1 - 4 kHz, this horn is adequate.

Both types of outputs have been adopted. The horns are mounted
in helmets while the headsets can be used without the helmet when it
is not desirable to wear it. A photograph of the complete intercom
system (without power supply) is shown in figure 74.

3.2.7 The Power Supply

In any powered vehicle there is normally a source of pneumatic
pressure already available from the engine in the form of a manifold
vacuum or compressor bleed. In any event, either mechanical or elec-
trical power is available to drive a pump. The power supply require-
ment for the audio portion is miniscule. A two-way circuit composed
of ten   amplifiers that consume 0.15 LPM of flow each and are
supplied from a 22 mmHg source require 73 milliwatts. Considering
that the supply is regulated and that say 10 kPa are driving the same

HELMET

AUDIO AMPLIFIER OUTPUT TUBE

THROAT MICROPHONE

AUDIO AMPLIFIER INPUT HORN
AUDIO AMPLIFIER

OUTPUT HORN

SPEECH INPUT TUBE
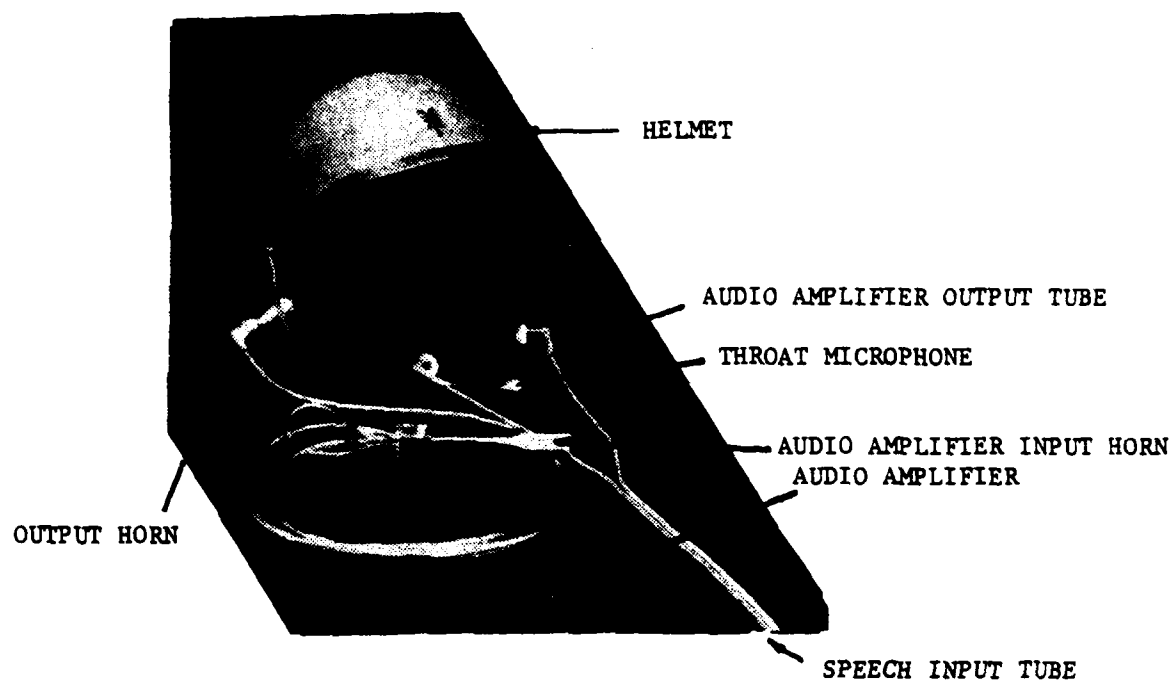
Figure 74. Photograph of the audio portion of the fluidic voice
communication system installed into a tankers helmet.

1.5 LPM, then 0.25 watts are required. If the data link circuit has the same order of magnitude requirement, then with a factor of safety of 2, a 1-watt supply is more than sufficient. This is a very small drain on the total vehicular system no matter which power source is used. For that matter human breath would be sufficient to operate the system in a pinch.

The question arises then which power source to use? Obviously, the system must work when the engines are off. This eliminates direct bleed from the engine. The engine could be used to charge an accumulator tank, however. This is very attractive since this approaches operating from bottled gas which is a very quiet power source. An accumulator, however, would be large and have to be pressurized quite high in order to provide long term power. In addition, a compressor would be required that delivers the high pressure. This is a distinct disadvantage. On the other hand, operating off the main batteries would be easy and, as pointed out above, would require little power drain.

Vibrating diaphragm, industrial grade air pumps are available in many sizes and are generally low cost. One such pump is manufactured by a company called WISA. The series 120 pumps shown in figure 75 and whose characteristics are given in figure 76 amply satisfy the pneumatic requirements set forth here. Electrical consumption is 4 watts. The model 120 is a pressure output pump that puts out over 15 kPa at a rated flow of 1.5 LPM which will be sufficient to drive a regulator (if desired) and the complete system. As it turns out, if the voltage is fixed to the pump and the load is fixed--as it will be, then the system supply pressure will be constant without the need of a regulator. Since d.c. drift does not affect the operation because of the high pass output filter used, small variations in supply will not materially affect the operation. Bandwidth is proportional to the square root of supply pressure so that variations in

Model 120

dimensions: area of base = 158 x 67 mm,
height = 80 mm, weight = 1.00 kilogram
dimensions without casing: area of base = 130 x 42 mm,
height = 50 mm, weight = 0.6 kilogram
consumption = 35 milliamp

Model 120

This is also a pressure pump, but smaller in size
and with a lower performance than Model 200.
This, of course, means a further saving in cost.
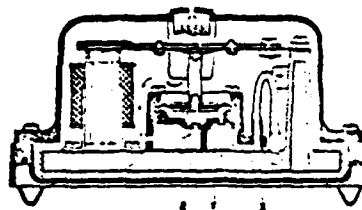
Model 120 VDS

This is a suction pump with these smaller dimensions.
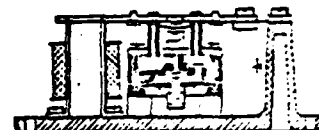
Model 120 VDS-vD

This is the same pump as before, designed for a
higher degree of vacuum. These two last-named
models are only available without casing, for incorporation.
The whole of the Model 120 series is suited to
constant running.

Figure 75. Physical characteristics of a WISA vibrating diaphragm pump
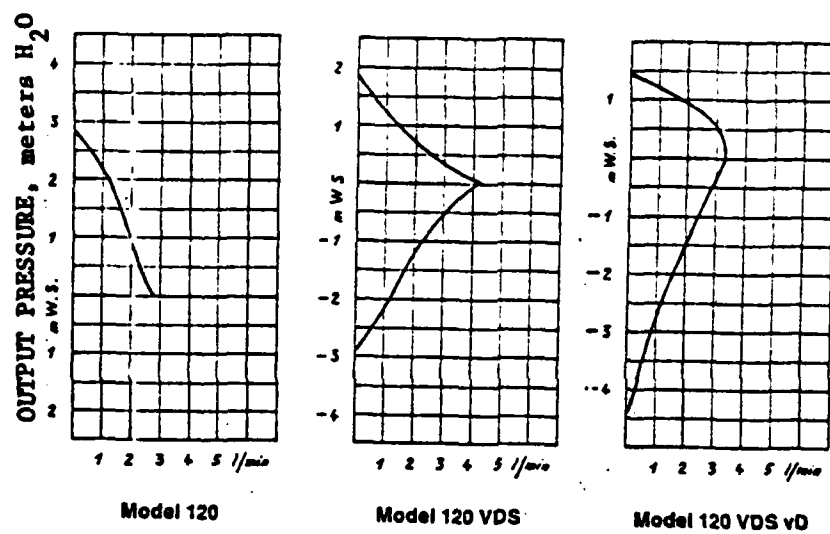
Figure 76.   Operating characteristics of the series 120 WISA pumps.

supply of as much as 10 percent will result in bandwidth changes of 5 percent or less. This is about $\pm$ 150 Hz and is tolerable.

The vibrating pump puts out a rippled pressure signal which is adequately damped out by a small volume tank and the volume and resistance in the supply lines. Notice that the preamplifier uses a dropping resistor to drop the common supply down. This fairly high resistance gives rise to a large time constant so that no ripple can be perceived at the output.

Although pumps and compressors are available, these industrial grade pumps (essentially aquarium-type pumps) have an extremely good history of reliability and low cost. They may operate continuously for several years (30,000 hours) and cost less than $30 each in quantity. These pumps have been extensively used by the HDL Fluid Control Branch for operating portable displays and the like with excellent results. For these reasons then, the WISA model 120 is chosen as the power supply for the system.

One should note here that this electrical component will not be adversely affected by EMI or radiation as would electronic components.

3.2.8 Interconnections

Two types of interconnections have been primarily discussed. Acoustic tee junctions and exponential horns. The tees are machined to maintain constant cross-sectional area. The horns, however, posed a problem, since machining various sizes to reduce or expand from the various size lines to fittings and so forth, would require mandrils or cams.

A simple solution was arrived at for the system put together in the laboratory. By heating a hard plastic tube over a given length

and then applying tension the heated portion will neck down into a shape
similar to that of an exponential horn. The large diameter is
chosen, and the neck down procedure is carried out until the desired
small diameter is achieved. Figure 74 shows the horn constructed in
this manner for the input to the audio amplifier. This does not appear,
however, to be a practical way of manufacturing metal parts that will
be required of a production system. Mandrils can be used then to cast
the desired shapes.

The output horns into the ear protection devices were available
as cast items from NASA, Langley Field, VA.

3.3 Human Engineering and Systems Engineering Considerations

Most good engineering design considers both the human and the
systems aspects of the problem by the very virtue of making a workable
system. Certainly if the intercom system caused unbearable discom-
fort, it would not be considered as a viable alternative. For this
reason wearer comfort has been considered. Unfortunately, the con-
straints of working with existing equipment, namely the standard issue
helmet, have not been conducive to ultimate comfort. Ideally, the
headset comfort of stereo headphones would be nice; however, only one
helmet type is manufactured. (The standard helmet will not fit people
with large heads, say size 7 5/8 and over.)

The current system uses an open-faced, boom microphone. This is
a mechanical protrusion in front of the face. While it in no way ob-
structs the field of vision when in the proper position, it does,
however, since it is moveable, offer the distinct possibility that it
can move up and obstruct vision and even poke at the face if pushed in,
say in a rough riding condition or a collision. The throat microphone

139

arrangement considered herein does not have these problems. It does, however, require the wearing of a device in addition to the helmet and may take a few seconds longer to put on and take off.

The output has been similarly considered. Attachment of tubes directly into the ear may be an additional chore or at least require manipulation of the ear protectors. This is really the device that can cause severe discomfort after wearing for a short time. Any one who has flown on a long trip on an airplane can attest to the fidgeting required to maintain comfort while watching the movie or listening to music. Operational suitability has to give way here to user comfort. The option is left for using insertion devices since it is simple to change over and because the fidelity of insertion devices is much better than that of the horns in the ear pads.

Since this system is envisioned as a backup to the standard system, it must be unobtrusive during non-use. This has been accomplished by the small size of the audio amplifiers. They can easily be made to fit in the standard interphone control box which has dimensions of roughly 15 x 10 x 10 cm. The laboratory outside dimensions of the audio amplifier are 1.5 x 2.5 x 2.5 cm. These dimensions can be reduced in an integrated bonded amplifier to 1.5 x 2.5 x 1.0 cm. An additional switch can be provided on the interphone control box, labeled for example "STANDBY" or "BACKUP," at the upper right corner of the commander's control box to turn on the air pressure to activate the system. The commander's control box is shown in figure 77. In such a way the fluidic audio system will readily integrate with the electronic system.

The only apparent hardware in the vehicle will be the transmission ducting. The commander, gunner and loader all sit within the cupola which rotates. The driver is in the tank hull. Emplacing the fixed
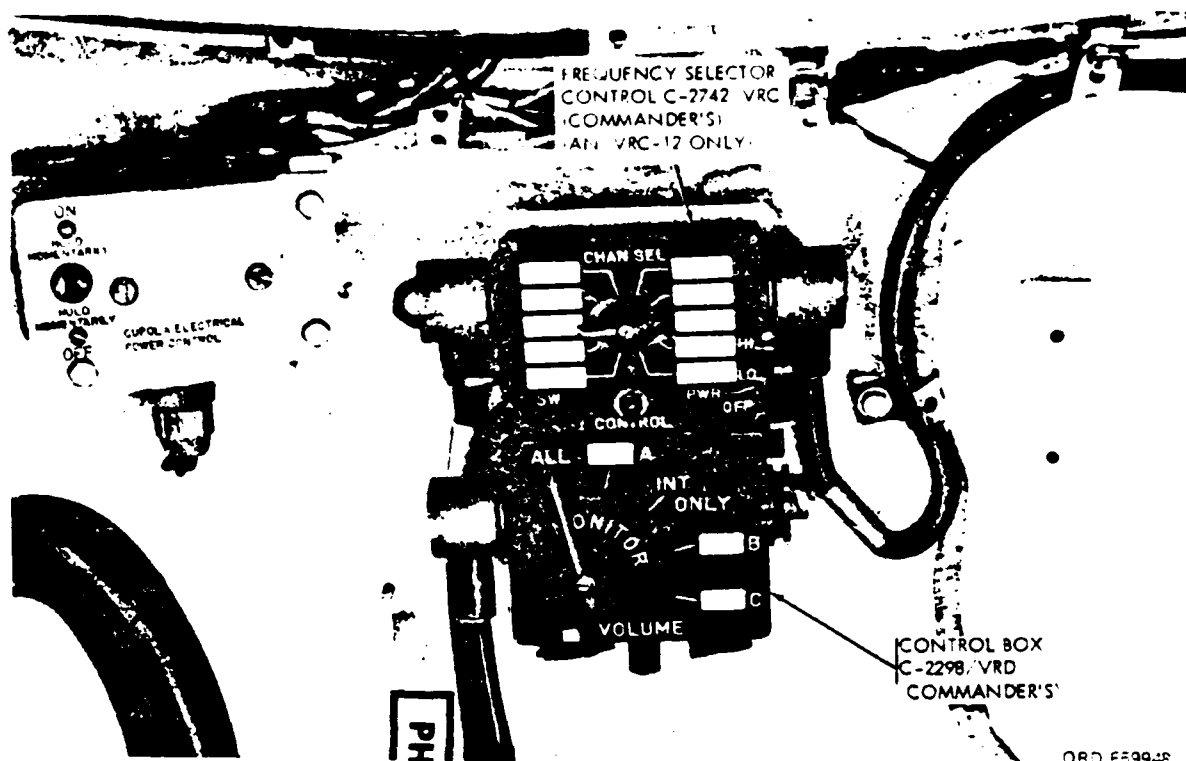
Figure 77. A view of the M60 commander's control box and frequency selector.

ducting in the cupola does not appear to be difficult. It needs only
to trace or follow the existing wiring which is shown in figure 78.
The difficulty arises in communicating with the driver. A pneumatic
slip-ring or rotating fitting must be provided and mounted near the
slip-ring box. Care must be taken that noise is not generated. The
dotted lines in figure 78 show a possible layout of the acoustic trans-
mission lines. As is observed, there is no particular disruption evi-
dent.

With regard to the systems engineering aspects of the intercom
the following morphology of design has been adopted, much as suggested
by Simon[46] in his excellent treatment on engineering design.

1. Needs analysis - was presented in the introduction.

2. Feasibility study - was conducted in the preliminary effort.

3. Preliminary design - was completed and demonstrated feasibility.

4. Detailed design - was completed.

5. Production - a brass-board system was built and considerations
for actual implementation were discussed.

Simon[46] considers the logical completion of total design to include
distribution, consumption and eventual retirement. This was not possible
under the present constraints.

The systematic approach to the choice of components and, wherever
possible, the logical arrival at a solution, has permitted a relatively
uncomplicated flow of design.
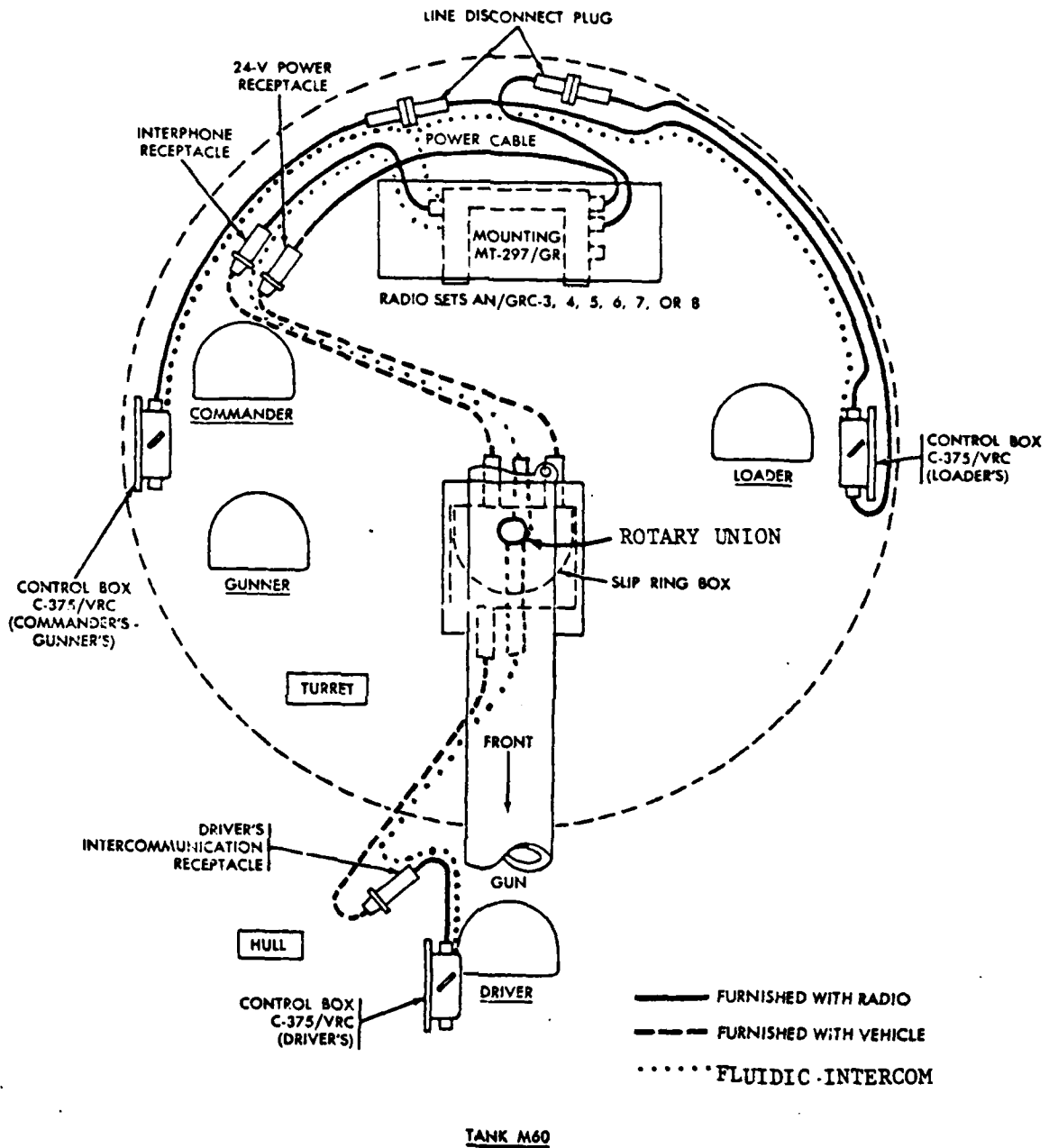
Figure 78. Cording diagram of the control boxes in an M60 tank showing the possible location of the acoustic transmission lines.

4. DATA LINK SUB-SYSTEM

This section will consider the design of a system to transmit
narrow band frequency modulated infcrmation that operates concurrently
with the broadband voice system. The applicability of such a system
to the tank becomes apparent when one considers the need to either
manually   or automatically control such devices as the engine or the
hydraulic turret drive. If it is possible to use the acoustic transmission
lines, then not much additional burden is placed on space requirements.

As was stated in section 3 and as is the intent of this design,
there are several components that overlap the audio and the data link
subsystems. These are the input connections, the transmission lines
and the interconnections. The items that differ are the signal gen-
erator and the amplifier/output configuration; these are treated
in this section.

4.1 Data Link Design

The data link system has been envisioned as having a high frequency
carrier that is inaudible so as not to disrupt the audio portion.
Initial studies were conducted to develop an oscillator of a frequency
greater than 20 kHz. An edgetone oscillator of about 37 kHz was fairly
quickly demonstrated; however, subsequent amplification and demodulation
of this signal fluidically proved to be beyond the capabilities of
the available hardware. In addition, signal attenuation at this fre-
quency was excessive. It was apparent, however, that since the audio
system was not passing signals beyond about 4 kHz, carriers above 4 kHz
could be acceptable as long as they could not be heard above the back-
ground noise. The sub-system components, therefore, that are described
in the following sections are based on this concept.

144

4.1.1 Input Narrow-band Oscillator

The determination of the carrier frequency will consider the tradeoff between signal attenuation and the availability of signal processing by standard fluidic amplifiers of the smallest practical size with nozzle widths of 0.25 mm as used in the audio portion. Maximum bandwidth occurs at the lowest aspect ratio and the highest supply pressure. Standard laminations are 0.05 mm thick so that two laminations will give the minimum acceptable aspect ratio, $\sigma = 0.4$. On the other hand at aspect ratio of over 1.5, usable high frequency gain occurs at the resonant peaks. From figure 53 it is apparent that the $\sigma = 1.5$ maximum bandwidth is about 10 kHz. For the low aspect ratios, the maximum normalized bandwidth is $F = 0.03$ corresponding to 14 kHz for an aspect ratio of 0.4 at a supply pressure of 135 mmHg. These numbers indicate that the carrier frequency must fall within the limits,

$$4 \text{ kHz} < f_{carrier} < 10 \text{ kHz}.$$

A convenient frequency in the mid-range is 7 kHz.

To design a 7 kHz oscillator, consider exciting the first edgetone or splitter resonance in an LPA which occurs at $F = 0.05$. This can be done by directly feeding back the outputs onto the inputs in the manner of a feedback oscillator. If the feedback line does not attenuate the signal to any great extent and the signal propagates acoustically, then an oscillator is generated since the feedback signal is large. For the feedback mechanism in the LPA, however, the developed feedback pressure near the splitter is low due to signal loss to the vent impedance. In the case of the oscillator, the entire jet dynamic head (less line losses) can be fed back to the inputs without encountering other losses such as the vent vanes, etc. The equation for frequency as a function

145

of supply pressure and size in terms of the normalized frequency F and convenient units of mmHg and mm is

$$f = \frac{F \times \sqrt{P_s \ (mmHg)} \times 10^4}{b_s \ (mm)} \tag{84}$$

For $f = 7000$ Hz and $F = 0.05$ and $b_s = 0.25$ mm, the supply pressure is $P_s = 12.25$ mmHg. But for moderate aspect ratios from the design guide, $N_R = 10^3$ and $N_R = 10^3 b_s \sqrt{P_s}$ so that $\sigma = 1.14$ and the nearest increment that can be built is $\sigma = 1.2$. An amplifier with an aspect ratio of $\sigma = 1.2$ amplifier was modified by the addition of short feedback lines of square cross-section 0.5 x 0.5 mm in the bottom cover plate. A sketch of the oscillator is given in figure 79 showing the location of the feedback lines, and figure 80 is a photograph of the physical arrangement of the oscillator with clear plastic cover plates showing the lines. The oscillator indeed meets the requirement of oscillating at about 7 kHz; in fact, its frequency output varies with supply pressure much as expected. The frequency versus supply pressure characteristic is given in figure 81 and is seen to be non-linear with supply pressure . Deviations from the exact value of frequency are due to the fact that the supply nozzles are not exactly 0.25 mm wide (they are slightly under) and the fact that the loading circuit affects the frequency. The output level right at the fitting is 100 db ref. 0.0002 μbar. It is virtually inaudible when placed in a baffle box and will certainly be inaudible in the 100 db background noise of a tank.
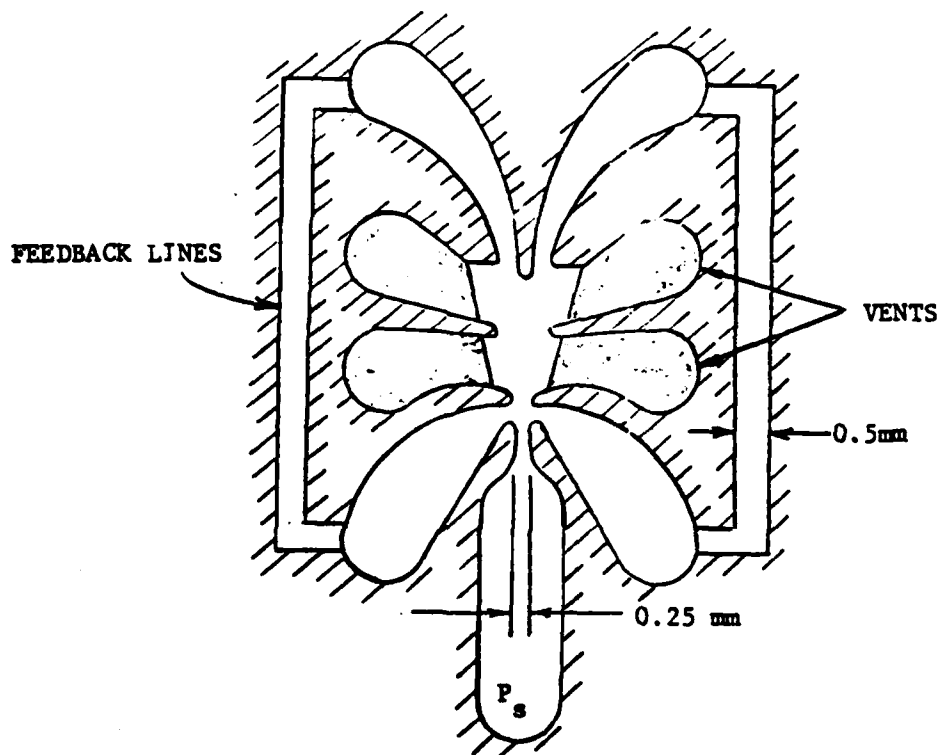
Figure 79. Sketch of an LPA oscillator designed for operation
at the first splitter resonance, F = 0.05.

OUTPUT HORN →

VARIABLE RESISITANCE
FREQUENCY MODULATING
SHUNT

FEEDBACK PASSAGES

$\sigma = 1.2$ HDL STD LPA
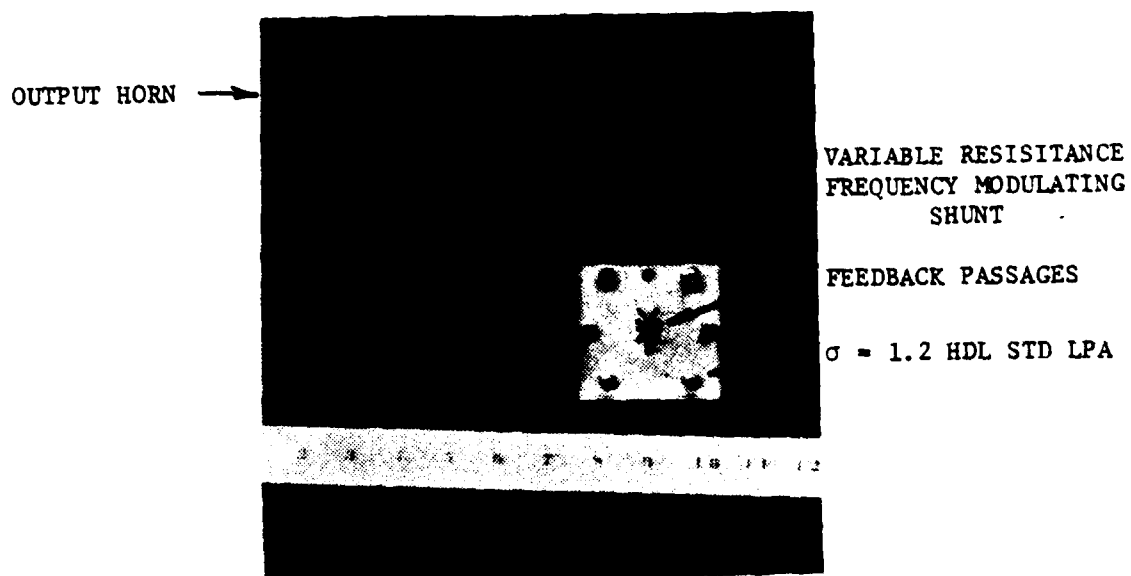
Figure 80.   Photograph of the embodiment of the frequency modulating
             oscillator for the data link sub-system.
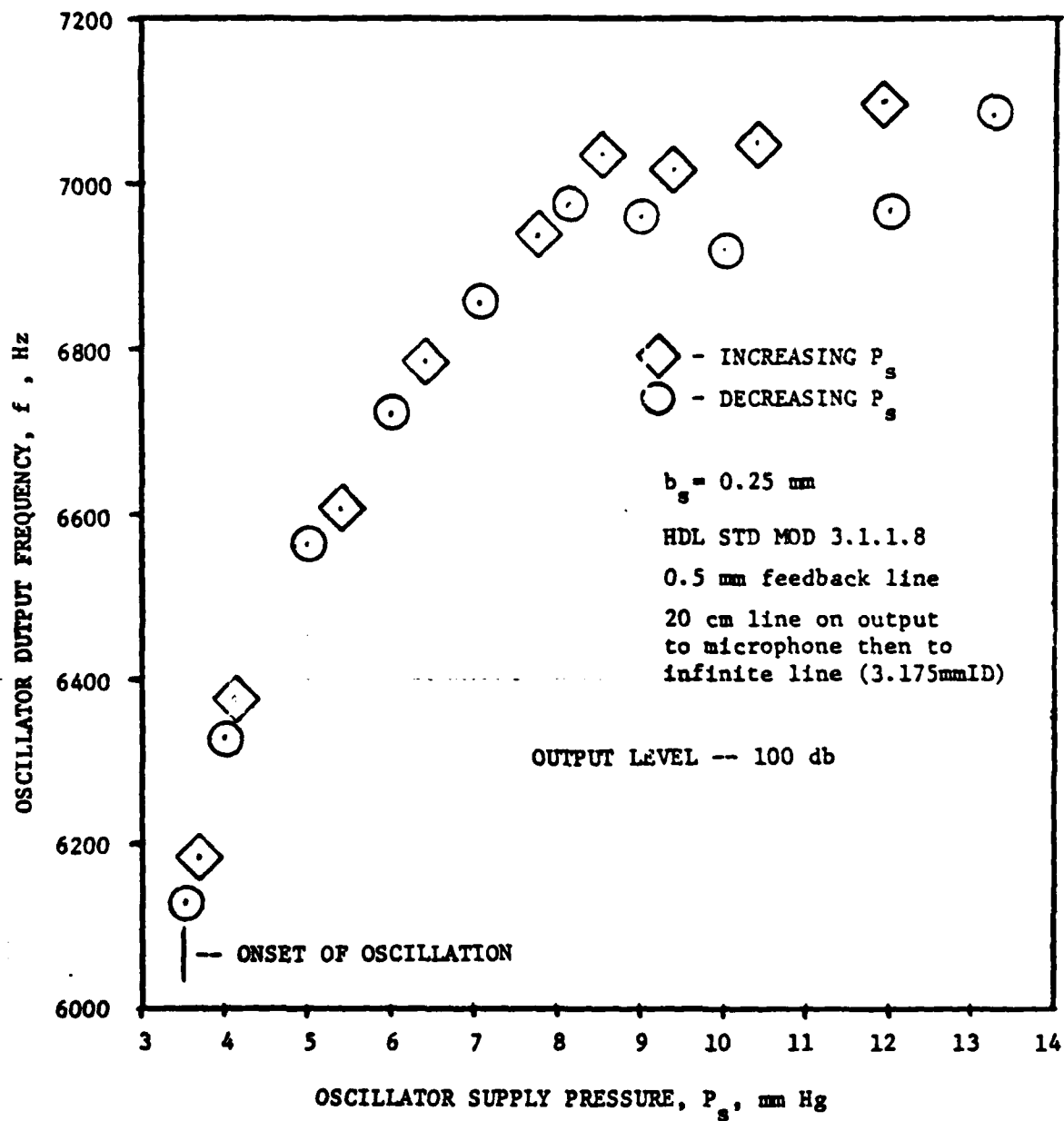
Figure 81. Experimental oscillator frequency output as a function of supply pressure.

149

Since the frequency shifts with oscillator supply pressure, this is one way to provide frequency modulation. One problem occurs, in that the amplitude also changes with supply pressure. It is, however, desirable to have a signal with constant amplitude since the demodulating scheme may be both amplitude and frequency dependent. The oscillator output may thus be fed into an amplifier stage with constant supply pressure and the output of this buffer amplifier can then be used as the frequency modulated signal.

A different modulating scheme was used in the final design. As observed previously, the frequency output is a function also of the load circuit on the feedback line. When a 3.175 mm ID line 10 cm long is connected to the unused output by an exponential horn, the frequency may be reduced by almost 300 Hz by merely blocking that tube. Virtually no change in amplitude at the active output occurs. Therefore, frequency modulation may be achieved by variation of either the active source or by variation of a passive component. The former is the basis for a pressure controlled oscillator which is basically an analog-to-frequency (A/F) converter. The latter may be used as a mechanical action-to-frequency converter.

For the problem at hand it is only desired to send two frequencies so that choosing a mid-range frequency of 6.58 kHz results in a reduction to 6.2 kHz when the line is blocked. Thus signal encoding can be achieved by a simple switching arrangement.

In order to prevent pressurization of the transmission line by the dc content of the oscillator, the output is blocked by a thin neoprene rubber membrane.

4.1.2 Signal Transmission

As stated before, the narrow band FM signal will be sent concurrently along the audio transmission lines. All that must be determined is the amplitude attenuation.

From equation (70) for the 5 m line with a hydraulic diameter of 1.667 cm, the attenuation is 13.5 db at 6.5 kHz.

4.1.3 Amplification and Demodulation

The demodulation of a flueric frequency signal into an analog signal is carried out by using the known amplitude/frequency relationship of some circuit. Typically, a first order lead or lag is used where the amplitude changes at 20 db/decade. The amplitude signal is rectified in a non-linear device and the output is then low-pass filtered to get the mean which is then a function of the input frequency. The non-linear device is called a flueric frequency multiplier/rectifier. It is a single output device with an identical input geometry to that of an LPA. The single output is centered on the location where the splitter would be in an LPA. In dc operation the output pressure mirrors the total head profile of the jet impinging on it as it is deflected as shown in figure 82. For small variations of the input, the output stays high since the jet is nearly centered on the output. For large variations the output excursions swing lower so that the mean pressure is lower also. In addition the output stays at only positive values of pressure and for each cycle of input variation, the output has two maxima; hence, if a given frequency is input, then the resultant output frequency is twice the input. This is shown in figure 83. This then means that the carrier will be 13 kHz when leaving the rectifier. This greatly eases the filtration of the output since relatively small volumes and moderate size resistors only will be required.

151

RECTIFIER

$\sigma = 0.5$

$P_s = 45$ mm Hg

$b_s = 0.25$ mm

LOAD.

$\sigma = 0.6$ HDL STD MOD 3.1.1.8

$b_s = 0.25$ mm

RECTIFIER OUTPUT PRESSURE, mm Hg

20

10

INPUT DIFFERENTIAL PRESSURE, mm Hg

-12   -8   -4   0.0   4   8   12
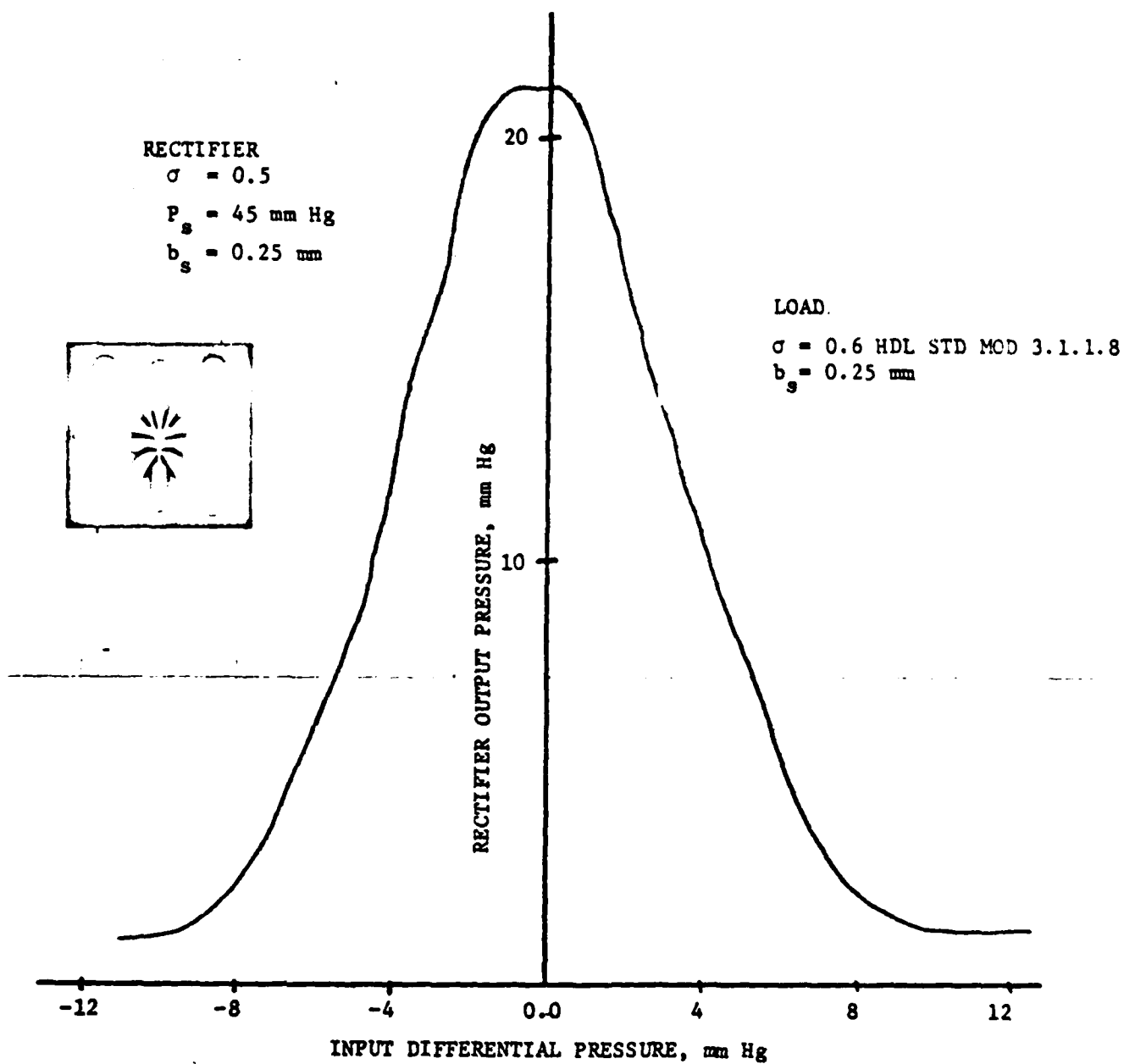
Figure 82. Fluidic multiplier/rectifier output characteristic ,low aspect ratio.
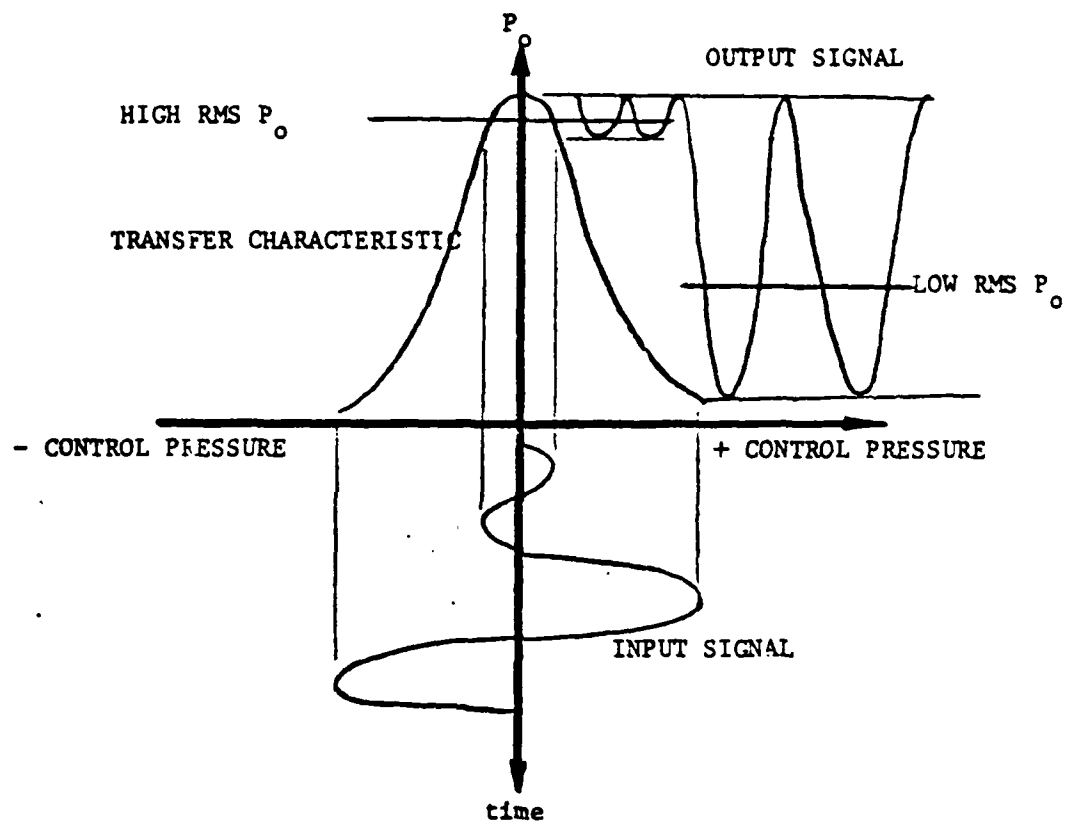
Figure 83. Schematic representation of the operation of the rectifier.

The input required to saturate the rectifier is about 8 mmHg. The input signal is attenuated by the line loss and the fitting loss of 23.2 db down to 76.8 db (10^{-3}mmHg) so that a gain of 8000 would be required for maximum dynamic range. Since only two discrete frequencies will be transmitted however, it is only necessary to have a usable output signal above the noise which is postulated to be 100 db. For a signal of 10 times the noise a 120 db (0.15 mmHg) output signal is needed. The slope of the rectifier transfer characteristic is about 3.0 so that an output change of 0.15 mmHg is attained with an input of 0.05 mmHg so that the .001 mmHg signal available must be amplified at least by a factor of 50. A three stage, self-staged amplifier provided a loaded gain of 120 when loaded into the controls of the rectifier.

The rectifier frequency response must be flat to include the carrier frequency so that at $F = 0.015$ from equation (84) with $b_s = 0.25$ mm and $f = 7000$, then the supply pressure must be $P_s = 135$ mmHg with $\sigma = 0.34$ for $\sigma N_R = 1000$. Rectifier laminations in the small size $b_s = 0.25$ mm come in increments of $\sigma = 0.25$ therefore one uses $\sigma = 0.5$ as the lowest acceptable aspect ratio. Amplifier laminations come in increments of 0.2 so that the amplifier can have $\sigma = 0.4$ or 0.6. It is most convenient to operate all the devices from a common pressure, and the supply pressure for $\sigma = 0.6$ is 45 mmHg, for $\sigma = 0.5$ it is 64 mmHg and for 0.4 it is 100 mmHg. It is easiest thus to use a gain block of $\sigma = 0.6$ with the rectifier running slightly low. The dc transfer characteristic for the gain block/rectifier circuit is shown in figure 84. Notice the offset from zero. This is caused by the null offset in the gain block. It, however, can easily be nulled out by use of a trim resistor on the opposite control of the pre-amplifier gain block in the same fashion as the null was removed from the audio amplifier.
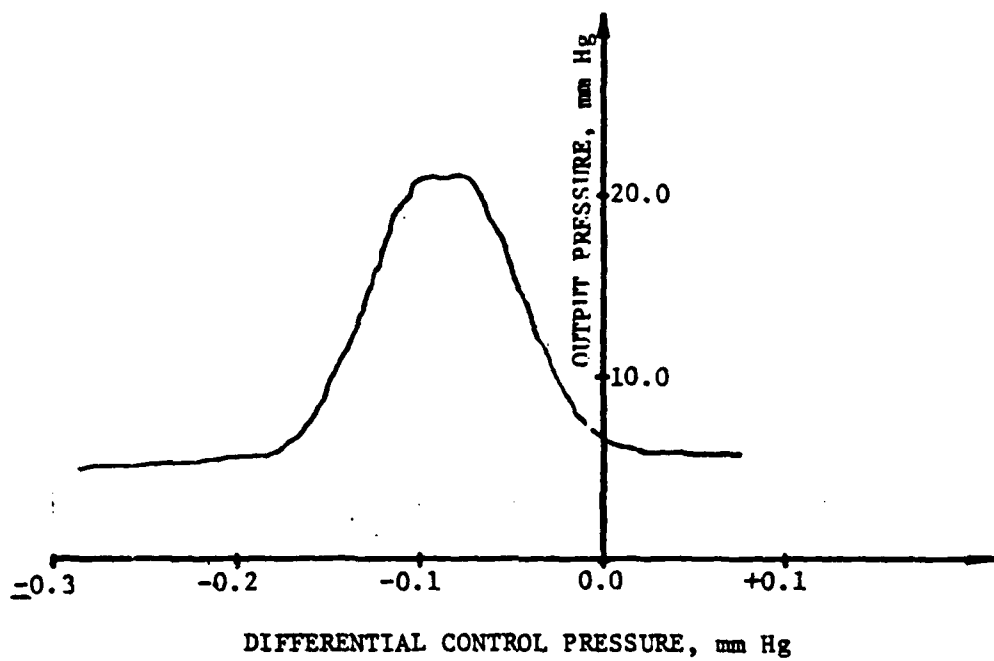
Figure 84. Experimental transfer function for the gain block/rectifier circuit.

155

The output now should have a flat response to frequencies beyond 7 kHz. If a resonant circuit is emplaced at the oscillator carrier frequency, then the RMS output will decrease dramatically at that frequency. Such a resonance can be induced in the amplifier circuit by placing acoustic cavities between stages of a length such that the resonant frequency equals the desired frequency. Randall[42] gives this frequency to be

$$f_{resonant} = \frac{1}{2\pi} c \sqrt{\frac{Area}{Volume \cdot \ell}} \tag{85}$$

and if the volume is a rectangular channel, then the resonance occurs at

$$f_{resonant\ channel} = \sqrt{\frac{c}{2\pi\ell}}$$

where c is the speed of wave propagation and ℓ is the length. This also requires a low resistance to eliminate damping. For a resonant frequency of 6.7 kHz, this requires an 8 mm channel. A gain block can be built by physically placing the amplifiers one after another. In so doing, with a standard format LPA, connectors of 16 mm in length can easily be machined in between stages. One expects multiple resonances to occur, the first at 3350 Hz and the second at 6700 Hz. Figures 85 and 86 respectively show a schematic of the gain block, with cavities and the rectifier and a photograph of the final embodiment of the circuit to include the RC low pass filter (valve and tank) on the output to provide the analog output level. From equation (73) for a pass band of 3 Hz, a volume of 12 cm^3 is needed. Figure 87 shows the rectified analog output of the device. Notice that there are indeed considerable notches at 3.5 and 6.7 kHz as expected from the resonances of the interconnecting volumes. The output is effectively the dc null output pressure for frequencies below 3 kHz since a high pass filter

156
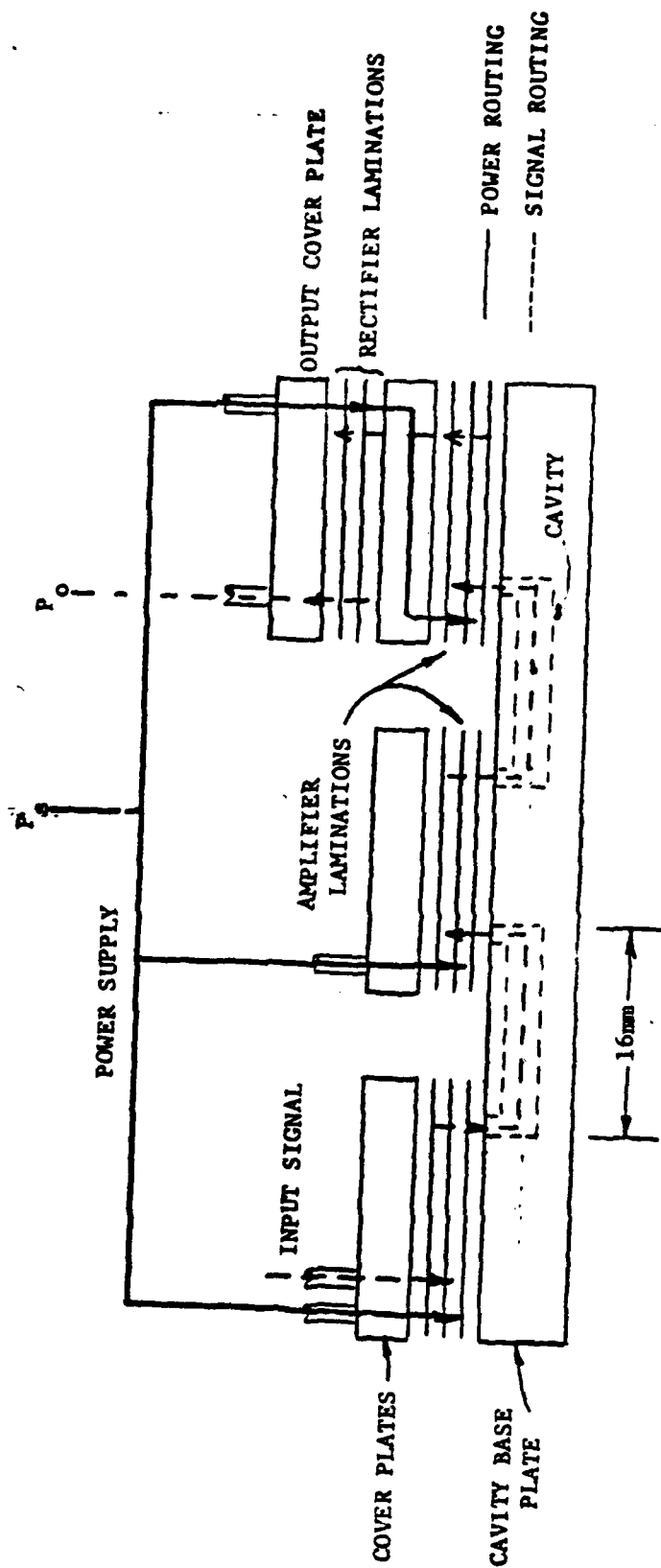
Figure 85. Schematic layout of the frequency demodulating and amplifying circuit block.
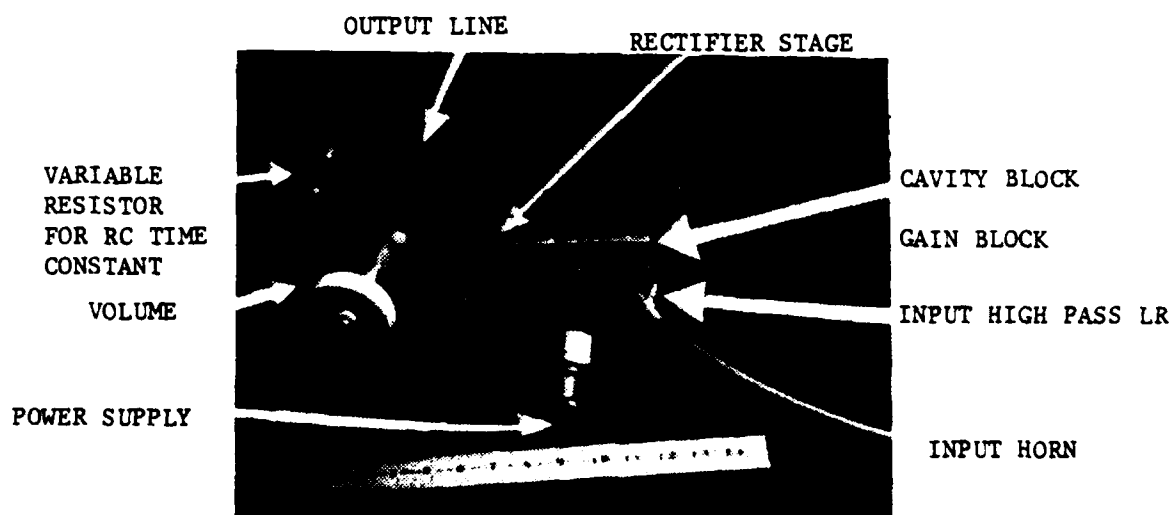
Figure 86. Photograph of the demodulating circuitry, $b_s = 0.25$ mm.
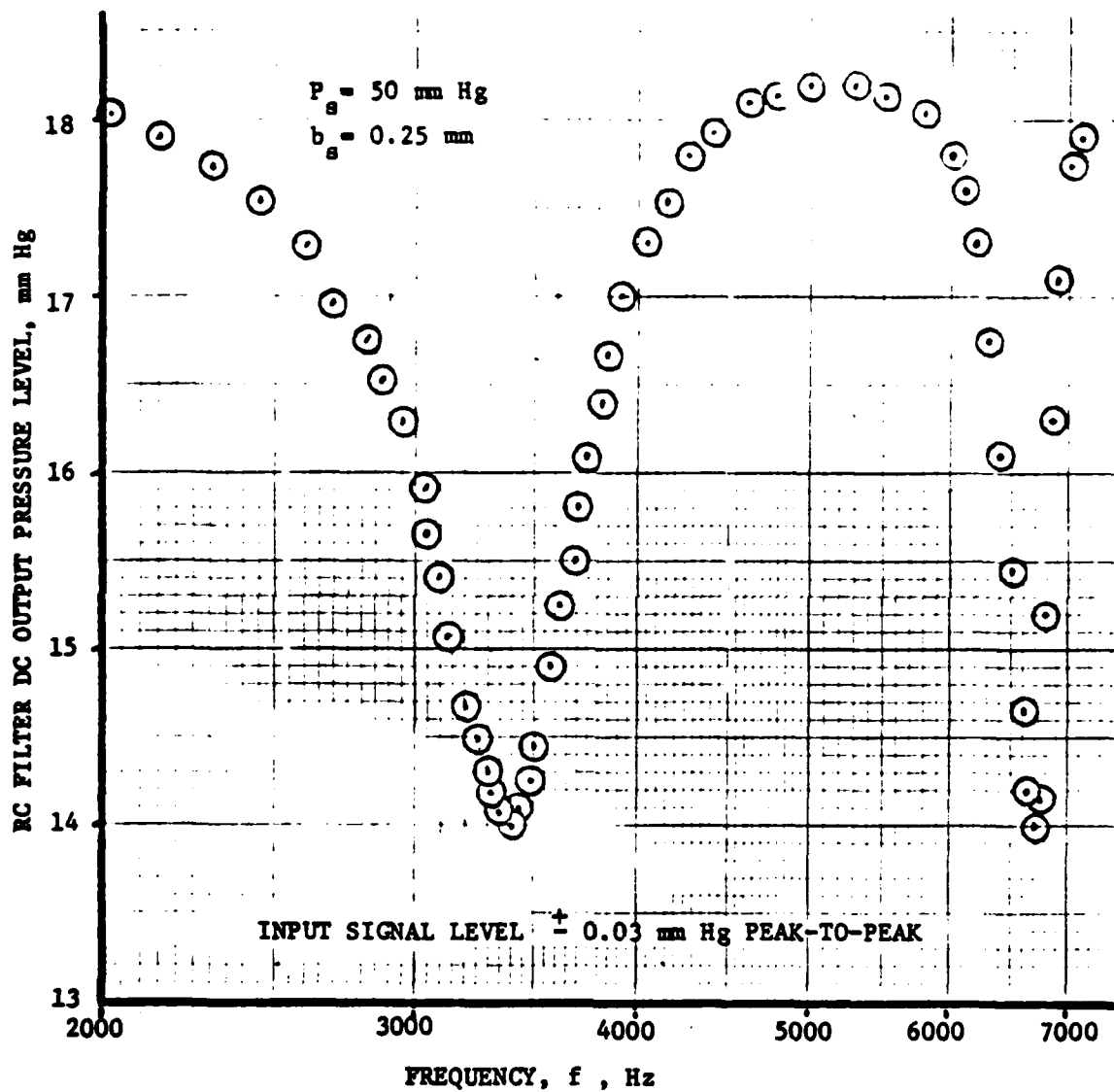
Figure 87. Experimental data for the analog output of the demodulating circuit as a function of frequency showing the two resonant notches due to the resonant cavities.

Is incorporated to filter out the low frequency audio portions. Figure 88 shows a linear plot expanding the data around the carrier frequency of 6.7 kHz. Notice that at this high input level, frequency discrimination is good. Certainly an output level of 0.05 mm can be discriminated which at 0.024 mmHg/Hz corresponds to less than 0.5 Hz over a band of 200 Hz which is a dynamic range of 400.

Figures 89(a) and (b) show the operation of the modulator/demodulator circuit under the extreme situation of transmission over a distance of 10 m in a 12.5 mm diameter line. The input signal level to the demodulating circuitry was 60 db. The noise level out of the RC filter was less than 0.01 mmHg, and an output signal of 0.1 mmHg was readily achieved for a step change in frequency of 380 Hz. Even at these low signal levels a frequency discrimination of less than 40 Hz is possible with the present system. Figure 89(b) shows an approximate frequency response of the system. The output filter was designed to break at 3 Hz and as the input is modulated (not sinusoidally unfortunately) by alternately blocking and unblocking the resonant line at a more rapid rate, one can observe that the amplitude does decrease. The amplitude is down to 70%(-3 db) of its original value at the point where 3 cycles per second occur. This is in good agreement with the desired design.

Most carrier systems reported on to date have been low frequency because of the limited bandwidth of the amplifiers. In their 1974 paper on fluidic carrier techniques, Boothe and Ringwall[47], cite the state of the art operating ranges of carrier systems as 100 Hz - 3 kHz but speculate about higher carriers of up to 100 kHz. The present carrier of 6.7 kHz, therefore, represents a significant step to the realization of the increased capabilities of fluidic carrier systems.
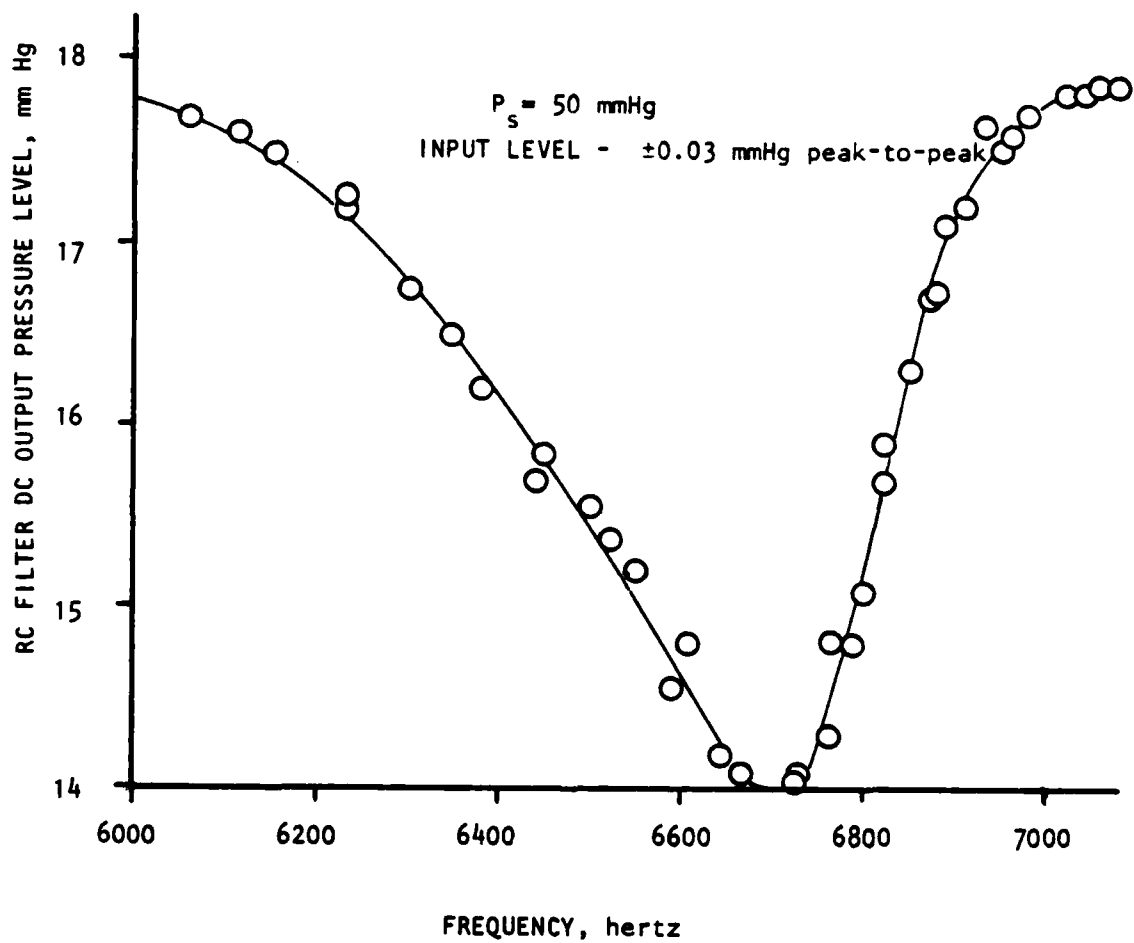
Figure 88. Expanded experimental plot of the first harmonic notch around the FM oscillator carrier frequency.

INPUT LEVEL - 60 db

0.1mmHg

6.2 kHz

6.58 kHz

.2s

(a)

0.07 mmHg(-3db)

1s
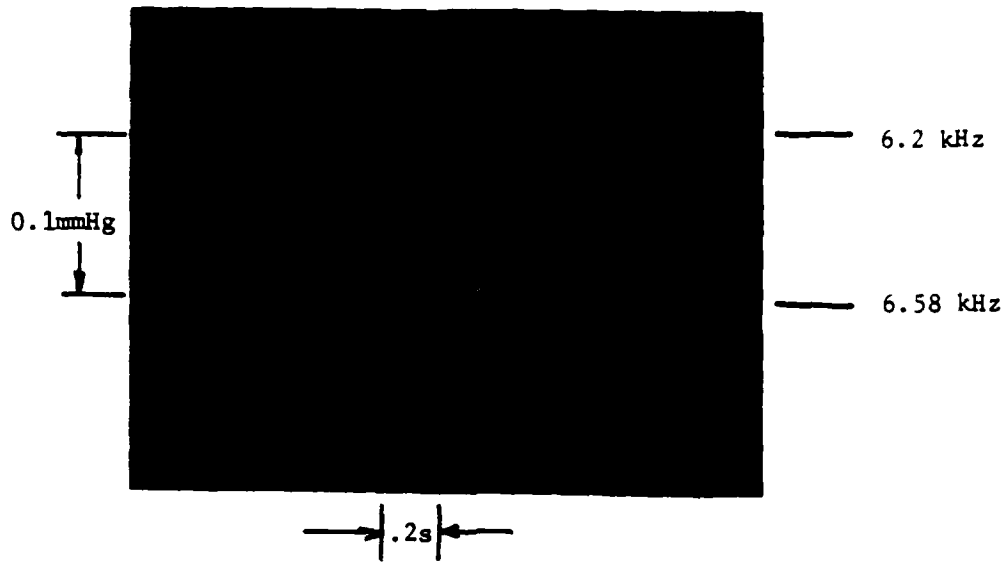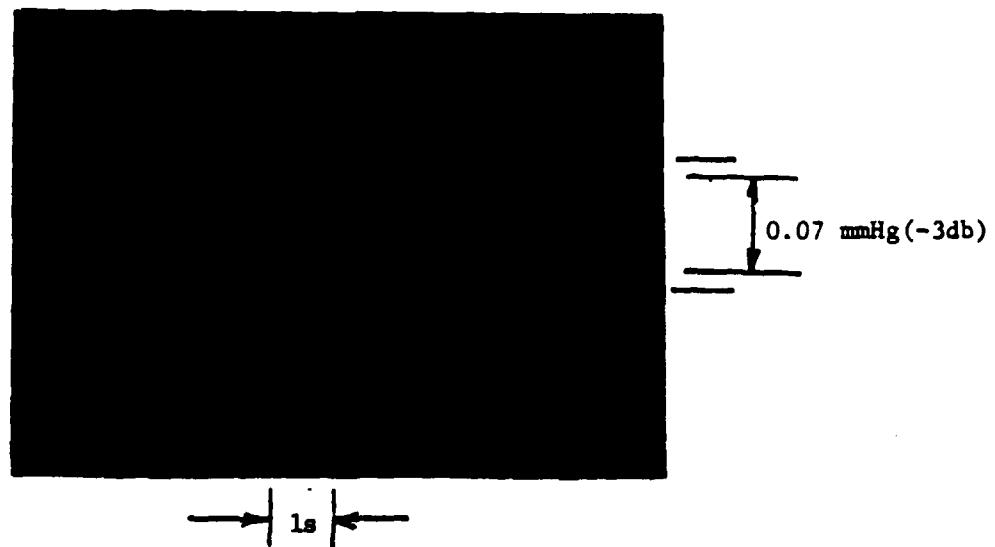
(b)

Figure 89. Oscilloscope traces of transient and frequency responses
of FM demodulator/modulator when signals are transmitted
10.0 m

4.2 Human Engineering Considerations

As mentioned previously, the carrier frequency is audible when the background levels are below 100 db. However, enclosing the oscillator in a small box packed with plastic foam provides for a considerable attenuation. Further attenuation is afforded by the audio headsets whether they are of the helmet or the airline types.

5. FLUIDIC VOICE COMMUNICATION SYSTEM AND DATA LINK IMPLEMENTATION

Sections 3 and 4 have separately considered the design of the two subsystems: the broadband voice subsystem and the narrow band data transmission system. This section will briefly deal with the implementation of the combined system in a vehicle. The complete system is shown schematically in figure 90. Only the power supply connections have been omitted for clarity.

Implementation of this system can be carried out in vehicles wherein the communication span is of the order of 5 - 10 m. The M60 class of tanks have the general dimensions of the generic species of armored vehicles to include the M48 and XM1 tank, the Infantry Combat Fighting Vehicle XM-2, and armored personnel carriers such as the Army's MICV and Marine Corps LVTP-7. In addition, this system may be implemented in such vehicles as the Army's Lighter, Air Cushion Vehicle (LACV-30), the Navy's V/STOL aircraft, and generically in most fighter aircraft. Control of the lifting surfaces and engine may possibly be done by the narrow band portion of this system. Voice or intercom functions in a fighter aircraft occur over a very short distance, normally about 2 m. In bomber aircraft the bombardier is often considerably removed so that this system may be inappropriate.

The audio and data link subsystems were integrated as shown schematically in figure 90. The total system operation was in accordance with the design goals. No mutual interference was noted. The FM carrier could only be detected in a quiet room within about 2 m of the baffle box. This indicates that the assumption made about its lack of interference was correct. When the head sets are in place, the carrier is inaudible. Speech between two rooms is of telephone quality. The speaker can be readily understood and recognized. FM signal transmission does not
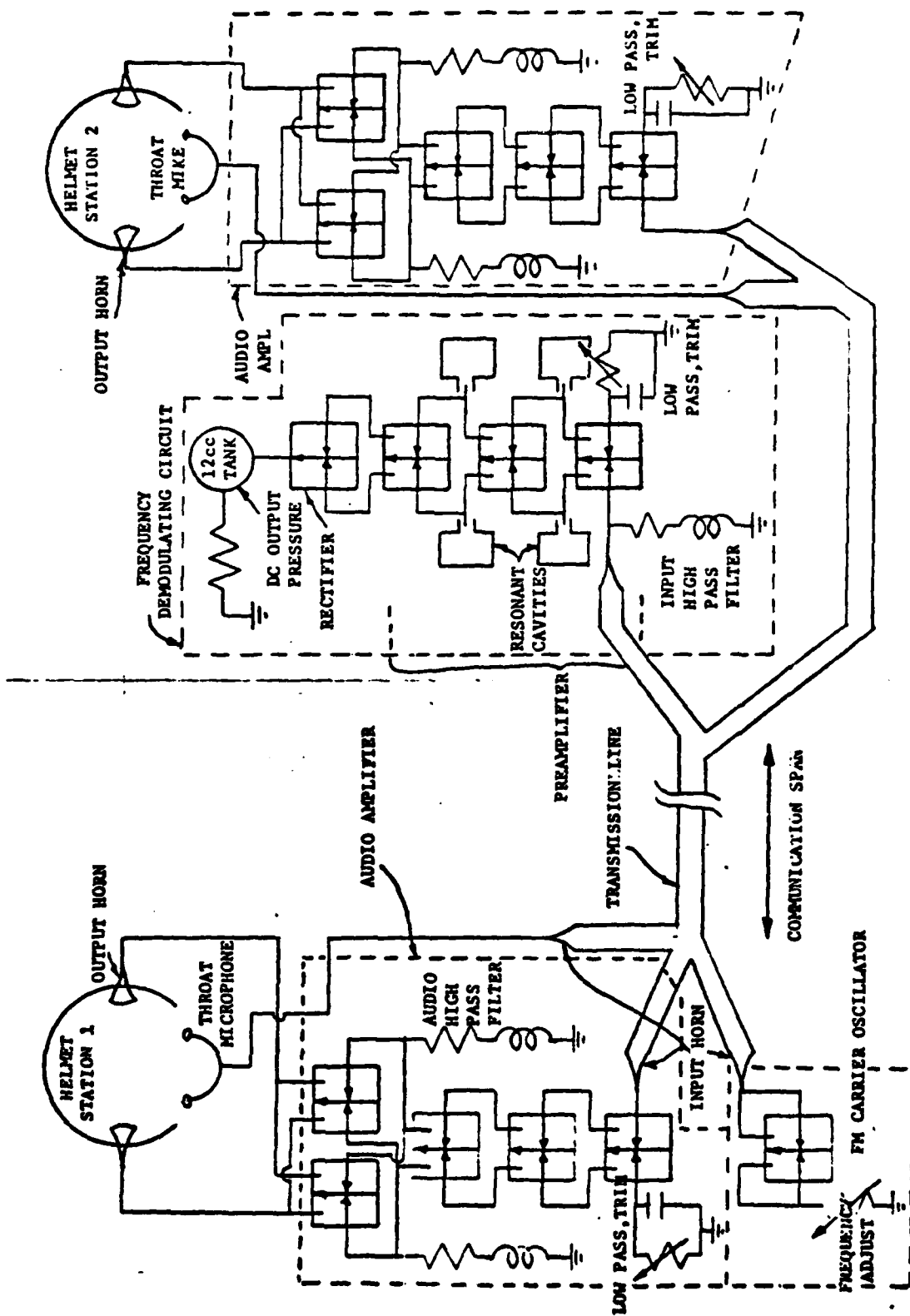
Figure 90. Schematic representation of the full Voice Communication System and Data Link.

165

affect speech transmission in the least. This demonstrates the feasi-
bility of dual mode signal transmission.

Qualitative tests of bandwidth show that the whole system indeed
does perform as the sum of its parts. The long distance, however, does
add phase shift to both the audio and data response. For the audio
portion, this merely appears as an undetectable delay. For the data
system this may prove to be a significant limitation if it is considered
for a closed loop control. Insufficient phase margin will significantly
affect the frequency response of a closed loop controller.

6. ENVIRONMENTAL SENSITIVITY

The operating characteristics of flueric laminar proportional amplifiers are dependent on the viscosity and the density of the medium in which they are operating through the Reynolds number and the Strouhal number (inverse of the normalized frequency).

The gain of an LPA decreases with decreasing N_R as shown in figure 91 which is a plot of the self-staged gain of an HDL standard LPA.
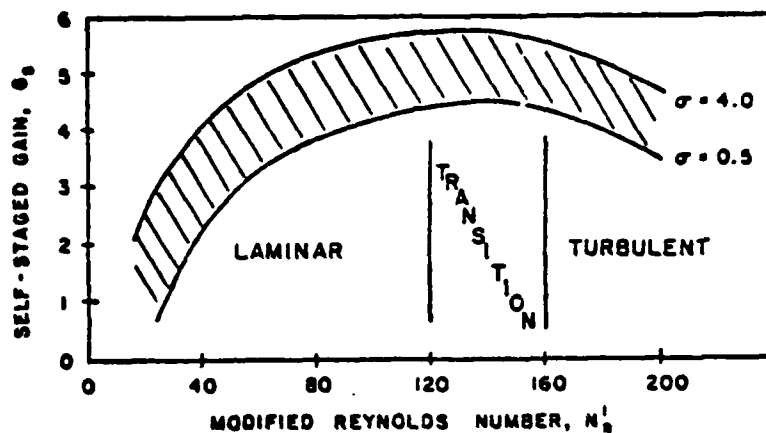
Figure 91. Self-staged gain as a function of modified Reynolds number for the HDL STD MOD 3.1.1.8 LPA.

For pneumatic operation the kinematic viscosity of air changes by a factor of two over the standard military temperature range -45°C to +80°C, hence the Reynolds number at constant supply pressure also changes by a factor of two. As is observed from figure 91, one may allow the Reynolds number to decrease from a nominal 120 to 60 and incur only about a 10 percent change in gain. The net change in gain for a gain block of n-stages is therefore approximately 10 n-percent. Since each device herein has four stages, that means that a gain change

167

of over 40 percent will occur if the supply pressure is held constant. A design around 20°C allowing for a $\pm$60°C shift in operating temperature will nominally give a $\pm$20 percent variation in gain. This will affect the audio portion to the greatest extent since there is just sufficient gain. However, since there is a factor of two margin incorporated, the voice signal will always be above the background noise.

The frequency response also suffers due to the change in density. The normalized bandwidth remains constant; hence, the bandwidth at constant supply pressure depends on the inverse square root of density. Density changes $\pm$20 percent for temperature changes of $\pm$ 60°C around 20°C. This results then in a $\pm$10 percent variation in bandwidth. This is definitely well within allowable bounds giving rise to a low end bandwidth of 3200 Hz at the highest temperature of 80°C. Since operation at the temperature extremes will probably occur infrequently, one may expect even smaller variations. Operation over the temperature range so far has been discussed assuming constant supply pressure. Consider, however, the operation of a pump loaded with a temperature sensitive resistance such as are the LPA supplies and the various manifolding resistors. As the viscosity increases, the air heats up, the resistance of the load increases so that the pressure actually increases somewhat. This effect therefore tends to compensate for temperature in that P_s increases as does ν. The amount of compensation, however, is small and should not be materially counted on.

Frequency of the oscillator is similarly affected. However, since the modulator and demodulator are affected in the same way the fact that the carrier frequency shifts slightly will have no effect on operation. Reduction in gain will have an effect in reducing the dc output slightly.

1.0

2.8   2.5

3.2   2.2

3.6

4.0   2.0

1.1

1.8

1.25   1.4   1.6

MICROCOPY RESOLUTION TEST CHART
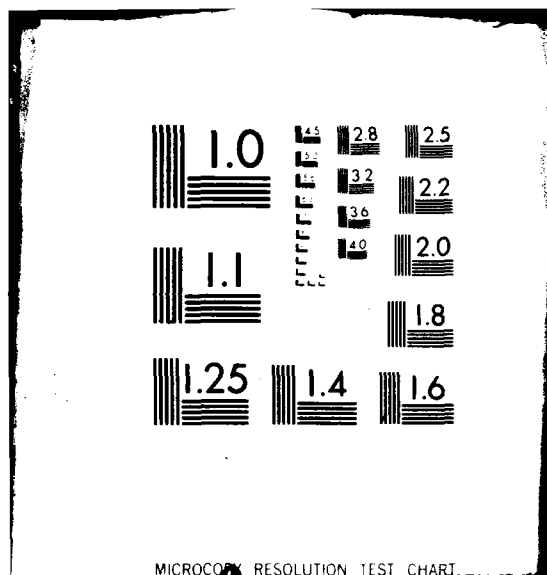
Variations in altitude will have a significant effect. At 10,000 meters altitude the ambient pressure is one-fifth that at sea level so that density also is one-fifth. This would considerably affect the bandwidth. However, if the device is emplaced in a pressurized box connected to ambient by a sonic orifice as is suggested for aircraft operation of fluidic devices by McDonnell-Douglas[48], then density variations will be greatly minimized. This has an additional benefit of isolating the amplifiers from ambient noise effects which cannot propagate across the sonic orifice.

Vibration has been demonstrated to have no effect on the dc operation of fluidic devices[24]. Frequency signals induced in the common mode also have little or no effect on the frequency content of the differential outputs. However, due to the low pass filters on the audio amplifier unused controls, vibrations in the transmission line will be transmitted if they are in the band-pass.

The most serious environmental problem is contamination. Particulate matter will eventually clog the LPA's. Based on accelerated time testing reported in the literature (see Drzewiecki[24,35] for a comprehensive listing), the mean time to failure, MTTF, for laminar devices operating off conventional power supplies will be in the area of 50,000 hours of continuous duty. This is almost 6 years. Since any vehicle operates only intermittently, say one-third of the time, conservatively, then the fluidics should be expected to operate for over 17 years. This undoubtedly approaches the useful life of most vehicles. Even armored vehicles such as the M48 tank that have seen service since the late 1940's (30 years) are periodically completely refurbished. A dust enclosure, however, is necessary to prevent blockage of the vents and also to serve as a baffle to wind currents that may temporarily saturate the amplifiers, rendering them useless.

The effects of nuclear radiation, electromagnetic interference
(EMI) and electromagnetic pulses (EMP) are essentially non-existent.
The fluidic circuit has only a possible sensitivity to the heat gen-
erated by some form of radiation. In most cases except perhaps at
the epicenter of an explosion, these heating effects are negligible.
Certainly fluidic circuits have demonstrated the capability to operate
at radiation levels far in excess of those above which life ceases.
Since this circuit requires a "live audience" is is immaterial if it
should fail under huge radiation doses.

Typical intercom systems are affected by EMI. Clicks are heard
when electrical components are turned on, interference and buzz occurs
when short-wave, micro-wave or other equipment is on. This fluidic
audio system has been tested in the presence of radio waves as gener-
ated by a citizens-band radio and in the presence of numerous electronic
devices which have been turned on and off. No effects could be heard
whatsoever. While these elementary tests do not comprise an exhaustive
set, they are indicative of the expected performance. Radio waves are not
expected to affect the performance of the audio portion.

As an aside, one should note that the output of the narrow band
sub-system is a dc pressure level. If it is incorporated in a control
system and must interface with electronics, the pressure transducer
interface may be EMI/EMP sensitive and thus require shielding.

If operation is caused to occur at a Reynolds number such that

$$c_d \, N_R / (1 + 1/\sigma)^2 > 180$$

then the flow is not entirely stable and may be transitional[35]. The
jet becomes sensitive to specific frequencies, the band of sensitivity
increasing with increasing Reynolds number. When the jet flow becomes
turbulent, a hissing noise is evident, clarity and fidelity are lost,
and considerable distortion occurs. Care must be taken, therefore, to
ensure that the Reynolds number stays in the laminar range for the
entire operating region.

7. COST AND RELIABILITY

The cost of a production version of the Fluidic Voice Communication System and Data Link (FVCSDL) may be estimated in two ways. The costs of the individual parts may be added up and added to estimates on labor, profit, overhead and so forth. Alternatively, a cost may be extrapolated from past experience on systems that include similar parts.

Typical production costs of photochemically etched metal LPA laminations are $0.25 each. Each amplifier consists of enough laminations to form the appropriate aspect ratio and laminations that form cross-coupling and venting. Normally, the venting dimensions require a height equal to or greater than the amplifier itself. However, since non-amplifier laminations do not require the same kind of precision (accuracy is proportional to etching depth), then the pieces may be thicker. As a rule one may count on a minimum of eight non-amplifier laminates per amplifier, four vent and four cross couplers, with integrated resistors, and perhaps as many as there are amplifier laminations in high aspect ratio cases.

The system uses 10 amplifiers in the audio portion and five in FM portion for a total of 15. The audio has six LPA's $\sigma = 1.2$ for 36 laminates and four at $\sigma = 0.8$ for another 16 laminates. The FM portion has one at $\sigma = 1.2$, three at $\sigma = 0.6$ and one at $\sigma = 0.5$ for a total of 26 laminates. The total number of HDL STD MOD 3.1.1.8 ($b_s = 0.25$ mm) LPA laminates is 78 for a cost of $19.50. Fifteen amplifiers with eight extra laminates each is another 120 laminations for $30.00.

The resonant cavity transfer blocks in the demodulation circuit require three piece construction, therefore add $1.50.

The individual components will have to be bonded together to prevent laminates from shifting. Diffusion bonding in a high vacuum furnace normally takes about one hour and the number of systems handled at once depends on furnace size. An hour of a technician and the furnace may cost $30 and assuming that five circuits at a time can be bonded, this reduces to $6/system.

The cost of the transmission line is about $2/meter or $10 total. Power supply lines, fittings and horns will run about $25. The pump cost $30 as previously mentioned.

System labor costs are based on time for semi-skilled personnel to assemble the parts. Mass production type facilities will allow no more than one hour and probably considerably less for assembly and a "go," "no-go," test. Typical production personnel costs are $20/hr. The following table itemizes the costs.

Item	Cost
Laminates	$ 51.00
Bonding	6.00
Fittings and lines	25.00
Pump	30.00
Labor	20.00
Sub total	$142.00
10% profit	14.20
Total	$156.20

The costs when determined by extrapolation are based on the production costs of DC-10 thrust reverser system manufactured by AiResearch

Corporation[49]. This is an 11 component device composed of metal etched laminations diffusion bonded together. It sells for an estimated cost of $220. This is a figure over that estimated above on a parts basis. The "true" cost probably lies somewhere in between.

It should be noted that a lack of competition in the fluidics area in recent years has given rise to unrestrained costs. Mass production of parts by competing sources will help keep costs down so that the figure of $156.20 per system may be realistic.

Life cycle costs for the fluidics are nil. The purchase price and installation costs can be amortized over the life of the vehicle so that for a 10-year life, the cost is only $15.62/year. This cost is negligible when compared to the total price of a fighting vehicle, say $1.5 million for an XM-1 and $4-5 million for a fighter aircraft.

Reliability has already been estimated by the system MTTF. The limiting factor will most probably be the pump. Experience has shown the pump life to be several years of continuous operation in an industrial environment. This, however, is a fairly constant temperature environment. The military environment includes extremes of heat and cold. This will undoubtedly affect the life of the rubber diaphragms and may actually dictate the use of a different pump should the problem be severe. Pump replacement at one year intervals seems appropriate. This then changes the life cycle costs to $30/year over the initial purchase price. This figure is still small compared with costs of a shielded electronic system. Overall reliability therefore as measured by pump life is about 9000 hours.

8. SUMMARY

This investigation has considered the analysis of the dynamics of laminar proportional amplifiers and the application of the analysis to the design of both a broad band voice and a narrow band frequency modulation demonstration system.

Beginning with first principles, the governing equations for the flow in the channels of an LPA have been developed. As a result, a complete equivalent circuit description for moderate frequencies that depends solely on the geometry has been evolved. The equivalent circuit for a duct in its simplest form has been determined to be a tee network composed of a resistance and inductance in series with a capacitance to ground from the RL node. This is in direct contradistinction to the lumped parameter model used up to now wherein the capacitance to ground comes after the RL series branch. The present model is in better intuitive agreement (not to mention qualitative agreement) with the physics of the problem since it seems that an average pressure should be used to determine the degree of compression in the duct. A basic analysis on the jet barrier compliance is combined with the channel analyses to develop a complete fifth order model for the input impedance of an LPA, that includes inertive effects of the clearance spaces between the jet and the control edges. The channel capacitance due to compressibility is shown to be significant for low aspect ratio operation and should not be neglected as has been done in previous analyses.

The input dynamics having been determined then allowed the modelling of the jet deflection in the LPA in the region between the controls and the outputs. A finite transport time of twice the average jet velocity has been shown to be the main cause for phase shift and gives excellent agreement with physical observations. Previous analyses used the average particle velocity and generally underestimated the

phase shift. By postulating an acoustic feedback along the sides of the jet of the pressure developed downstream before the vents due to spilled jet flow, an augmentation in gain is computed and verified. The locations of resonances, so prevalent in high aspect ratio LPA's, have been precisely determined, and the amplitudes are generally well represented. Accuracy is especially good for frequencies up to the first splitter induced resonance. Recognizing that the acoustic feedback phenomenon is the basic mode of operation in edgetone systems, it has been found that the LPA resonances line up almost exactly with the edgetone eigen-frequencies with the main difference being that in the LPA the resonant regions are merely augmented gain regions not sustained oscillations. It has been demonstrated, however, that sustained oscillations can be induced by appropriate choice of geometric configuration both analytically and experimentally. A computer based algorithm has been developed and is listed in the Appendix 1.

Based on the insight developed by the modelling and the actual ability to compute bandwidth, gain and impedances, a dual purpose system was designed and built. A broad band voice spectrum audio ampli-fier was designed for operation as an intercom in an Army tank. In addition a narrow band frequency modulating system to transmit digital pulses was also designed and built. As a result of both designs, the state of the art in frequency response of fluidic systems was dramatically advanced. The audio system operates to 4 kHz but does not push the capability of the size LPA used. A 10 kHz system could easily be built. Similarly, a 6.7 kHz FM carrier system was built that exceeds the state of the art by at least a factor of two. Again the capability has not been stretched. Consideration of even smaller LPA's (b_s = 0.1 mm) in-dicates the possibility--even the feasibility--of operating ultrasonically.

The fluidic components of the demonstration system will operate for the expected life of a military vehicle. The system is so designed

as to be applicable to a wide range of military vehicles to include tanks, armored personnel carriers, air cushion vehicles and fighter aircraft. The specifications are summarized below in Table II.

Table II Fluidic Voice Communication System and Data Link (FVCSDL) Specifications

PARAMETER	VOICE SYSTEM	DATA LINK
Overall dimensions	2.0 x 1.5 x 3.0 cm per channel	2.0 x 1.5 x 6.5 cm (demodulator) 1.0 x 3.0 x 3.0 cm (oscillator)
LPA nozzle width	$b_s = 0.25$ mm	
Power supply	4 watts at 120 VAC (50 mmHg at 2.25 LPM $\pm$ 10%)	
Bandwidth	1 - 4 kHz	6 - 6.7 kHz
Bandwidth temperature variation -45°C - +80°C	$\pm$ 400 Hz for +60°C around 20°C	N/A
Output level	110 PNDB at 20°C	2.6×10^{-4} mmHg/Hz at 60 db input level 6.7×10^{-3} mmHg/Hz at 105 db input level
Threshold	limited only by ambient noise	40 Hz at 60 db 1.5 Hz at 105 db
Output	Exponential horns in helmet or direct insertion headsets	static pressure in a volume
Input	Throat clamped "U" tube "throat microphone"	Mechanical switch or motion of tube
Operating temperature	-45°C - +80°C	
EMI/EMP sensitivity	None	None on fluidics some possible on pressure transducer if used.
Cost	$156.00	

9. CONCLUSIONS

As a result of the successful analysis of the dynamic behavior of LPA's, two main conclusions can be made:

1. Fluidic systems can operate over bandwidths in excess of 10 kHz with standard size components.

2. Fluidic systems can operate well into the ultrasonic range when nozzle widths are about 0.1 mm.

The implications of operating at ultrasonic frequencies are interesting, however. Note that the definition of high frequencies in fluidics differs by a factor of 10^6 from that in electronics. This is the ratio of the speed of electromagnetic propagation to that of sound. This implies then that 1 Hz operation in air is akin to 1 megahertz operation electronically and 10 kHz fluidic is like 10 gigahertz electronically. In electronics, various three-dimensional effects (skin effects) occur at the elevated frequencies, similarly in fluidics when the wavelengths approach the device dimensions lumped approximations fail. In addition, the viscous signal losses are tremendous at ultrasonic frequencies. For example, a 30 kHz signal is attenuated at a rate of 10 db/meter in a 1 cm ID tube. This means that signals cannot be transmitted far without use of relay amplifiers. A signal loss of 100 db may be tolerated from a source at 150 db but what are the physiological implications and effects of sustained exposure to ultrasonic sound at high amplitudes.

Certainly one can conclude that high frequency operation in a densely packed integrated circuit will allow an increase in the computational capability of fluidics, especially on the speed of computation.

One other conclusion, which is perhaps more far reaching, is that the LPA may be considered as a pressure transducer of extremely good

177

resolution with wide bandwidth. A typical dynamic range for an LPA gainblock of a gain of 10^3 operating at a first stage supply of 10 mmHg is 10^5. This indicates that if the maximum output differential is of the order of the supply, then the input threshold is of the order of 10^{-7} mmHg (2×10^{-9} psi) for an output signal of 10^{-4} mmHg. Now consider the measurement of pressure differentials of the order of just 10^{-5} mmHg. If an electronic transducer is used, a large diaphragm device must be used. Typically, an electronic manometer (Barocel) transducer may be used; however, the bandwidth is limited to about 20 Hz so that if dc is desired to say 5 kHz, an electronic transducer cannot do the job. A microphone will not go to dc. However, if the signal is fluerically preamplified without loss of bandwidth, then a low cost, pressure sensitive transistor can easily transduce the 0.01 mmHg LPA output, with the result of a hybrid pressure transducer...a flueric pressure preamplifier and an electronic interface. This then allows a host of low pressure output sensors to be utilized where before their use was impractical.

This program has provided design algorithms for the practical utilization of standard LPA's and for the customization of LPA design to a particular application. The broadband amplifier concept is one such outcome of this program. The ability to *a priori* predict the frequency response of LPA's will allow the shaping of desired frequency characteristics to meet specifications. Indeed, the ability to produce a specified shape frequency response may in the future obviate the need for passive circuitry. Resonant circuits may be replaced by edgetone augmented amplifiers, thus considerably simplifying circuit construction by eliminating the need for separate volumes and resistors.

The design algorithm also has specified the input impedance of LPA's so that rational design can be used for complex computation

178

circuits. While LPA input impedance was not directly measured and the fifth order model was not directly verified, its validity has been established indirectly from the good agreement of the complete LPA response model with experimental data.

10. RECOMMENDATIONS

This program has pointed out several areas of possible additional fundamental research and several areas of developmental interest. Perhaps the area of greatest fundamental interest is the relationship between the onset of edgetone oscillations and turbulence. This phenomenon appears to involve such areas as the hydrodynamic stability of jets and confined flows. The present research has been on a macroscopic level and efforts should be tied to some microscopic level evaluation of the actual velocities and spatial distributions of energy.

Another area of fundamental interest is the examination of the transition of flows from the acoustic to the fluidic region. Clearly LPA's can operate at large signal levels as well as small. What is the relationship between the highly nonlinear step response observed and the large signal sinusoidal response? How do induced secondary flows interact with the large deflections of an oscillating jet?

Yet another possible area for basic research is the solution of the flow between a solid wall and a jet boundary as found in the control-jet edge interaction. While a plausible engineering analysis has been made, certain assumptions do not hold at low and negative biases. The reverse or counterflow condition accounts for the physical explanation of digital amplifiers, yet the actual values of impedance have analytically eluded researchers.

An area for future development is certainly the high volume public address systems as originally desired for aircraft carrier flight deck operation. The development of acoustic summing to provide high volume output (140 db) should be reexamined.

The area of compensation circuit techniques using active devices should receive attention.

The development and refinement of the present algorithm to include interactive circuit analysis should be pursued. This will allow closer examination of system stability and aid in the design of pressure controlled oscillators. These devices are useful as pressure-to-frequency transducers. The output pressure of a fluidic sensor or preamplifier becomes the supply pressure of an oscillator which gives out a frequency related to the supply pressure. By appropriate choice of feedback circuitry, the relationship may be made linear or as in the case shown here. If the feedback is allowed to be purely acoustic, then the frequency is related to the square root of pressure. Low cost pressure transducers can easily read the pressure frequency and the signal can be directly used with digital microprocessors.

The use of high frequency fluidic amplifiers is limited only by the imagination. It is hoped that this present work will stimulate the development of new systems. Plans are already in the works for developing generalized circuit analysis programs for the LPA so that it can be used as a standard circuit element just like a resistor and an op amp or a capacitor, based on the above recommendations.

11. BIBLIOGRAPHY

1. Alexander, G. and Drzewiecki, T. M., "Fluidic Voice
    Communication Systems," SIGNAL, Vol. 33, No. 4, Jan 79.

2. Kirshner, J. M, Editor, Fluid Amplifiers, McGraw-Hill,
    NY, 1966.

3. Manion, F. M. and Mon, G., "Fluerics 33: Design and Staging of
    Laminar Proportional Amplifiers," HDL-TR-1608, NTIS No. AD751182,
    Sep 72.

4. Manion, F. M. and Drzewiecki, T. M., "Analytical Design of Laminar
    Proportional Amplifiers," Proc. HDL Fluidic State-of-the-Art
    Symposium, Oct 74.

5. Drzewiecki, T. M., Wormley, D. N., and Manion, F. M., "Computer-
    Aided Design Procedure for Laminar Fluidic Systems," J. Dynamic
    Systems, Measurement and Control, Trans ASME, 97, 4, series G,
    Dec 75.

6. Drzewiecki, T. M., "Fluerics 38: A Computer-Aided Design Analysis
    for the Static and Dynamic Port Characteristics of Laminar Pro-
    portional Amplifiers," HDL-TR-1758, Jun 76.

7. Horton, B. M., "Fluid Operated System," US Patent 3,425,430,
    4 Feb 69 (filed 24 Aug 60).

8. Roffman, G. L., and Deadwyler, R., "Direct Flueric Amplification
    and Transmission of Speech," Final Report to Naval Applied Sciences
    Lab under NAVSHIPS Development Task 4956, Code 03414.

9. Fisher, S., "Pneumatic Audio Heads Tenth Year of Fluidics,"
    Product Engineering, 3 Aug 70.

10. Roffman, G. L. and Deadwyler, R., "Flueric Amplification and
    Transmission of Speech," Proc. Joint Automatic Controls Conference,
    paper no. 5-E3, St. Louis, MO, 11-13 Aug 71.

11. Anonymous (HDL staff), "1977 Annual Posture Report," Harry Diamond
    Labs, 1977 (limited to government agencies only).

12. Unfried, H. H., "An Approach to Broad Band Fluid Amplification at Acoustic Frequencies," Proc. HDL Fluid Amplification Symposium, Vol I, Oct 65.

13. Sato, H., "The Stability and Transition of a Two-Dimensional Jet," J. Fluid Mechanics, 1960.

14. Roffman, G. L. and Toda, K., "A Discussion of the Effects of Sound on Jets and Flueric Devices," ASME Vibrations Conference, paper no. 69-Vibr-3, Mar 69.

15. Kirszenblat, A., "Transmission of a Fluidic Signal at Intermediate Distances," ASME Winter Annual Meeting paper no. 70-WA/Flcs-15 Dec 70.

16. Rschevkin, S. N. A Course of Lectures on the Theory of Sound, editor P. E. Doak, Macmillan Co., NY 1963.

17. Kirshner, J. M. and Katz, S., Design Theory of Fluidic Components, Academic Press, NY 75.

18. Roffman, G. L. and Katz, S., "Predicting Closed Loop Stability of Fluid Amplifiers From Frequency Response Measurements," Proc. HDL Fluid Amplification Symposium, Vol. I, Oct 65.

19. Moore, L., Zaloudek, J. and Turek, R., "Fluidic AC Amplifiers," Final Report to Harry Diamond Labs by Bowles Fluidics Corp. on Contract no. DA-49-186-AMC-325(D), Jun 67.

20. Healey, A. J. and Shipp, E., "Vent Length Effects on a Proportional Amplifier," Army Research Office Technical Report, Durham, N. C., Sep 73.

21. Healey, A. J., "Jet Deflection Proportional Amplifier," Proc. HDL Fluidic State-of-the-Art Symposium, Vol I, Adelphi, MD, Oct 74.

22. Griffin, W. S. and Gebben, V. D., "A Proportional Fluid Jet Amplifier with Flat Saturation Characteristics and Its Application to a Gain Block," NASA TM X-1915, Nov 69.

23. Kelley, L. and Boothe, W., "Hydraulic Fluidics," Trans. ASME, J. Dynamic Systems Measurement and Control, Jun 73/originally ASME WAM paper no. 68-WA/Aut-26, Nov 69).

24. Drzewiecki, T. M., "Design Considerations for a Flueric Laminar Jet Angular Rate Sensor," ASME WAM, Dec 79, paper no. 79-WA/DSC-3. Dec 79.

25. Kirshner, J. M., and Manion, F. M., "The Jet Deflection Proportional Amplifier," ASME publication, 70-Flcs-17, Jun 70.

26. Foster, K., and Parker, G., Fluidics, Wiley-Interscience, 70.

27. Belsterling, C., Fluidic System Design, Wiley-Interscience, 71.

28. Iseman, J. M., "A Circuit Analysis Approach to the Solution of Passive Pneumatic Fluidic Compensation Networks," Proc. HDL Fluidic State of the Art Symposium, Vol IV, Oct 74.

29. Zalmanzon, L. A., Components for Pneumatic Control Instruments, Pergamon Press, Oxford, 65, pp 244-6.

30. Cornish, R. J., "Flow in a Pipe of Rectangular Cross-section," Proc. Roy. Soc. A, CXX (1928).

31. Blackburn, J. F., Reethof, G. and Shearer, J. L. Fluid Power Control, Wiley, NY, 1960.

32. Drzewiecki, T. M., "The Design of Flueric, Turbulent, Wall Attachment Flip-Flops," Proc. HDL Fluidic State of the Art Symposium, Vol I, Oct 74.

33. Drzewiecki, T. M., "Planar Nozzle Discharge Coefficients," Developments in Mechanics, Vol 7, Proc. 13th Midwestern Mechanics Conference, Aug 73.

34. Drzewiecki, T. M., "Fluerics 37: A General Planar Nozzle Discharge Coefficient Representation," HDL-TM-74-5, Aug 74.

35. Drzewiecki, T. M. and Manion, F. M., "Fluerics 40: LJARS-the Laminar Jet Angular Rate Sensor," HDL-TM-79-7, 1979.

36. Hoglund, R. and Simcox, C., "The Effects of Acoustic Inputs on Turbulent Jets," Purdue Univ. report on US Army contract DAAG39-67-6-0022, April 68.

37. Shields, W. L. and Karamcheti, K., "An Experimental Investigation of the Edgetone Flow Field," SUDDAR No. 304, Stanford U., Feb 67.

38. Stiffler, A. K. and Shearer, J. L., "Sinusoidal Exitation of a Free Turbulent Jet with Constant Amplitude Transverse Pressure Gradients Near the Nozzle Exit," Trans. ASME, J. Dynamic Systems Measurement and Control, June 1973.

39. Beranek, L. L. Acoustic Measurements, Wiley and Sons, N.Y., 49.

40. Brown, G. B., "The Vortex Motion Causing Edgetones," Proc. Phys. Soc. London, 49,493, (1937).

41. Brown, Forbes T. and Humphrey, R. A., "Dynamics of a Proportional Amplifier," ASME papers 69-WA/Fics-2,3, J. Basic Engineering series D, 92, 1970.

42. Randall, R. H., An Introduction to Acoustics, Addison-Wesley Press, Cambridge, Mass, 51.

43. Drzewiecki, T. M., and Manion, F. M., "The Laminar Flip-Flop," Proc. HDL Fluidics State-of-the-Art Symp., Vol II, Oct 74.

44. Drzewiecki, T. M. and Manion, F. M., "Flueric Laminar Digital Amplifier," U. S. Patent 3,958,602, 27 Apr 76.

45. Drzewiecki, T. M., Phillippi, R. M., and Paras, C. E., "Fluidics - A New Potential for Energy Conservation by Continuous High Temperature Monitoring and Control," ASME Publication Heat Transfer in Energy Conservation, Nov 77.

46. Simon, H. A., A Students Introduction to Engineering Design Pergammon Press Inc., N. Y., 1975.

47. Boothe, W. A. and Ringwall, C. G., "Fluidic Carrier Techniques," Proc. HDL Fluidic State of the Art Symposium, Vol III, Oct 74.

48. Westerman, W. J. and Wright, R. E., "Evaluation Program - Fluidic Laminar Rate Sensor - Final Report, " McDonnell-Douglas NAVAIR report L0252, under contract N00019-73-C-0265, 8 Mar 74.

49. Sutton, T. G., and Anderson, W. J., "Aerospace Fluidics Applications and Circuit Manufacture," Proc. HDL Fluidic State of the Art Symposium, Vol V, Oct 74.

```
**** TWO FORTRAN HARDCOPY ****
DSNAME FORWARC.DYN2.FORT


C*************************** D Y N 2 *********************************
C THIS PROGRAM WILL DETERMINE THE FREQUENCY RESPONSE OF A FLUIDIC
C LAMINAR PROPORTIONAL AMPLIFIER (LPA) FROM THE GEOMETRY ALONE.
C
C IN ORDER TO COMPILE AND RUN THIS PROGRAM THE TEKTRONICS TERMINAL
C PLOTTING LIBRARY PACKS MUST BE ATTACHED. THE FOLLOWING STATEMENT
C MUST BE MADE AT THE BEGINNING OF EACH DAY :
C
C FTXCLG DYN2 LIB('SYS1.TEKTCS.LOAD' 'SYS1.TEKAG2.LOAD')
C
C THEREAFTER DURING THE DAY ONE NEED ONLY "CALL DYN2" TO RUN.
C
C ALL INPUT SHOULD BE IN THE FREE FLOATING POINT FORMAT AS BELOW:
C
C INPUT THROAT WIDTH,ST,NOZZLE LENGTH,XN
C ?
C 1.25 1.0
C
C ANSWER ALL QUESTIONS AS INDICATED
C
C
C
C SET ASIDE SPACE FOR VARIABLES TO COMPUTE DISCHARGE COEFFICIENT
C
      DIMENSION G(25),F0(25)
C
C SET ASIDE SPACE FOR VARIABLES TO BE PLOTTED
C
      DIMENSION F(300),AR(300),PHS(300)
C
C DEFINE ALL COMPLEX VARIABLES
C
      COMPLEX S,T,Z,ZV,ZC,ZK,ZJ,ZP,ZFB,ZO,ZV1,ZV2,ZIN,ZL,BK1,BK2
1999  WRITE(6,2000)
2000  FORMAT(' ***************** D Y N 2 ******************-')
      WRITE(6,2001)
2001  FORMAT(' THIS PROGRAM WILL COMPUTE THE FREQUENCY RESPONSE OF AN')
      WRITE(6,2002)
2002  FORMAT(' LPA GIVEN ITS GEOMETRY AND OPERATING POINT')
      WRITE(6,999)
999   FORMAT(' IF THIS IS AN HDL STD MOD 3.1.1.8 LPA ENTER 1')
      READ(5,*) HDLSTD
      IF(HDLSTD.EQ.1) GO TO 998
      WRITE(6,1000)
1000  FORMAT(' INPUT THROAT WIDTH,ST,NOZZLE LENGTH,XN')
      READ(5,*) ST,XN
      WRITE(6,1001)
1001  FORMAT(' INPUT CONTROL LNGTH,XC,AVG WDTH,BCBAR,MIN WDTH,BCMIN')
      READ(5,*) XC,BCBAR,BCMIN
      WRITE(6,1002)
1002  FORMAT(' INPUT SPLITTER LNGTH,XSPL,WDTH,BSP,OUTPUT WIDTH,BO')
      READ(5,*) XSPL,BSP,BO
      WRITE(6,1003)
1003  FORMAT(' INPUT ENTRAINMT RADIUS,RE,BIAS PRESSURE,PB')
      READ(5,*) RE,PB
      WRITE(6,1004)
```

```
1004   FORMAT(' INPUT REYNOLDS NO.,FNR,ASPECT RATIO,SIGMA,NOZZLE WIDTH,
      1 ,IN MM')
       READ(5,*) FNR,SIGMA,BS
       WRITE(6,1005)
1005   FORMAT(' INPUT CONTROL WIDTH,BC,SPLITTER DIST.,XSPL')
       READ(5,*) BC,XSP
       WRITE(6,800)
800    FORMAT(' INPUT LENGTHS OF VENTS, XLV1,XLV2')
       READ(5,*) XLV1,XLV2
       WRITE(6,801)
801    FORMAT(' VENTVANE DIST,XV1,OUTPUT LGTH,XOUT,AVG WDTH,BOBAR')
       READ(5,*) XV1,XOUT,BOBAR
998    CONTINUE
       WRITE(6,802)
802    FORMAT(' INPUT NUMBER OF STAGES')
       READ(5,*) NSTAGE
       WRITE(6,804)
804    FORMAT(' IF YOU WANT TABULATION OF EACH POINT SET PRINT=1.')
       WRITE(6,805)
805    FORMAT(' PRINT= ')
       READ(5,*) PRINT
       WRITE(6,806)
806    FORMAT(' IF YOU WANT BLOCKED RESPONSE SET AA=1.0')
       WRITE(6,807)
807    FORMAT(' INPUT AA=')
       READ(5,*) AA
       IF (HULSTD.NE.1) GO TO 997
C
C THIS IS THE HUL STD MOD 3.1.1.8 GEOMETRY
C
       BT=1.25
       XV=1.0
       XC=10.0
       BOBAR=2.75
       BCMIN=1.0
       XSPL=0.75
       BSP=0.5
       BO=1.5
       RE=0.25
       PB=0.0
       BC=1.0
       XSP=6.0
       XV1=5.0
       XOUT=12.0
       BOBAR=2.35
       XLV1=1.0
       XLV2=0.75
C
C ENTER VALUES OF REYNOLDS NO., ASPECT RATIO AND SIZE
C
       WRITE(6,810)
810    FORMAT(' INPUT ENR,SIGMA,NOZZLE WIDTH BS IN MM')
       READ(5,*) FNR,SIGMA,BS
997    CONTINUE
C
C   COMPUTE THE MODIFIED REYNOLDS NUMBER
C
       ENRMOD=FNR/(XN+1.0)/(1.+1./SIGMA)**2
C
C   COMPUTE DISCHARGE COEFFICIENT BY REGULA FALSI ON THE IMPLICIT
```

187

```
C     UNIVERSAL DISCHARGE FUNCTION.
C
      DO 1006 J=1,24
      IF(J.GT.1) GO TO 1007
      C(J)=0.5
      GO TO 1009
1007  IF(J.GT.2) GO TO 1008
      C(J)=0.6
1009  FO(J)=2.407/C(J)*(EXP(6.6*C(J)**2)-1.0)-SIGMA0
      IF(J.LT.2) GO TO 1006
      C(J+1)=C(J)-FO(J)*(C(J)-C(J-1))/(FO(J)-FO(J-1))
      IF(ABS(FO(J)).LT.0.01) GO TO 1010
1008  CONTINUE
1010  CO=C(J)
C
C COMPUTE 2D DISCHARGE COEFFICIENT,O
C          ENTRAINED FLOW TO CONTROL,QE
C          ENTRAINED FLOW TO VENT VANE,QEVV
C          JET EDGE SPACE AT CONTROL,SE
C          JET EDGE SPACE AT VENT VANE,SEVV
C          CONTROL SPILLBACK FLOW,OCSB
C          VENTVANE SPILLBACK FLOW,QVVSB
C          NET ENTRAINMENT COEFFICIENTS,A1,A11
C          SPILLBACK LOSS COEFFICIENT,CSB
C
      O=(1.-SIGMA)/2.+SQRT((SIGMA+1.)**2/4.-SIGMA*(1.-CO))
      QE=1.5519*(.00772+1.32*(FO+RF)/(CO*ENR))**(.3333)-.5
      QEVV=1.6019*(.00772+1.32*XV1/(CO*ENR))**(.3333)-.5
      AK=1./(CO*QE+1/2.)
      SE=0.5*(BT-(1.+FO/.021/CO/ENR)**0.6666657)
      SEVV=0.5*(3.1-(1.+XV1/.021/CO/ENR)**.6665657)
      TT1=ALOG((1.+.5*O*AK)/(1.-.5*O*AK))/2.
      AK3=4./(EXP(TT1)+EXP(-TT1))**2
      AK4=AK3/2./CO
      OCSB=QE*EXP(-AK4*SE)/2.
      A1=AK4*QCSB*2.
      CSS=1.-3.6363*AK4*QCSB**2
      AKVV=1./(CO*QEVV+O/2.)
      TT1VV=ALOG((1.+.5*O*AKVV)/(1.-.5*O*AKVV))
      AK3VV=4./(EXP(TT1VV)+EXP(-TT1VV))**2
      AK4VV=AK3VV/QEVV/CO
      QVSB=QEVV*EXP(-AK4VV*SEVV)/2.
      A11=AK4VV*QVSB+1.
C
C COMPUTE JET EDGE RESISTANCE,RV, BY RECTANGULAR INTEGRATION
C OF THE 2D LAMINAR JET VELOCITY PROFILE FOR BIAS PRESSURES
C FROM 0.1 TO 0.5.
C
      R4=0.
      DO 1020 J=1,9
      P1=J
      P1=0.05+P1/20.
      P=P1**.25
      S1=ALOG(1./P+SQRT(1./P/P-1.))
      YO=S1/AK
      D1=(BT/2.-YO)/10.
      AI=0.
      AII=0.
1030  Y1=YO+AII*D1
      S2=2./(EXP(Y1*AK)+EXP(-Y1*AK))
```

188

```
           A=(SQRT(G.**4.+P1)-S2**2)*D1
           AI=AI+A
           AII=AII+1.0
           IF(Y1.LT.T/2.) GO TO 1040
           GO TO 1050
1040       R1=D*P1/R1
           R4=R4+R1
1050       CONTINUE
           RV=R4/10.
C
C  COMPUTE CHANNEL RESISTANCE CORRECTION AND COEFFICIENTS
C
           IF(BCBAR/SIGMA.GT.2.0) GO TO 690
           AK2=0.35
           GO TO 700
690        AK2=0.5
700        T4=24.*PO*CD*(SIGMA/BCBAR+BCBAS/SIGMA+AK2)/(BCBAR**2*SIGMA
          1*ENR)
           T5=0.91*(CD/BCMIN)**2
           CTHETA=1.0*CD*CD
           IF(CD.GT.0.5) GO TO 770
           ENO=2.*CD
           GO TO 790
770        ENO=1.
790        CONTINUE
C
C  COMPUTE   DISPLACEMENT THICKNESS,DO
C            EFFECTIVE NOZZLE LENGTH,X
C            CORE LENGTH,XO
C            VIRTUAL ORIGIN,XVO
C
           DO=(1.+SIGMA)/4.-.5*SQRT((1.+SIGMA)**2/4.-(1.-CD)*SIGMA)
           X=ENR*(DO*10./3.)**2/25.*ENO
           XO=X*(.27/(DO*1.4)**2-1.)
           XVO=0.0158*CD*ENR
C
C  CHOOSE BOUNDARY LAYER COEFFICIENTS FOR PLATE LOSSES FOR LOW
C  ASPECT RATIOS AND HIGH ASPECT RATIOS
C
           IF(SIGMA.LT.1.) GO TO 826
           EN5=4.
           EN6=5.6
           GO TO 830
826        EN5=3.
           EN6=3.
830        CONTINUE
C
C  COMPUTE PLATE LOSS COEFFICIENT,CO
C
           IF(XO.GT.0.) GO TO 850
           CO=(1.+XSO/XVO)**(-2./3.)
           GO TO 900
850        IF(XO.GT.XS2) GO TO 890
           IF(CD.GT..5) GO TO 860
           CO=(1.+(XS2-XO)/XVO)**(-2./3.)
           GO TO 870
860        CO=(1.+(XS2-XO)/XVO)**(-2./3.)*(1.-EN5*SQRT((X+XO)/ENR)
          1/SIGMA)/(1.-EN6*SQRT(X/ENR)/SIGMA)
870        CONTINUE
           GO TO 900
```

189

```
880    CO=(1.-SNS*SQRT((XSF+X)/CNR)/SIGMA)/(1.-SNS*SQRT(X/CNR)/SIGMA)
       SNS=1.
900    CONTINUE
C
C      COMPUTE THE BLOCKED PRESSURE RECOVERY,PR
C
       PC=PB
       QC=-0.5*(T4+RV)/T5+SQRT(.25*((T4+RV)/T5)**2+(PC+RV*(QE-QCSB))
      1/T5)
       RC=T4+T5*QC
       PJ=(PC/RC-(QE-QCSB))*RC*RV/(RC+RV)
       A3=QC+.5
       B2=3./(1.+XSP/.021/CO/CNR)**(2./3.)
       IF(QC.LT.B2) GO TO 920
       B2=QC
920    PR=CO*(1.-1.1*BSP/(SQRT(CO*CNR*BSP/2.)))*CTHETA/BC*CSB*
      1(1.5+2.*CO*PJ*SQRT(ABS(PJ))/(RV*CTHETA))
C
C      COMPUTE THE OUTPUT CHARACTERISTIC AND INPUT CHARACTERISTIC
C
       RCL=24.*XCUT*CO*(SIGMA/BOBAR+BOBAR/SIGMA+AK2)/(BOBAR**2*SIGMA
      1*CNR)
       AK5=.45*CO*CO/BO**2
       AICH=0.
       I6=0
       T7=0.
       Z3=1.
       DO 1470 K=1,51
       QO=K
       QO=QO/100.-.01
       IF(I6.EQ.1) GO TO 1170
       IF(SIGMA.LT.2.) GO TO 1140
       Z3=2./SIGMA
1140   PO=PR*(1.-2.*QO*CO/SQRT(PR*BO))/(1.-CO*CO/BO/SQRT(BO*PR))
      1-RCL*QO-AK5*QO*QO+CO*SQRT(PR/BO)*QO*.25*SIGMA*Z3+(CO*QO/BO)
      2**2*4.
       R6=CO*SQRT(PR/BO)/(1.-CO*CO/BO/SQRT(PR*BO))*(-2.+(1.-2.*QO
      1*CO/SQRT(PR*BO))/BO/(1.-QO*CO/BO/SQRT(PR*BO)))-RCL-2.*AK5*
      2QO+CO*SQRT(PR/BO)*.25*SIGMA*Z3+8.*(CO/BO)**2*QO
       ZZ=RCL+AK5*QO+PO/(QO+.00000001)
       A4=.5/A3
       IF(A4.LT.ZZ) GO TO 1180
       IF(PO/(A3-QO).LT.-R6) GO TO 1180
       I6=1
       A7=QO
       A8=PO
1170   PO=A8/(A3-A7)*(A3-QO)
       R6=-A8/(A3-A7)
1180   CONTINUE
       QC=QO
       RC=T4+T5*QC
       PC=-(QE-QCSB)*RV+(RV+RC)*CC
       SF=PO-PC
       JAICH=AICH
       IF(SF.GT.0.) GO TO 1420
       IF(T7.EQ.1.) GO TO 1420
       T7=1.
       ROUTSS=R6
       POUTSS=PO
       RCSS=RC
```

.190

```fortran
      RCSS=RC
      GO TO 1480
1420  IF(AICH-JAICH.GT.0.1) GO TO 1450
1450  AICH=AICH+.2
      IF(PC.LT.C.) GO TO 1480
1470  CONTINUE
1480  CONTINUE
C
C     COMPUTE BIAS JET EDGE PRESSURE,PJ,BIAS PRESSURE RESISTANCE,RK
C     AND SPILLBACK RESISTANCE , RD.
C
      PJ=(PBOTSS/RCSS-(1.-QCSS))*RCSS*RV/(RCSS+RV)
      RK=2.*CTHETA*CD*CD/((BC+2.*RE)**2*SQRT(PJ))
      RD=4.*CTHETA/(RI*(BC+2.*RE)**2)
C
C     COMPUTE THE INDUCTANCES:
C                 CONTROL,ELC
C                 BIAS PRESSURE,ELK
C                 JET EDGE SPACE,ELV
C                 UPSTREAM VENT,ELV1
C                 DOWNSTREAM VENT,ELV2
C                 OUTPUT,ELO
C
      ELC=2.*CD*CD*XC/BCBAR
      ELK=4.*CD*CTHETA*CD/((BC+2.*RE)**2*PJ)
      ELV=2.*CD*CD/(.5*RT-.5)
      ELV1=2.*CD*CD/(XV1-(BC+RE))*XLV1
      ELV2=2.*CD*CD/(XSP+XSPL-XV1)*XLV2
      ELO=2.*CD*CD*ACUT/BCBAR
C
C     COMPUTE PARASITIC CAPACITANCE,CP,AND JET COMPLIANCE,CJ
C
      CP=BCBAR*XC*(ENR/1000./BS)**2/760.0
      CJ=(BC+2.*RE)**3/(7.92*CD*CD)
C
C     COMPUTE THE RESISTANCES:
C                 CONTROL,RC
C                 UPSTREAM VENT,RV1
C                 DOWNSTREAM VENT,RV2
C                 OUTPUT , RO
C
      BV1=XV1-(BC+RE)
      BV2=XSP+XSPL-XV1
      RC=RCSS
      RV1=24.*XLV1*CD*(SIGMA/BV1+BV1/SIGMA+.5)/(BV1**2*SIGMA*ENR)
      RV2=24.*XLV2*CD*(SIGMA/BV2+BV2/SIGMA+.5)/(BV2**2*SIGMA*ENR)
      RO=-ROUTSS
      WRITE(6,954)
954   FORMAT(' THE FOLLOWING ARE A FEW VALUES FOR A CHECK')
      WRITE(6,950)
950   FORMAT('    RC       RV       RD       RO       PR')
      WRITE(6,951) RC,RV,RD,RO,PR
951   FORMAT( 5E10.5)
      WRITE(6,4000)
4000  FORMAT('    RV1      RV2      PJ       RK       CP')
      WRITE(6,4040) RV1,RV2,PJ,RK,CP
4040  FORMAT( 5E10.4 )
      WRITE(6,952)
952   FORMAT('    LC       LV       LK       LV1      LV2      LO')
      WRITE(6,953) ELC,ELV,ELK,ELV1,ELV2,ELO
```

```
953     FORMAT( 6F10.4)
        WRITE(6,955)
955     FORMAT(' IN ORDER FOR THE PROGRAM TO CONTINUE ENTER ANY NO.')
        READ(5,*) XXXX
C
C COMPUTE PRELIM CONSTANTS:
C                       TRANSPORT DELAY TO SPLITTER,TI
C                       TRANSPORT DELAY T. VANE,T2
C                       JET DEFLECTION COEFFICIENT,AKJ
C                       NOZZLE WIDTH IN METERS,BS
C
        T1=2.*XSP
        T2=2.*XV1
        AKJ=(BC+2.*BS)**2/(5.25*CD*CD)
        BS=BS/1000.
C
C PROGRAM AIR KINEMATIC VISCOSITY IN (M*M/S)
C
        DVISC=1.41643-5
C
C THIS  LOOP COMPUTES THE GAIN AND PHASE SHIFT OF THE LPA
C TRANSFER FUNCTION AT DISCRETE VALUES OF NORMALIZED FREQUENCY,F.
C
        DO 10 I=1,250
C
C INCREMENT FREQUENCY F
C
        F(I)=10.**(I*.01-3.)
C
C COMPUTE NORMALIZED RADIAN FREQUENCY,W AND LAPLACE OPERATOR,S.
C
        W=2.*3.14159*F(I)
        S=CMPLX(0.,W)
C
C   COMPUTE THE ACOUSTIC ATTENUATION FACTOR,ZFB
C
        ZFB=10.**(-2.767E-5*SQRT(CD*DVISC*ENR*F(I))*XSP/(BS*SIGMA))
C
C   COMPUTE THE COMPLEX IMPEDANCES:
C                       UPSTREAM VENT,ZV1
C                       DOWNSTREAM VENT, ZV2
C                       JET EDGE ,ZV
C                       JET BARRIER, ZJ
C                       BIAS PRESSURE,ZK
C                       CONTROL, ZC
C                       LOAD,ZL
C                       INPUT,ZIN
        ZV1=RV1+S*LV1
        ZV2=RV2+S*LV2
        ZV=RV+FLV*S
        ZJ=1./(CJ*S)+5.0*CD*CD/BC**2
        ZK=RK+ELK*S
        ZO=RO+LO*S
        ZC=RC+LC*S
        Z=1./(1./ZV+1./ZK+1./ZJ+1./RO)
        ZP=1./(1./(2.+LC*S)+S*CP)
        ZIN=ZP*Z/(RC+ZP)/(Z+S*LC)
        IF (AA .EQ.1.0) GO TO 34
        ZL=RC+ZP
        GO TO 35
```

```
   34   ZL=CMPLX(9.0099.,1.099499.)
   35   CONTINUE
C
C   ADJUST VENT IMPEDANCE BY ACOUSTIC ATTENUATION FACTOR
C
      ZV2=ZV2*2.F5
      ZV1=ZV1*2.F5/2.
C
C COMPUTE COMPLEX TRANSFER FUNCTION VALUE,T
C
      BK1=AKJ*CEXP(-T1*S)*(2.*XSP/(SC+2.*RE)-1.)/(1.+AKJ*CEXP
     1(-T2*S)*(2.*XV1/(SC+2.*RE)-1.)*A11*ZV2)
      BK2=4.*BK1*FR/(1.+BK1*ZV2)
      T=(BK2*ZL)*ZL/(Z0+ZL-BK2*ZV2))**NSTAGE
C
C COMPUTE MAGNITUDE OF TRANSFER FUNCTION T,AR
C
      AR(I)=20.*ALOG10(CABS(T))
      AR1=CABS(T)
C
C COMPUTE PHASE SHIFT AS ARCTAN(IMAGINARY/REAL)
C
      TR=REAL(T)
      TI=AIMAG(T)
      PH=ATAN2(TI,TR)
      PHASE=PH*180./3.14159
      PHS(I)=PHASE
      IF (PRINT.EQ.1.00) GO TO 27
      GO TO 10
C
C PRINT VARIABLES OF INTEREST IF DESIRED
C
   27 WRITE(6,*) F(I),AR(I),PHASE,AR1
   10 CONTINUE
C
C CALL PLOT 10 ROUTINE AND PLOT OF AMPLITUDE RATIO AND PHASE
C SHIFT VERSUS FREQUENCY ON A SEMILOG GRID.
C
      CALL QLGPLT(F,1,AR,0,250,1,'NORMALIZED FREQUENCY,F',22,
     1'GAIN, DB',8,'FREQUENCY RESPONSE OF AN LPA',28,2,IER)
      CALL QLGPLT(F,1,PHS,0,250,1,'NORMALIZED FREQUENCY,F',22,
     1'PHASE SHIFT,DEGREES',19,'FREQUENCY RESPONSE OF AN LPA',28,2
     2,IERR)
      WRITE(6,3000)
 3000 FORMAT(' IF YOU WANT TO DO ANOTHER CASE ENTER 1.0')
      READ(5,*) AGAIN
      IF(AGAIN.EQ.1.0) GO TO 1999
C
C   END OF PROGRAM
C
      STOP
      END
```

```
IF YOU WANT TO DO ANOTHER CASE ENTER 1.0
?
1.
***********************  D Y N 2  ***********************
THIS PROGRAM WILL COMPUTE THE FREQUENCY RESPONSE OF AN
LPA GIVEN ITS GEOMETRY AND OPERATING POINT
IF THIS IS AN HDL STD MOD 3.1.1.8 LPA ENTER 1
?
1
INPUT NUMBER OF STAGES
?
1
IF YOU WANT TABULATION OF EACH POINT SET PRINT=1.
PRINT=
?
1.
IF YOU WANT BLOCKED RESPONSE SET AA=1.0
INPUT AA=
?
0.
INPUT EHR,SIGMA,NOZZLE WIDTH BS IN MM
?
330.0 3.0 0.5
THE FOLLOWING ARE A FEW VALUES FOR A CHECK
      RC         RV         RD         RO         PR
    0.1367     1.8995     8.1203     0.2608     0.3591
      RV1        RV2        PJ         RK         CP
    0.0031     0.0023     0.2792     0.5329     0.0158
      LC         LV         LK         LV1        LV2        LO
    3.5626     7.8377     2.0170     0.2613     0.1959     5.0028
IN ORDER FOR THE PROGRAM TO CONTINUE ENTER ANY NO.
?
```

Table A-1. Computer printout of the frequency response of the LPA in figure 42.

F	G_p (db)	PHASE (degrees)	G_p (ratio)
.512863323E-02	14.5327063	-42.2685089	5.32897459
.524808466E-02	14.5241499	-43.2798920	5.32352747
.537033007E-02	14.5149717	-44.3161469	5.31800461
.549542531E-02	14.5050726	-45.3779391	5.31194496
.562343374E-02	14.4944115	-46.4654368	5.30543327
.575441122E-02	14.4829054	-47.5795288	5.29841042
.588845462E-02	14.4705219	-48.7203625	5.29095732
.602561235E-02	14.4571848	-49.8900452	5.28274155
.616597012E-02	14.4427967	-51.0876160	5.27399635
.630953751E-02	14.4273143	-52.3133954	5.26452648
.645655786E-02	14.4106407	-53.5700226	5.25458706
.660695500E-02	14.3926649	-54.8552469	5.24364471
.676085427E-02	14.3732926	-56.1731415	5.23195793
.691831857E-02	14.3524904	-57.5211029	5.21944839
.707947463E-02	14.3300743	-58.9010773	5.20599747
.724437833E-02	14.3059855	-60.3172782	5.19157791
.741312653E-02	14.2800760	-61.7583313	5.17611694
.758579091E-02	14.2522439	-63.2365578	5.15955544
.776248425E-02	14.2223473	-64.7424293	5.14182663
.794330239E-02	14.1902742	-66.2944641	5.12287331
.812833811E-02	14.1559390	-67.8748016	5.10260582
.831766739E-02	14.1199451	-69.4897919	5.08098030
.851140171E-02	14.0794325	-71.1394683	5.05791955
.870966166E-02	14.0371770	-72.8242953	5.03334618
.891254097E-02	13.9919167	-74.5440826	5.00721169
.912013650E-02	13.9435159	-76.2929502	4.97944641
.933256608E-02	13.8921099	-78.0685620	4.95000648
.954994932E-02	13.8371563	-79.9131622	4.91878788
.977240130E-02	13.7786655	-81.7721252	4.88577271
.100000291E-01	13.7164896	-83.6650543	4.85092735
.102329254E-01	13.6504793	-85.5917664	4.81419754
.104712881E-01	13.5804510	-87.5516052	4.77554321
.107152015E-01	13.5062962	-89.5439385	4.73494530
.109647997E-01	13.4279659	-91.5677032	4.69240570
.112201758E-01	13.3451729	-93.6219482	4.64792051
.114815347E-01	13.2579899	-95.7060394	4.60150146
.117489807E-01	13.1662493	-97.8168171	4.55315590
.120226555E-01	13.0699453	-99.9589386	4.50295448
.123027079E-01	12.9690027	-102.125168	4.45092392
.125892572E-01	12.8634214	-104.315364	4.39714813
.129825033E-01	12.7531843	-106.530304	4.34169399
.131825767E-01	12.6383591	-108.766479	4.28467559
.134896450E-01	12.5189848	-111.023239	4.22619438
.138038434E-01	12.3951788	-113.298584	4.16638374
.141253844E-01	12.2670028	-115.591492	4.10535431
.144544169E-01	12.1346360	-117.900253	4.04328918
.147911124E-01	11.9983578	-120.223465	3.98031999
.151356049E-01	11.8582678	-122.559189	3.91663742
.154881701E-01	11.7146311	-124.906799	3.85240354
.158489458E-01	11.5677385	-127.264755	3.78779984
.162181221E-01	11.4179239	-129.631561	3.72302818
.165958703E-01	11.2654991	-132.006226	3.65826416
.169824325E-01	11.1108370	-134.387802	3.59370041

195

.173780136E-01	10.9542609	-136.775665	3.52952576
.177820111E-01	10.7954201	-139.168823	3.46594048
.181970033E-01	10.6775675	-141.565635	3.40313149
.186209782E-01	10.4790005	-143.955564	3.34127003
.190546252E-01	10.3183497	-146.375412	3.29065763
.194984749E-01	10.1602221	-148.785089	3.22115326
.199526474E-01	10.0026445	-151.208424	3.16724043
.204173774E-01	9.84672356	-153.619141	3.10606802
.208929740E-01	9.69315624	-156.042984	3.05251694
.213796459E-01	9.54248714	-159.472122	3.00002239
.218776539E-01	9.39543819	-160.907639	2.94966125
.223872028E-01	9.25267220	-163.349976	2.90157509
.229086901E-01	9.11488342	-165.801025	2.85590935
.234423056E-01	8.98282814	-168.261735	2.81291853
.239883624E-01	8.85730839	-170.733826	2.77246284
.245470926E-01	8.73910236	-173.218669	2.73498726
.251188937E-01	8.62909412	-175.712765	2.70056534
.257039666E-01	8.52815914	-178.235947	2.66936493
.263027065E-01	8.43725872	179.227402	2.64157486
.269153416E-01	8.35741205	176.662411	2.61748494
.275422968E-01	8.28970718	174.083939	2.59703023
.281838551E-01	8.23528290	171.471085	2.58005823
.288403593E-01	8.19539261	168.825912	2.56903267
.295120701E-01	8.17136383	166.144913	2.56193542
.301935166E-01	8.16470146	163.422791	2.55997086
.309029705E-01	8.17696190	160.654907	2.56358719
.316228122E-01	8.20993519	157.835358	2.57333755
.323594213E-01	8.26555443	154.957733	2.58986855
.331131294E-01	8.34598637	152.014459	2.61396217
.338844210E-01	8.45366237	148.996414	2.64656830
.346737094E-01	8.59131527	145.893204	2.69284468
.354813859E-01	8.76209831	142.692383	2.74223709
.363078080E-01	8.96952438	139.379120	2.80851364
.371535495E-01	9.21774101	135.934280	2.88592882
.380189903E-01	9.51151562	132.334793	2.98931264
.389045887E-01	9.85644054	128.550980	3.11044121
.398107022E-01	10.2589865	124.544434	3.25798798
.407380387E-01	10.7270460	120.262939	3.43355784
.416869745E-01	11.2696486	115.636871	3.66001129
.426580161E-01	11.8973988	110.568634	3.93432235
.436515510E-01	12.6222630	104.919403	4.27674484
.446683541E-01	13.4569340	98.4829407	4.70911462
.457088426E-01	14.4115267	90.9530029	5.25504494
.467735678E-01	15.4858809	81.8657634	5.94694710
.478629991E-01	16.6492462	70.5429993	6.79927626
.489779040E-01	17.7953595	56.1161499	7.75887299
.501187779E-01	18.6800079	37.9605560	8.59015556
.512861758E-01	19.9363251	16.8639679	8.84742737
.524808168E-01	18.3627167	-4.31075001	8.28202249
.537031814E-01	17.1624298	-22.6918335	7.21310043
.549541228E-01	15.7023296	-37.4893799	6.09700594
.562342033E-01	14.2310289	-49.3251953	5.14696312
.575441019E-01	12.8566952	-59.0664825	4.39374542
.588843450E-01	11.6125612	-67.3926392	3.80739784
.602559745E-01	10.5006571	-74.7704010	3.34991074
.616595559E-01	9.51336193	-91.5065002	2.98997879
.630958080E-01	8.64060116	-87.8063354	2.70414543
.645654202E-01	7.87302494	-93.8100128	2.47543335
.660693645E-01	7.20272255	-99.6164551	2.29153592
.676083565E-01	6.62372684	-105.295837	2.14331027
.691831702E-01	6.13164043	-110.899918	2.02573204
.707945824E-01	5.72360229	-116.467345	1.93276978

|			
.724436045E-01	5.39811325	-122.029114	1.86168289
.741310716E-01	5.15305600	-127.697773	1.81030941
.758573777E-01	4.99506655	-133.221573	1.77737141
.776246786E-01	4.92215067	-138.883469	1.76242065
.794328451E-01	4.93701048	-144.605515	1.76500311
.812830925E-01	5.05125399	-150.393768	1.78900501
.831764935E-01	5.26703603	-156.252197	1.83380935
.851139426E-01	5.59656334	-162.179626	1.90470695
.933255553E-01	8.40714645	173.710297	2.63243234
.954992771E-01	9.64395864	167.813974	3.03492546
.977237821E-01	11.2156897	162.233261	3.63734627
.100000024	13.2571526	157.373505	4.60106887
.102329433	16.0074615	154.258549	6.31500435
.104712344	19.9391479	156.133299	9.93019485
.107151985	25.5266266	177.719162	18.8943939
.109647930	25.7541962	-123.078156	19.3959503
.112202048	20.6945953	-102.367034	10.8325405
.114815295	17.3294525	-101.910599	7.35314941
.117489755	15.2020550	-107.293148	5.75576210
.120226502	13.8691139	-115.124054	4.93691026
.123027027	13.1223803	-124.873856	4.53022003
.125892520	12.6626261	-136.405991	4.39674759
.128825009	13.0362816	-150.147110	4.48553467
.131825686	13.5809393	-167.034637	4.77581215
.134896398	14.3231916	171.437363	5.20187378
.138038635	14.7903968	144.109543	5.49471474
.141253769	14.3267870	113.257629	5.20402527
.144544065	12.0215322	84.9260101	4.37599564
.147911012	10.9354753	62.3596191	3.52187347
.151356399	9.20531150	44.8325553	2.88596344
.154881597	7.85816060	30.9503021	2.46892549
.158489347	6.93881702	19.9460144	2.22300720
.162181139	6.49946785	11.8230972	2.11335945
.165958941	6.52739239	7.45955849	2.12016487
.169824243	6.88230801	8.88873863	2.20959146
.173780084	6.96171693	18.4622845	2.20897421
.177828014	5.65444565	33.2551422	1.91744232
.181970298	2.91877556	43.5293427	1.39939022
.186208665	-.145062269	45.9943425	.983437777
.190546155	-2.91349597	43.1085359	.715031365
.194984674	-5.24223604	37.2337494	.546875000
.199526370	-7.12857723	29.7724457	.440120101

FREQUENCY RESPONSE OF AN LPA
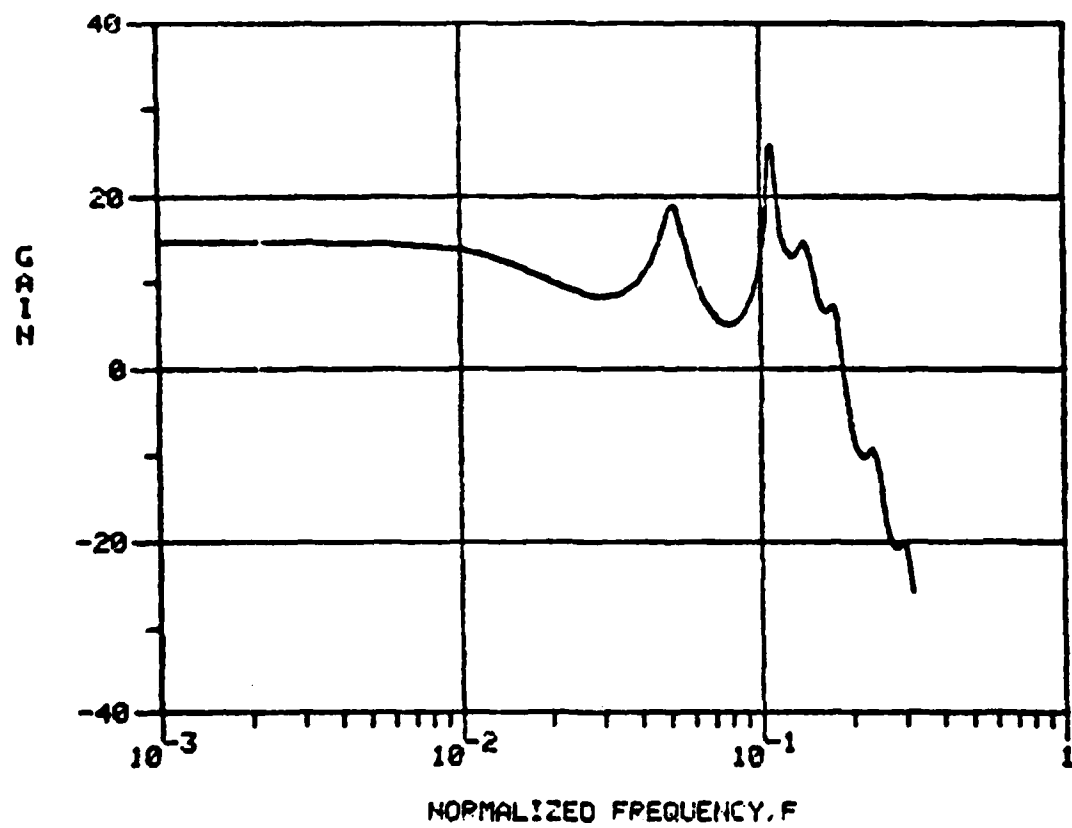
Figure A-1. Frequency response plot from Table A-1.

APPENDIX II.   The Experimental Method

The data collected on characteristics for the verification of the analysis presented in sections 2, 3 and 4 was comprised of:

1. Measurements of mean jet edge pressure.
2. Bode plots or pressure gain and phase shift versus frequency.
3. Static transfer characteristics.
4. Output pressure noise spectral analysis.
5. Carrier oscillator output frequency versus supply pressure.
6. Rectifier static transfer characteristic
7. Demodulator analog output level versus frequency.
8. Demodulator transient response.
9. Demodulator frequency response.

This appendix will specify the experimental techniques and apparatus used for each test and in the case of the LPA Bode plots will compare the numerous results with the computer model.

A.1   Measurement of Mean Jet Edge Pressure

The static pressure at the end of the control channel is to be measured as close to the jet edge as possible. To this end a 0.4 mm static tap was drilled in the cover plate of an LPA with $b_s = 0.5$ mm in the location already shown in figure 27. A low 10 Hz bandpass electronic manometer, tradename BAROCEL, was connected by a tank and plastic tubing to the tap. In this manner the frequency component (ripple) will be filtered out and the mean level only can easily be observed. A buffer amplifier of the same aspect ratio was used to drive the test amplifier so that operation was self-staged. The buffer amplifier was driven by an acoustic driver. The amplitude of the input signal was maintained at a constant level of 80 db by a General Radio Company 1569 Automatic Level Regulator tied to a 1/4 in (6.35 mm) B & K microphone placed at the fitting to the test LPA. Three different aspect ratio LPA's were tested $\sigma = 0.5$, $\sigma = 1.0$, $\sigma = 2.0$. Figure A1 shows the test arrangement schematically. The test data has already been presented in figure 28.
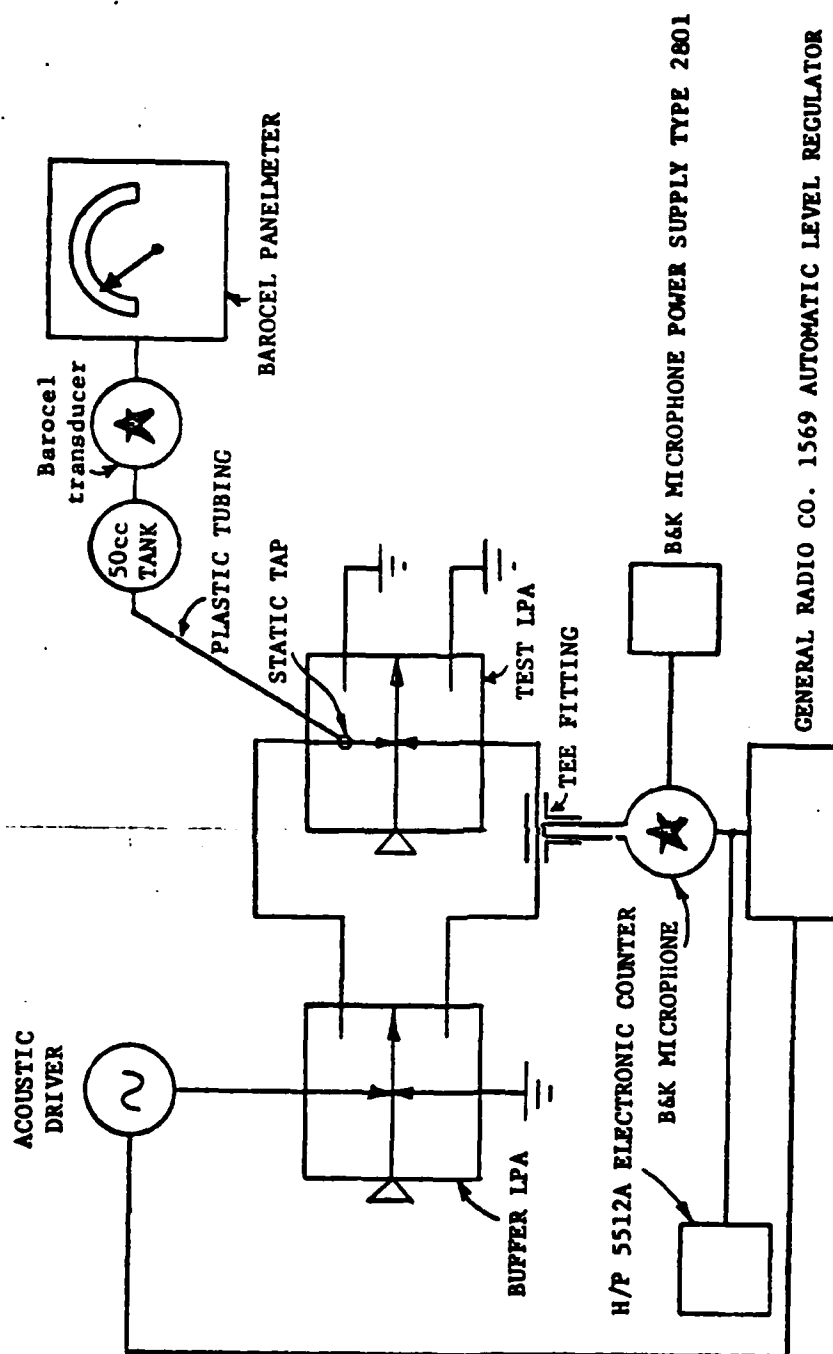
Figure A1. Schematic of the test apparatus for determining the mean jet edge pressure in an LPA.

A2. Measurement of LPA Frequency Response (Bode Plots)

The measurement of the LPA transfer function (gain) as a function of applied frequency is of the greatest importance to this research and development program. It is critically important that the measurement means not affect the LPA performance and that the data is truly representative of the LPA.

One means of estimating the LPA frequency response is called an insertion gain measurement which is described in detail by Toda et al. (Toda, K. Roffman, G., and Talkin, A., "The Matched Acoustic Generator," J. Dyn. Syst. Meas. and Control, March 1972). This gives a measure of the insertion gain of an LPA loaded into an infinite line. This, however, is not sufficient data for staged operation. It is necessary to avoid reflections and this is afforded by the infinite line.

If one were to measure the pressures directly at the port locations in a configuration where the distances between any two adjacent nodes is less than a wavelength, then reflections and standing waves should not develop. In addition, a meaningful gain measurement is desired of the LPA under loaded conditions on both the controls and outputs. Furthermore, it is desired to produce a truly differential (push-pull) control signal. To this and it was decided that mounting matched microphones flush in the control and output ports of an LPA driven by a buffer LPA and driving a load LPA would allow the measurement of self-staged gain. The microphone is not a differential device, so that the signals measured are one half the differential signal, but since gain is the ratio of output to output, this factor is common and cancels out resulting in a true gain measurement. (Note that when a single side acoustic input is measured, this is the whole input (since $P_2 = 0$) but the output is push-pull, hence, only half the output is measureed thus the ratio of the microphone signals is 6 db down (a factor of two)

from the true gain. (This was the case with the measurement of the Corning gain block.)

Figure A2 shows schematically the microphone emplacement and the buffer and load LPA arrangement. Figure A3 shows the complete apparatus schematically.

Figures A4 - A12 are Bode plots taken in this manner. The xy recorder plots give the data points. In some cases a Hewlett Packard 3575A Gain-Phase meter was used for point by point measurement when the BAFCO was down. Notice that blocked output response is obtained by placing a metal rod in the output manifold so that it is flush with the plane of the lower bounding plate of the test LPA. Each data set has the corresponding theoretical prediction plotted with it. Agreement on the whole is satisfactory.

Care must be exercised in not allowing standing waves to occur anywhere in the test arrangement. When the supply line to the LPA's was long, about 25 cm, an anomalous Bode plot could be generated with a resonance augmenting the $F = .01$ peak as shown in figure A13. This frequency, $f \sim 300$ Hz is very close to the quarter wavelength of the tubes ($f = 330$ Hz). Perhaps standing waves are generated in the supply so that the supply pressure may appear to increase at that frequency. This effect can be eliminated by using short tubing or manifolding to break up any standing waves. It is interesting to note, however, how the gain of an LPA may be shaped by external circuitry. This is an area of current interest. It may be useful or detrimental.
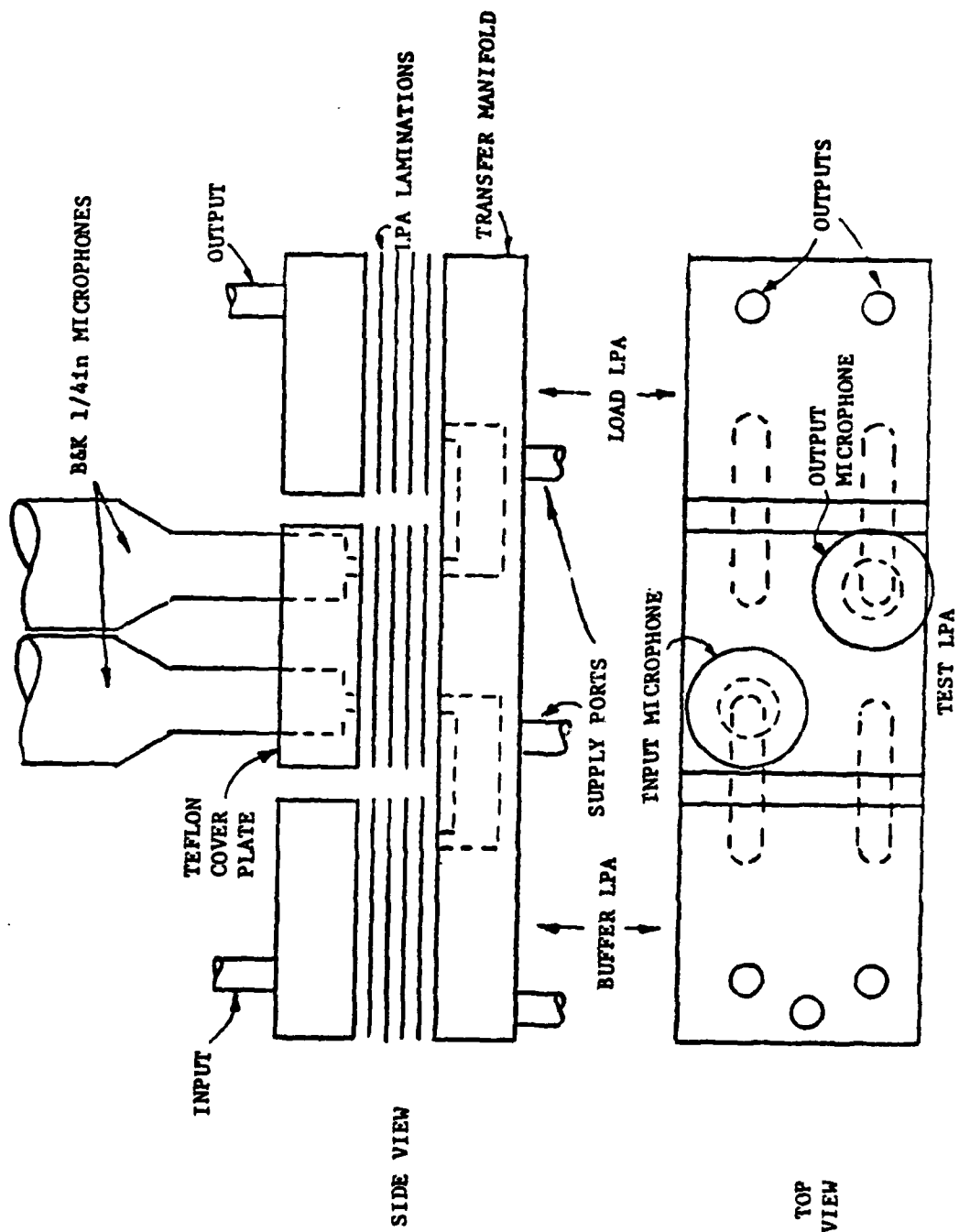
202

B&K 1/4in MICROPHONES

OUTPUT

LPA LAMINATIONS

TRANSFER MANIFOLD

TEFLON COVER PLATE

LOAD LPA

SUPPLY PORTS

INPUT MICROPHONE

BUFFER LPA

INPUT

SIDE VIEW

OUTPUTS

OUTPUT MICROPHONE

TEST LPA

TOP VIEW

Figure A2. Schematic drawing of the test setup for measuring self-staged dynamic gain of an LPA.

Figure A3. Schematic layout of the test apparatus for the dynamic testing of LPAs.
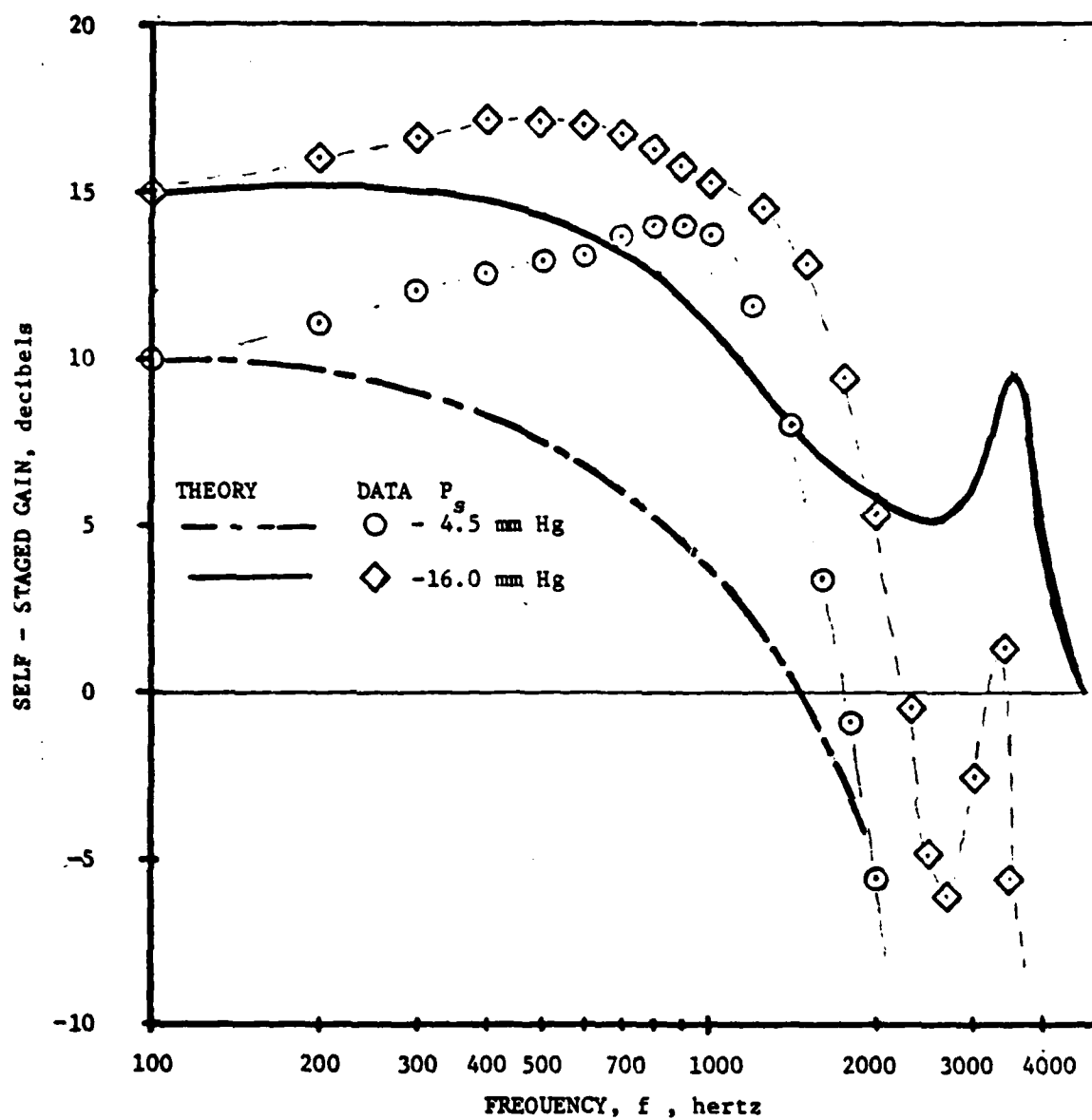
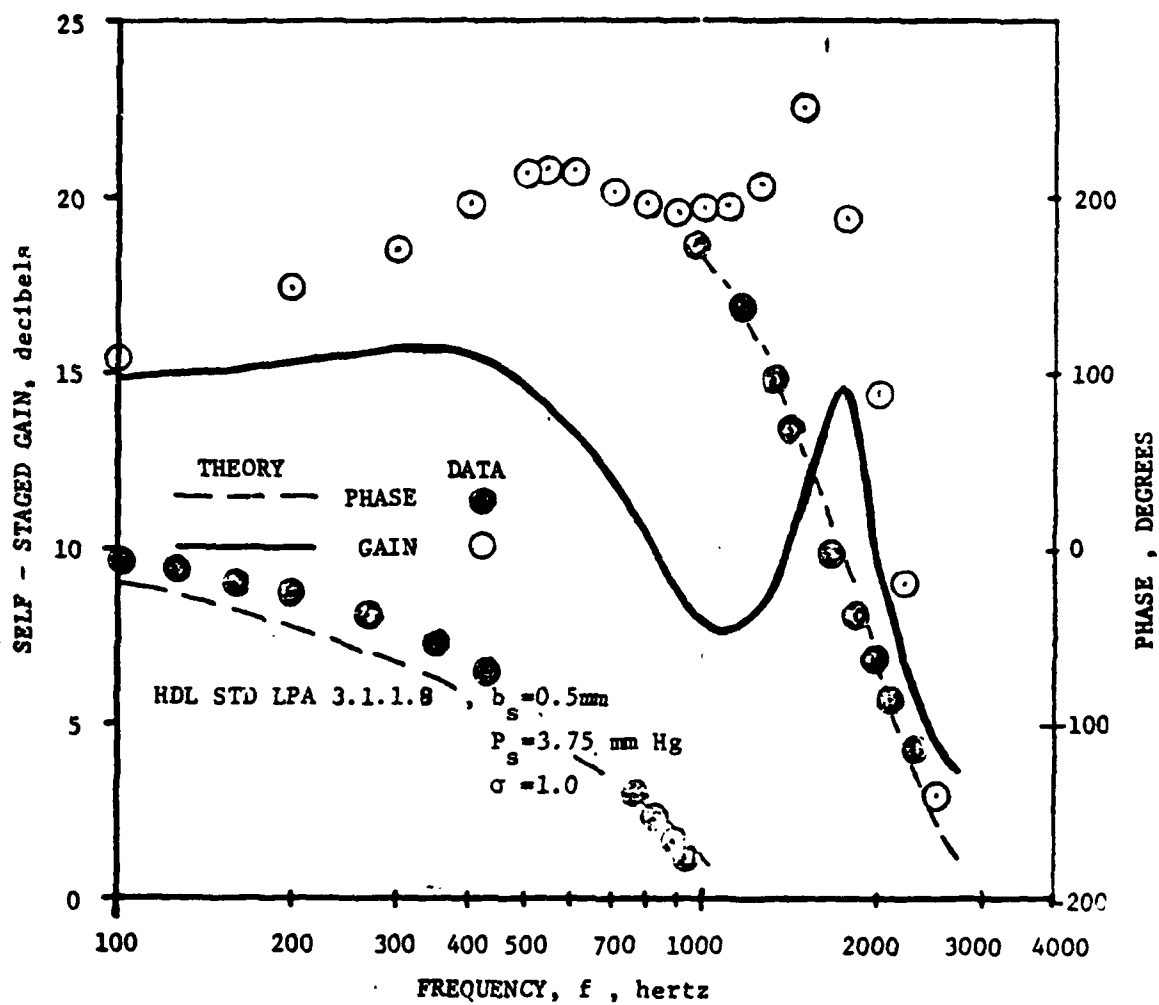Figure A4. Bode plot of self-staged gain for an HDL STD LPA,$\sigma = 0.5$. ($b_s = 0.5$ mm)

205

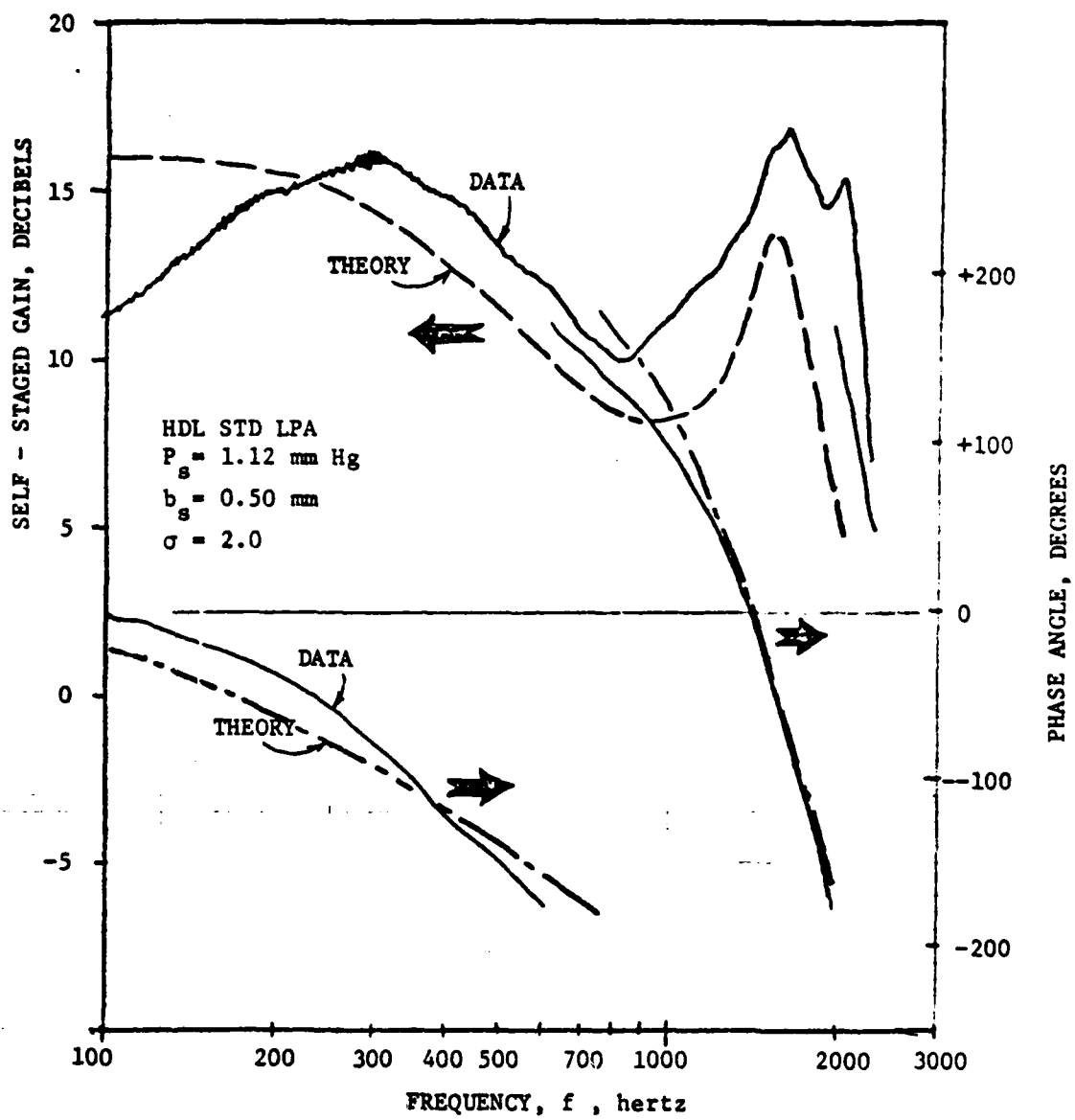Figure A5. Bode plot of self-staged gain of HDL STD LPA, $\sigma=1.0$, $b_s=0.5$mm.

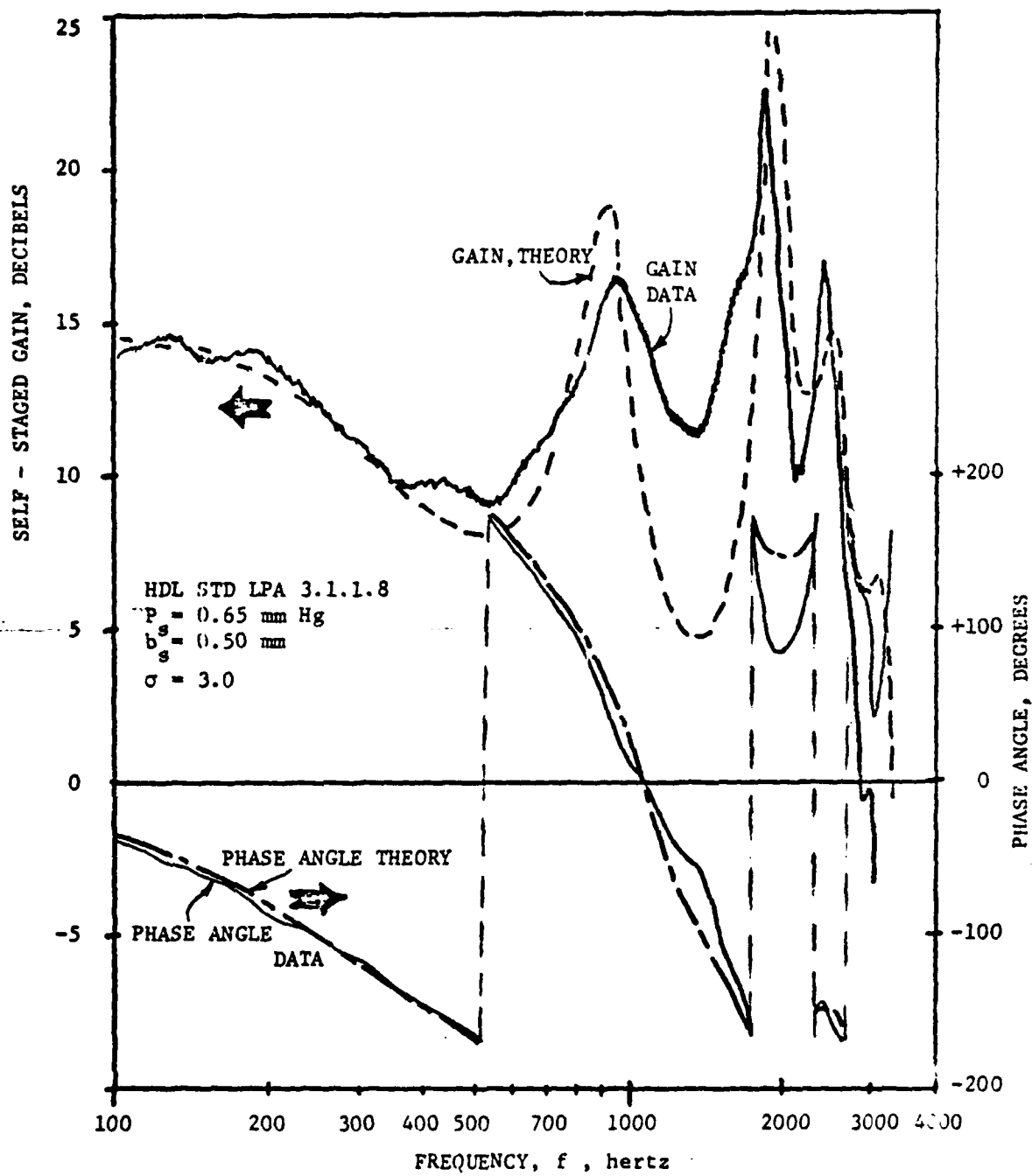Figure A6. Bode plot of HDL STD LPA self-staged gain and phase, σ= 2.0.

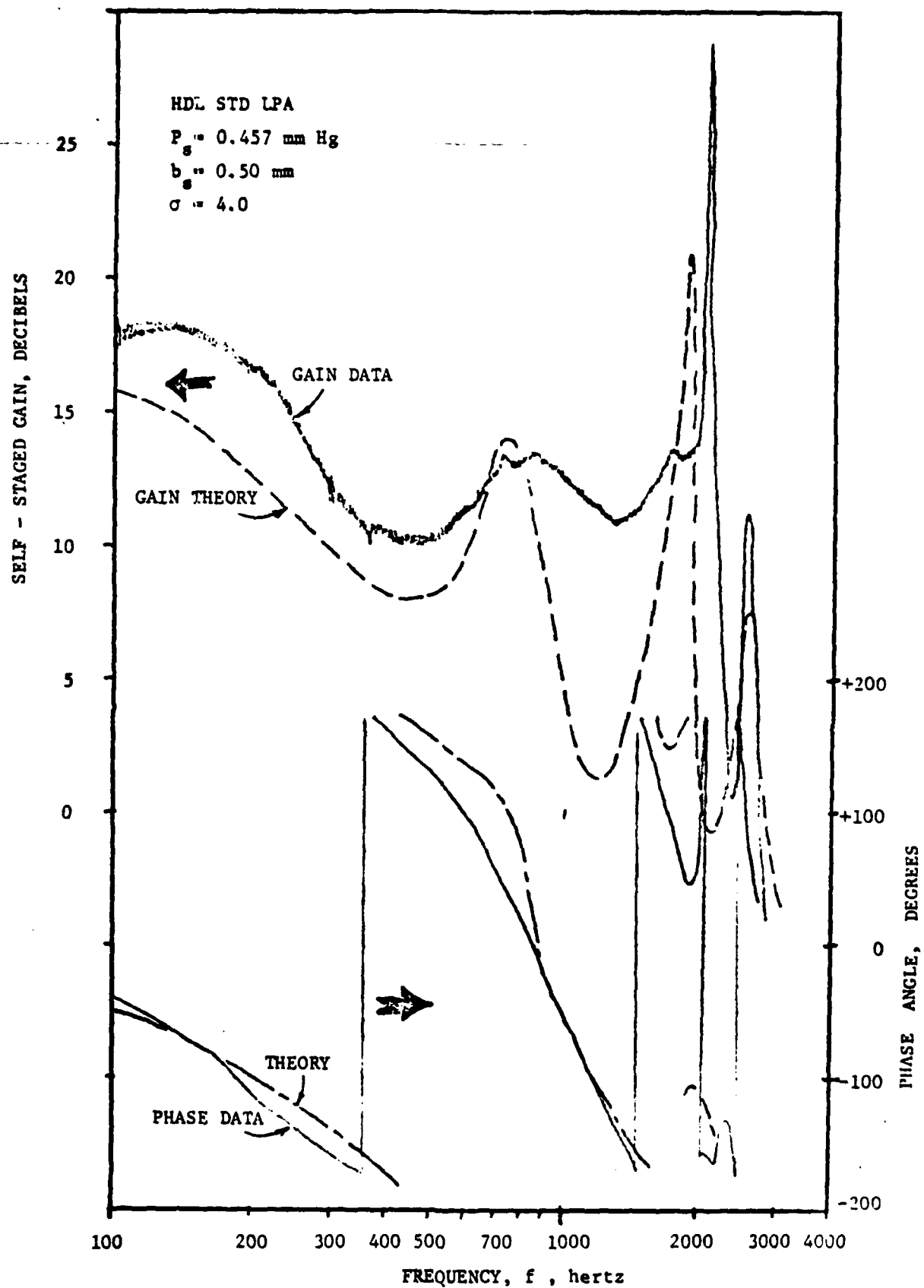Figure A7.   Bode plot of gain and phase for HDL STD LPA, σ = 3.0.

Figure A8.   Bode plot of self-staged gain for HDL STD LPA, σ =4.0.

209
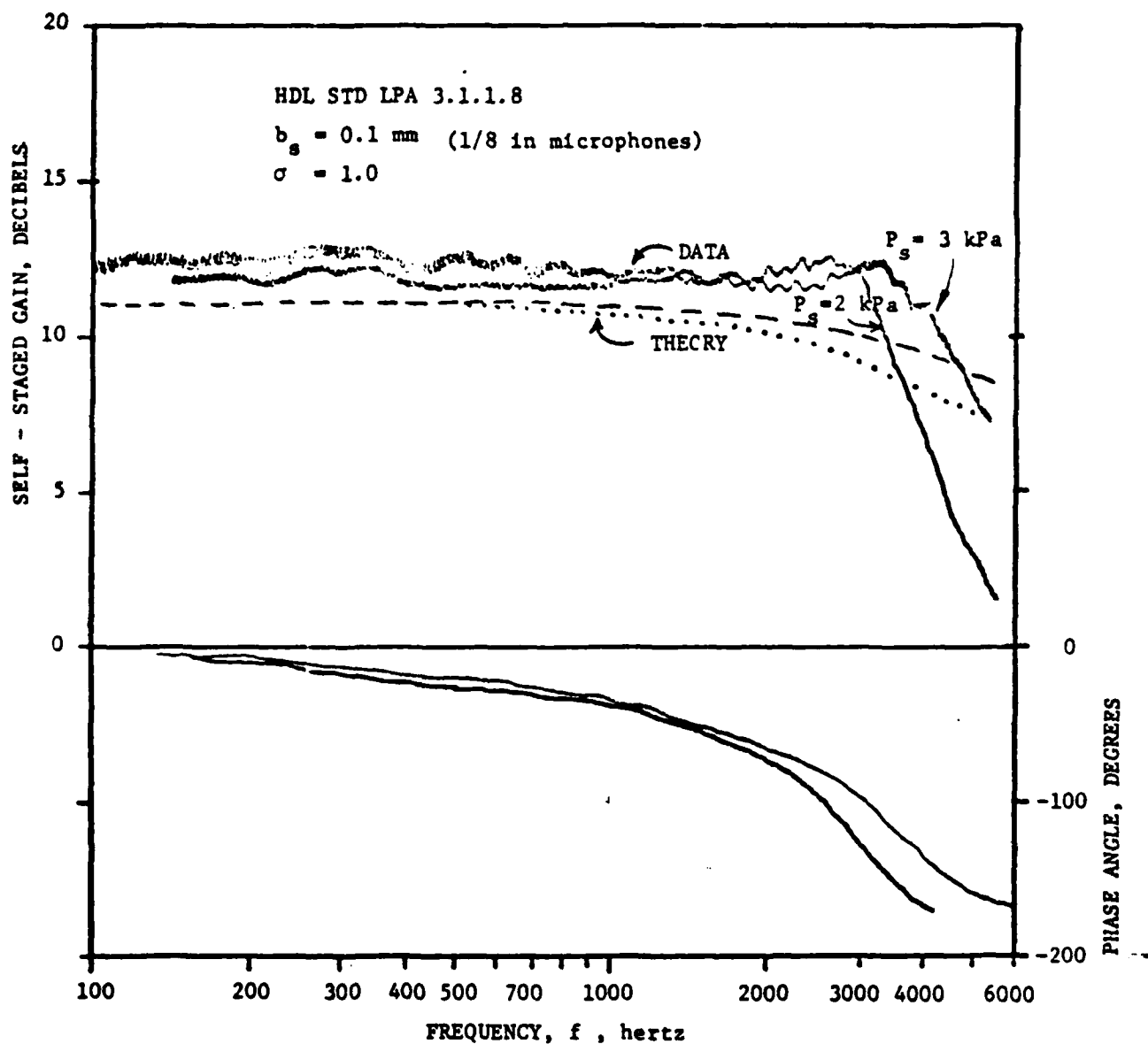
Figure A9. Bode plot of self-staged gain for a microminiature LPA
of standard format, $b_s = 0.1$ mm, $\sigma = 1.0$.

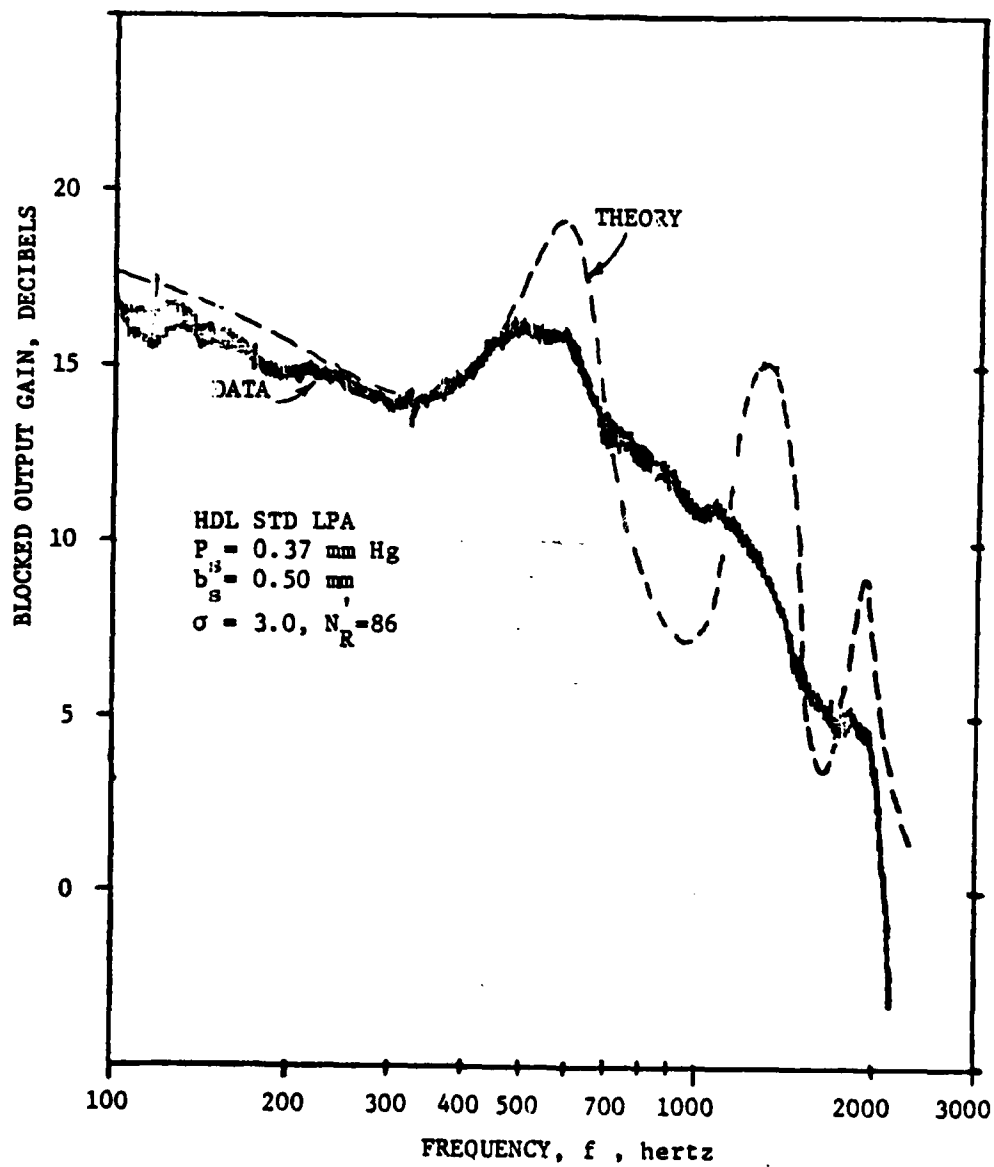Figure A10. Bode plot of the blocked gain of an HDL STD LPA, $\sigma = 3.0$, low Reynolds number.
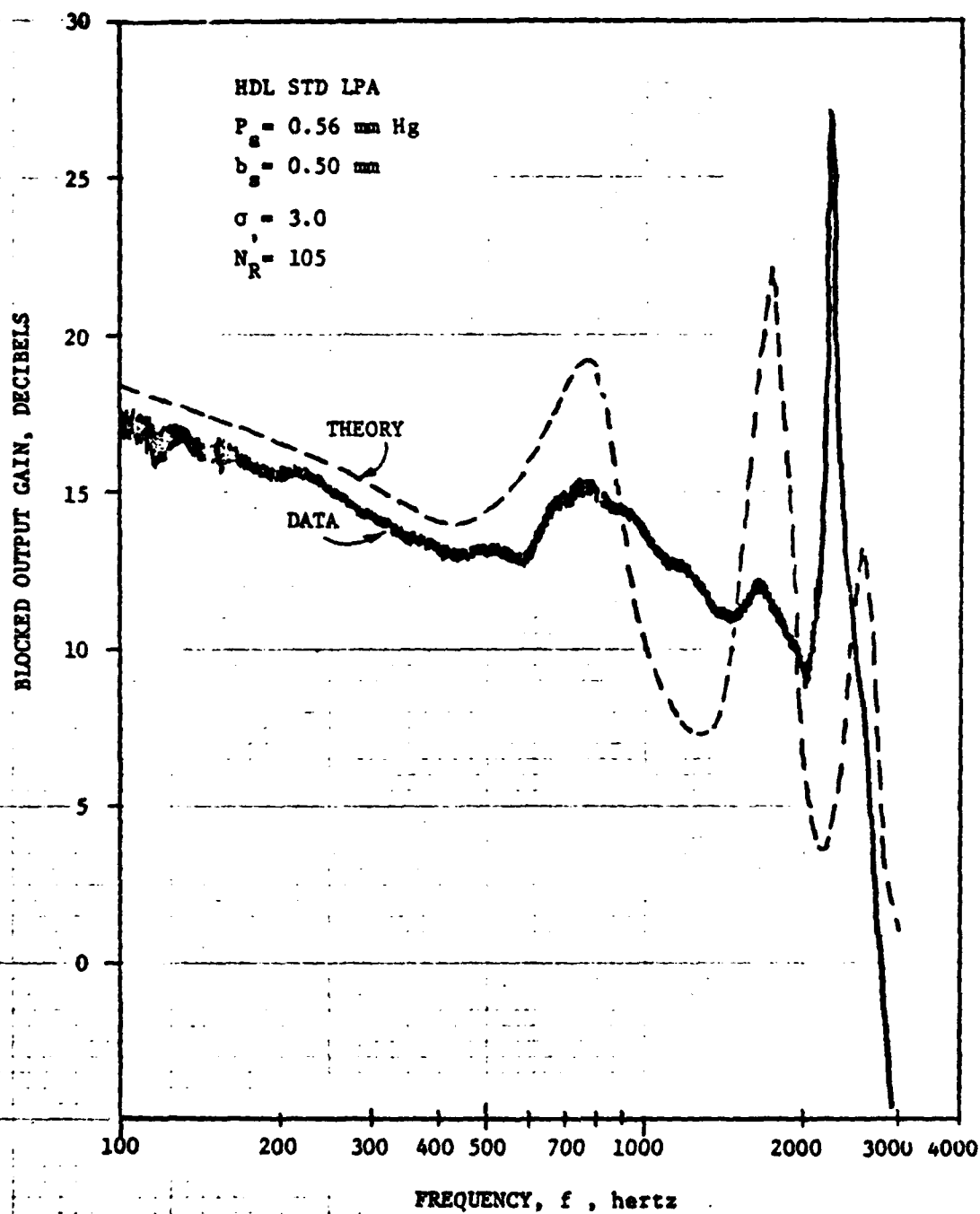
Figure A11. Bode plot of the blocked gain of an HDL STD LPA, σ = 3.0, and moderate Reynolds number.

242
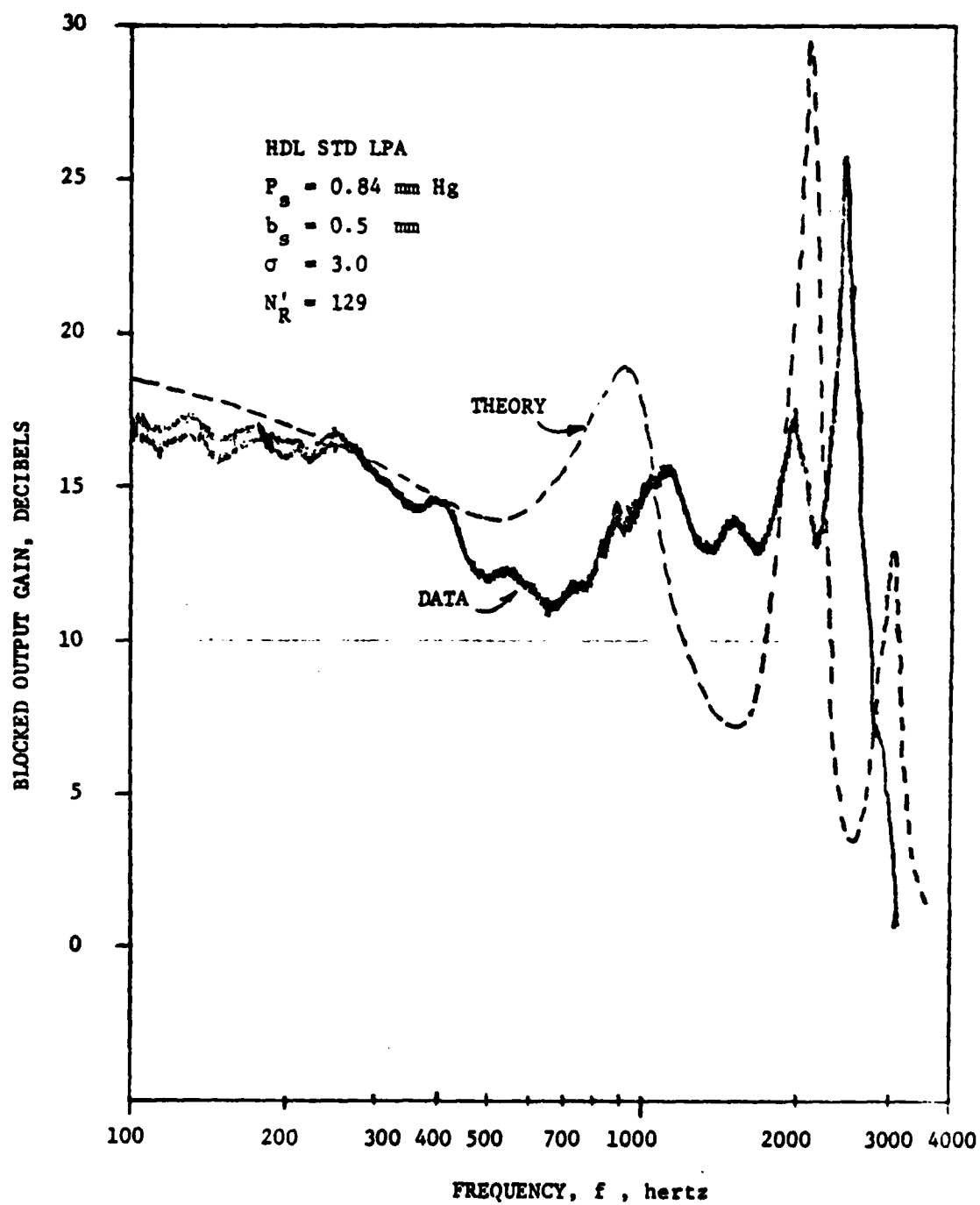
Figure A12. Bode plot of blocked gain of an HDL STD LPA, $\sigma = 3.0$, for high Reynolds number.

SELF - STAGED GAIN, DECIBELS

30

1st SUPPLY
LINE
RESONANCE

HDL STD LPA
P_s = 1.12 mm Hg
b_s = 0.5 mm
σ = 2.0

25

2nd RESONANCE

20

GAIN

15

PHASE ANGLE, DEGREES

200

10

100

5

θ

PHASE ANGLE

0

-100

-5

-200

100   200   300 400 500 700 1000   2000   3000 4000

FREQUENCY, HERTZ

Figure A13. Bode plot affected by resonances in supply lines of 25cm length.

A.3. Static Transfer Characteristic

This test is conducted under the same input loading conditions
as the dynamic tests. A buffer amplifier is used to drive the test
amplifier. Differential control and blocked output pressures are
measured with Barocel Electronic Mamometer pressure transducers. The
setup is shown in figure A14. Test data was shown in figure 70.

A.4. Output Pressure-Noise Spectral Analysis

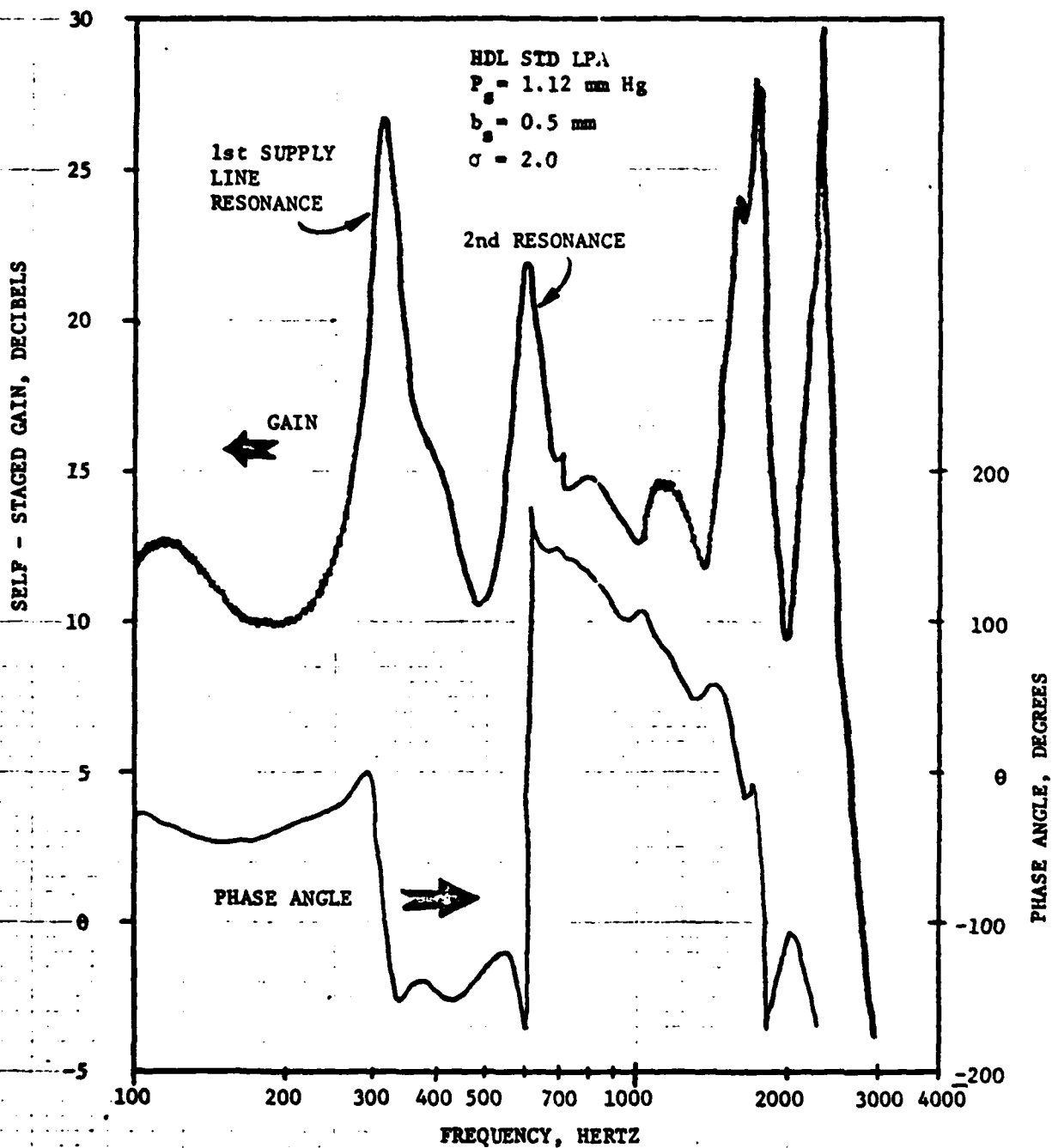To determine such quantities as dynamic range and transition-to-
turbulence, the output noise level spectrum is required. An LPA is
block loaded (worst case with maximum adverse pressure gradient) by a
flush mounted microphone and the noise spectrum is examined on a Hewlett
Packard 3580 A spectrum analyser.

The procedure results in a conservative measurement since dif-
ferential noise is not measured. It is expected that differential noise
is at least an order of magnitude lower than the single sided noise
measured by the microphone. This is because if there is any isotropy
or homogeneity to the disturbances, they will tend to make themselves
felt equally on both outputs so that differential signals are small.
With the development of ultrasensitive pressure sensitive transistors,
a differential measurement may one day be possible. Currently, these
sensors are proprietary laboratory curiosities. The use of PVF2
(polyvinylate difluoride) sheet may allow a differential measurement;
however, noise and impedance mismatches do not yield the present
threshold of microphones.

The procedure is generally to obtain a spectrum with the LPA turned
off and then with it turned on. If the traces are identical as in figure
A15a and b, then the LPA is considered to be operating laminar. If
noise appears, then the output level increases over the laminar op-
eration as already discussed (see section 2, figure 52). This is shown
in the analyser trace of figure A15c.
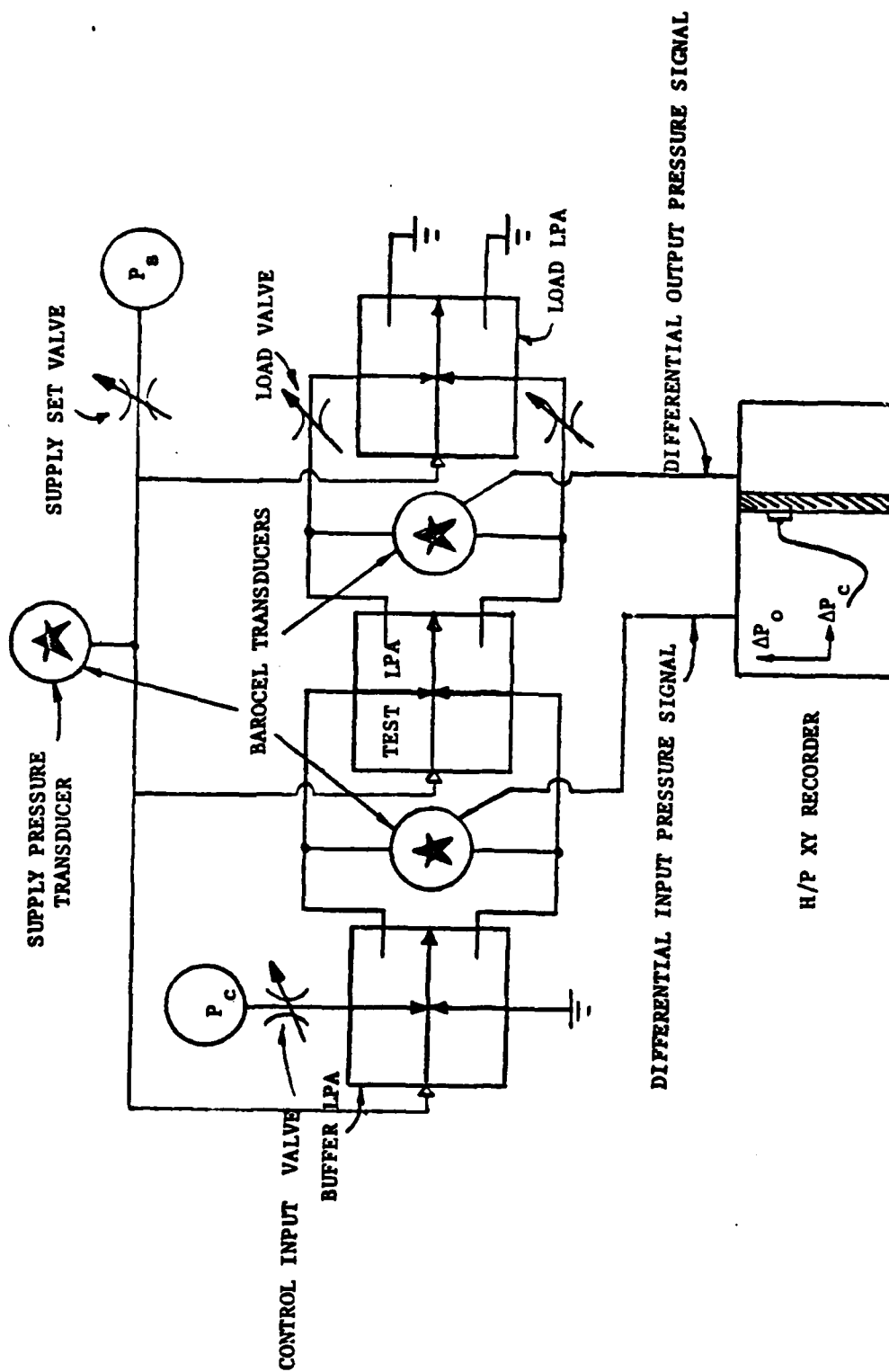
Figure A14. Schematic drawing of the test apparatus for in-stage dc gain measurement.

216
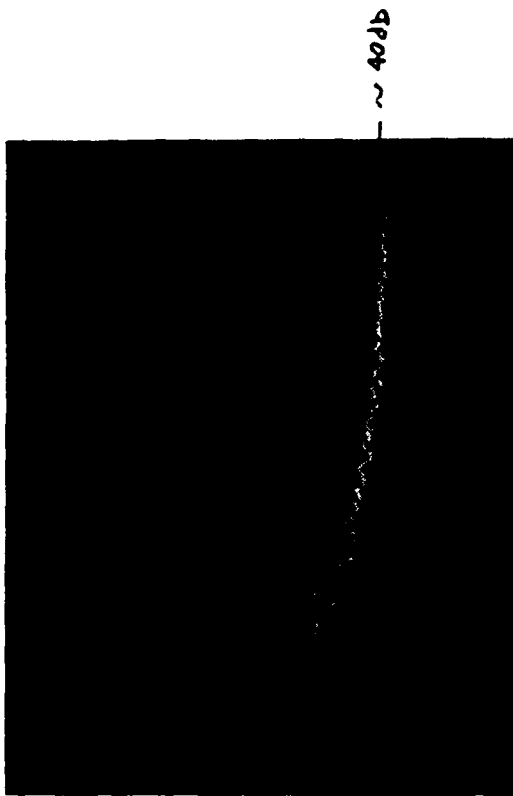
(a) Spectrum of
Room Noise, Electronic Noise
Jet Off

~ 40db

(b) Spectrum of
Room Noise, Electronic Noise
Plus Laminar Jet
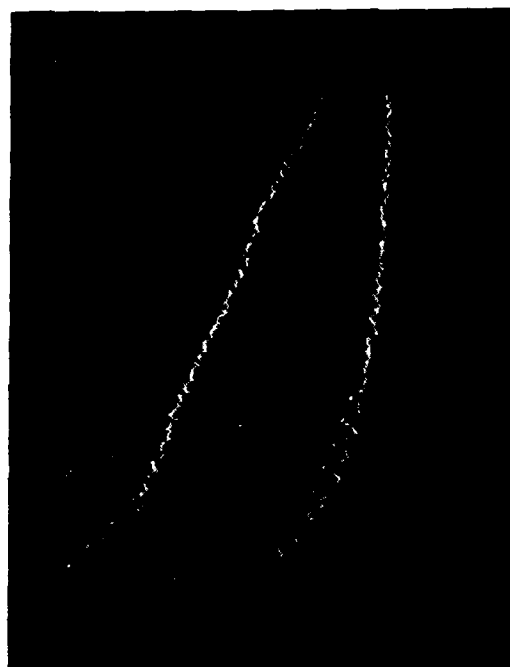
(c) Spectrum of Room Noise
Electronic Noise, Laminar Jet
and Superimposed Turbulent Jet

Total Frequency Range ≈ 5000 Hz
Turbulent/Laminar Noise Ratio
for f < 100 Hz ≈ 70 db

Figure A15. Spectrum analyser
traces of the noise in an LPA.

217

Using this technique, the empirical guide for transition used in section 3 was established. If $c_d N_R / (1 + 1/\sigma)^2 < 180$, the flow will be laminar.

A.5. Carrier Oscillator Frequency Versus Supply Pressure

The oscillator was connected to a supply of air. A tee in the large diameter line (3.175 mm compared with the 0.25 mm nozzle width) measures the stagnation supply pressure. A microphone is "teed" into the output line so that the microphone cavity is negligible (for high resonant frequency) as shown in figure A16. The amplified microphone output is connected to an H/P 5512A electronic counter that displays the frequency. Figure A17 shows a schematic of the test arrangement.

A.6. Rectifier Static Transfer Characteristic

This test was conducted in an identical manner to the LPA static transfer characteristic test with the exception that the rectifier is a single output device so that the Barocel used on the output had one port grounded to atmosphere.

A.7. Demodulator Analog Output Level Versus Frequency

This test was conducted in a similar fashion to the oscillator frequency/output test. The output pressure level is measured in a 12 cc tank with a Barocel transducer. The input frequency is measured with a B/K 1/4 in. microphone in a "tee" as in figure A16 at the input to the block. The schematic is shown in figure A18.

A.8. Demodulator Transient and Frequency Response

A Barocel has a frequency response of about 10 Hz. Since the output transient response is expected to be less than this (3 Hz),

218

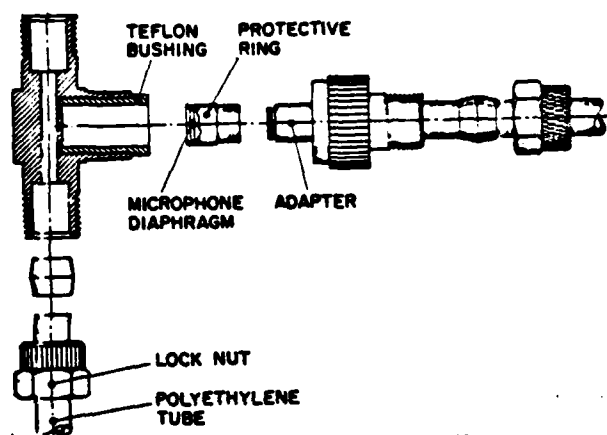Figure A16. Exploded view of the microphone holder "tee" with small
            parasitic volume for high frequency response.(volume
            Helmholtz frequency is 24.5kHz).
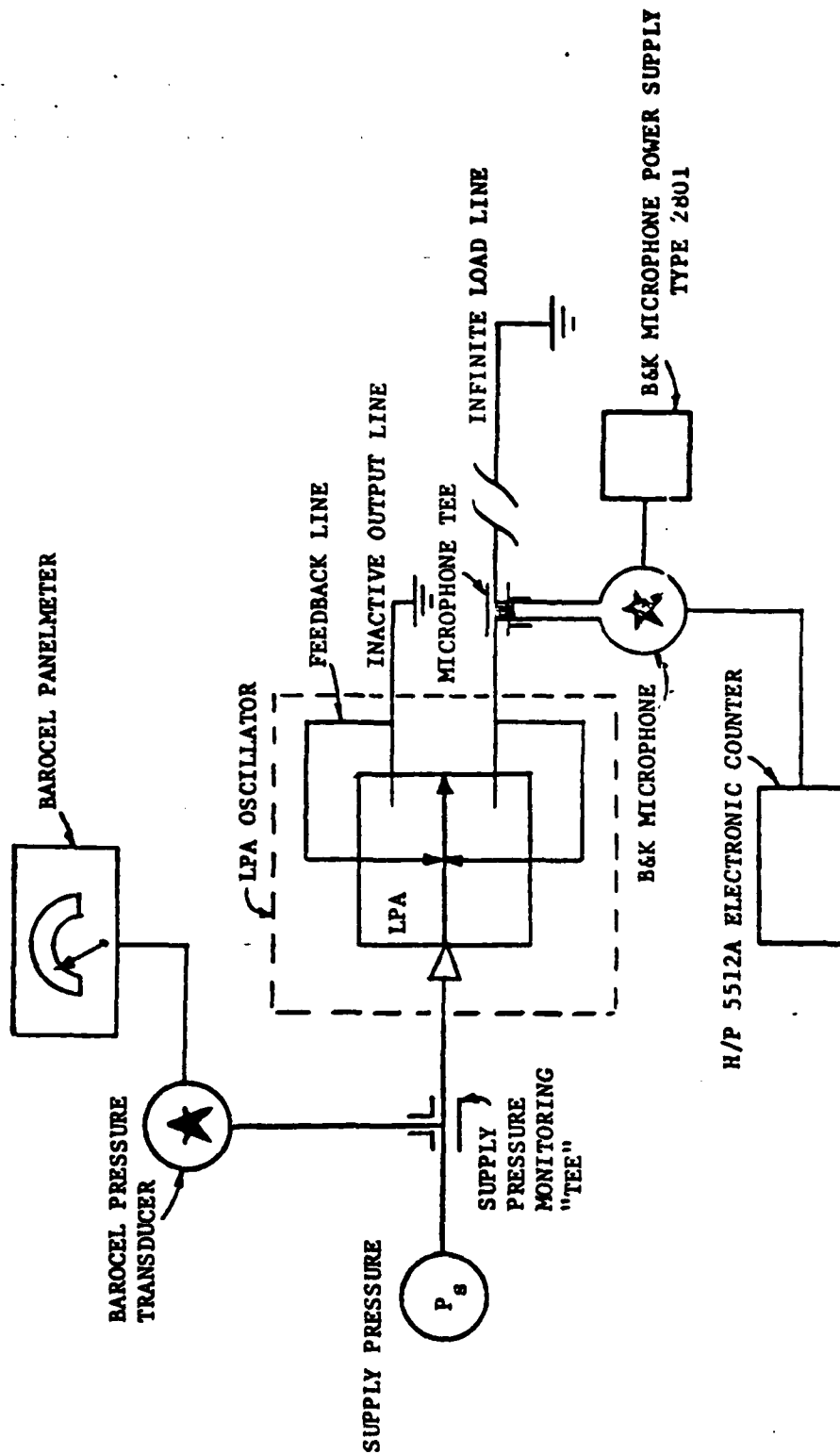
Figure A17. Schematic drawing of the test apparatus for measuring LPA oscillator output frequency as a function of supply pressure.

220
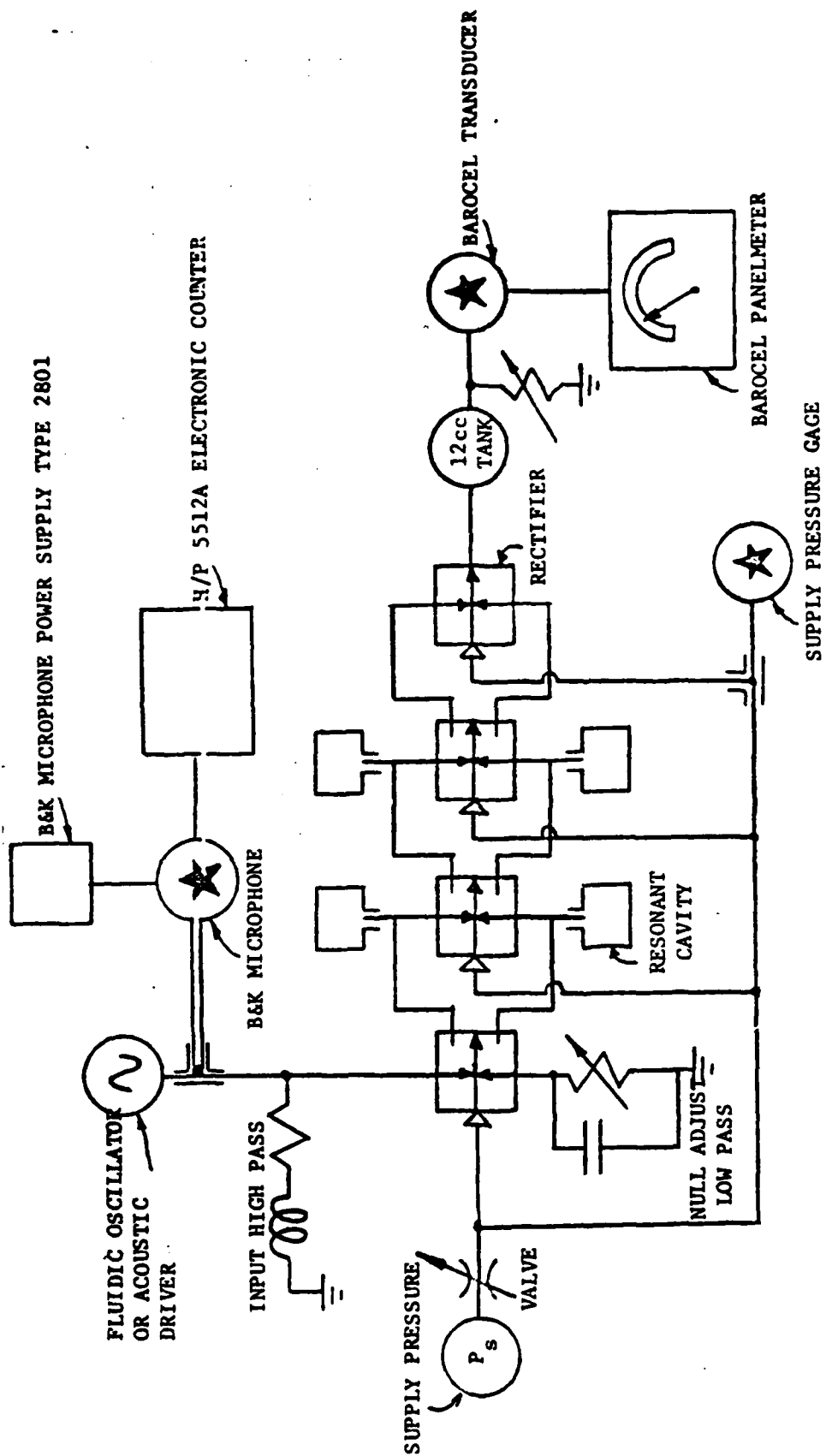
Figure A18. Schematic of the test apparatus used in obtaining the frequency demodulator characteristics.

221

then a Barocel transducer closely coupled to the output (the line volume is much less than the output volume) will not affect operation. A 10 cm, 3.175 mm line has a volume of 0.74 cc compared to the 12 cc of the tank.

The oscillator output is connected to the demodulator input by a 10 m, 12 mm diameter copper line. The oscillator step output is generated by quickly blocking the offside output. This can be achieved in less than 0.05 seconds. The output changes 380 Hz. This then produces a demodulator output shown in figure 89a. The test arrangement is shown in figure A19.

The frequency response is approximated by repeating the transient response test but repeatedly blocking and unblocking the oscillator output at an increasing rapid rate. The results were shown in figure 89b.

Figure A19. Schematic drawing of the test arrangement for measuring the transient and frequency response of the narrow band data link system.

223

A3. US PATENT DISCLOSURE, " FLUERIC BROAD BAND AMPLIFIER ".

Name of Inventor: Tadeusz M. Drzewiecki

Serial No.

Filing Date

Title: BROAD BAND FLUERIC AMPLIFIER

ABSTRACT OF THE DISCLOSURE

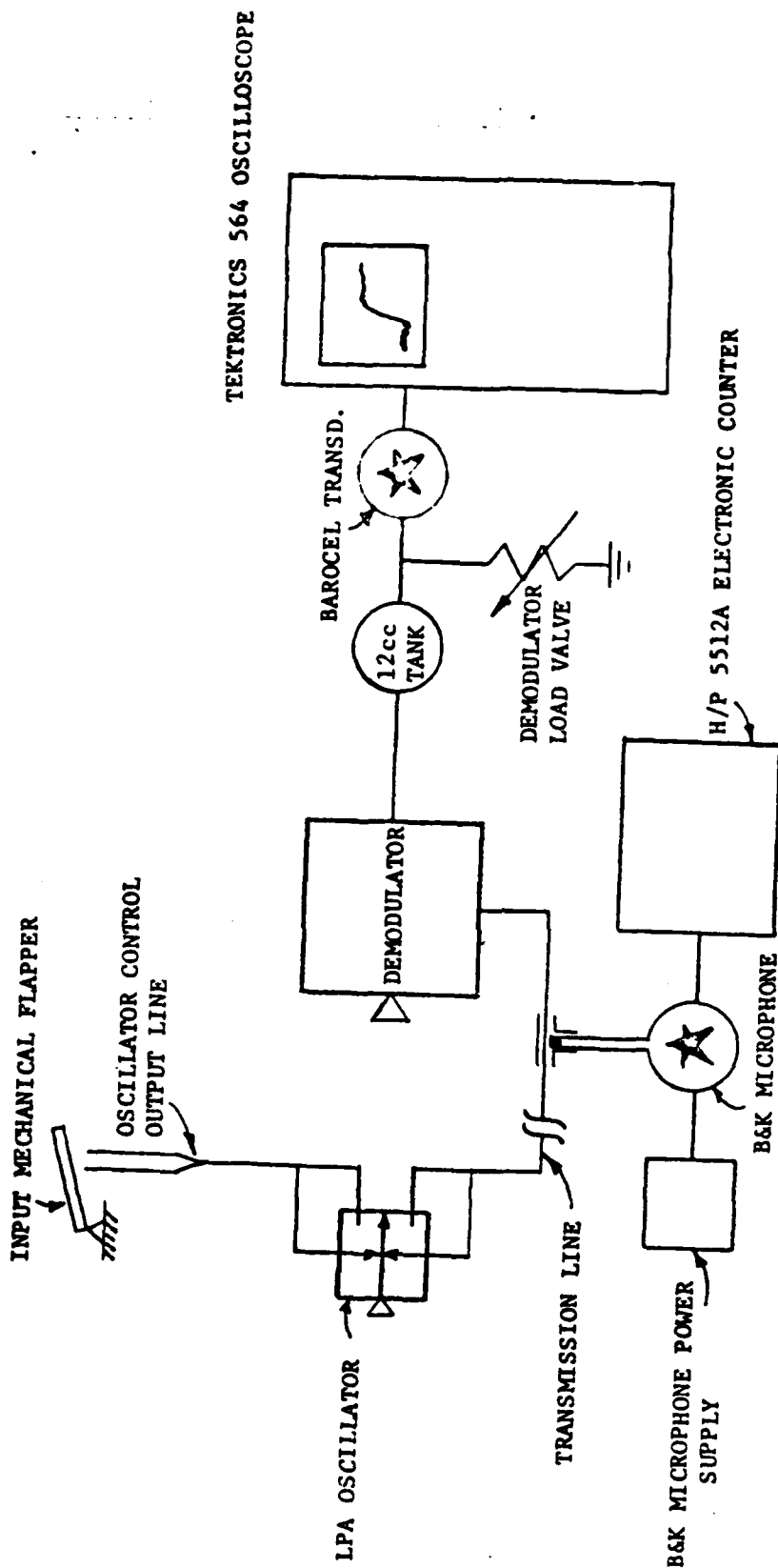A broad band flueric amplifier is disclosed which comprises means to increase the deflection of the fluid jet within the amplifier at higher frequencies of oscillation of the jet. The means for increasing jet deflection comprises vanes or protrusions positioned closely adjacent the jet path at selected distances from the nozzle. Acoustic feedback from these vanes or protrusions will assist the control pulse in deflecting the jet at selected frequencies of oscillation.

RIGHTS OF THE GOVERNMENT

The invention described herein may be manufactured, used and licensed by or for the United States Government for governmental purposes without the payment to me of any royalty thereon.

BACKGROUND OF THE INVENTION

Typically, the bandwidth of AC fluidic or flueric amplifiers has been limited by the dynamic response of the input impedance. This impedance is such that the input control signal is generally attenuated significantly at higher frequencies. Often the bandwidth of available devices is insufficient for many purposes. Particularly, the increasing use of flueric amplifiers for FM and speech processing requires a wider band of operating frequencies.

Accordingly, it is an object of the invention to overcome the deficiencies of the prior art devices noted above.

Specifically, it is an object of the invention to provide a flueric or fluidic amplifier having a significantly increased bandwidth.

It is an object of the invention to provide a fluidic amplifier which will operate at a broad range of frequencies yet be simple in structure, having no moving parts.

SUMMARY OF THE INVENTION

Fluidic amplifiers such as the laminar proportional amplifier (LPA) are generally designed with a low aspect ratio (height/width ratio) to get wide bandwidth. This invention makes use of observed performance of high aspect ratio devices, having an aspect ratio greater than two. By placing multiple protrusions in an LPA amplifier, multiple peaks in gain can be achieved. Pressure feedback from the protrusions provides an amplification of jet deflection. This is the result of a phenomenon not unlike edgetones except that there is no instability present. This results in a device which has an order of magnitude wider bandwidth. Data shows that a device normally having a bandwidth of 300 Hz can exhibit a bandwidth of 3,000 Hz when this feedback is provided.

Several of the amplifiers of the invention can be operated in parallel, the peaks in gain of one amplifier being shifted in relation to the peaks in gain of another amplifier. The result will be an output which is smoother, having increased gain across a broad continuum of frequencies.

BRIEF DESCRIPTION OF THE DRAWINGS

Figure 1 illustrates an exemplary embodiment of the amplifier of the present invention.

Figure 2 graphically illustrates the relationship between frequency of oscillation and the effective control energy applied to an oscillating jet in a laminar proportional amplifier.

Figure 3 shows the relationship between frequency of oscillation and gain in the amplifier of the present invention.

Figure 4 illustrates an embodiment of the invention comprising two modified amplifiers operating in parallel.

Figure 5 graphically illustrates the gains of the respective amplifiers of figure 4 as they relate to frequency, and the effective gain of the composite system shown in figure 4.

DESCRIPTION OF THE PREFERRED EMBODIMENT

Referring to figure 1, there is shown an amplifier comprising the essential features of the present invention. Supply 3 comprises a pressurized source of fluid which directs a jet out of nozzle 4. Control inputs 6 and 8 direct control pressure pulses through outlets 10 and 12, respectively. Vents 14 and 16 are maintained at constant pressure in the usual and well known manner for such devices. Either or both of outlets 18 and 20 will receive the fluid of the jet depending upon the position of the jet resulting from deflection by pressure pulses through outlets 10 or 12.

Vanes 1 and 2 are placed within the vent region between nozzle 4 and splitter S which separates outputs 18 and 20. The vanes extend to a position closely adjacent the path of the jet. The outer-most edge of each vane should extend to a position which is at a distance from the edge of the undeflected jet which does not exceed one-half the width of nozzle 4. The deflected jet should just touch the vane when the output of the amplifier is fully saturated.

In operation, fluid from supply 3 exits as a jet through nozzle 4 toward splitter S. Control pressures through inputs 6 and 8 generate control pulses at ports 10 and 12, respectively. These control pulses act to deflect the jet toward either output 18 or output 20. As the control pulses at ports

10 and 12 are reversed due to a frequency input, the jet will oscillate back and forth between the outputs 18 and 20 at the same frequency.

As the jet passes closely adjacent the edge of one of the vanes 1 or 2 acoustic energy will be generated and fed back toward the nozzle 4. This will also occur as the jet passes closely adjacent the splitter S. This acoustic energy will provide a pressure on the side of the jet adjacent the protrusion or vane. This pressure, along with the pressure pulses from ports 10 and 12, will act on the jet to determine the deflection thereof. If the acoustic feedback pulse and the control pulse from the port 10 or 12 are exactly in phase with one another, the two will combine to significantly increase the deflection of the jet. However, since there is a finite transport time for the fluid of the jet from nozzle 4 to any point downstream of the nozzle the acoustic pulse cannot be precisely in phase with the pulse from the control port. Therefore, the two pulses will combine to increase the deflection of the jet when they are 360° out of phase with one another, or exactly one wavelength apart.

At low frequencies of oscillation of the control pulse the position of the jet with respect to the outputs will always be substantially in phase with the control pulse. For example, when a positive pulse is applied at port 10, the jet will follow a path through output 20. As the frequency of oscillation of the control pulse is increased, the downstream position of the jet moves out of phase with the control pulse. As seen in figure 1, the control pulse P_j is applied through port 10 while the downstream position of the jet, shown by dashed lines, is at output 18. The position of the jet at splitter S is therefore 180° out of phase wtih the pressure pulse P_j. Also, there is a normal phase lag between the jet position downstream and the control signal of 180° due to the finite jet transport time between the upstream and downstream positions. (This lag can be observed in a stream of water exiting from the nozzle of a garden hose as the hose is rapidly moved back and forth.) The result is that the acoustic feedback, shown by

arrow F in figure 1, generated at the splitter is 360° out of phase with
the control impulse at port 10. Since the acoustic energy travels at the
speed of sound, much more rapidly than does the jet, the acoustic pressure
may be considered to instantly combine with the pulse from port 10 to increase
the deflection of the jet.

The manner in which this phenomenon increases the operation bandwidth
of the amplifier will be described with reference to figures 2 and 3. In
figure 2, P_c represents the control pressure which exists at input 6 or 8
of the amplifier, while P_j represents the actual pressure pulse generated at
the output ports 10 and 12. Since the input signal P_c is fed through an
impedance, the signal P_j becomes significantly attenuated at higher frequen-
cies. This is illustrated in figure 2 by the rapidly decreasing ratio of
P_j to P_c at increasing frequencies. Due to this loss of control pressure
at higher frequencies, the gain of prior art amplifiers significantly dimin-
ished or disappeared at such frequencies. The present invention alleviates
this problem by providing the above discussed acoustic pressure signals in
the higher frequency range, thus increasing the gain of the amplifier in this
range.

Figure 3 graphically illustrates the relationship between frequency
and the ratio of the output pressure to the control pressure (gain) in the
amplifier of the present invention. At lower frequencies the device operates
substantially in the same manner as the prior art devices. This can be seen
in that portion of the gain curve which terminates at point N along the axis
which represents frequency. Point N signifies the normal bandwidth of a
prior art amplifier since it is at this point where the gain diminishes sub-
substantially due to the loss of pressure at the control port, as discussed
with reference to figure 2. In this device of the present invention, as the
frequency increases beyond the value N, the wavelength of the deflected jet
becomes such that the position of the wave at the splitter S becomes 180° out
of phase with the control pulse as discussed with reference to figure 1. At

that point the acoustic pressure signal is 360° out of phase with the control
pulse, and combines therewith to increase the deflection of the jet, thereby
increasing the gain of the amplifier. The acoustic signal generated by the
device compensates for the loss in pressure at the control ports.

As the frequency of oscillation increases still further, the acoustic
pulse generated at the splitter moves further out of phase with the pulse
at the control port, and therefore will not combine therewith to effectively
increase the deflection of the jet. However, the increasing frequency will
shorten the wavelength of the deflected jet to the extent that the jet posi-
tion at vane 2 will then be 180° out of phase with the pulse at the control
port. The acoustic signal generated at vane 2, as shown by arrow H in figure
1, will then be 360° out of phase with the signal at the control port, and
will combine therewith to again increase the deflection of the jet. The result
will be a second increase in the gain of the amplifier, as shown by point 2 in
figure 3. The same will again occur as the frequency is increased to bring
the deflected jet 180° out of phase with the control signal at vane 1.

As can be seen in figure 3, the successive peaks in the gain of the
amplifier at higher frequencies extend the operational bandwidth of the device
to a frequency represented by point B. While figure 1 illustrates a device
having two sets of vanes 1 and 2, it is to be noted that any number of vanes
may be used. The position of the vane, that is the distance of the vane from
the nozzle 4, will determine the frequency at which the acoustic energy will
be effective to assist the control pulse in deflecting the jet. Therefore,
an amplifier may be readily designed which will generate peaks in the gain
thereof at preselected frequencies.

Figure 4 illustrates an embodiment of the invention which comprises two
amplifiers of the invention operating in parallel. It is to be understood
that three or more amplifiers may also be operated in parallel as shown in
the drawing. The embodiment of figure 4 comprises commmon inputs 6 and 8
for the control pulses of the respective amplifiers, and common outputs 18 and
20. The upper-most amplifier comprises vanes 1 and 2 positioned at distances

d_1 and d_2 from the nozzle 4, respectively. The lower-most amplifier comprises nozzles 31 and 32 set at distances d_{31} and d_{32} from nozzle 4, respectively. It is noted that the distances d_1, d_2, d_{31}, d_{32} are all different from one another. Assuming that the velocities of the respective jets in the amplifiers are equal the peaks in gain generated by vanes 1 and 2 will be generated at frequencies different from the peaks in gain generated by vanes 31 and 32.

Figure 5 graphically illustrates the gain of the composite amplifier of figure 4. The lower curves marked LPA 1 and LPA 2 signify the gain curves of the respective individual amplifiers of figure 4. It is noted that each of these lower curves corresponds in shape generally to that of figure 3. The composite curve of figure 5 illustrates the effective gain of the composite device shown in figure 4. Note that since the peaks in gain of the respective lower curves are shifted relative one another the summation of the two results in a curve which is much smoother, having less sharply defined peaks and valleys. The result is an amplifier which has a much more even operation across a wide continuum of frequencies.

As noted above the frequency at which an amplifier of the invention will generate a peak in amplifier gain is determined by the position of the protrusions or vanes in the device. This frequency may also be affected by varying the velocity of the jet from nozzle 4. The velocity of the jet determines the transport time of the fluid to a position adjacent one of the protrusions or vanes, thereby affecting the time at which the jet will be in or out of phase with the pulse at the control port.

While the invention has been disclosed with reference to the specification and attached drawings, I do not wish to be limited to the specific details disclosed therein as obvious modifications can be made by one of ordinary skill in the art.

CLAIMS:

1. A broadband flueric amplifier comprising;

    means for directing a jet of fluid outwardly from a nozzle;

    output means comprising at least two output channels;

    control means for deflecting the jet toward an output channel and for

    causing the jet to oscillate between output channels; and

    means for increasing the deflection of the jet at specific frequencies

    of oscillation thereof.

2. An amplifier as in claim 1, wherein said means for increasing the deflec-

tion of the jet comprises means for generating acoustic feedback.

3. An amplifier as in claim 2, wherein said means for increasing the deflec-

tion of the jet comprises at least one protrusion having an edge situated

closely adjacent the path of the jet between said nozzle and said output

means.

4. An amplifier as in claim 3, which comprises at least one set of said

protrusions situated closely adjacent opposite sides of the jet path.

5. An amplifier as in claim 3 or 4, wherein said means for directing the

jet/fluid comprises a nozzle having a given width, and said protrusions

are situated at a distance from the edge of said jet which does not exceed

one-half said width.

6. An amplifier as in claim 2, wherein a splitter is positioned between

said output channels to separate said channels, and interaction of said jet

with said splitter generates acoustic feedback.

7. An amplifier as in claim 3, wherein the frequency at which the jet deflection will be increased is determined by the distance between the nozzle and said protrusion.

8. An amplifier as in claim 4 comprising more than one set of protrusions positioned at selected distances from said nozzle, whereby the deflection of said jet will be increased at several frequencies of oscillation thereof.

9. An amplifier as in claim 1 or 7, wherein the frequency at which the jet deflection will be increased is determined by the velocity of said jet.

10. A system comprising at least two amplifiers as in claim 4, wherein the amplifiers have common output channels and a common control means, wherein the distances of the protrusions from the nozzle in one of said amplifiers differs from said distances in other of said amplifiers, whereby the respective amplifiers will increase the deflection of their respective jets at differing frequencies of oscillation.

FIG. 1

FIG. 2

FIG. 3

235
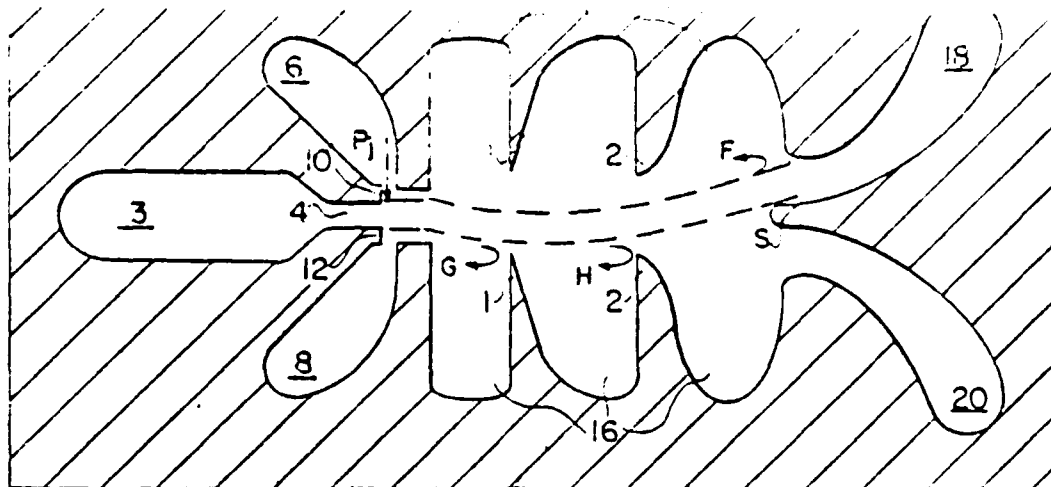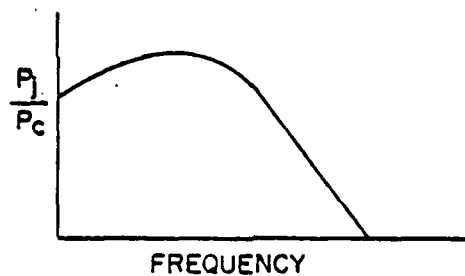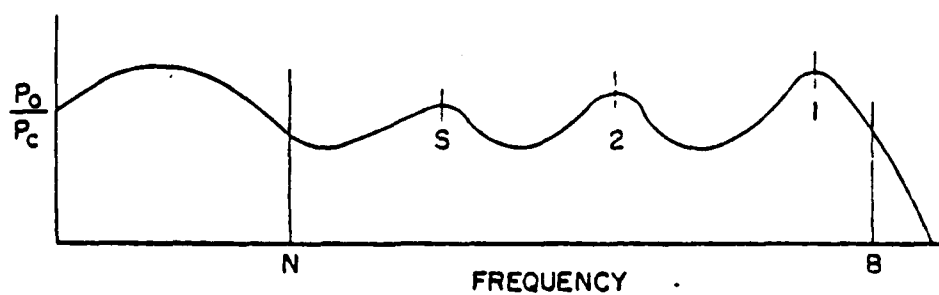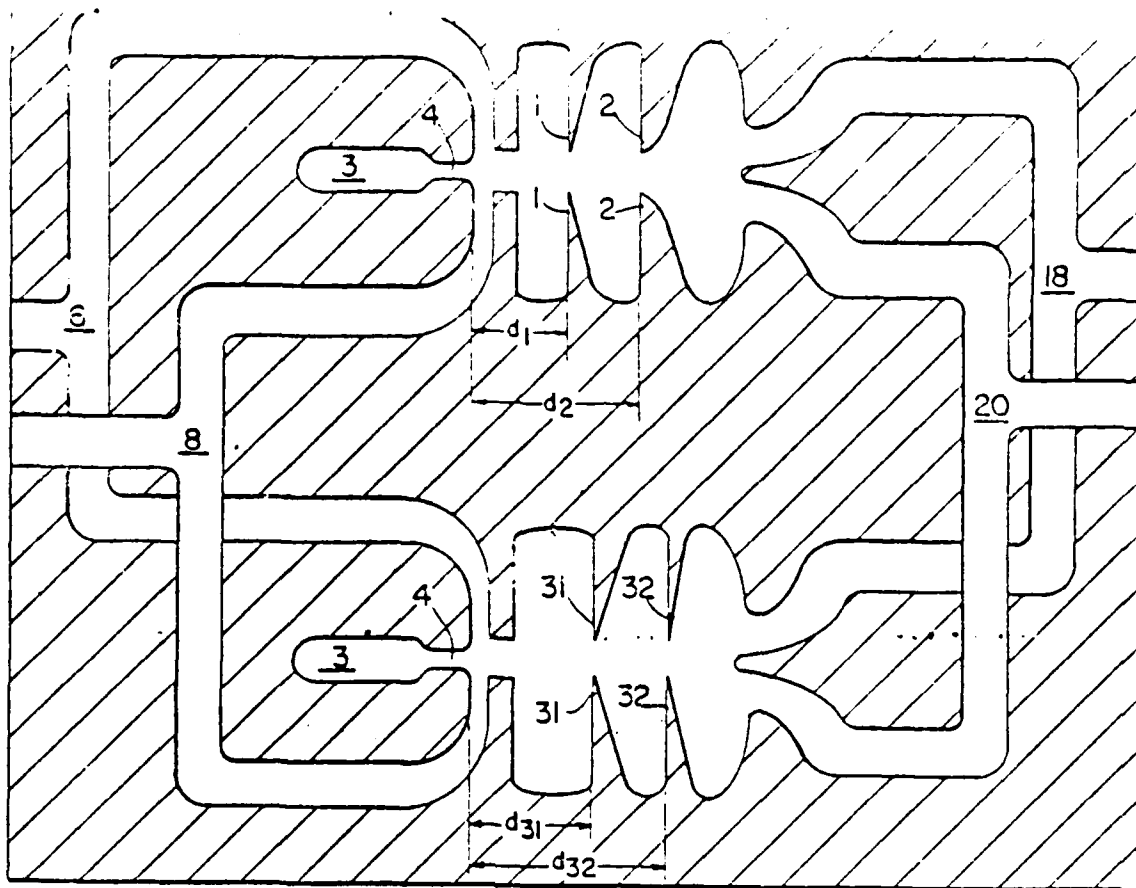
FIG. 4

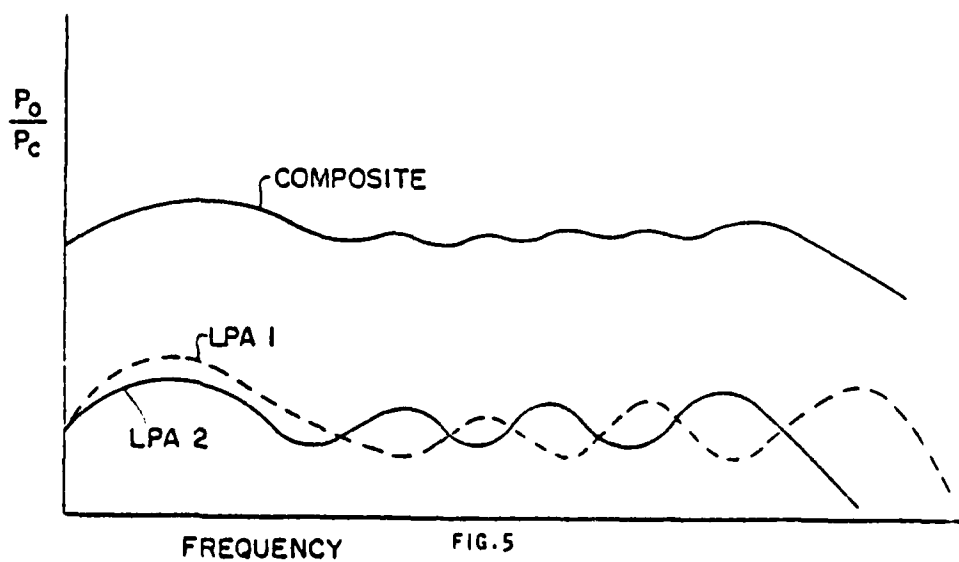
FIG. 5

INITIAL DISTRIBUTION

No. Copies

Defense Documentation Center
Cameron Station   2
Alexandria, VA 22134

Naval Postgraduate School
Monterey, CA 93940
  Department of Mechanical Engineering
     Prof. P. J. Marto, Code 69Mx   1
     Assoc. Prof. R. H. Nunn, Code 69Nn   1
  Department of Electrical Engineering
     Prof. D. E. Kirk, Code 62Ki   1
     Assoc. Prof. R. D. Strum, Code 62St   1
  Department of Aeronautics
     Prof. D. J. Collins, Code 67Co   1
  Library, Code 0142   2

Dr. T. M. Houlihan   1
Propulsion Dynamics Inc.
2200 Somerville Road
Annapolis, MD 21401

Mr. J. M. Kirshner   1
9234 E. Parkhill Drive
Bethesda, MD 20014

Commander
Harry Diamond Laboratories
2800 Powder Mill Road
Adelphi, MD 20783
  ATTN: DELHD-CM-FS-4 T. M. Drzewiecki   1
                        R. M. Gottron   1
                        J. M. Goto   1
  ATTN: DELHD-CM   R. McCoskey   1

Prof. Latif M. Jiji   1
City College of the City Univ. of New York
Department of Mechanical Engineering
139th Street at Convent Avenue
New York, NY 10031

Prof. David Wormley   1
Massachusetts Institute of Technology
Mechanical Engineering Department, Rm. 3-146
77 Massachusetts Ave.
Cambridge, MA 02139

Naval Air Systems Command   1
Department of the Navy
Washington, DC 20360
  ATTN: Code AIR-52022E (D. Houck)

237

No. Copies

Air Force Institute of Technology   1
Wright-Patterson Air Force Base
Ohio 45433
  ATTN: AFIT (ENM) Dr. Milton Franke

DATE
FILMED

-8